Final report

1.1 Project details

Project title	ECONOMIC MODEL PREDICTIVE CONTROL SCHEME FOR DEMAND RESPONSE OF SPACE HEATING IN RESIDENTIAL BUILDINGS (READY.DK)
Project identification (program abbrev. and file)	ForskEl, grant number 12305
Name of the programme which has funded the project	ForskEL (now EUDP)
Project managing company/institution (name and address)	Aarhus University
Project partners	Aarhus University
CVR (central business register)	31119103
Date for submission	07-09-2019

1.2 Short description of project objective and results

The objective of this project was to investigate the potential of economic model predictive control (MPC) of residential space heating systems to provide demand response. The case investigated was existing multifamily residential buildings facing retrofit.

Using time varying tariffs from the day-ahead wholesale power market, MPC of the retrofitted buildings can achieve operational cost savings of up to 13% - and up to 19% if intraday trading was included. Moreover, CO_2 emissions associated with the power production was reduced with up to 3%, and consumption in peak periods was reduced by up to 50%.

Consequently, MPC of heating systems in retrofitted residential buildings can be a valuable assert in the balancing of the energy system, while also saving operational cost and CO_2 emissions.

Formålet med dette projekt var at undersøge om det er muligt at opnå smart grid fordele ved model-baseret styring (MPC) af boligvarmeanlæg i eksisterende etageboliger.

Projektet demonstrerer, at man ved hjælp af MPC og tidsvarierende takster fra elmarkedet (day-ahead) kan opnå driftsbesparelser på op til 13% - og op til 19%, hvis intra-day markedet blev inkluderet. Derudover blev CO_2-emissioner fra energiproduktionen reduceret med op til 3%, og forbruget i spidsbelastningsperioder blev reduceret med op til 50%. Disse potentialer afhænger af bygningers energieffektivitet.

Konklusionen er, at MPC af bygningers varmesystemer kan bruges til at balancere energisystemet, spare driftsomkostning hos forbrugeren, og reducere samfundets CO_2-emissioner.

1.3 Executive summary

Economic model predictive control (MPC) of heating systems in retrofitted residential buildings are able to provide demand response for balancing of the energy system, end-user energy savings, and reduction in CO_2 emissions.

1.4 Project objectives

The overall objective of the project was to investigate the ability of residential buildings to participate actively in smart grids – before and after an energy-retrofit. After a review of energy consumption in these type of buildings, the remaining project focused on investigating whether the energy use for space heating could be made flexible for smart grid purposes using model predictive control to store and release heat in the thermal mass of the building according to the need of the energy system as a whole.

The intended method of the project was to make theoretical investigations of potentials in simulation-based studies, and then test whether it was possible to redeem these potentials in actual buildings which was a part of the much larger EU-funded project READY. However, due to large delays in the READY project, it was not possible to use the buildings in READY.dk.

The initial intention of making simulation-based investigations was fulfilled where it was demonstrated that retrofitted buildings has the potential to become a viable assert in a smart grid system.

Since it was not practical possible to test the findings in real buildings, focus was put on another initial objective of the project, namely the methodology to identify and quantify the smart grid potential that is related to energy-retrofit of existing buildings – both on building scare and city scale. Furthermore, several simulation-based investigations were conducted to contribute to the development of a reliable economic model predictive control scheme suitable for real application.

Finally, the project managed to test the simulated potential in a real setting – but not in a real building as initially intended. A laboratory experiment of an implemented prototype of the two-level economic model predictive control scheme was performed, and the results suggested that the prototype successfully exploited the ability to store heat in thermal mass to minimize heating consumption during high price periods. Further experimental studies are required to verify whether the theoretical potentials can be realised in practice.

1.5 Project results and dissemination of results

The main activities in the project was to conduct simulation-based studies of the smart grid potential of using MPC for building space heating, as well as contribute to the development of a reliable economic model predictive control scheme and software/hardware for real application. Furthermore, it was a main activity to test the setup in a laboratory setting.

The technical results is the formulation and implementation of algorithms for MPC suitable for the purpose. Furthermore, the laboratory experiment demonstrated that it is technically possible to use existing building energy management hardware (for office buildings) to control actual heating systems with the algorithms. Further technical development is needed before it is economical feasible to invest in the hardware needed for MPC in residential buildings

The project succeeded to meet its objective to a large extent. Unfortunately it was not possible to test the technology in actual buildings but this was compensated making relevant experiments in a laboratory setting.

The project was a research project and turnover, exports and employment was not an aspect considered in the project. However, the research project has led to three new projects involving industrial partners who are interested in implementing the controller as a part of their commercial business.

The project results have been disseminated through numerous activities: several invited talks about the project (domestic and international), participation in IEA annex 67, M.Sc. courses at Aarhus University, and a total of seven papers in scientific international journals with high impact factors, and six international scientific conference papers. The written dissemination is compiled in the PhD thesis of Theis Friis Pedersen.

1.6   Utilization of project results

Aarhus University, the only contributor in this project, has already utilised the results to establish three new R&D project together with several partners in the industry. A total of three new PhD students have started in the second half of 2019 on new studies helping companies to make a scientifically sound implementation and test of the technology in their current product portfolio.

The project results is an integrated part of the teaching activities at Aarhus University, where new M.Sc. projects featuring further development of the technology has been and is currently conducted. Several scientific papers (a total of 13) about the project has been published, and there will be more based on recent activities.

1.7   Project conclusion and perspective

The theoretical potential of MPC of heating system in retrofitted buildings is operational cost savings of up to 19%. Moreover, CO_2 emissions associated with the power production can be reduced with up to 3%, and consumption in peak periods was reduced by up to 50%. MPC of heating systems in retrofitted residential buildings is therefore potentially a valuable assert in the balancing of the energy system, while also saving operational cost and CO_2 emissions.

Provided that the potential can be realised in practice, buildings should now be regarded as an active assert in the energy system rather than a passive consumer of energy. Consequently, it is not only the energy-efficiency of buildings that should be of interest to building owners and society but also energy flexibility potential of buildings should be considered. Future building regulatory demands in terms of energy efficiency should not only reflect a balance between investments in energy-efficiency and energy production but also include the potential of investments in energy flexibility technologies.

Annex
https://www.researchgate.net/profile/Theis_Pedersen
https://www.researchgate.net/profile/Steffen_Petersen4

Economic model predictive control scheme for demand response of space heating in residential buildings

Theis Friis Pedersen

Aarhus University
Department of engineering

April 2018

Preface

This thesis reports on the Ph.D. work carried out from May 2015 to April 2018 in the research project *READY.DK* financed by Energinet.dk (ForskEl) under grant number 12305. It has been prepared at the Department of Engineering at Aarhus University under the supervision of Associate Professor Steffen Petersen.

The thesis contributes to the development of a reliable model predictive control scheme suitable for real application in residential buildings to enable non-dispatchable demand response programs of space heating. The work investigates the theoretical demand response potentials in residential buildings using economic model predictive control and, in particular, addresses some of the practical aspects involved when applying model predictive control schemes for real applications.

The main body of the thesis starts with a brief introduction to the general principle of non-dispatchable demand response and demand response assessment together with a description of a generic model predictive control formulation. As such, these two sections provide an overview of the theoretical basis for the thesis work. The following sections report on the main contributions of the thesis, based on a collection of seven primary scientific papers. Four of the papers are published in peer-reviewed scientific journals, two papers are published at peer-reviewed scientific conferences, while the seventh manuscript is under review at a scientific journal.

I would like to express my thanks to my supervisor Steffen Petersen for his continuous guidance and suggestions during the last three years. I would also like to thank my great colleagues Michael Dahl Knudsen, Martin Kristensen and Rasmus Elbæk Hedegaard for their collaboration and contribution to this thesis work.

Finally, I would like to express my gratitude to my friends and family, and in particular, to my wife Sidse, who has been an unyielding source of support, patience and inspiration during the highs and lows of the years of thesis work.

Aarhus, April 2018

Theis Friis Pedersen

Aarhus University
Department of Engineering

Abstract

The concept of demand response covers a wide range of services whereby consumers make permanent or temporary adjustments of their consumption in response to an external request from the energy system. The work presented in this thesis concerns temporary demand response. More specifically, it concerns the application of economic model predictive control to enable non-dispatchable demand response programs of space heating in response to a time-varying cost signal. The work investigates the theoretical potential of non-dispatchable demand response programs and, in particular, addresses some of the practical aspects involved when applying economic model predictive control schemes. The overall aim of the thesis work was to contribute to the development of a reliable economic model predictive control scheme suitable for real application in residential buildings, with a focus on existing residential buildings facing retrofits.

The simulation-based investigations indicated that residential buildings participating in non-dispatchable demand response programs can provide substantial balancing services to the energy system, while simultaneously achieving operational cost savings. Furthermore, the results indicate that buildings with a higher energy efficiency engaged in demand response more frequently and, consequently, achieved higher relative performance. Simulation results suggested that an energy-efficient residential building participating in non-dispatchable demand response programs considering time varying tariffs from the day-ahead wholesale power market achieved operational cost savings of up to 13%, while considering intraday trading simultaneously increased the total operational cost savings by up to 19%. Moreover, non-dispatchable demand response enabled significant benefits for the energy systems, e.g. reductions of CO_2 emissions associated with the power production of up to 3%, while at the same time reducing space heating consumption in peak periods by up to 50%.

To achieve the maximum benefits of participating in demand response programs, while still ensuring thermal comfort, a two-level economic model predictive control setup is suggested to be the most appropriate for real applications. In an attempt to move towards a practical verification of the theoretical identified potentials, a proof-of-concept laboratory experiment of an implemented prototype of the two-level economic model predictive control scheme was performed. The preliminary results suggested that the implemented prototype successfully exploited the ability to store heat in thermal mass to minimize heating consumption during high price periods. Further experimental studies are, however, required to definitively verify the theoretical potentials.

Resumé

Begrebet efterspørgselsreaktion (*demand response*) dækker over en portefølje af tjenester, hvor forbrugere foretager permanente eller midlertidige ændringer af deres forbrug som reaktion på en ekstern anmodning fra energisystemet. Nærværende afhandling vedrører anvendelsen af økonomisk model-baseret prædiktiv kontrol i beboelsesejendomme til at aktivere efterspørgselsreaktion af rumopvarmning som en reaktion på et tidsvarierende prissignal. Arbejdet undersøger de teoretiske potentialer ved at deltage i efterspørgselsreaktion, men behandler især nogle af de praktiske aspekter der er involveret i anvendelsen af økonomisk model-baseret prædiktiv kontrol. Formålet er at bidrage til udviklingen af en pålidelig økonomisk model-baseret prædiktiv kontrol, der egner sig til anvendelse i beboelsesejendomme med særligt fokus på eksisterende beboelsesejendomme, der står over for behov for omfattende renovering.

De simuleringsbaserede undersøgelser viste, at beboelsesejendomme der tilbyder efterspørgsels-reaktion kan levere betydelige balanceringstjenester til energisystemet samtidig med, at de private husejere opnår driftsbesparelser. Endvidere indikerer resultaterne, at bygninger med højere energieffektivitet oftere deltager i efterspørgselsreaktion og derved opnår større udbytte. Simuleringsresultater for en energieffektiv beboelsesejendom viser, at tidsvarierende priser fra *day-ahead* el-engrosmarkedet medførte driftsbesparelser på op til 13%, mens *intraday* handel øgede de samlede driftsbesparelser op til 19%. Endvidere muliggjorde efterspørgselsreaktion betydelige fordele for energisystemerne, f.eks. reduktion af CO_2-emissioner på op til 3% i forbindelse med produktion af elektricitet, samtidig med at rumvarmeforbruget i spidsbelastninger blev reduceret med op til 50%.

Til virkelige applikationer viste en to-niveau økonomisk model-baseret prædiktiv kontrolopsætning sig at være den mest hensigtsmæssige opsætning for at opnå de maksimale fordele ved at deltage i efterspørgselsreaktion og samtidig sikre termisk komfort. I et forsøg på en praktisk verifikation af de teoretisk identificerede potentialer, blev der udført et *proof-of-concept* laboratorieeksperiment af en prototype af den to-niveau økonomiske model-baseret prædiktive kontrolopsætning. De foreløbige resultater indikerer, at den implementerede prototype med succes udnyttede evnen til at lagre varme i den termisk masse for at minimere rumopvarmningsforbruget i højpris perioder. Yderligere eksperimentelle undersøgelser er imidlertid påkrævet for at verificere de teoretiske potentialer endeligt.

Publications

Primary

[P1] Theis Heidmann Pedersen, Kasper Ubbe Nielsen and Steffen Petersen, "Method for room occupancy detection based on trajectory of indoor climate sensor data", *Building and Environment 155* (2017) 147-156. doi: 10.1016/j.buildenv.2017.01.023

[P2] Theis Heidmann Pedersen, Rasmus Elbæk Hedegaard and Steffen Petersen, "Space heating demand response potential of retrofitted residential apartment blocks", *Energy and Buildings 141* (2017) 158-166. doi: 10.1016/j.enbuild.2017.02.035

[P3] Rasmus Elbæk Hedegaard, Theis Heidmann Pedersen and Steffen Petersen, "Multi-market demand response using economic model predictive control of space heating in residential buildings", *Energy and Buildings 150* (2017) 253-261. doi: 10.1016/j.enbuild.2017.05.059

[P4] Theis Heidmann Pedersen, Michael Dahl Knudsen, Rasmus Elbæk Hedegaard and Steffen Petersen, "Comparison of centralized and decentralized model predictive control in a building retrofit scenario", *Energy Procedia 122 – CISBAT 2017 International Conference* (2017) 979-984. doi: 10.1016/j.egypro.2017.07.456

[P5] Theis Heidmann Pedersen, Rasmus Elbæk Hedegaard, Michael Dahl Knudsen and Steffen Petersen, "Handling thermal comfort in economic model predictive control schemes for demand response", *Energy Procedia 122 – CISBAT 2017 International Conference* (2017) 985-990. doi: 10.1016/j.egypro.2017.07.458

[P6] Theis Heidmann Pedersen and Steffen Petersen, "Investigating the performance of scenario-based model predictive control of space heating in residential buildings", *Journal of Building Performance Simulation* (2017). doi: 10.1080/19401493.2017.1397196

[P7] Theis Heidmann Pedersen, Rasmus Elbæk Hedegaard, Kristian Fogh Kristensen, Benjamin Gadgaard and Steffen Petersen, "The effect of including hydronic radiator dynamics in model predictive control of space heating", *Energy and buildings* (2018), *under review.*

Secondary

[S1] Steffen Petersen, Theis Heidmann Pedersen, Kasper Ubbe Nielsen and Michael Dahl Knudsen, "Establishing an image-based ground truth for validation of sensor data-based room occupancy detection", *Energy and Buildings 130* (2016) 787-793. doi: 10.1016/j.enbuild.2016.09.009

[S2] Theis Heidmann Pedersen, Michael Dahl Knudsen, Rasmus Elbæk Hedegaard and Steffen Petersen, "Handling Stochastic Occupancy in an Economic Model Predictive Control Framework for Heating System Operation in Dwellings", *CLIMA2016 – proceedings of the 12th REHVA World Congress:* vol. 10 (2016).

[S3] Rasmus Elbæk Hedegaard, Theis Heidmann Pedersen, Michael Dahl Knudsen and Steffen Petersen, "Identifying a Comfortable Excitation Signal for Generating Building Models for Model Predictive Control: A Simulation Study", *CLIMA2016 – proceedings of the 12th REHVA World Congress:* vol. 10 (2016).

[S4] Michael Dahl Knudsen, Rasmus Elbæk Hedegaard, Theis Heidmann Pedersen and Steffen Petersen, "Model Predictive Control of Space Heating and the Impact of Taxes on Demand Response: A Simulation Study", *CLIMA2016 – proceedings of the 12th REHVA World Congress:* vol. 10 (2016).

[S5] Michael Dahl Knudsen, Rasmus Elbæk Hedegaard, Theis Heidmann Pedersen and Steffen Petersen, "System identification of thermal building models for demand response – A practical approach", *Energy Procedia 122 – CISBAT 2017 International Conference* (2017) 937-942. doi: 10.1016/j.egypro.2017.07.426

[S6] Rasmus Elbæk Hedegaard, Theis Heidmann Pedersen, Michael Dahl Knudsen and Steffen Petersen, "Towards practical model predictive control of residential space heating: Eliminating the need for weather measurements" *Energy and buildings 170* (2018) 206-216. doi: 10.1016/j.enbuild.2018.04.014

Table of contents

Nomenclature

Abbreviations

CCP	Critical peak prices
DH	District heating
DMI	Danish Meteorological Institute
DMPC	Deterministic model predictive control
DR	Demand response
DSM	Demand-side management
EED	Energy efficiency directive
E-MPC	Economic model predictive control
EPBD	Energy performance of buildings directive
EU	European Union
ITH	Intraday trading horizon
KPI	Key performance indicator
MPC	Model predictive control
NRMSE	Normalized root mean square error
PB	Performance bound
PI	Proportional-Integral
PMV	Predicted mean vote
PPD	Predicted percentage dissatisfied
RBC	Rule-based control
RES	Renewable energy sources
RTP	Real-time prices
SB-MPC	Scenario based model predictive control
SSM	Supply-side management
TOU	Time-of-Use
TSO	Transmission system operator

Symbols

The following fonts are used to display mathematics: Scalar variables are italic, vectors are bold italic and matrices are bold Roman.

$\mathbf{A}$	State matrix	
$\mathbf{B}$	Input matrix	
$\mathbf{C}$	Output matrix	
c_p	Specific heat capacity	[J/(kg·K)]
$\boldsymbol{d}$	Disturbance vector	
$\mathbf{E}$	Disturbance matrix	
F	Total operational cost	[€]
$\boldsymbol{f}$	Cost signal vector	
J	Total objective value	
K	Number of disturbances scenarios	
KG	Kalman gain	
N	Prediction horizon	[h]
P	Period	
q	Flow rate	[m³/s]
t^{max}	Upper thermal comfort bound	[°C]
t^{min}	Lower thermal comfort bound	[°C]
t^{return}	Return temperature	[°C]
t^{supply}	Supply temperature	[°C]
$\boldsymbol{u}$	Input vector	[W]
$\boldsymbol{u}^{\mathrm{max}}$	Maximum heating power	[W]
V	Cost function	
$\boldsymbol{x}$	State vector	[°C]
$\boldsymbol{y}$	Output vector	[°C]
$\boldsymbol{y}^{meas}$	Measured output vector	[°C]
$\boldsymbol{y}^{set}$	Output setpoint vector	[°C]
$\varPhi$	Heating power	[W]
θ	Valve opening	
ρ	Density	[kg/m³]
τ	Time step	
$\Delta\boldsymbol{t}^{\mathrm{max}}$	Maximum rate of temperature change	[°C/h]
$\Delta\boldsymbol{t}^{\mathrm{min}}$	Minimum rate of temperature change	[°C/h]
$\Delta\varPhi^{\mathrm{charge}}$	Storage capacity	[kWh]
$\overline{\Delta\varPhi}$	Relative heating difference	
$\overline{\Delta\varPsi}$	Relative shift of heating consumption	
η^{shifting}	Storing efficiency	
τ^{charge}	Charge period	[h]
$\tau^{\mathrm{discharge}}$	Discharge period	[h]
ΔC	Thermal comfort violations	[°Ch]
ΔF	Operational cost savings	[€]
$\Delta\varPhi$	Absolute heating difference	[W]
$\Delta\varPsi$	Absolute shift of heating difference	[W]

1 Introduction

In the pursuit of minimizing the effects of global warming, the Danish government has stated an ambitious climate policy, partly driven by international obligations and partly by ambitious national targets, to aid the transition towards a sustainable low-emission society independent of fossil fuels by 2050. The Danish government has formulated several milestones to help achieve this target, e.g. that 30% and 50% of the energy consumed in Denmark should be covered by renewable energy sources (RES) by 2020 and 2030, respectively [1, 2]. Consequently, there has been a particular focus on increasing the share of wind power in Denmark to achieve these milestones, thus wind power production covered approx. 43% of the total national electricity consumption in 2017 [3]. However, this increasing penetration of intermittent RES such as wind power complicates the important task of maintaining an instantaneous balance between electricity supply and demand. Supply-side management (SSM) today almost exclusively ensures this balance, where a dedicated power plant or supply-side storage – often using fossil fuels – ramps up or down their electricity generation and consumption for the required durations and magnitudes. As the penetration of RES increases, the task of ensuring this balance in a cost-effective manner by SSM becomes similarly challenging, since the power output of RES is highly dependent on meteorological conditions. It would require that traditional supply-side flexibility sources, such as power plants, operate in ways that cause low efficiency and, consequently, high operational costs. Therefore, the recent focus has been on demand-side management (DSM) measures to assist in continually balancing supply and demand. DSM covers a wide range of services where consumers make permanent or temporary adjustments to their consumption in order to meet the needs of the system [4-7]. Traditionally, temporary DSM measures are generally considered in relation to power systems; however, district heating (DH) networks may equally benefit from temporary DSM measures, as DH networks, in the near future, will be strongly coupled with the power grid to further increase the integration of RES [8, 9].

The building sector has been identified as a major focus area regarding permanent DSM, i.e. increasing the energy efficiency of buildings, due to their long lifetime and significant energy consumption. Therefore, it has been mandatory since 2006 for countries in the European Union (EU) to follow a regulatory framework that is laid out in the *Energy Performance of Buildings Directive* (EPBD) [10] and E*nergy Efficiency Directive* (EED) [11]. Among other aspects, the directives state that each EU country must define minimum requirements for the energy performance of new buildings and building elements (in EPBD), and that EU countries must make a long-term retrofit strategy of the national building stock (in EED). A proposal for an amendment of the EPBD was presented in 2016 [12], in which the introduction of a *smartness indicator* that evaluates the building's technological readiness to efficiently interact with the grid was suggested:

> *"The smartness indicator shall cover flexibility features, enhanced functionalities and capabilities resulting from more interconnected and built-in intelligent devices being integrated into the conventional technical building systems. The features shall enhance the ability of occupants and the building itself to react to comfort or operational requirements, take part in demand response and contribute to the optimum, smooth and safe operation of the various energy systems and district infrastructures to which the building is connected."* [12]

The energy performance requirements for new buildings and the selection of retrofit measures are currently based on a cost-optimal balance between investment costs and energy savings. However, the introduction of a smartness indicator in EPBD might influence this balance; the challenge is now to identify the cost-optimal balance between investment costs, energy savings and the ability of buildings to provide balancing services to the energy systems through DSM measures.

1.2 Demand-side management

The term demand-side management (DSM) was first introduced in the early 1980s [4] and extensive reviews on the concept can be found in [13, 14]; thus, only a short overview of DSM is provided in the following to introduce the concept for the reader. DSM covers a wide span of categorized measures that are designed to influence consumers' electricity[1] use in various ways, as given in Fig. 1, which is a reproduction of the concept as defined in [14]. The overall aim of these measures is to change consumers' electric consumption pattern, i.e. the time pattern and magnitude, to attain a desired load shape, which depends on the characteristics and state of the energy system [5, 15]. In the power system, as the penetration of wind power increases, one objective is, for example, to shift the bulk of the energy consumption to periods of high production from wind turbines. Another objective could be to shift the energy consumption to periods of low CO_2 emissions stemming from production, which is not necessarily correlated with the wind power production [16]. In district heating networks, one objective is, for example, to minimize peak consumption to ensure a higher production efficiency and to increase network capacity.

Encouraging consumers to adjust their consumption in response to an external request is referred to as demand response (DR). There is no commonly agreed upon distinction between the immediately similar terms DSM and DR and they are often used interchangeably. In this thesis, the definition that DSM is a parent term that includes DR as a designation for ranges of measures (see Fig. 1) is adopted. In this definition, there is a clear distinction between *permanent demand response* and *temporary demand response* programs. Permanent DR consists of measures that aim at changing the consumption pattern on a long-term horizon, i.e. retrofitting with low-energy windows and extra insulation (*energy efficiency*), changing occupant behavior (*conservation*) or to convert the load to another type of energy (*load building*). Temporary DR aims at changing consumption on a shorter time horizon when temporary adjustments are sought by the supply side of the energy system. Temporary DR is divided into dispatchable and non-dispatchable programs. To some extent, the terminologies dispatchable and non-dispatchable DR overlap with other categorizations such as direct and indirect control or incentive- and price-based DR [17]. Dispatchable DR programs refer to resources where the consumer is obliged to allow transmission system operators (TSO) or other market entries direct control to modulate the demand to meet their objective, e.g. deliver up- and/or downwards adjustments with a short notification time (*reliability*) or participate on equal terms on various energy markets (*economy*). Non-dispatchable DR programs imply the use of economic incentives, for instance by broadcasting a time-varying cost signal to the consumers to achieve an expected response. The term cost signal does not necessarily refer to economic aspects, but could just as well be a signal that reflects the share of wind power in the energy system or a CO_2 intensity signal. The most common cost signal is time-of-use (*TOU*) tariffs, which have replaced fixed-price tariffs for small consumers in many countries [17]. TOU tariffs refer to static prices that are set in advance but vary over the day. Since TOU tariffs are static, they do not represent the current state of the energy systems, and are thus not suitable to address issues regarding intermittent imbalances. Therefore, TOU tariffs are typically used to shift energy consumption from fixed peak to off-peak periods. Critical peak prices (*CPP*) tariffs are superimposed on TOU tariffs at critical peak periods, for instance at times of extremely high wholesale prices, to better reflect the state of the energy system. Dynamic real-time prices (*RTP*) best reflect the current state of the energy system and represent the most suitable cost signal to handle imbalances. In most cases, day-ahead wholesale electricity prices are used as RTP tariffs; however, in some situations, intraday prices may be favorable (for a brief review on the power markets see e.g. [P3]).

---

[1] As previously mentioned, this early definition unnecessarily restricts DSM to power systems. However, other energy systems such as district heating networks could also benefit from DSM.
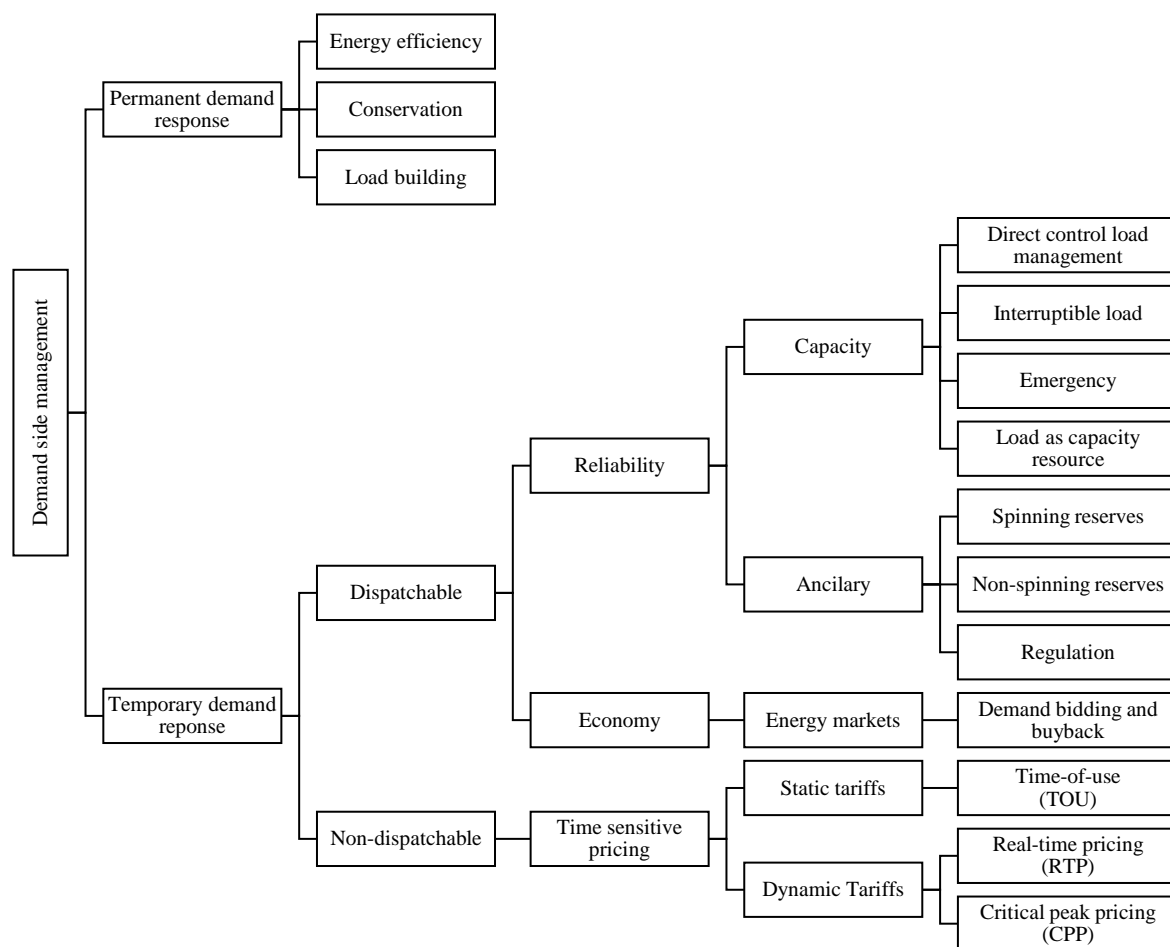
Fig. 1. Schematic overview of DSM measures. Reproduction from [14].

There is a great political awareness and focus on ensuring feasible permanent DR from buildings, for example, through legislations that require increasing energy efficiency, while temporary DR programs have primarily been offered to individual large-scale industrial and commercial consumers [18, 19]. However, residential consumers as a group represent a significant share of the total energy consumption. Private households accounted for approx. one-third of the total gross energy consumption in Denmark in 2016, of which space heating and heating of domestic hot water constituted approx. 83%, and the remaining 17% was used for electrical appliances and lighting [20]. Therefore, several recent studies have suggested that residential buildings also constitute a significant potential for temporary DR.

1.3 Residential energy flexibility

In the context of residential buildings, several studies have demonstrated the ability to perform temporary DR using, for example, wet appliances [21-24], electrical storage [25-27], active thermal storage (e.g. domestic hot water tanks) [28, 29] or passive thermal storage [30-36]. All resources entail pros and cons in terms of charging capacity, storing efficiency, discharging duration and investment costs. Because passive thermal storage is already available in the form of structural thermal mass, the investment cost of utilizing such storage is limited to an upgrade of the space heating control system. Therefore, this capacity has been demonstrated to be a cost-effective storage resource compared to other storage options to enable DR programs [37, 38]. Utilizing the structural thermal mass as heat storage inherently requires modulations of the indoor temperature to charge and discharge the storage. It is thus important to constrain the modulations to comply with thermal

comfort requirements. Consequently, the optimal use of the passive thermal storage for temporary DR requires reliable control strategies that explicitly ensure thermal comfort.

Research in the energy flexibility of residential buildings commonly concerns non-dispatchable DR programs as a result of the large number of participants. Furthermore, non-dispatchable DR programs allow individual consumers to decide when to participate in DR programs based on the broadcasted cost signal and to ensure that thermal comfort requirements are respected. One control approach is to establish simple control rules for the heating system based on the variations in the time-varying cost signal. Thus, the thermal storage is charged, i.e. the temperature is raised, or discharged, i.e. the temperature is decreased, if the cost is below a lower threshold or exceeds an upper threshold, respectively. Rule-based control (RBC) is generally used to characterize the flexibility potential of buildings [35, 39, 40]. However, Le Dréau and Heiselberg [30] applied such RBC and achieved operational cost savings by modulating the temperature setpoint depending on a lower or upper threshold on the day-ahead wholesale electricity prices. However, applying such RBC for flexibility purposes inherently suffers from two main limitations:

I. Determining adequate thresholds is difficult as the storage capacity and efficiency of the thermal mass depends on the boundary conditions (e.g. weather conditions and occupancy). Furthermore, the variations in the cost signal may vary between weeks, months or seasons.
II. Applying RBC do not guarantee optimal utilization of the thermal storage.

Therefore, the concept of model predictive control (MPC) has recently received significant research attention [41]. MPC is an optimization-based control scheme that relies on a simplified control-model of the building thermodynamics, predictions of boundary conditions and explicit constraints on inputs (i.e. space heating control inputs) and outputs (i.e. room air temperatures). The objective is to determine an optimal control strategy that minimizes a certain cost function, e.g. minimizing operational cost based on a time-varying cost signal. Several studies have investigated the potential of applying MPC schemes to enable DR [31-33]. Although several studies have suggested a significant theoretical potential of applying MPC to enable non-dispatchable DR [14, 32, 33], Killian and Kozek [42] identified the development of a reliable MPC scheme as a main barrier for large-scale applications in residential buildings.

1.4 Thesis objectives

The aim of this thesis is to contribute to the development of a reliable MPC scheme suitable for real application in residential buildings to enable non-dispatchable DR programs of space heating consumption in the heating-dominated climate of Denmark. The focus is on the application in existing residential buildings facing retrofits to improve their energy efficiency.

Previous studies [30, 39] have suggested that the ability to exploit the thermal mass as heat storage depends on the energy efficiency of the building envelope. The thesis work therefore includes investigations on existing and retrofitted buildings with varying thermal characteristics. The objective is to identify any trade-off between energy efficiency and the ability to participate in non-dispatchable DR programs. Furthermore, it is to identify potential benefits, both for private households and for the energy system, of residential buildings participating in DR programs, which should encourage investments in updated space heating control systems. However, it is outside the scope of this thesis to evaluate the cost-optimal balance of retrofit measures or investments in control systems update.

As mentioned, the thesis work focuses on applying MPC schemes to enable non-dispatchable DR programs in existing buildings facing retrofits. While the mathematical aspects of MPC (stability, optimization algorithms, etc.) are well described in literature [43-45], using MPC for real applications depends on multiple technical aspects that largely come from experience. Therefore, the thesis work addresses these practical challenges related to the real application of MPC schemes. The objective is to formulate a reliable yet simple MPC scheme to reduce the technical infrastructure and hardware requirements.

Moreover, studies have indicated that the type of heat emitter (floor heating system or baseboard heaters) affects the potential for utilizing the thermal mass as heat storage [30, 39]. However, only investigations featuring baseboard heaters, which represent the typical heat emitter in existing residential buildings in Denmark, were considered within the scope of the thesis work.

Another prerequisite is that the DR programs used throughout the thesis work are primarily orientated towards the state in the power system, as it is expected that the coupling degree between the power grid and DH network will increase in the future, principally through the deployment of central and local heat pumps. However, considerations on the efficiency factor in the conversion of electricity to thermal energy are considered to fall outside the scope of the thesis work.

1.5 Thesis outline

The main body of the thesis starts with a brief introduction of the general principle of non-dispatchable DR and DR assessment in section 2. It is not an attempt to provide a comprehensive and final take on these issues, but merely to reflect on the experience from the years of thesis work. A description of a generic MPC formulation is provided in section 3 to introduce the reader to the MPC concept used throughout the thesis work. As such, these two sections form an overview of the theoretical basis for the thesis work.

The following sections, 4, 5 and 6, report on the main outcome of the thesis work as extracts of the scientific papers [P1-P7], structured in three parts as depicted and explained in Fig. 2. Parts I and II cover simulation-based investigations on the DR potential and development of a reliable MPC scheme, respectively. Part III deals with proof-of-concept laboratory experiments of an implemented prototype of the MPC scheme developed in Part II, in an attempt to move towards a practical verification of the theoretical potentials identified in Part I.
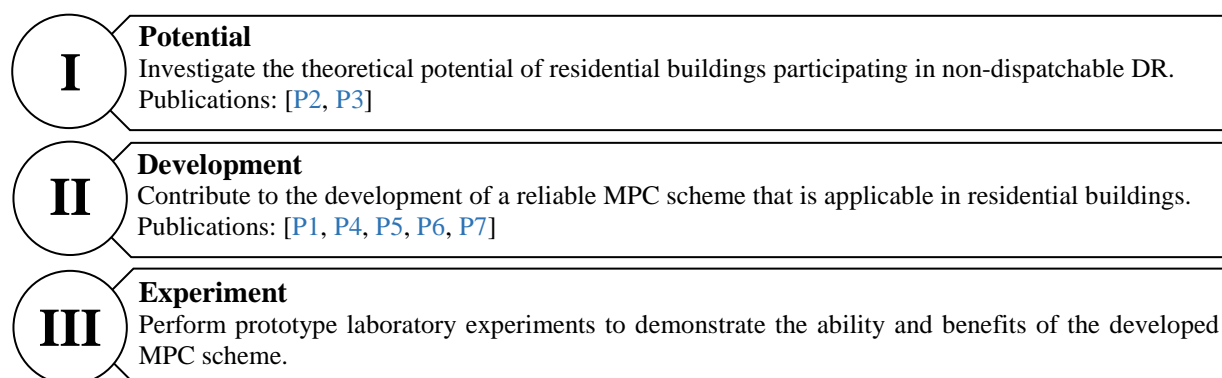
I **Potential**
Investigate the theoretical potential of residential buildings participating in non-dispatchable DR.
Publications: [P2, P3]

II **Development**
Contribute to the development of a reliable MPC scheme that is applicable in residential buildings.
Publications: [P1, P4, P5, P6, P7]

III **Experiment**
Perform prototype laboratory experiments to demonstrate the ability and benefits of the developed MPC scheme.

Fig. 2. The structure of the main body of the thesis work.

Finally, a main conclusion based on the thesis work together with perspectives and recommendations for future research efforts are provided in section 7.

2 Principle of non-dispatchable demand response

The basic principle of non-dispatchable DR is to determine a control strategy in response to a time-varying cost signal, with the objective of minimizing the total cost for a finite horizon. An illustration of a single DR event, which is defined as a temporary deviation from normal behavior, is given in Fig. 3. In this case, normal behavior corresponds to a reference constantly tracking the lower constraint bound $t^{\min}$, which represents the most energy-efficient control policy. The top figure shows the cost signal, which consists of a low price (f^{charge}) period followed by a high price ($f^{\mathrm{discharge}}$) period. The second figure depicts the resulting room air temperatures in response to the cost signal. While the reference controller discarded the variations in the cost signals, the DR controller used the thermal mass as heat storage[2] by raising the room air temperature during the low price period to charge the thermal mass and, in contrast, discharge during the high price period. The temperature modulations were restricted by the thermal comfort requirements defined by the lower and upper bounds $t^{\min}$ and $t^{\max}$, respectively. The bottom two figures show the heating power and the resulting heating difference during the charging τ^{charge} and discharging $\tau^{\mathrm{discharge}}$ periods. The DR controller increases the heating consumption in the charging period significantly, while reducing the heating consumption moderately but over a considerably longer discharge period.
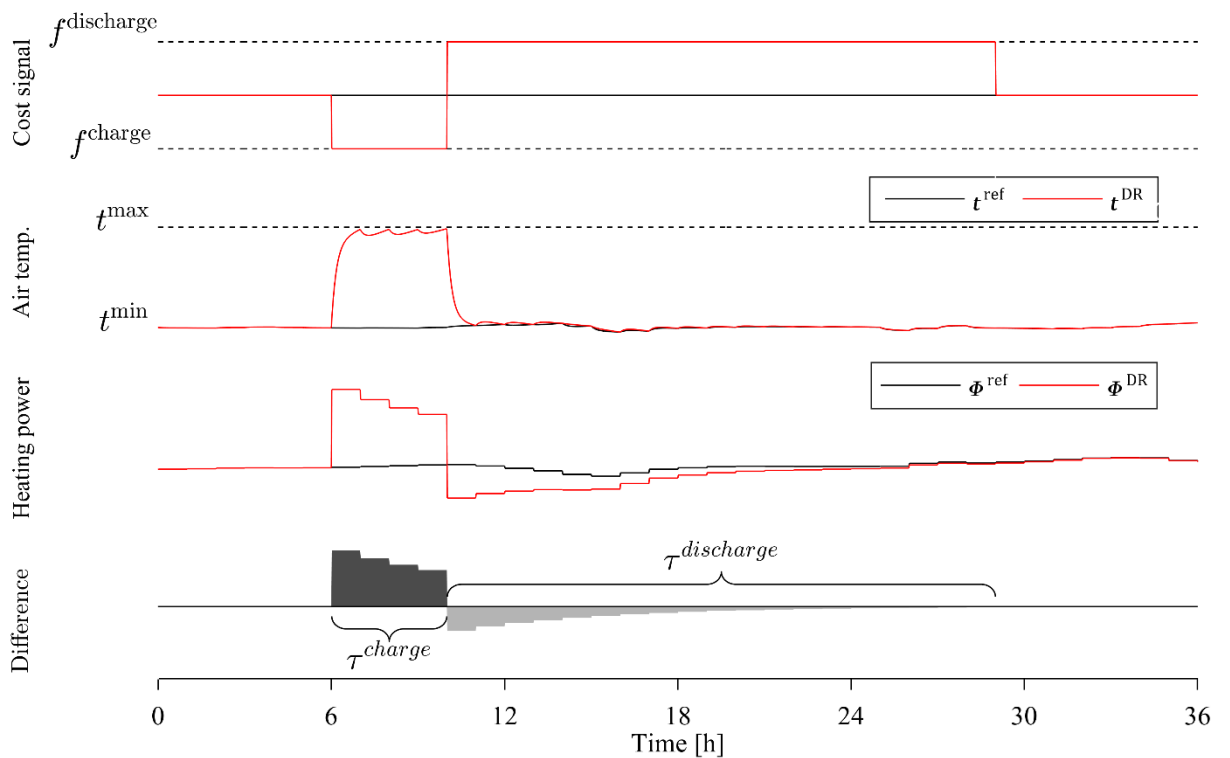

Fig. 3. Principle of non-dispatchable DR

---

[2] The same principle applies for active heat storages resources (e.g. domestic hot water tanks), considering different constraints.

Principle of non-dispatchable demand response

The total cost over the charging and discharging periods for the reference and DR controller denoted F^{ref} and F^{DR}, respectively, are specified in Eqs. (1) and (2).

$$F^{\text{ref}} = \int_0^{\tau^{\text{charge}}} \Phi^{\text{ref}}(\tau) \cdot f^{\text{charge}}(\tau) \, d\tau \; + \int_0^{\tau^{\text{discharge}}} \Phi^{\text{ref}}(\tau) \cdot f^{\text{discharge}}(\tau) \, d\tau \tag{1}$$

$$F^{\text{DR}} = \int_0^{\tau^{\text{charge}}} \Phi^{\text{DR}}(\tau) \cdot f^{\text{charge}}(\tau) \, d\tau \; + \int_0^{\tau^{\text{discharge}}} \Phi^{\text{DR}}(\tau) \cdot f^{\text{discharge}}(\tau) \, d\tau \tag{2}$$

As seen in Fig. 3 the prices f^{charge} and $f^{\text{discharge}}$ are assumed to be time-invariant, thus Eqs. (1) and (2) simplify to the discrete Eqs. (3) and (4), where the heating consumption is summarized for each time step and $\Delta\tau$ represents the duration between time steps.

$$F^{\text{ref}} = f^{\text{charge}} \cdot \sum_{\tau=1}^{\tau^{\text{charge}}} \Phi^{\text{ref}}[\tau] \cdot \Delta\tau \; + f^{\text{discharge}} \cdot \sum_{\tau=1}^{\tau^{\text{discharge}}} \Phi^{\text{ref}}[\tau] \cdot \Delta\tau \tag{3}$$

$$F^{\text{DR}} = f^{\text{charge}} \cdot \sum_{\tau=1}^{\tau^{\text{charge}}} \Phi^{\text{DR}}[\tau] \cdot \Delta\tau \; + f^{\text{discharge}} \cdot \sum_{\tau=1}^{\tau^{\text{discharge}}} \Phi^{\text{DR}}[\tau] \cdot \Delta\tau \tag{4}$$

As previously mentioned, the objective is to minimize the total cost function, i.e. fulfilling the condition that $F^{\text{DR}} < F^{\text{ref}}$, which equals the condition stated in Eq. (5).

$$F^{\text{DR}} - F^{\text{ref}} < 0 \tag{5}$$

Inserting Eqs. (3) and (4) into Eq. (5) yields the condition stated in Eq. (6). It is noted that the quantity $\Delta\Phi^{\text{charge}}$ corresponds to the storage capacity as defined by Reynders [39], which represents the amount of heat that can be stored in the thermal mass given the boundary conditions without violating thermal comfort.

$$f^{\text{charge}} \cdot \underbrace{\sum_{\tau=1}^{\tau^{\text{charge}}} \left(\Phi^{\text{DR}}[\tau] - \Phi^{\text{ref}}[\tau] \right) \cdot \Delta\tau}_{\Delta\Phi^{\text{charge}}} \; + f^{\text{discharge}} \cdot \underbrace{\sum_{\tau=1}^{\tau^{\text{discharge}}} \left(\Phi^{\text{DR}}[\tau] - \Phi^{\text{ref}}[\tau] \right) \cdot \Delta\tau}_{\Delta\Phi^{\text{discharge}}} < 0 \tag{6}$$

Eq. (6) simplifies to the conditional statement given in Eq. (7).

$$\frac{f^{\text{charge}}}{f^{\text{discharge}}} < \frac{-\Delta\Phi^{\text{discharge}}}{\Delta\Phi^{\text{charge}}} \tag{7}$$

The ratio between the discharged and charged heat on the right side of the inequality sign corresponds to the storing efficiency, defined by Le Dréau and Heiselberg [30], as stated in Eq. (8).

$$\eta^{\text{shifting}} = \frac{-\Delta\Phi^{\text{discharge}}}{\Delta\Phi^{\text{charge}}} \tag{8}$$

Inserting Eq. (8) into (7) gives the condition stated in Eq. (9) which describes the relationship between the thermal building characteristics, in the form of the shifting efficiency, and the variations in the cost signal. The condition demonstrates that a larger ratio between f^{charge} and $f^{\text{discharge}}$ entails a lower acceptable η^{shifting}.

$$\eta^{\text{shifting}} > \frac{f^{\text{charge}}}{f^{\text{discharge}}} \tag{9}$$

Inserting the definitions of $\Delta\Phi^{\text{charge}}$ and $\Delta\Phi^{\text{discharge}}$ from Eq. (6) into Eq. (8) gives the definition of the building-specific characteristic η^{shifting} as stated in Eq. (10) [30]. This definition highlights that η^{shifting} depends on both the magnitude of the difference of heating consumption and the durations τ^{charge} and $\tau^{\text{discharge}}$, which may both differ for each DR event.

$$\eta^{\text{shifting}} = \frac{-\sum_{\tau=1}^{\tau^{\text{discharge}}}\left(\Phi^{\text{DR}}[\tau] - \Phi^{\text{ref}}[\tau]\right) \cdot \Delta\tau}{\sum_{\tau=1}^{\tau^{\text{charge}}}\left(\Phi^{\text{DR}}[\tau] - \Phi^{\text{ref}}[\tau]\right) \cdot \Delta\tau} \tag{10}$$

Let us now consider two scenarios:

Scenario #1: $\eta^{\text{shifting}} = 1$ (a utopia scenario), i.e. it possible to discharge the entire amount of heat stored in the thermal mass as stated in Eq. (11). When inspecting Eq. (9), this scenario implies that even the smallest variations in the cost signal would be sufficient to enable non-dispatchable DR programs, given that $f^{\text{charge}} < f^{\text{discharge}}$.

$$\Delta\Phi^{\text{charge}} = -\Delta\Phi^{\text{discharge}} \tag{11}$$

Scenario #2: $\eta^{\text{shifting}} < 1$, i.e. a certain amount of the charged heat is lost to the ambient surroundings, thus it is not possible to discharge the entire amount of stored heat, as specified in Eq. (12).

$$\Delta\Phi^{\text{charge}} = -\Delta\Phi^{\text{discharge}} + \Phi^{\text{loss}} \tag{12}$$

Inserting Eq. (12) into Eq. (8) gives the definition of η^{shifting} as specified in Eq. (13).

$$\eta^{\text{shifting}} = \frac{\Delta\Phi^{\text{charge}} - \Phi^{\text{loss}}}{\Delta\Phi^{\text{charge}}} \tag{13}$$

Eq. (13) simplifies to Eq. (14) which states that η^{shifting} depends on the ratio between the magnitude of lost and stored heat, which are often conflicting. For instance, a building with an energy-efficient building envelope and corresponding low heat loss coefficient would have a low storage capacity $\Delta\Phi^{\text{charge}}$ because of the generally limited space heating demand. On the contrary, a building with a higher heat loss would have a greater general space heating demand and, accordingly, a higher storage capacity.

$$\eta^{\text{shifting}} = 1 - \frac{\Phi^{\text{loss}}}{\Delta\Phi^{\text{charge}}} \tag{14}$$

The simplistic principle of non-dispatchable DR presented in Eqs. (1) to (14) describes the necessary conditions to be fulfilled. However, for real applications this is not a trivial process for several reasons:

I.   The cost signal is assumed to consist of time-invariant prices during the entire charging and discharging periods; however, this is not the case when considering dynamic RTP tariffs such as day-ahead whole electricity prices.
II. The characteristic parameter η^{shifting} is not static, but depends on the boundary conditions.
III. The relationship between the heat loss and storage capacity as specified in Eq. (14) addresses the tradeoff between energy efficiency and the ability to exploit the thermal mass as heat storage. However, this relationship strongly depends on the time-varying boundary conditions.

To reliably handle the abovementioned non-trivial challenges and to investigate the building during a longer period under time-varying boundary conditions, a dynamic assessment of demand response is required.

2.1 Demand response assessment

Evaluating the benefits of participating in DR programs is a subject of considerable research concern, and also of great relevance regarding the introduction of a smartness indicator in EPBD [12]. Currently, significant work on this topic is taking place in the research framework of IEA EBC Annex 67 on *Energy flexible buildings* [46], with the aim of developing a common flexibility classification method. Clauß et al. [40] conducted a comprehensive review on multiple key performance indicators (KPIs) used to evaluate energy flexibility and DR, and found that the choice of KPIs strongly depends on whether the aim is to classify the energy flexibility of a building or to develop control strategies to enable DR. Another key issue is to define the reference control, i.e. normal behavior. In Denmark, one of the most common control schemes for space heating operation is conventional proportional-integral (PI) control. In the thesis work the reference control was, therefore, chosen as a PI controller constantly tracking the lower comfort bound, which constitutes the most energy-efficient control policy.

The KPIs considered in this work differ between the investigations as a result of the different focuses. However, some of the most commonly used KPIs were absolute $\Delta\Phi$ and relative $\overline{\Delta\Phi}$ space heating difference for each time step τ during the evaluation period P as specified in Eqs. (15) and (16). Furthermore, the KPIs operational cost savings ΔF and thermal comfort violations ΔC, denoting the number of degree hours [°Ch] violating $t^{\min}$ and $t^{\max}$, were taken into account as defined in Eqs. (17) and (18), respectively, where $\Delta\tau$ represents the duration between time steps.

$$\Delta\Phi[\tau] = \Phi^{\mathrm{DR}}[\tau] - \Phi^{\mathrm{ref}}[\tau] \qquad \forall \tau = 1, \dots, P \tag{15}$$

$$\overline{\Delta\Phi}[\tau] = \frac{\Phi^{\mathrm{DR}}[\tau] - \Phi^{\mathrm{ref}}[\tau]}{\Phi^{\mathrm{ref}}[\tau]} \qquad \forall \tau = 1, \dots, P \tag{16}$$

$$\Delta F \quad = \sum_{\tau=1}^{P} f[\tau] \cdot \Delta\Phi[\tau] \tag{17}$$

$$\Delta C \quad = \sum_{\tau=1}^{P} \left[\max\left(t^{\min} - t[\tau], 0\right) + \max(t[\tau] - t^{\max}, 0) \right] \cdot \Delta\tau \tag{18}$$

3   Model predictive control

MPC is an optimization-based control scheme that minimizes a cost function for a finite prediction horizon N to determine an optimal sequence of controllable decision variables $\boldsymbol{u}$ [41, 43, 47-49]. The first input of the control sequence is implemented in the plant, and the optimization problem is solved again at the next discrete time step with a prediction horizon shifted one step ahead in time. This receding horizon approach introduces feedback, since the optimal control strategy is a function of the current state. A generic formulation of a MPC scheme is given in Eqs. (19a-f):

$$
\underset{\boldsymbol{u}_0,\dots,\boldsymbol{u}_{N-1}}{\text{minimize}} \quad J \quad = \sum_{\tau=0}^{N-1} \mathrm{V}_\tau(\boldsymbol{y}_\tau, \boldsymbol{u}_\tau) \qquad\qquad \textit{cost function} \qquad\qquad (19a)
$$

subject to

$$
\begin{aligned}
\boldsymbol{x}_{\tau+1} &= \mathrm{g}_\tau(\boldsymbol{x}_\tau, \boldsymbol{u}_\tau, \boldsymbol{d}_\tau) & \textit{dynamics} && (19b)\\
\boldsymbol{y}_\tau &= \mathrm{h}(\boldsymbol{x}_\tau) & \textit{outputs} && (19c)\\
\boldsymbol{x}_0 &= \boldsymbol{x} & \textit{current states} && (19d)\\
\boldsymbol{u}_\tau &\in \mathcal{U}_\tau & \textit{decision variable constraints} && (19e)\\
\boldsymbol{y}_\tau &\in \mathcal{Y}_\tau & \textit{output constraints} && (19f)
\end{aligned}
$$

where J is the total objective value and V_τ denotes the cost function at time step $\tau \in \mathbb{N}$, which is a function of the outputs $\boldsymbol{y}_\tau \in \mathbb{R}^{n_y}$ and decision variables $\boldsymbol{u}_\tau \in \mathbb{R}^{n_u}$. The function g_τ represents the time-dependent control-model that describes the plant dynamics as a function of the states $\boldsymbol{x}_\tau \in \mathbb{R}^{n_x}$, $\boldsymbol{u}_\tau$ and uncontrollable disturbances $\boldsymbol{d}_\tau \in \mathbb{R}^{n_d}$. The function h maps $\boldsymbol{x}_\tau$ to $\boldsymbol{y}_\tau$. Measurements of the current states $\boldsymbol{x}$ are used as initial states $\boldsymbol{x}_0$. Furthermore, the decision variables and outputs are restricted by the constraint sets $\mathcal{U}_\tau$ and $\mathcal{Y}_\tau$, respectively. The length of the finite prediction horizon N depends on the cost function and process dynamics; however, multiple studies have suggested the use of a sufficiently long N to ensure stability of MPC in practice [50, 51].

The generic MPC formulation is applicable for control of a wide range of processes. However, in the remainder of this thesis work the following definitions are introduced: The controllable decision variables $\boldsymbol{u}_\tau$ are space heating control inputs and the constraint set $\mathcal{U}_\tau$ is given by the physical limitations of the heating system. The output variables $\boldsymbol{y}_\tau$ are the indoor air temperatures, which are constrained by thermal comfort requirements $\mathcal{Y}_\tau$. The functions V_τ, g_τ and h are elaborated in sections 3.1 and 3.2, and the constraint sets are elaborated in section 3.3.

3.1 Cost function

The cost function describes the desired objective and can be tailored to various performance targets, e.g. maximizing thermal comfort, minimizing energy consumption or minimizing operational cost. Preferably, convex cost functions are formulated, e.g. linear and quadratic functions, since they can be solved very efficiently and reliably [45].

Several approaches exist to maximize thermal comfort. Morales-Valdés et al. [52] suggested a nonlinear cost function expressing Fanger's predicted mean vote (PMV) index or predicted percentage dissatisfied (PPD) index [53]. However, there are, in general, no effective methods for solving a nonlinear optimization problem [45]. Therefore, Cigler et al. [54] proposed a convex approximation of the PMV index. Nonetheless, the PMV index relies on comprehensive measurements of air speed, relative humidity and the mean radiant temperature together with assumptions on clothing level and metabolic rate.

Instead, traditional reference tracking control of a preferred setpoint temperature $\boldsymbol{y}_\tau^{set}$ is a favored approach to ensure thermal comfort. The objective is to minimize the square of setpoint deviations, thus penalizing larger deviations the most, as specified in the quadratic cost function in Eq. (20), where $\mathbf{I} \in \mathbb{R}^{n_y \times n_y}$ is an identity matrix.

$$V_\tau(\boldsymbol{y}_\tau, \boldsymbol{u}_\tau) = (\boldsymbol{y}_\tau^{set} - \boldsymbol{y}_\tau)^T \cdot \mathbf{I} \cdot (\boldsymbol{y}_\tau^{set} - \boldsymbol{y}_\tau) \tag{20}$$

To minimize the sum of a quantity, e.g. energy consumption or operational cost, linear cost functions are more suitable, as given in Eq. (21) with cost signal $\boldsymbol{f} \in \mathbb{R}^{n_u}$. When $\boldsymbol{f}$ is constant, the sole objective is to minimize $\boldsymbol{u}_\tau$, i.e. the total energy use. On the contrary, using RTP tariffs as a time-varying $\boldsymbol{f}$ serves as weights of $\boldsymbol{u}_\tau$ between time steps and the objective is consequently to minimize the total operational cost – often denoted economic MPC (E-MPC).

$$V_\tau(\boldsymbol{y}_\tau, \boldsymbol{u}_\tau) = \boldsymbol{f}_\tau^T \cdot \boldsymbol{u}_\tau \tag{21}$$

Exploiting the thermal mass as heat storage inherently relies on modulations of the air temperature, suggesting that the cost functions in Eqs. (20) and (21) are conflicting, i.e. there is generally no unique solution that optimizes both simultaneously. Therefore, a useful definition is that of non-dominated Pareto optimal solutions that are equally acceptable from a mathematical point of view and, consequently, form a Pareto front [55, 56]. The simplest method to obtain a Pareto optimal solution is the weighted sum approach, i.e. a convex combination of the two cost functions as given in Eq. (22) [57].

$$V_\tau(\boldsymbol{y}_\tau, \boldsymbol{u}_\tau) = \lambda \cdot (\boldsymbol{y}_\tau^{set} - \boldsymbol{y}_\tau)^T \cdot \mathbf{Q} \cdot (\boldsymbol{y}_\tau^{set} - \boldsymbol{y}_\tau) + (1 - \lambda) \cdot \boldsymbol{f}_\tau^T \cdot \boldsymbol{u}_\tau, \qquad \lambda \in [0,1] \tag{22}$$

The performance of the weighted sum approach significantly depends on the choice of λ, which can be difficult to choose since thermal comfort has no direct economic translation in residential buildings[3]. Thus, in the majority of the thesis work $\lambda = 0$ was chosen; however, this choice was investigated in detail in paper [P5].

3.2 Control model

An indispensable component of MPC schemes is the control-model, given by the function g_τ, which describes the dynamics of the system to be controlled. The aim of g_τ is to sufficiently represent the dynamics in a form readily applicable for control and optimization. In general, three modeling approaches exist to derive such simplified reduced-order (resistance-capacitance) models, depending on the balance between use of measurement data and prior physical knowledge:

I.   Data-driven *black-box models* where methods from the field of system identification and measured data are used to identify the inputs-outputs relation.
II. First principle *white-box models* where (simplified) fundamental heat-balance equations, detailed building information and detailed material properties are used to form the model.
III. *Grey-box models* start from a physics-based model structure but rely on measured data to estimate physically interpretable parameters using system identification techniques.

The choice of modeling approach for MPC depends on multiple factors, which fall outside the scope of this thesis, but the reader is referred to, for example, [58-62]. In this thesis work, a grey-box modeling approach was chosen since such models are expected to be more robust towards changes in operating conditions. Furthermore, two central model characteristics regarding the control-model g_τ were assumed. Firstly, the model was assumed to be time-invariant, i.e. model parameters were static. Secondly, in relation to the previously mentioned desire for convex optimization problems, the control-model was assumed to be linear, thus approximating any nonlinear building phenomena.

---

[3] In industrial and office buildings, the objective of productivity could be used as economic translation.

The resulting state space formulation of g to describe the thermodynamics in buildings is given in Eq. (23) with state matrix $\mathbf{A} \in \mathbb{R}^{n_x \times n_x}$, input matrix $\mathbf{B} \in \mathbb{R}^{n_x \times n_u}$ and disturbance matrix $\mathbf{E} \in \mathbb{R}^{n_x \times n_d}$. The control-model was estimated in continuous time and then discretized using the zero-order hold method.

$$x_{\tau+1} = \mathbf{A} \cdot x_\tau + \mathbf{B} \cdot u_\tau + \mathbf{E} \cdot d_\tau \tag{23}$$

The function h maps x_τ to y_τ as given in Eq. (24) with output matrix $\mathbf{C} \in \mathbb{R}^{n_y \times n_x}$.

$$y_\tau = \mathbf{C} \cdot x_\tau \tag{24}$$

Current measurements of the room air temperatures y_τ^{meas} at each time step τ, were used to correct the states predicted at previous time step $x_{\tau|\tau-1}$ using a Kalman filter to update the observed and unobserved states according to Eq. (25), where KG is the Kalman gain [63].

$$x_{\tau|\tau} = x_{\tau|\tau-1} + KG \cdot \left(y_\tau^{\text{meas}} - \mathbf{C} \cdot x_{\tau|\tau-1}\right) \tag{25}$$

3.3 Constraints

The space heating control inputs u_τ were restricted by the physical limitations of the heating system as specified in Eq. (26). Since only heating was considered, the minimum power was 0 and u^{max} specifies the maximum power.

$$0 \le u_\tau \le u^{\text{max}} \tag{26}$$

The indoor air temperatures y_τ were restricted according to Eq. (27), by the time-invariant lower and upper comfort bounds t^{min} and t^{max}, respectively. Since the potential for exploiting the structural thermal storage is a function of the allowable temperature modulations, the values of t^{min} and t^{max} vary between studies. In general, the size of the comfort band can be perceived as a measure of the willingness to provide DR.

$$t^{\text{min}} \le y_\tau \le t^{\text{max}} \tag{27}$$

Another important restriction with respect to temperature modulations is the rate of change as specified in Eq. (28), restricting the minimum and maximum rate of change Δt^{min} and Δt^{max}, respectively. As suggested by ASHRAE [64], the values of Δt^{min} and Δt^{max} depend on the duration between times steps given by $\Delta \tau$.

$$\Delta t^{\text{min}} \le \frac{y_\tau - y_{\tau-1}}{\Delta \tau} \le \Delta t^{\text{max}} \tag{28}$$

The control input constraints given by Eq. (26) were implemented as hard constraints. However, to ensure the feasibility of the MPC scheme, the output constraints given by Eqs. (27) and (28) were softened by introducing non-negative slack variables, thus transforming the inequality constraints to equality constraints [45, 47]. Moreover, the introduction of slack variables allowed for different penalty weights of violating t^{min}, t^{max}, Δt^{min} and Δt^{max}, respectively.

4   Part I - Potential

The objective of Part I was to examine the ability and theoretical benefits of residential buildings participating in non-dispatchable DR programs, using an E-MPC scheme with the objective of minimizing operational costs. Parts I and II relied on simulation-based case studies, which, compared to laboratory or field experiments, are better suited for developing and evaluating an immature technology, as they allow for rapid and repetitive performance assessments under similar controllable boundary conditions. Historical data of power production, trading activities, and prices from the day-ahead and intraday wholesale power markets were acquired for bidding area DK1 through the Danish TSO, Energinet.dk and power market Nord Pool. The simulations were performed for ten apartments that constitute the third floor of an existing multi-story apartment building and eight retrofit scenarios thereof, see Table 1.

Table 1. Case buildings notation and total reference space heating consumption during the 4-month simulation period. See paper [P2] for detailed explanation of the retrofit scenarios.

Case building		Reference space heating consumption
Existing building	(R0)	59.9 kWh/m^2
Retrofit scenario 1	(R1)	28.1 kWh/m^2
Retrofit scenario 2	(R2)	25.0 kWh/m^2
Retrofit scenario 3	(R3)	27.3 kWh/m^2
Retrofit scenario 4	(R4)	24.0 kWh/m^2
Retrofit scenario 5	(R5)	23.0 kWh/m^2
Retrofit scenario 6	(R6)	19.8 kWh/m^2
Retrofit scenario 7	(R7)	22.0 kWh/m^2
Retrofit scenario 8	(R8)	18.6 kWh/m^2

The focus of the work reported in paper [P2] was to evaluate the benefits of residential buildings participating in non-dispatchable DR programs, both in terms of the benefits for the private householders and for the energy system. For this purpose, a cost signal consisting of time-varying weights of historical day-ahead market prices, grid load, CO_2 intensity and wind power production was generated, as proposed in [S4]. Using this cost signal in the associated E-MPC scheme led to operational cost savings for the end-user of up to 6% while simultaneously reducing CO_2 emissions related to the energy production by up to 3%.

Furthermore, the ability to simultaneously shift heating consumption from peak load periods was evaluated. Therefore, each hour of the simulation period P was categorized based on historical grid load data as either a low (below the first quantile), high (between the first and third quantile) or peak (above the third quantile) load period, i.e. $s[\tau] = 1$, $s[\tau] = 2$ or $s[\tau] = 3$, respectively. The absolute and relative shift of space heating consumption was determined according to Eqs. (29) and (30), where $\Delta\Phi$ is defined by Eq. (15).

$$\Delta\Psi[j] = \sum_{\tau=1}^{P} \Delta\Phi[\tau] \cdot \pi[\tau] \qquad \forall j = 1, 2, 3 \qquad (29)$$

$$\overline{\Delta\Psi}[j] = \frac{\Delta\Psi[j]}{\sum_{\tau=1}^{P} \Phi^{\mathrm{ref}}[\tau] \cdot \pi[\tau]} \qquad \forall j = 1, 2, 3 \qquad (30)$$

$$\text{where } \pi[\tau] = \begin{cases} 1 & s[\tau] = j \\ 0 & \text{otherwise} \end{cases}$$

The achieved results are depicted in Fig. 4. Compared to the reference controller, applying the E-MPC scheme in case buildings R1 to R8 consistently reduced space heating consumption in peak and high load periods with around 2.2 kWh/m² and 1.2 kWh/m², respectively, while consumption in low load periods increased by approx. 4.5 kWh/m². In fact, $\Delta\Psi$ was consistent even though the storage capacity $\Delta\Phi^{charge}$ decreased with the extent of retrofit measures [39]. The reason for this consistency is, as stated in Eq. (14), that the efficiency $\eta^{shifting}$ depends on the time-varying ratio between $\Delta\Phi^{charge}$ and Φ^{loss}. Therefore, despite of a lower $\Delta\Phi^{charge}$ the applied retrofit measures led to an increased $\eta^{shifting}$, which allowed for a lower ratio between low and high prices as given by the conditional statement in Eq. (9). Inspecting the simulation results in detail showed precisely that an increased energy efficiency, as a consequence of the retrofit measures, resulted in a higher number of DR events. Because of the generally lower reference consumption in each retrofit scenario, $\overline{\Delta\Psi}$ increased with the extent of retrofit measures, thus confirming the increasing $\eta^{shifting}$.
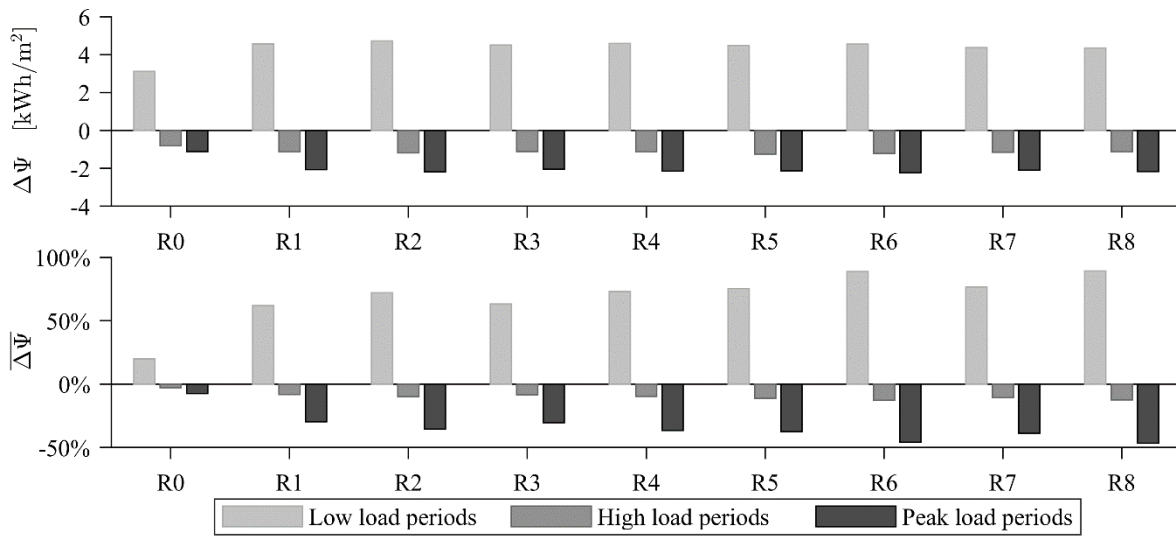

Fig. 4. Absolute and relative shift of space heating consumption [P2].

The same tendencies was observed in paper [P7] where day-ahead market prices were used together with an E-MPC scheme to minimize operational costs. One-week simulation results are depicted in Fig. 5. The same number of DR events was observed in case buildings R0 and R8 during the week, indicating that the variations in the cost signal were sufficient to enable DR events in both case buildings. The week was divided into six DR events, each consisting of a charging τ^{charge} and discharging $\tau^{discharge}$ period. In contrast to previous studies on this subject [30, 39], the duration of τ^{charge} and $\tau^{discharge}$ for each event was optimized by the E-MPC scheme. Fig. 5 shows that R0 allowed for the highest magnitude of consumption shift due to the generally higher reference consumption, while R8 allowed for shifts over longer periods. Further inspection of the simulation results indicated that R8 allowed for complete space heating shut-off for extended periods, while R0 was incapable of maintaining thermal comfort without space heating consumption.
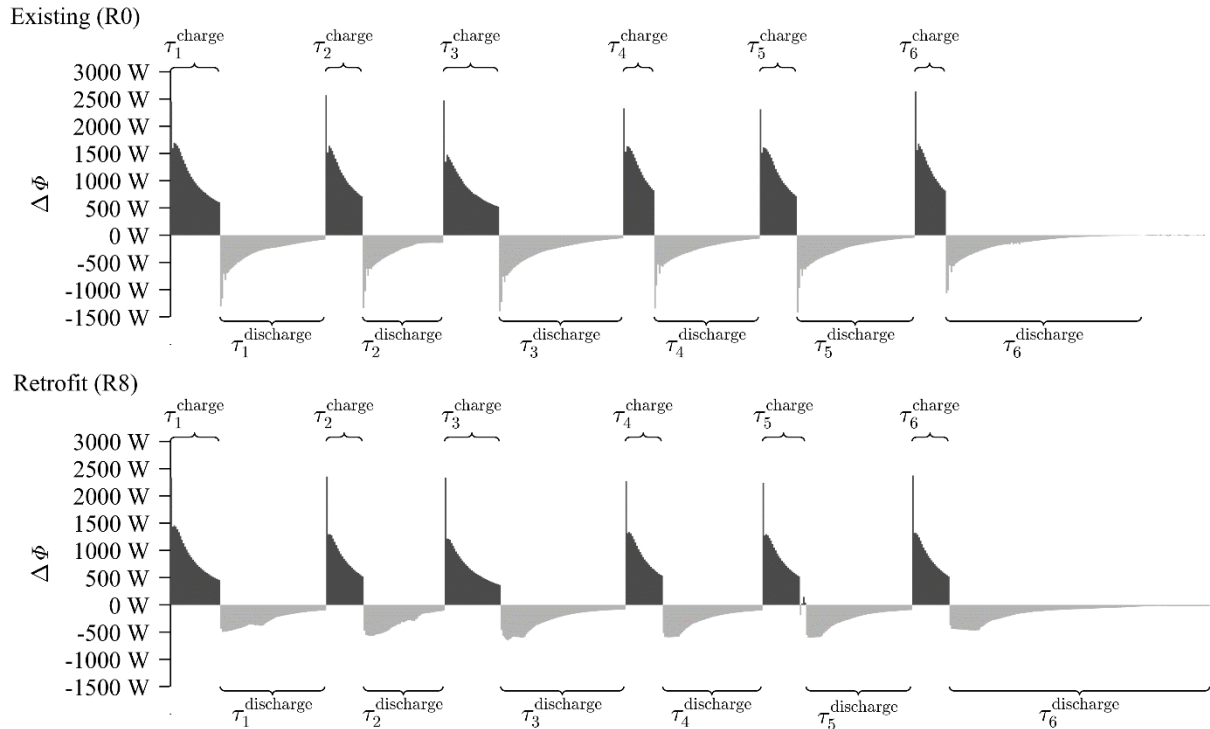
Fig. 5. Absolute shifting potential for the existing and retrofitted building [P7].

Table 2 lists the storage capacity $\Delta\Phi^{charge}$, discharging capacity $\Delta\Phi^{discharge}$ and the resulting efficiency $\eta^{shifting}$ for each DR event. As expected, $\Delta\Phi^{charge}$ was highest for the existing building, while $\eta^{shifting}$ was highest for the retrofitted building. In fact, the efficiency of DR event 6 was even above 100%, since heat stored at previous DR events was not yet fully discharged coming into this DR event.

Table 2. Summarized heating differences and storing efficiency of each event [P7].

Case building		$\Delta\Phi^{charge}$	$\Delta\Phi^{discharge}$	$\eta^{shifting}$
Existing (R0)	Event 1	108.1 Wh/m^2	-65.4 Wh/m^2	60.6%
	Event 2	86.8 Wh/m^2	-52.9 Wh/m^2	61.0%
	Event 3	102.8 Wh/m^2	-74.3 Wh/m^2	72.4%
	Event 4	79.7 Wh/m^2	-57.6 Wh/m^2	72.3%
	Event 5	88.5 Wh/m^2	-62.5 Wh/m^2	70.6%
	Event 6	79.4 Wh/m^2	-60.0 Wh/m^2	75.5%
Retrofit (R8)	Event 1	89.0 Wh/m^2	-57.9 Wh/m^2	65.1%
	Event 2	68.5 Wh/m^2	-53.3 Wh/m^2	77.9%
	Event 3	81.4 Wh/m^2	-69.3 Wh/m^2	85.1%
	Event 4	70.1 Wh/m^2	-56.6 Wh/m^2	80.7%
	Event 5	71.7 Wh/m^2	-57.7 Wh/m^2	80.5%
	Event 6	69.3 Wh/m^2	-70.4 Wh/m^2	101.5%

While papers [P2] and [P7] aimed at non-dispatchable DR programs based on RTP tariffs with horizons upwards of days to store heat in the thermal mass, little is known about the ability and benefits of residential buildings participating in DR programs on a shorter time-scale. Therefore, the work reported in paper [P3] investigated whether residential buildings may benefit from day-ahead and intraday market prices in parallel. To accommodate this, a hieratical control structure was adopted. First, an E-MPC scheme considering day-ahead market (spot) prices over a 3-day prediction horizon was solved. Subsequently, an E-MPC scheme considering available offers on the intraday

market within a shorter intraday trading horizon (ITH) was solved, treating the consumption procured on the day-ahead market as a trade commodity.

The simulation results, depicted in Fig. 6, showed that engaging in intraday trading increased the operational cost savings from 3%, 8% and 13%, to 6%, 13% and 19% in R0, R1 and R8 case buildings, respectively. Fig. 6 also indicates that the majority of economic benefits from intraday trading can be achieved considering a one-hour ITH, due to a strong correlation between intraday and day-ahead market prices. Furthermore, the simulation results showed that the traded volume on the intraday market of R0 was 12.7 kWh/m^2 corresponding to approx. 21% of the reference heating consumption, while R1 and R8 traded 12.1 kWh/m^2 (43%) and 9.6 kWh/m^2 (52%), respectively. The achieved results therefore suggest that a wide range of buildings would benefit from participating in DR programs considering both day-ahead and intraday market trading.
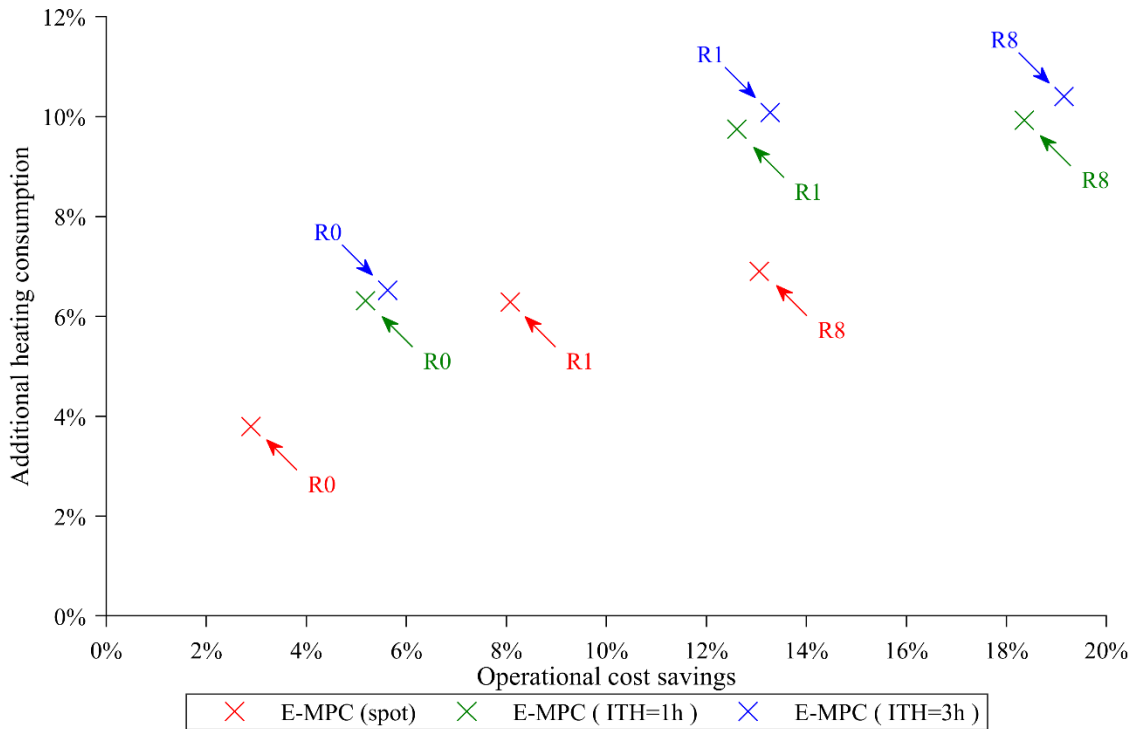
Fig. 6. Operational cost savings and additional heating consumption summarized for all apartments [P3].

5 Part II - Development

The results obtained in Part I indicated that significant benefits can be achieved by residential buildings participating in non-dispatchable DR programs using E-MPC to exploit the thermal mass as heat storage. However, the applied E-MPC scheme in Part I suffers from a range of practical challenges and therefore requires further development before implementation in real residential buildings. The objective of Part II was therefore to develop solutions to address some of these practical challenges. Since Part I suggested that the ability to participate in non-dispatchable DR depended on the thermal characteristics of the building, the case buildings listed in Table 1 also formed the basis for the investigations in Part II.

5.1 Centralized or decentralized control scheme

When designing control schemes for multi-zone buildings, centralized and decentralized control approaches exist, where heat transfer between adjacent zones is accounted for or neglected, respectively [65, 66]. Decentralized control schemes will, in theory, return a sub-optimal solution compared to centralized control schemes. However, decentralized control schemes may constitute a more practical approach for real application, since they do not require mapping of zone-adjacency or exchange information between controlled-zones during operation. Furthermore, decentralized control schemes are preferable in multi-apartment residential buildings because they allow individual apartment owners to specify control objectives and to decide when to engage in DR programs. The work reported in paper [P4] therefore investigated the performance of centralized and decentralized MPC as a function of the coupling degree between apartments, i.e. before and after (indicated by superscript $^+$) adding 100 mm of insulation to the partition walls.

The simulation results for each of the three control schemes (reference, centralized E-MPC and decentralized E-MPC) are listed in Table 3. The total operational cost, operational cost savings ΔF (according to Eq. (17)) and relative cost savings are summarized for all ten apartments, while thermal comfort violations ΔC (according to Eq. (18)) are given as the mean across the ten apartments. Furthermore, the standard deviations are specified in the parentheses. Overall, the centralized and decentralized E-MPC schemes achieved similar operational cost savings; however, the standard deviations across the apartments indicate that applying decentralized E-MPC without insulated partition walls led to unevenly distributed cost savings across the apartments. This effect was significantly reduced in the case buildings R0$^+$ and R8$^+$ with insulated partition walls. Furthermore, decentralized E-MPC even out-performed centralized E-MPC in terms of maintaining thermal comfort in R0$^+$ and R8$^+$.

Table 3. Simulations results for all ten apartments [P4].

Case building		Total cost	Cost savings	Relative cost saving	Mean comfort violations
Existing (R0)	reference	€1040			89.7 (4.3) °Ch
	centralized	€1010	€30 (0.66)	2.9%	18.1 (9.8) °Ch
	decentralized	€1011	€29 (1.37)	2.8%	22.7 (9.4) °Ch
Existing$^+$ (R0$^+$)	reference	€1001			84.4 (2.9) °Ch
	centralized	€977	€24 (0.42)	2.4%	15.9 (2.6) °Ch
	decentralized	€979	€22 (0.50)	2.2%	11.2 (1.5) °Ch
Retrofit (R8)	reference	€327			43.9 (3.0) °Ch
	centralized	€293	€34 (0.86)	10.4%	9.3 (8.7) °Ch
	decentralized	€293	€34 (1.59)	10.4%	18.0 (8.7) °Ch
Retrofit$^+$ (R8$^+$)	reference	€323			38.5 (1.7) °Ch
	centralized	€287	€36 (0.55)	11.1%	7.5 (3.0) °Ch
	decentralized	€287	€36 (0.63)	11.1%	6.9 (2.2) °Ch

5.2 Stochastic disturbances

The DR potentials suggested in Part I constitute a causal upper theoretical performance bound (PB) which, in practice, is unachievable, since the E-MPC scheme is affected by various structural uncertainties (i.e. building/control-model mismatch) and uncertain disturbance predictions (i.e. weather forecast and stochastic occupancy). Recent research has therefore focused on scenario-based MPC (SB-MPC) schemes [67], which take the stochastic properties of the uncertainties into consideration. Furthermore, SB-MPC enables probabilistic output constraints (so-called chance constraints), thus allowing the constraints to be violated with a small probability [68, 69].

A key issue in applying SB-MPC is to obtain reliable detections and predictions of disturbance scenarios. The SB-MPC proposed in paper [P6] relied on on-site weather measurements and weather forecast ensembles provided by Danish Meteorological Institute (DMI). However, detecting the current occupancy and generating reliable predictions of occupancy are difficult because of the stochastic nature of humans. The aim of paper [P1] was therefore to propose a novel non-intrusive method to detect occupancy by applying a set of rules on the trajectory of indoor climate related sensor data. The detection method obtained maximum accuracies of 78% and 98% in a dorm apartment and a single-person office, respectively. The achieved results during a 6-day period in the single office are depicted in Fig. 7.
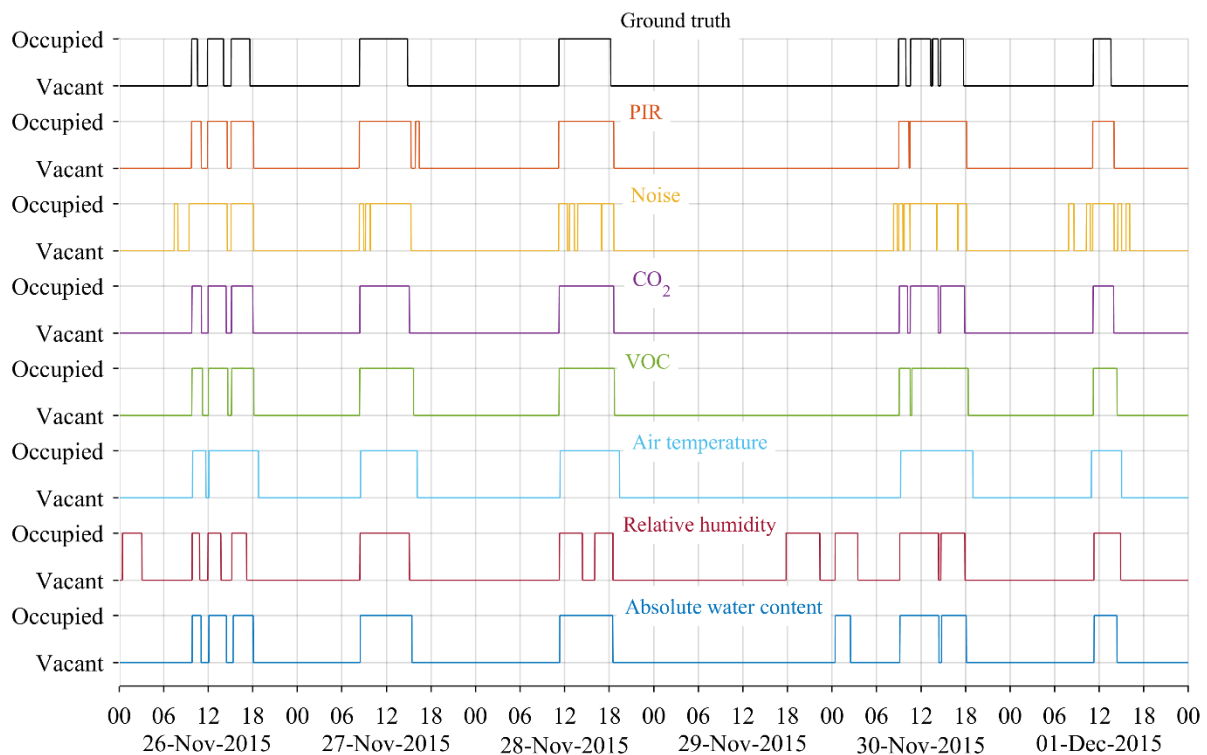

Fig. 7. Ground truth and detection results using sensor data from six days at a single-person office [P1].

In paper [P6], the abovementioned occupancy detection method was used to obtain occupancy schedules for four single-person dorm apartments based on CO_2 measurements. These schedules were then randomly combined for each of the ten apartments, assuming that the presence of individual occupants was independent. Predictions of occupancy were generated using a higher-order inhomogeneous Markov chain model, which was continually trained to adapt to changes in room usage.

The simulation results during the simulation period are given in Table 4 for the reference, three SB-MPC schemes with a varying number of considered disturbance scenarios K and the PB (i.e. perfect information on disturbances), respectively. The total operational cost and operational cost savings ΔF (according to Eq. (17)) are summarized for all ten apartments, while thermal comfort violations ΔC (according to Eq. (18)) are given as the mean across the ten apartments. Compared to deterministic MPC (DMPC), i.e. $K = 1$, the simulation results suggested that applying SB-MPC with $K > 1$ reduced comfort violations significantly while operational cost savings were affected to a limited extent.

Table 4. Summarized operational costs and mean thermal comfort violations for all ten apartments [P6].

Case building		Operational cost	Cost savings	Comfort violations	Comfort difference
Existing (R0)	reference	€534		12.2°Ch	
	SB-MPC (K=1)	€519	€15 (2.8%)	27.1°Ch	14.9°Ch (122.1%)
	SB-MPC (K=9)	€523	€11 (2.1%)	15.1°Ch	2.9°Ch (23.8%)
	SB-MPC (K=100)	€527	€ 7 (1.3%)	8.6°Ch	-3.6°Ch (-29.5%)
	PB	€520	€14 (2.6%)	14.0°Ch	1.8°Ch (14.8%)
Retrofit (R8)	reference	€137		20.6°Ch	
	SB-MPC (K=1)	€115	€22 (16.1%)	28.4°Ch	7.8°Ch (37.9%)
	SB-MPC (K=9)	€118	€19 (13.9%)	20.7°Ch	0.1°Ch (0.5%)
	SB-MPC (K=100)	€119	€18 (13.1%)	15.6°Ch	-5.0°Ch (-24.3%)
	PB	€116	€21 (15.3%)	17.7°Ch	-2.9°Ch (-14.1%)

Simulation results for a 4-day period for case building R8 are depicted in Fig. 8. The results indicate that multiple scenarios ($K = 100$) on several occasions ensured compliance with $t^{\max}$ (dashed line) while DMPC led to constraint violations. Inspecting the results more closely also indicated that SB-MPC, regardless of the choice of K, did not affect the charging periods but merely the magnitude of the estimated storage capacity $\Delta \Phi^{\text{charge}}$. A practical and computationally tractable alternative to SB-MPC could therefore be to implement DMPC as high-level control together with a low-level PI controller, where the latter ensures thermal comfort when the DMPC scheme underestimates/overestimates the uncertain disturbances.
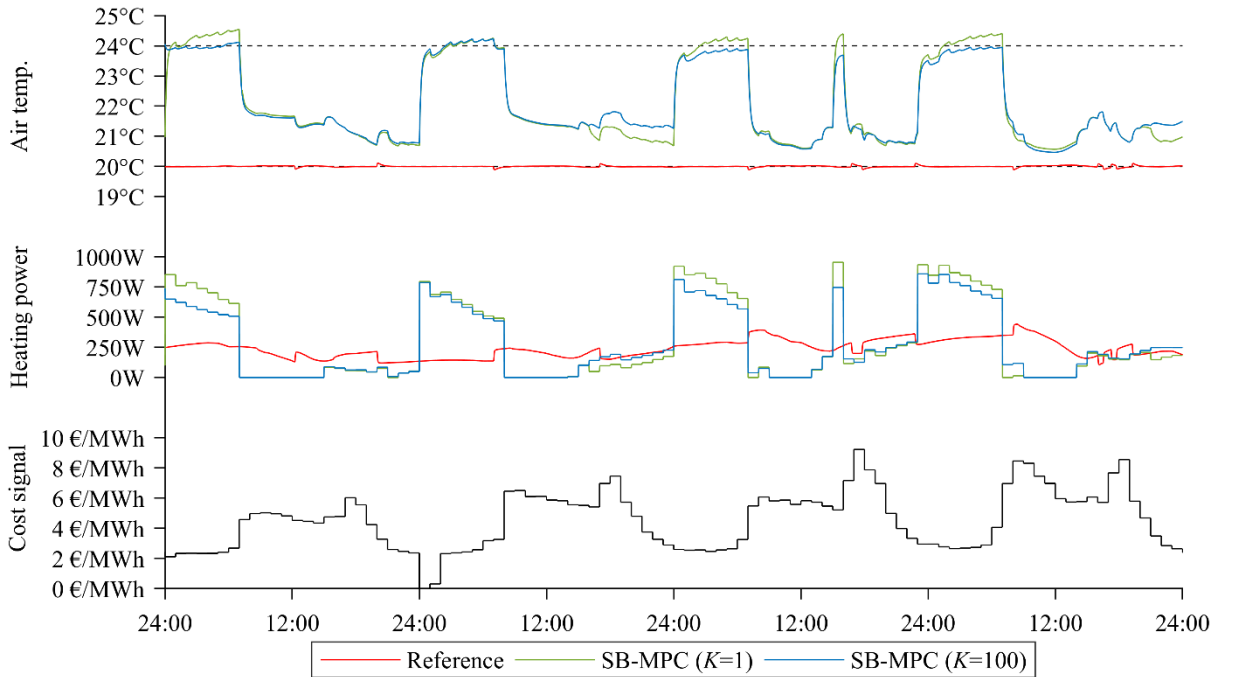

Fig. 8. Four-day simulation results of one apartment in case building R8 [P6].

5.3   Ensuring thermal comfort

Exploiting the thermal mass as heat storage to enable non-dispatchable DR inherently depends on modulations of the room air temperatures, and it is therefore necessary to ensure that DR benefits are not at the expense of violations of thermal comfort. As stated in sections 3.1 and 3.3, thermal comfort can be handled as an optimization objective (Eq. (20)) or as output constraints (Eqs. (27) and (28)). The objective of paper [P5] was therefore to provide a quantitative performance assessment in terms of operational cost savings and thermal comfort violations of four different MPC formulations:

I.   Single-objective: Minimize temperature deviations from preferred temperature (Eq. (20)).
II. Single-objective: Minimize operational cost (Eq. (21)).
III. Multi-objective: Compromise solution (a special case of Eq. (22)).
IV. Single-objective: Minimize operational cost (Eq. (21)), but with additional output constraints.

The resulting air temperature (solid red line) of applying the four MPC schemes and the associated cost signal during a one-week period are depicted in Fig. 9. While formulation I ensured a temperature close to the preferred temperature of 21.5°C at all times, the three other formulations utilized the thermal comfort band (dashed lines) to minimize the operational cost. It is difficult to state which of the four formulations are preferable, since the distinct cost functions and constraints imposed on the four MPC schemes render any direct comparison of results unfair from a mathematical point of view. Furthermore, it depends on whether – and how much – occupants are willing to deviate from their preferred air temperature to minimize operational cost. However, the proposed single-objective problem formulation IV introduces a parameter ε^{max}, which describes the maximum negative acceptable deviations from the preferred indoor air temperature, in other words, an indicator of their 'DR willingness'.
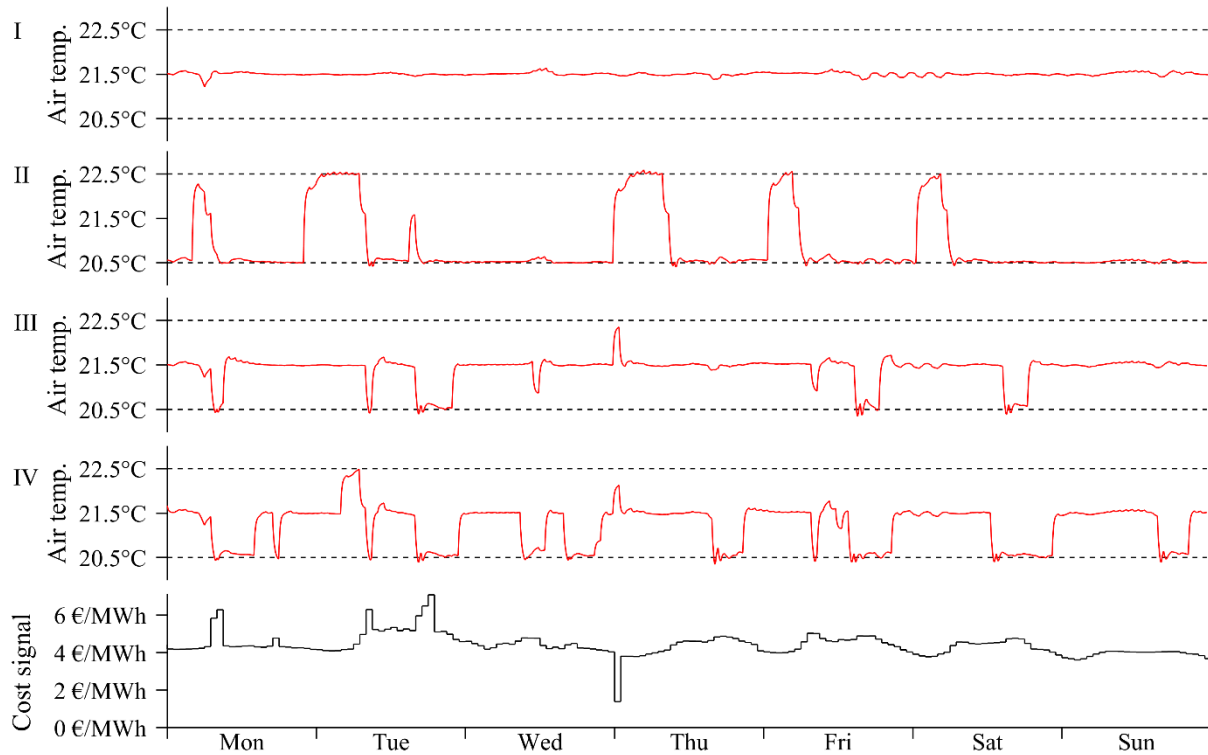

Fig. 9. One-week simulation results for one apartment in case building R8 [P5].

5.4 Hydronic heat emitters

The work reported in papers [P2] to [P6] makes use of electrical convective baseboard heaters that behave linearly. However, in buildings connected to DH networks, the typical heating systems consist of hydronic heat emitters, such as radiators, that are characterized by nonlinearities in their heat output driven by the temperature difference between the radiator and room. The objective of paper [P7] was therefore to investigate the effect on the DR potential when including the hydronic radiator dynamics, and to address the nonlinearities when applying an E-MPC scheme.

To reliably evaluate the impact of the dynamics of a hydronic radiator, a nonlinear grey-box model that adequately represents the thermodynamics of a hydronic radiator was established as a system of nonlinear ordinary differential equations, i.e. the radiator was lumped into N_S equally sized homogeneous horizontal sections in serial connection. The model parameters were calibrated with the objective of minimizing the outlet temperature residuals based on data from experiments where the flow rate was modulated to excite the radiator. Simulated model states and output compared to measurements (validation data) are depicted in the left column of Fig. 10, while histograms of the residuals appear in the right column. The top, middle and bottom sections refer to measurements taken at the first, second and third quarter of the radiator height, respectively, whereas the bottom chart displays the outlet temperature.
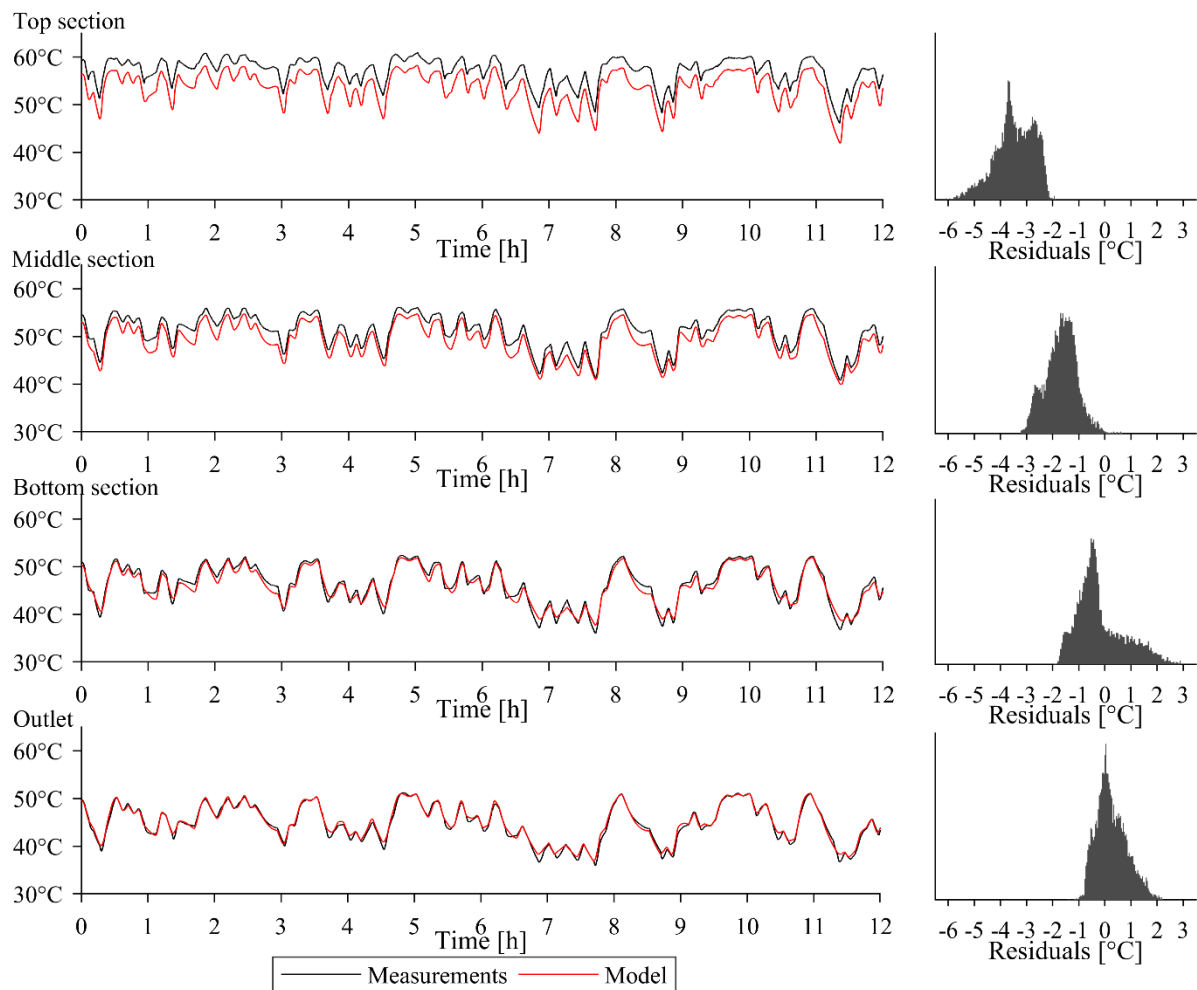

Fig. 10. Simulated model states and output compared to measurements [P7].

25

Simulations of three E-MPC setups were carried out to investigate the effect on the DR potential when including the hydronic radiator dynamics:

I.   Linear E-MPC controlling an electrical baseboard heater (as used in papers [P2] to [P6]).
II. Two-level control where a linear E-MPC determined the optimal heating setpoint. This setpoint was then communicated to a conventional PI-controller that adjusted the water flow to the hydronic radiator model.
III. Nonlinear E-MPC scheme, i.e. including the hydronic radiator when optimizing the control strategy.

The resulting air temperature (solid red line) for the reference and the three E-MPC schemes during a one-week period are depicted in Fig. 11 together with the cost signal. Compared to the reference controller, all the E-MPC setups raised the air temperatures within the thermal comfort band (dashed lines) during low price periods to charge the thermal mass. In general, Fig. 11 indicates that the three E-MPC setups resulted in similar space heating strategies. This was supported by the summarized results, which suggested that the three E-MPC setups achieved similar operational cost savings ΔF (according to Eq. (17)) of approx. 5% and 19% relative to the reference for case buildings R0 and R8, respectively. Furthermore, similar and limited levels of thermal comfort violations ΔC (according to Eq. (18)) for all E-MPC setups were achieved.
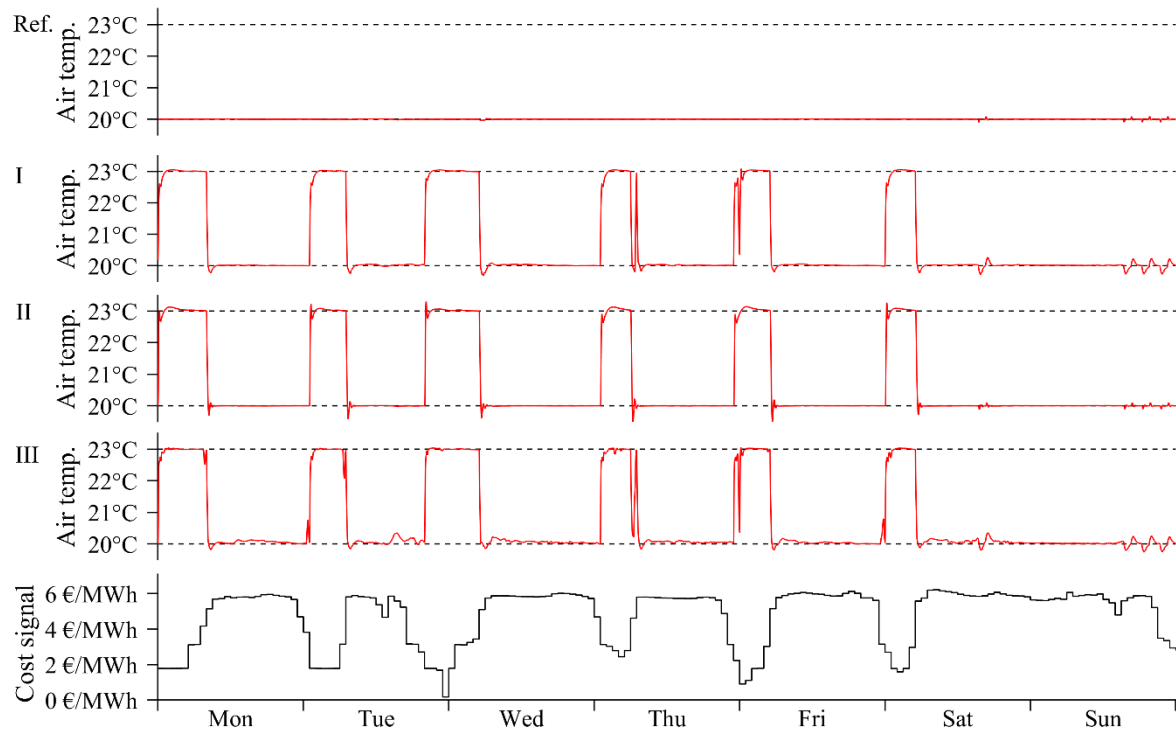

Fig. 11. One-week simulation results of one apartment in case building R0 [P7].

The simulation results suggested, just as proposed in paper [P6], that the performance of a two-level E-MPC scheme for practical coupling of the E-MPC scheme with typical setpoint-tracking controllers appears to be an appropriate control setup for real applications.

6   Part III – Experiment

The objective of Part III was to conduct a proof-of-concept laboratory experiment for the proposed E-MPC scheme developed based on experiences from Parts I and II before moving onto field experiments. The first task of Part III was therefore to develop the necessary hardware/software infrastructure to enable the laboratory experiments. However, the establishment of the experimental infrastructure proved to be more time-intensive and troublesome than expected; as a consequence, no complete and successful experiments were obtained within the time-frame of the thesis work. Part III of this thesis is therefore dedicated to documenting the work put into the development of an experimental setup to test E-MPC at Aarhus University during the thesis period. The second task was to obtain a few preliminary results from tests of applying the prototype E-MPC scheme, which are also presented here.

6.1   Experimental setup

The daylight laboratory at Aarhus University, located on the roof of the Navitas building (see Fig. 13) was used as the test facility, and consists of two similar experiment rooms, a control room, a staircase, a hallway and a technical room as illustrated in the floor plan in Fig. 12. The floor plan also indicates that the window-to-floor area ratios in the experiment rooms are unrealistic compared to existing residential buildings. Therefore, and in order to increase the mutual comparability of the experiment rooms, aluminum foil was attached on the interior of the windows and skylights except for a minor window area on the south-facing façade. Furthermore, insulation panels were added to the fixed casement windows, as illustrated in Fig. 12 and depicted in Fig. 13. In addition, a number of bricks were stacked in each room to increase the structural capacity, as depicted in Fig. 13.
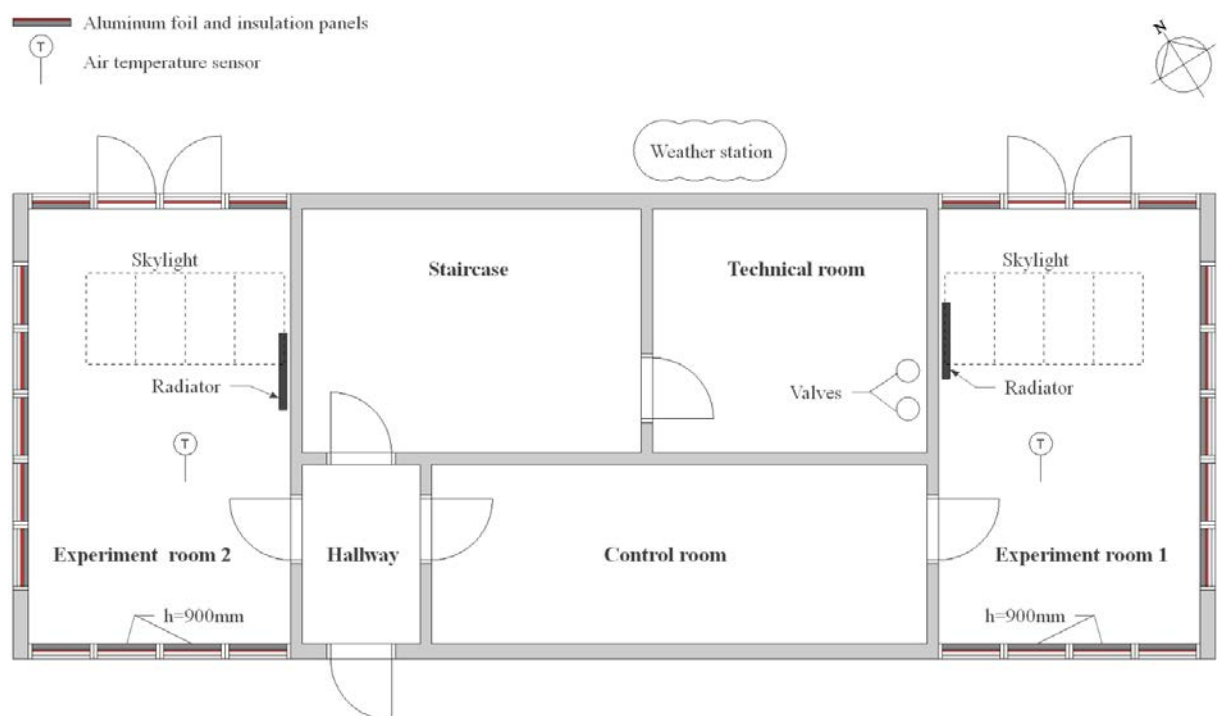

Fig. 12. Floor plan of the daylight laboratory at Navitas, Aarhus University.

Fig. 13. Top: Satellite view of the Navitas building and the daylight laboratory facility.
Bottom: Pictures of the insulation panels, aluminum foil and the stack of bricks.

To estimate a grey-box control-model (as given in Eq. (23)) for each experiment room, a 4-week excitation experiment was carried out, where temperature setpoints of 20.5°C and 25.5°C fluctuated randomly on a weekly pattern. During the experiment, the mechanical ventilation was shut off to ease the control-model identification. Furthermore, electrical heaters were used during this excitation experiment due to practical issues with the hydronic heating system. Measurements of the air temperature y^{meas_1} and y^{meas_2} in the two experiment rooms, respectively, together with ambient weather conditions measured on the roof of the laboratory, are displayed in Fig. 14. In general, the temperatures in the two experiment rooms behave similarly during temperature ramp up and down periods. However, on days with particularly high solar gains, the temperature in experiment room 1 occasionally exceeds 25.5°C, suggesting that experiment room 1 was more sensitive towards solar heat gains. The heating consumption in the two rooms during the experiment period were 22.2 kWh/m² and 24.3kWh/m², respectively.
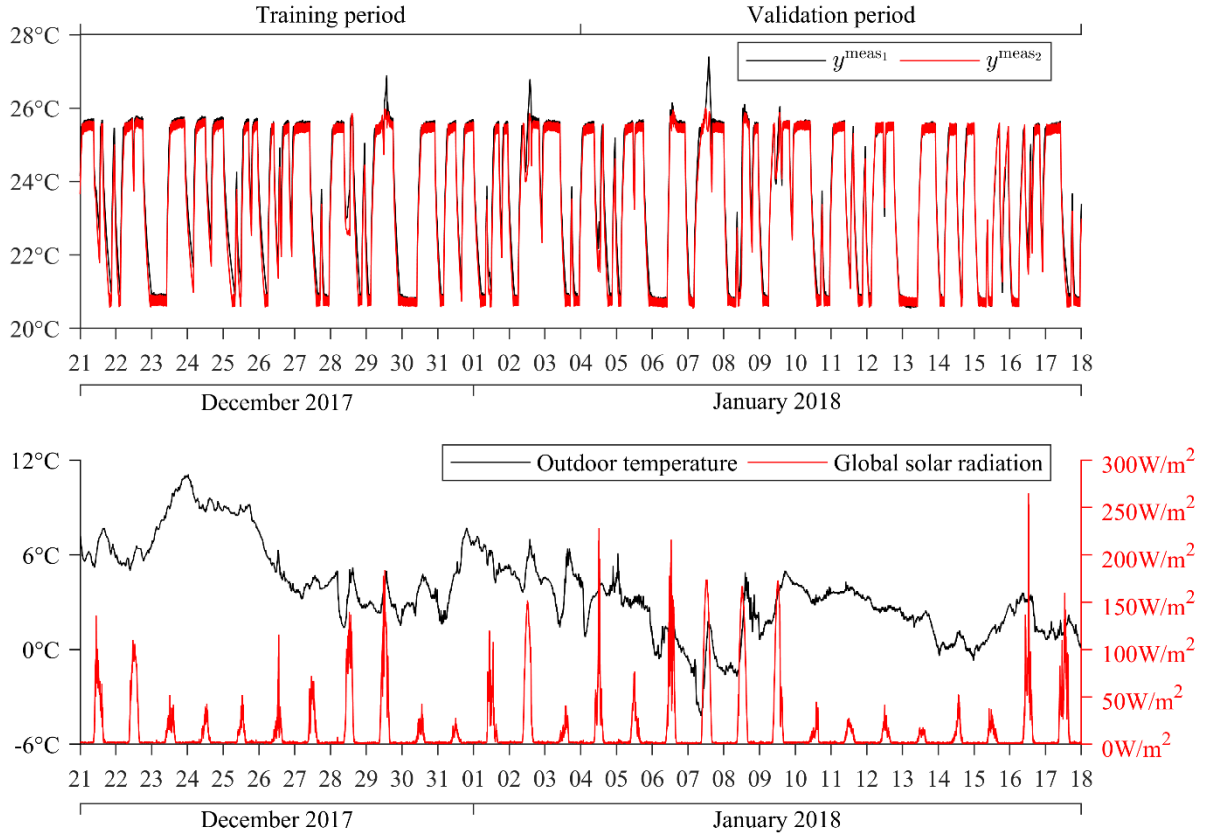
Fig. 14. 4-week excitation experiment data

As illustrated in Fig. 14, the experiment period was divided in to a training and validation period. Data obtained during the training period were used to estimate control-model parameters by minimizing the multiple-step ahead prediction error, while the remaining data were used for control-model validation. The control-models were evaluated in terms of the standard metric *normalized root mean square error (NRMSE)* as given in Eq. (31), where y^{meas} and $\hat{y}$ denote the time series of the measured data and the control-model output, respectively, and $\|\cdot\|$ denotes the Euclidean norm.

$$NRMSE = \left(1 - \frac{\|y^{\mathrm{meas}} - \hat{y}\|}{\|y^{\mathrm{meas}} - \mathrm{mean}(y^{\mathrm{meas}})\|}\right) \cdot 100 \tag{31}$$

The control-model was formulated as a linear two-state grey-box model representing the lumped thermal capacity of the room air and the construction elements (a graphical representation of the model structure is given in paper [P2]). The control-model was estimated in continuous time and then discretized using the zero-order hold method with a time step of 60 seconds. The outputs of the final selected control-models, with a NRMSE during the validation period of 65% and 71% for experiment room 1 and 2, respectively, are depicted in Fig. 15.
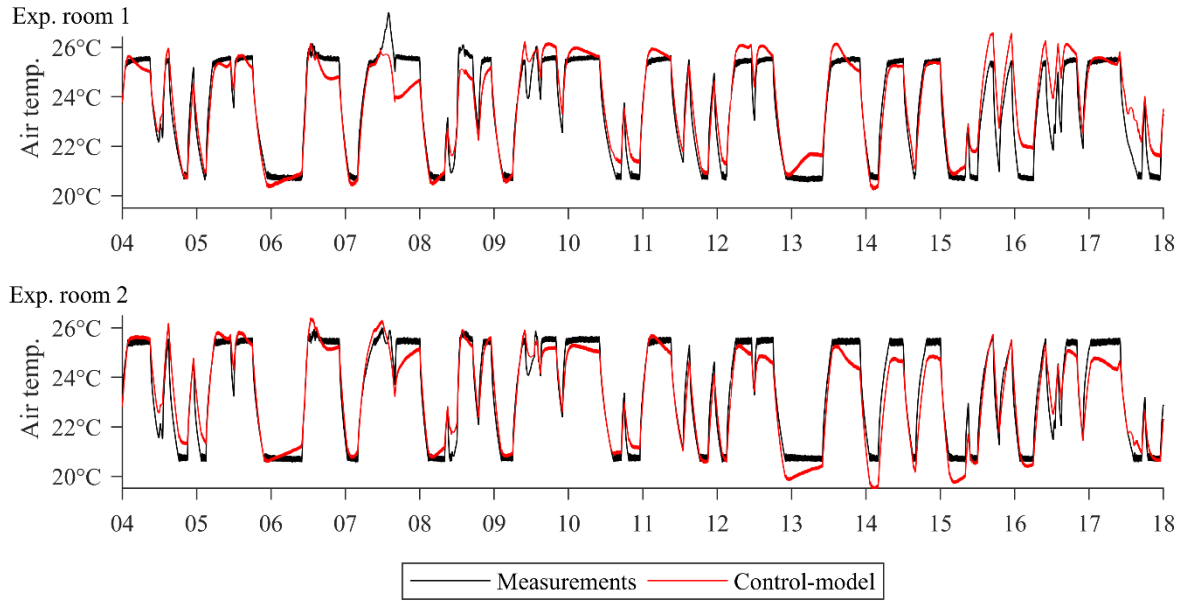
Fig. 15. Measurements and control-model output during the validation period.

The implemented prototype MPC scheme corresponded to E-MPC setup II as suggested in paper [P7], which is illustrated as a block diagram in Fig. 16. A linear E-MPC scheme based on the abovementioned control-models determines an optimal heating setpoint y_τ^{set} at each time step τ, constrained according to Eq. (27) by the time-invariant bounds t^{min} and t^{max} of 20°C and 26°C, respectively. A conventional PI-loop then adjusts the valve opening θ_τ and a driver consequently adjusts the water flow q_τ to the hydronic radiator to achieve y_τ^{set}. The heat delivered to the room and the air temperature denoted Φ_τ and y_τ, respectively, are measured and returned to the MPC scheme, thus introducing feedback. Disturbances $\boldsymbol{d}_\tau$ acting on the room, i.e. outdoor temperature and global solar radiation, are likewise measured and returned to the E-MPC scheme. Furthermore, weather forecast provided by DMI of the disturbances and the cost signal $\boldsymbol{f}$ for the prediction horizon N are communicated to the E-MPC scheme.
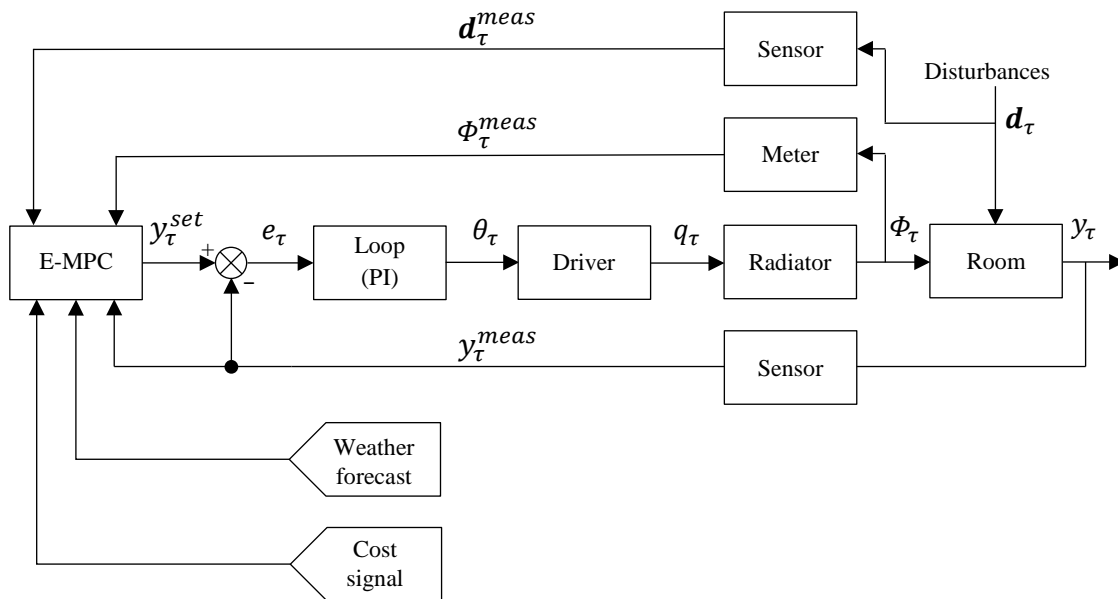

Fig. 16. Block diagram of implemented prototype E-MPC setup.

6.2 E-MPC results

Measurements of the air temperatures, heating power and ambient disturbances during a 6-day period are depicted in Fig. 17. The heating power Φ_τ^{meas} was calculated as the change in energy of the water according to Eq. (32), based on measurements of the accumulated flow since previous time step denoted q_τ and the instantaneous supply and return temperature referred to as t_τ^{supply} and t_τ^{return}, respectively. The specific heat capacity and density of the water are denoted c_p^{water} and ρ^{water}, respectively.

$$\Phi_\tau^{\text{meas}} = c_p^{\text{water}} \cdot \rho^{\text{water}} \cdot q_\tau \cdot \left(t_\tau^{\text{supply}} - t_\tau^{\text{return}} \right) \tag{32}$$

The prototype E-MPC scheme was applied in experiment room 2 while the reference control constantly tracking t^{min} was applied in experiment room 1. As previously mentioned, the experiment rooms are very sensitive towards solar heat gains, which was also shown on two occasions where the air temperature significantly exceeded t^{max} while the heating power was 0W. The small oscillations of the air temperature were due to delays in the hydronic heating system, tuning of PI gains and building/control-model mismatch.
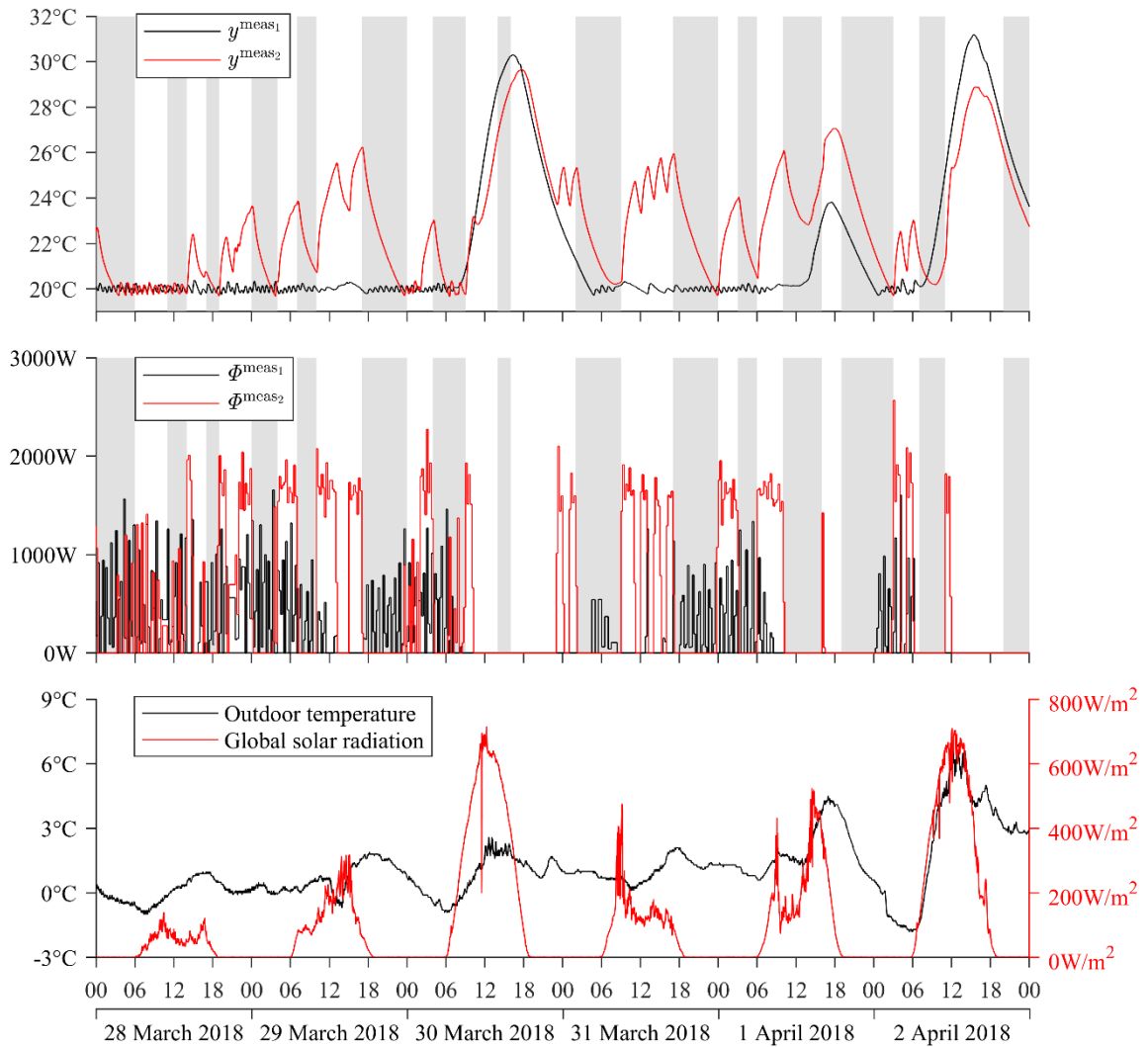

Fig. 17. Measurements obtained during a 6-day period.

The objective of the MPC scheme was to minimize heating consumption in high price periods (marked with grey), by increasing the air temperature during low price periods and, consequently, charge the thermal mass. The achieved results are listed in Table 5, where the heating consumption during the 6-day period is summarized for the two experiment rooms. Compared to the difference in heating consumption during the excitation experiment, the results show a significant difference in total heating consumption Φ between the two experiment rooms when using the hydronic heating systems. An obvious reason is the application of the E-MPC scheme; however, another important factor is the uninsulated pipe lengths between the radiators and the valves (where the meters measuring t_τ^{supply} and t_τ^{return} are mounted), see Fig. 12. In fact, a difference of approx. 2°C between the measured supply and return temperature difference at the meter and radiator was observed in experiment room 2. Thus, the quantity Φ^* approximates this observation by constantly subtracting 2°C from the measured supply temperature to experiment room 2. The variables $\overline{\Phi}^{\text{high}}$ and $\overline{\Phi}^{\text{low}}$ specifies the relative amount of Φ that was consumed during high and low price periods, respectively.

Table 5. Summarized experiment results.

	Φ	Φ^*	$\overline{\Phi}^{\text{high}}$	$\overline{\Phi}^{\text{low}}$
Experiment room 1 *(reference control)*	1.4kWh/m^2	1.4kWh/m^2	54.5%	45.5%
Experiment room 2 *(two-level E-MPC scheme)*	2.9kWh/m^2	1.9kWh/m^2	26.4%	73.6%

7 Conclusions

This thesis reported on the potential and development of a reliable economic model predictive control scheme suitable for real application in residential buildings to enable non-dispatchable demand response programs for space heating consumption in the heating-dominated climate of Denmark. The focus was on its application in existing residential buildings facing retrofits and any trade-off between energy efficiency and ability to participate in non-dispatchable demand response programs. The main contributions of the thesis work were structured into three parts based on extracts of the scientific papers [P1-P7].

The objective of Part I was to examine the theoretical benefits and ability of an existing residential buildings and eight retrofit scenarios thereof participating in non-dispatchable DR programs based on several simulation-based studies. The results suggest that an energy-efficient residential building considering time varying tariffs from the day-ahead whole power market can achieve operational cost savings of up to 13%, while considering intraday trading simultaneously increased the total operational cost savings by up to 19%. The absolute magnitude of the DR potentials was fairly consistent across the varying retrofit scenarios, whereas the relative ability to exploit the thermal mass as heat storage depended significantly on the thermal characteristics of the building and, consequently, the storing efficiency. Moreover, non-dispatchable demand response enabled significant benefits for the energy systems, for example, reductions of CO_2 emissions associated with the power production of up to 3% while at the same time reducing space heating consumption in peak periods by up to 50%.

However, several practical challenges complicate the task of implementing economic model control schemes in residential buildings. The objective of Part II was therefore to address some of these practical challenges, focusing on formulating a reliable and computational tractable economic model predictive control scheme. Part II contains several separate investigations with multiple individual conclusions; however, the main findings of the different studies amount to the recommendation of a two-level economic model predictive control setup to obtain the overall aim of reliable operation. In several investigations, the two-level setup achieved the maximum benefits of participating in demand response programs, while ensuring thermal comfort at the same time. Moreover, the two-level economic model predictive control scheme builds on the typically current control scheme in residential buildings, thus reducing investment costs.

The objective of Part III was to conduct a proof-of-concept laboratory experiment of a prototype of the two-level economic model predictive control setup, including the necessary hardware and technological infrastructure, to demonstrate the ability and benefits of participating in non-dispatchable DR programs. The preliminary results suggested that the implemented prototype economic model predictive control scheme successfully shifted heating consumption by exploiting thermal mass as heat storage.

7.1 Future work

A general subject that calls for future research efforts is the definition of suitable KPIs related to non-dispatchable demand response programs. Firstly, the assessment of demand response significantly depends on the definition of a reference representing normal behavior, which still needs further research. Secondly, non-dispatchable demand response programs can be tailored to multiple objectives depending on the construction of the time varying cost signal. To further highlight the benefits of residential buildings participating in non-dispatchable demand response, steps should be taken to engage various stakeholders in the energy systems to define relevant and exact objectives.

By this time, there appear to be multiple simulation-based theoretical studies, e.g. [16, 30, 33, 39] and the thesis work presented in the scientific papers [P1-P7], which suggest that residential buildings exploiting their structural thermal storage form an excellent resource for non-dispatchable demand response. However, in order to definitively verify the identified theoretical potentials, many more reliable experimental studies are necessary. The preliminary results presented in section 6 indicated that buildings have the ability to shift space heating consumption; however, the proof-of-concept experiment gave rise to several challenges to be addressed when transitioning from simulation-based investigations to laboratory/field experiments, including:

I.   The task of obtaining a suitable control-model for economic model predictive control schemes (which was largely considered outside the scope of this thesis). It seems that different elements involved when obtaining an adequate control-model, for example, experiment design, amount and resolution of required data, modeling technique etc., constitute a significant practical challenge to implementing economic model predictive control in actual buildings.

II. The role of occupants needs further research efforts. Firstly, occupant acceptance of temperature modulations must be investigated, since utilization of the thermal as heat storage inherently relies on modulations of the air temperature. These investigations must be associated with the discussions presented in paper [P5]. Secondly, the simulation results reported in paper [P6] indicated that the two-level economic model predictive scheme adequately handled stochastic occupancy; however, these suggestions call for verification through real experiments.

8 References

[1] Official Journal of the European Union, "Directive 2009/28/EC of the European parliament and of the council of 23 April 2009 on the promotion of the use of energy from renewable sources and amending and subsequently repealing Directives 2001/77/EC and 2003/30/EC" (2009).

[2] Regeringen, "Regeringsgrundlag. For et friere, rigere og mere trygt Danmark." (2016). Statsministeriet. København,

[3] Energinet, (11 01 2018). [Online]. Available: https://energinet.dk/Om-nyheder/Nyheder/2018/01/09/Baade-vind-og-sol-slog-rekord-i-2017-leverede-459-procent-af-stroemmen [Accessed 09-04-2018].

[4] C. W. Gellings, "The Concept of Demand-Side Management for Electric Utilities", Proceedings of the IEEE, vol. 10, (Oct. 1985) 1468-1470. doi: 10.1109/PROC.1985.13318.

[5] A. F. Meyabadi and M. H. Deihimi, "A review of demand-side management: Reconsidering theoretical framework", Renewable and Sustainable Energy Reviews 80 (2017) 367-379. doi: 10.1016/j.rser.2017.05.207.

[6] N. O'Connell, P. Pinson, H. Madsen and M. O'Malley, "Benefits and challenges of electrical demand response: A critical review", Renewable and Sustainable Energy Reviews 39 (2014) 686-699. doi: 10.1016/j.rser.2014.07.098.

[7] B. P. Esther and K. S. Kumar, "A survey on residential Demand Side Management architecture, approaches, optimization models and methods", Renewable and Sustainable Energy Reviews 59 (2016) 342-351. doi: 10.1016/j.rser.2015.12.282.

[8] H. Lund, A. N. Andersen, P. A. Østergaard, B. V. Mathiesen and D. Connolly, "From electricity smart grids to smart energy systems - A market operation based approach and understanding", Energy 42 (2012) 96-102. doi: 10.1016/j.energy.2012.04.003.

[9] J. Wang, H. Zhong, Z. Ma, Q. Xia and C. Kang, "Review and prospect of integrated demand response in multi-energy system", Applied Energy 202 (2017) 772-782. doi: 10.1016/j.apenergy.2017.05.150.

[10] Official Journal of the European Union, "Directive 2010/31/EU of the European Parliament and of the Council of 19 May 2010 on the energy performance of buildings (recast)" (2010).

[11] Official Journal of the European Union, "Directive 2012/27/EU of the European Parliament and of the Council of 25 October 2012 on energy efficiency" (2012).

[12] European Commission, "Proposal for a Directive of the European Parliament and of the Council amending Directive 2010/31/EU on the energy performance of buildings" (2016). Brussels,

[13] North American Electric Reliability Corporation (NERC), "2011 Demand Response Availability Report" (2013). [Online]. Available: http://www.nerc.com/docs/pc/dadswg/2011%20DADS%20Report.pdf [Accessed 26-02-2018].

[14] M. D. Knudsen, "Evaluation of Price-Based Demand Response Potential using Economic Model Predictive Control for Residential heating" (2016). Aarhus University.

[15] S. Wang, X. Xue and C. Yan, "Building power demand response methods toward smart grid", HVAC&R Research 20:6 (2014) 665-687. doi: 10.1080/10789669.2014.929887.

[16] M. D. Knudsen and S. Petersen, "Demand Response Potential of Model Predictive Control of Space Heating based on Price and Carbon Dioxide Intensity Signals", Energy and Buildings 125 (2016) 196-204. doi: 10.1016/j.enbuild.2016.04.053.

[17] J. M. Morales, A. J. Conejo, H. Madsen, P. Pinson and M. Zugno, "Integrating Renewables in Electricity Market. Operational Problems" (2014). International Series in Operations Research & Management Science. Springer US.

[18] M. Gweder, D. Gyalistras, C. Sagerschnig, R. S. Smith and D. Sturznegger, "Final Report: Use of Weather And Occupancy Forecasts For Optimal Building Climate Control -Part II: Demonstration (OptiControl-II)" (2013). Automatic Control Laboratory, ETH Zürich, Switzerland..

[19] K. O. Aduda, T. Labeodan, W. Zeiler, G. Boxem and Y. Zhao, "Demand side flexibility: Potentials and building performace implications", Sustainable Cities and Society 22 (2016) 146-163. doi: 10.1016/j.apenergy.2015.05.101.

[20] Energistyrelsen, "Energistatistik 2016" (2016). Energi-, Forsynings- og Klimaministeriet. København K.

References

[21] R. D'Hulst, W. Labeeuw, B. Beusen, S. Claessens, G. Deconinck and K. Vanthournout, "Demand response flexibility and flexibility potential of residential smart appliances: Experiences from large pilot test in Belgium", Applied Energy 155 (2015) 79-90. doi: 10.1016/j.apenergy.2015.05.101.

[22] Y. F. Du, L. Jiang, J. Counsell and J. S. Smith, "Multi-objective demand side scheduling considering the operational safety of appliances", Applied Energy 179 (2016) 864-874. doi: 10.1016/j.apenergy.2016.07.016.

[23] M. R. Staats, P. D. de Boer-Meulman and W. G. van Sark, "Experimental determination of demand side management potential of wet appliances in the Netherlands", Sustainable Energy, Grids and Networks 9 (2017) 80-94. doi: 10.1016/j.segan.2016.12.004.

[24] D. Setlhaolo, X. Xia and J. Zhang, "Optimal scheduling of household appliances for demand response", Electric Power Systems Research 116 (2014) 24-28. doi: 10.1016/j.epsr.2014.04.012.

[25] C. O. Adika and L. Wang, "Smart charging and appliance scheduling approaches to demand side management", International Journal of Electrical Power and Energy Systems 57 (2014) 232-240. doi: 10.1016/j.ijepes.2013.12.004.

[26] D. Newbery, "Shifting demand and supply over time and space to manage intermittent generation: The economics of electrical storage", Energy Policy 113 (2018) 711-720. doi: 10.1016/j.enpol.2017.11.044.

[27] G. Lorenzi and C. A. S. Silva, "Comparing demand response and battery storage to optimize self-consumption in PV systems", Applied Energy 180 (2016) 524-535. doi: 10.1016/j.apenergy.2016.07.103.

[28] M. D. Knudsen and S. Petersen, "Model predictive control for demand response of domestic hot water preparation in ultra-low temperature district heating systems", Energy and Buildings 146 (2017) 55-64. doi: 10.1016/j.enbuild.2017.04.023.

[29] S. Stinner, K. Huchtemann and D. Müller, "Quantifying the operational flexibility of building energy systems with thermal energy storages", Applied Energy 181 (2016) 140-154. doi: 10.1016/j.apenergy.2016.08.055.

[30] J. Le Dréau and P. Heiselberg, "Energy flexibility of residential buildings using short term heat storage in the thermal mass", Energy 111 (2016) 991-1002. doi: 10.1016/j.energy.2016.05.076.

[31] J. Široký, F. Oldewurtel, J. Cigler and S. Prívara, "Experimental analysis of model predictive control for an energy efficient building heating system", Applied Energy 88 (2011) 3079-3087. doi: 10.1016/j.apenergy.2011.03.009.

[32] M. Avci, M. Erkoc, A. Rahmani and S. Asfour, "Model predictive HVAC load control in buildings using real-time electricity pricing", Energy and Buildings 60 (2013) 199-209. doi: 10.1016/j.enbuild.2013.01.008.

[33] G. Bianchini, M. Casini, A. Vicino and D. Zarrilli, "Demand-response in building heating systems: A Model Predictive Control Approach", Applied Energy 168 (2016) 159-170. doi: 10.1016/j.apenergy.2016.01.088.

[34] J. Kensby, A. Trüschel and J.-O. Dalenbäck, "Potential of residential buildings as thermal energy storage in district heating systems - Results from a pilot test", Applied Energy 137 (2015) 773-781. Doi: 10.1016/j.apenergy.2014.07.026.

[35] G. Reynders, T. Nuytten and D. Saelens, "Potential of structural thermal mass for demand-side management in dwellings", Building and Environment 64 (2013) 187-199. doi: 10.1016/j.buildenv.2013.03.010.

[36] E. Nyholm, S. Puranik, É. Mata, M. Odenberger and F. Johnsson, "Demand response potential of electrical space heating in Swedish single-family dwellings", Building and Environment 96 (2016) 270-282. doi: 10.1016/j.buildenv.2015.11.019.

[37] S. Sabihuddin, A. E. Kiprakis and M. Mueller, "A Numerical and Graphical Review of Energy Storage Technologies", Energies, no. 8, (2015) 172-216. doi: 10.3390/en8010172.

[38] K. Hedegaard, B. V. Mathiesen, H. Lund and P. Heiselberg, "Wind power integration using individual heat pumps - Analysis of different heat storage options", Energy 47 (2012) 284-293. doi: 10.1016/j.energy.2012.09.030.

[39] G. Reynders, "Quantifying the impact of building design on the potential of structural storage for active demand response in residential buildings" (2015). PhD Dissertation. KU Leuven,

[40] J. Clauß, C. Finck, P. Vogler-Finck and P. Beagon, "Control strategies for building energy systems to unlock demand side flexibility – A review," IBPSA Building Simulation, (2017).

[41] F. Oldewurtel, A. Parisio, C. N. Jones, D. Gyalistras, M. Gwerder, V. Stauch, B. Lehmann and M. Morari, "Use of model predictive control and weather forecasts for energy efficient building climate control", Energy and Buildings 45 (2012) 15-27. doi: 10.1016/j.enbuild.2011.09.022.

[42] M. Killian and M. Kozek, "Ten questions concerning model predictive control for energy efficient buildings", Building and Environment 105 (2016) 403-412. doi: 10.1016/j.buildenv.2016.05.034.

[43] M. L. Darby and M. Nikolaou, "MPC: Current practice and challenges", Control Engineering Practice 20 (2012) 328-342. doi: 10.1016/j.conengprac.2011.12.004.

[44] D. Mayne, "Robust and stochastic model predictive control: Are we going in the right direction?", Annual Reviews in Control 41 (2016) 184-192. doi: 10.1016/j.arcontrol.2016.04.006.

[45] S. Boyd and L. Vandenberghe, "Convex optimization" (2004). Cambridge University Press.

[46] S. Ø. Jensen, A. Marzal-Pomianowska, R. Lollini, W. Pasut, A. Knotzer, P. Engelmann, A. Stafford and G. Reynders, "IEA EBC Annex 67 Energy Flexible Buildings", Energy and Buildings 155 (2017) 25-34. doi: 10.1016/j.enbuild.2017.08.044.

[47] J. B. Rawlings and D. Q. Mayne, "Model predictive control: theory and design. 2nd edition" (2016). Madison: Nob Hill Publishing, LLC.

[48] D. Q. Mayne, "Model predictive control: Recent developments and future promise", Automatica 50 (2014) 2967-2986. doi: 10.1016/j.automatica.2014.10.128.

[49] S. J. Qin and T. A. Badgwell, "A survey of industrial model predictive control technology", Control Engineering Practice 11 (2003) 733-764. doi: 10.1016/S0967-0661(02)00186-7.

[50] L. Grüne, "Economic receding horizon control without terminal constraints", Automatica 49 (2013) 725-734. doi: 10.1016/j.automatica.2012.12.003.

[51] A. Jadbabaie and J. Hauser, "On the stability of receding horizon control with a general terminal cost", IEEE Transactions on Automatic Control, vol. 50, no. 5, (2005) 674-678. doi: 10.1109/TAC.2005.846597.

[52] P. Moreles-Valdés, A. Flores-Tlacuahuac and V. M. Zavala, "Analyzing the effects of comfort relaxation on energy demand flexibility of buildings: A multiobjective optimization approach", Energy and Buildings 85 (2014) 416-426. doi: 10.1016/j.enbuild.2014.09.040.

[53] P. O. Fanger, "Thermal comfort: Analysis and applications in environmental engineering" (1970). Copenhagen: Danish Technical Press.

[54] J. Cigler, S. Prívara, Z. Váňa, E. Žáčeková and L. Ferkl, "Optimization of Predicted Mean Vote index within Model Predictive Control framework: Computationally tractable solution", Energy and Buildings 52 (2012) 39-49. doi: 10.1016/j.enbuild.2012.05.022.

[55] I. Das and J. E. Dennis, "Normal-boundary intersection: A new method for generating the Pareto surface in nonlinear multicriteria optimization problems", SIAM Journal on Optimization, vol. 8, no. 3, (1998) 631-657. doi: 10.1137/S1052623496307510.

[56] V. M. Zavala, "Real-Time Resolution of Conflicting Objectives in Building Energy Management: An Utopia-Tracking Approach," in Fiftth National Conference of IBPSA-USA, Madison, Wisconsin, 2012.

[57] I. Y. Kim and O. L. de Weck, "Adaptive weighted-sum method for bi-objective optimization: Pareto front generation", Structural and Multidisciplinary Optimization, vol. 29, no. 2, (2005) 149-158. doi: 10.1007/s00158-004-0465-1.

[58] S. Prívara, J. Cigler, Z. Váňa, F. Oldewurtel, C. Sagerschnig and E. Žáčeková, "Building modeling as a crucial part for building predictive control", Energy and Buildings 56 (2013) 8-22. doi: 10.1016/j.enbuild.2012.10.024.

[59] P. Bacher and H. Madsen, "Identifying suitable models for the heat dynamics of buildings", Energy and Buildings 43 (2011) 1511-1522. doi: 10.1016/j.enbuild.2011.02.005.

[60] S. Goyal, C. Liao and P. Barooah, "Identification of multi-zone building thermal interaction model from data", 50th IEEE Conference on Decision and Control (2011). doi: 10.1109/CDC.2011.6161387.

[61] S. Prívara, Z. Váňa, D. Gyalistras, J. Cigler, C. Sagerschnig, M. Morari and L. Ferkl, "Modeling and Identification of a Large Multi-Zone Office Building", IEEE International Conference on Control Applications (CCA) (2011). doi: 10.1109/CCA.2011.6044402.

[62] J. Cigler and S. Prívara, "Subspace Identification and Model Predictive Control for Buildings", 11th International Conference Control, Automation, Robotics and Vision (2011). doi: 10.1109/ICARCV.2010.5707821.

[63] R. E. Kalman, "A New Approach to Linear Filtering and Prediction Problems", Journal of basic engineering 82(1) (1960) 35-45.

References

[64] ASHRAE Standard 55-2010, "Thermal environmental conditions for human occupancy" (2010).

[65] P.-D. Moroşan, R. Bourdais, D. Dumur and J. Buisson, "Building temperature regulation using a distributed model predictive control", Energy and Buildings 42 (2010) 1445-1452. doi: 10.1016/j.enbuild.2010.03.014.

[66] V. Chandan and A. G. Alleyne, "Decentralized architectures for thermal control of buildings", American Control Conference (ACC) (2012). doi: 10.1109/ACC.2012.6315599.

[67] G. Schildbach, L. Fagiano, C. Frei and M. Morari, "The Scenario Approach for Stochastic Model Predictive Control with Bounds on Closed-Loop Constraint Violations", Automatica 50 (2014) 3009-3018. doi: 10.1016/j.automatica.2014.10.035.

[68] G. C. Calafiore, "On the Expected Probability of Constraint Violation in Sampled Convex Programs", Journal of Optimization Theory and Applications, vol. 143, no. 2, (2009) 405-412. doi: 10.1007/s10957-009-9579-3.

[69] M. C. Campi and S. Garatti, "A Sampling-and-Discarding Approach to Chance-Constrained Optimization: Feasibility and Optimality", Journal of Optimization Theory and Applications, vol. 148, no. 2, (2011) 257-280. doi: 10.1007/s10957-010-9754-6.

P1 Method for room occupancy detection based on trajectory of indoor climate sensor data

Contents lists available at ScienceDirect

Building and Environment

journal homepage: www.elsevier.com/locate/buildenv

ELSEVIER

Method for room occupancy detection based on trajectory of indoor climate sensor data

CrossMark

Theis Heidmann Pedersen[*], Kasper Ubbe Nielsen, Steffen Petersen

Department of Engineering, Inge Lehmanns Gade 10, Aarhus University, DK-8000 Aarhus C, Denmark

ABSTRACT

Significant energy savings can be achieved by operating heating, ventilation and air conditioning controllers using a feedback from sensor-based occupancy detection methods. This paper presents a novel plug-and-play occupancy detection method based on the trajectory of various indoor climate sensor data. Sensor data obtained from two different building zones was used to test the efficacy of the method. For a simple test room, occupancy detection based on CO_2 sensor data had the best performance with a mean absolute error (MAE) of 2%, closely followed by PIR and volatile organic compound (VOC) with a MAE of 3% and 4%, respectively. For a real dorm apartment with three rooms, but only one data logger, the best performance was found when PIR was used to determine when the apartment went from unoccupied to occupied and either VOC or CO_2 sensor data was used to determine when the apartment went from occupied to unoccupied (MAE of 22% and 26%, respectively). Compared to more complex detection methods that require detailed information about the physical conditions of rooms or extensive training data sets, the proposed plug-and-play method that employs simple trajectory of CO_2, PIR and VOC sensor data resulted in similar occupancy detection accuracies.

© 2017 Elsevier Ltd. All rights reserved.

1. Introduction

Heating, ventilation and air conditioning (HVAC) systems currently account for approximately half of the energy consumed in buildings in developed countries [1]. It is therefore essential to design and operate HVAC systems in an energy-efficient manner to meet low-energy targets. The HVAC need is strongly related to the occupancy of the building due to the air pollution and heat load generated by human metabolism, and their use of electrical equipment [2–5]. Conventional rule-based HVAC operation typically relies on a daily static occupancy schedule and real-time measurements of air temperature and/or CO_2 concentration to determine the HVAC need. However, several studies have suggested that significant energy savings can be achieved by using feedback from sensor-based occupancy detection when operating HVAC systems [6–14] and lighting [15–18]. Agerval et al. [6] used occupancy information in a rule-based HVAC control scheme and obtained electrical energy savings of up to 16% compared to a baseline control. Dong and Lam [10] compared a conventional set-

point schedule to an occupancy based control approach in a simulation study, which suggested that energy savings of 18.5% could be achieved. Labeodan et al. [16] included occupancy information in the lighting control in an office building and achieved energy savings of 28%. Even greater energy savings can be obtained when applying occupancy predictions based on occupancy detection data as input to more complex control schemes, such as model predictive control (MPC) [19–28]. For example, simulation results of Goyal et al. [21] achieved energy savings of 50% on average when including occupancy information in a rule-based control scheme compared to a conventional baseline controller, but an additional energy saving of 1–13% were achieved when using occupancy predictions in a MPC scheme. The same tendency was demonstrated by Oldewurtel et al. [25], where occupancy information in an MPC scheme led to energy savings of up to approx. 34%. The above-mentioned studies demonstrate a significant theoretical energy-saving potential, i.e. when perfect occupancy detection and predictions are assumed. However, simulation results of Pedersen et al. [29] show that the accuracy of occupancy detection and predictions affects the theoretical energy-saving potential significantly. This calls for the development of reliable yet simple and inexpensive real-time occupancy detection approaches to include occupancy information when optimizing real-time HVAC

* Corresponding author.
  E-mail address: thp@eng.au.dk (T.H. Pedersen).

operation.

1.1. Related work and aim of paper

Current occupancy detection approaches can be split into two groups: image-based methods and data-based methods. Image-based methods [30–33] rely on camera technology to detect occupancy. Zhang et al. [32] utilized the depth-frame data from a Kinect camera to detect and track moving people 4.0 m below with a precision of 99.7%. Petersen et al. [33] applied the same approach with an accuracy of approx. 99% when detecting and tracking people 2.3–3.0 m below the camera. However, installing cameras can be perceived as a privacy violation and often represents an additional investment and running cost to a building project. Zhao et al. [34] obtained convincing occupancy detection in offices using a Bayesian belief network together with information from e.g. Wi-Fi, GPS location, chair sensor, and keyboard and mouse sensor. However, some occupants may still consider these sensor data to be intrusive. An inexpensive and non-intrusive alternative is to use indoor climate data from sensors already installed in today's buildings for other purposes than occupancy detection. Currently, the most commonly used sensor data for occupancy detection is data from passive infrared (PIR) sensors [20,26,35–37] which are installed primarily for energy efficient operation of lighting. However, relying solely on PIR sensor data as a detection of occupancy is rather uncertain since the sensors do not capture immobile occupants or occupants that are outside the PIR sensor's field-of-view [38]. Data from indoor climate sensors already used for conventional HVAC control seems like another obvious basis for occupancy detection. The carbon dioxide (CO_2) level in a room is an attractive indicator as it is a direct consequence of human presence and, to some extent, independent of whether the occupants are moving or not. Detecting occupant presence based on changes in CO_2 level has demonstrated acceptable accuracy in a simple study with a difference of maximum ± 50 PPM between simulated and measured CO_2-concetration for one day [38]. Using data from CO_2 sensors in conjunction with building models to solve a CO_2 mass balance equation has been applied to detect occupancy in Refs. [39–42]. Calì et al. [42] used the CO_2 mass balance equation to detect occupant presence in a two-person office room and a residential room. Applying the proposed algorithm led to an accuracy of 88% and 79%, respectively while it accurately detected the number of occupants 70% and 46% of the time in the two cases, respectively. The disadvantage of using the CO_2 mass balance equation is that it requires detailed information about the physical room conditions (e.g. room volume, mechanical air change rate, window/door openings, occupant CO_2 production, outdoor CO_2 concentration) which can be difficult to determine and vary in time, thus making it subject to some uncertainty.

Utilizing sensor data to establish statistical models is another widely used approach [10,37,43–47]. For example, Rye and Moon [46] used machine learning techniques to detect occupancy in a controlled test-room using indoor climate sensors and energy consumption meters, and found that the CO_2 concentration yielded the highest information gain. Jiang et al. [43] identified an occupancy estimator based on CO_2-measurements in an office room occupied with up to 35 persons. Considering a tolerance in person counting of zero and three people, the estimator achieved an accuracy of 50% (mainly due the unoccupied hours) and 89%, respectively. Data-based occupancy detection based on measurements of CO_2, carbon-monoxide (CO), total volatile organic compounds (TVOC), small particles (PM2.5), acoustics, illumination, PIR, temperature and relative humidity (RH) from an open-plan office environment was reported in Refs. [10,37,44]. Correlation between the number of occupants and sensor data ranked the individual sensor data in terms of relative information gain, which suggested that RH (77.65%), Acoustic (73.42%), CO_2 (67.14%) and Temperature (37.39%) yielded the largest correlation [44]. Combining features involving RH, CO_2 and acoustic sensor data led to a relative information gain of 90%. In Ref. [37] the authors investigated three different statistical methods for the estimation of occupancy numbers (Support Vector Machines (SVM), Artificial Neural Networks (ANN) and Hidden Markov Models (HMM)) and found that data from CO_2 and acoustic sensors had the largest correlation with the number of occupants. All three models had an average accuracy of approx. 75%, however, the authors stated that the HMM method more realistically described an occupancy presence profile compared to SVM and ANN due to its ability to discount sudden brief changes in occupancy levels as well as maintain a constant level during static occupancy periods. In Ref. [10] the authors continued the work and added a Gaussian Mixture Model (GMM) in the HMM approach. The GMM was used to categorize the changes of the selected features involving sensor data from acoustic, lighting, CO_2 and PIR sensors. These categorizations were then used as observations for the HMM to estimate number of occupants. Adding the GMM to the HMM improved the accuracy of the combined model to between 82% and 85%.

The disadvantage of current methods for data-based occupancy detection is that they need prior information to work in practice. The above-mentioned methods based on physical models (mass balance equation) require detailed a priori information about physical conditions of each room in the building. This type of method therefore needs to be set up manually before application. The above-mentioned statistical models need extensive training data and can therefore not be applied right after they are installed. An alternative method to occupancy detection that overcomes the practical disadvantage of the model-based approaches is the novel plug-and-play method presented in this paper which applies a set of rules on the trajectory of sensor data to detect occupancy. The proposed method was tested in two long-time duration tests and evaluated in terms of its ability to detect occupancy compared to the ground truth.

2. Method

The proposed occupancy detection method tracks the trajectory of sensor data and applies a set of rules to determine a probability of occupancy. This probability is translated into a binary signal that states whether a room is occupied or vacant based on user-defined thresholds. Two different sets of rules are developed: one for impulse-based sensor data (PIR and noise) and one for sensor data governed by the mass balance equation (air temperature, relative humidity, CO_2 concentration and VOC). The following sections explain in detail the two different sets of rules.

2.1. PIR and noise

The principle of occupancy detection based on PIR and noise sensor signals is illustrated in Fig. 1. Let S be a sensor signal, P the probability of occupancy and C a binary indicator of occupancy. The PIR sensor signal in a discrete time step k (S_{PIR}^k) is considered an indicator of occupancy if $S_{PIR}^k = 1$, thus the room is considered occupied ($C_{PIR}^k = 1$) with probability $P_{PIR}^k = 1$. When the noise sensor signal S_{noise}^k is larger than an empirically specified threshold (T_{noise}), the signal is considered to indicate occupancy ($C_{noise}^k = 1$) with $P_{noise}^k = 1$. The reason for T_{noise} is to ensure robustness towards background noise in the microphone. In the next discrete time step $k+1$, the probability of occupancy for each sensor data decreases
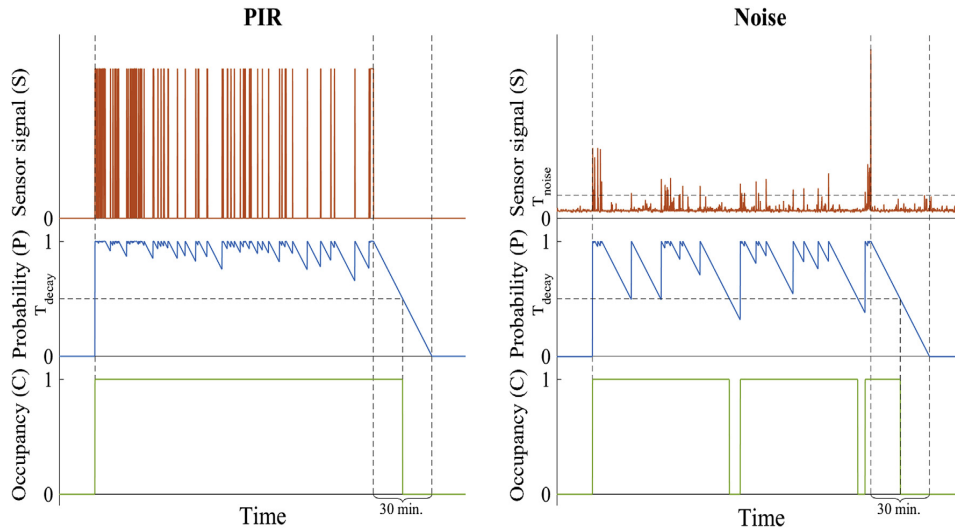
PIR

Noise

Fig. 1. Illustration of the principle of occupancy detection. Left: PIR sensor signals. Right: Noise sensor signals.

linearly if $S_{PIR}^{k+1} = 0$ and $S_{noise}^{k+1} < $ T$_{noise}$, respectively. After 30 min the probability equals $P_{PIR}^{k+30min} = 0$ and $P_{noise}^{k+30min} = 0$. The binary state of 'no occupancy' ($C_{PIR}^{k+i} = 0$ and $C_{noise}^{k+i} = 0$) is determined with respect to a user-defined threshold regarding the probability (T$_{decay}$), i.e C$_{PIR} = 0$ and C$_{noise} = 0$ after $i = \left(1 - T_{decay}\right) \cdot 30$ minutes.

2.2. Air temperature, humidity, CO₂ and VOC

To minimize the risk of false detections due to measurement noise and irregular air movement, it is necessary to filter the indoor climate sensor data prior to any analysis of trajectory to smoothen measurement spikes (see Fig. 2). The Exponential Moving Average (EMA) filter, eq. (1), was chosen due to its computational efficiency and causality which are important in real-time applications.

$$\bar{x}_k = \frac{n}{n+1}\bar{x}_{k-1} + \left(1 - \frac{n}{n+1}\right)x_k \tag{1}$$

where $\bar{x}_k$ is the EMA filtered value at time step k, $\bar{x}_{k-1}$ is the EMA filtered value at time step k-1, x_k is the actual sensor data value at time step k, and n is a factor expressing the tolerated lag between the actual sensor data and EMA filtered data in time step k. This lag is reduced according to eq. (2) resulting in a zero lag exponential moving average (ZLEMA), $\bar{z}_k$ [48].

$$\bar{z}_k = \bar{x}_k + \left(\bar{x}_k - \left(\frac{2n}{2n+1}\bar{x}_{k-1} + \left(1 - \frac{2n}{2n+1}\right)x_k\right)\right) \tag{2}$$

In case of a linear trend, the ZLEMA approach eliminates the lag. However, using this approach on a non-linear trend (which is the case for indoor climate sensor data) only reduces the lag. When detection state changes from 'occupied' to 'unoccupied' and vice versa, a low value of n is preferred since the changes caused by occupants are much greater than the measurement noise. However, when the measurement data is stagnating for a long consecutive period, a large value of n is preferred since the greatest part of the measurement changes is due to sensor noise. This makes the selection of an appropriate value of n a critical task.

Fig. 2 shows that the ZLEMA filtered data corresponds better to the actual data trajectory when having different values of n depending on whether the indoor climate sensor data increases, decays or stagnates. A ZLEMA filter using $n = 50$ (approx. 4 min) results in a highly fluctuating trajectory of the filtered data in
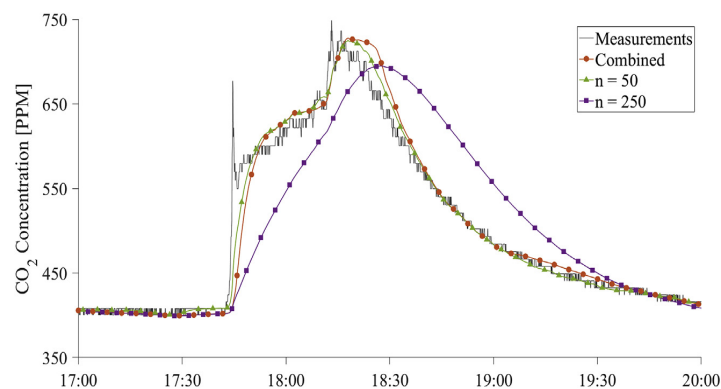

Fig. 2. Example of trajectory of filtered data using different lag factors in the ZLEMA filter.

situations where the sensor data is only affected by measurement noise (e.g. time 17.00−17.45) but results in a fast-reacting and smooth approximation to sensor data when persons enter or leave the room (e.g. 17.45−18.45 and 18.45−20.00, respectively). A ZLEMA filter using $n = 250$ (approx. 20 min) results in a smooth trajectory of sensor data in situations where the sensor data is only affected by measurement noise (e.g. time 17.00−17.45) but yields a poor approximation when persons enter or leave the room compared to $n = 50$. A combination of the filter lags (red line in

Fig. 2) seems to be a suitable solution for eliminating measurement noise while maintaining a trajectory of data which is similar to the raw measurement data. The combination is based on the slopes of the linear trends (Fig. 3(a−e)) where $n = 250$ if the slope is below a threshold (a_{max}) or if the slope is larger than a threshold (a_{min}), otherwise $n = 50$. The thresholds a_{min} and a_{max} are specified empirically for each individual sensor. Furthermore, n increases and decreases linearly with a maximum time delay of 2 min from $n = 250$ to $n = 50$ to prevent undesired leaps in the sensor data

(a) Increasing five-minute linear trend   (b) Increasing two-minute linear trend

(c) Stagnating five-minute linear trend   (d) Stagnating two-minute linear trend

(e) Decreasing five-minute linear trend   (f) Decreasing two-minute linear trend
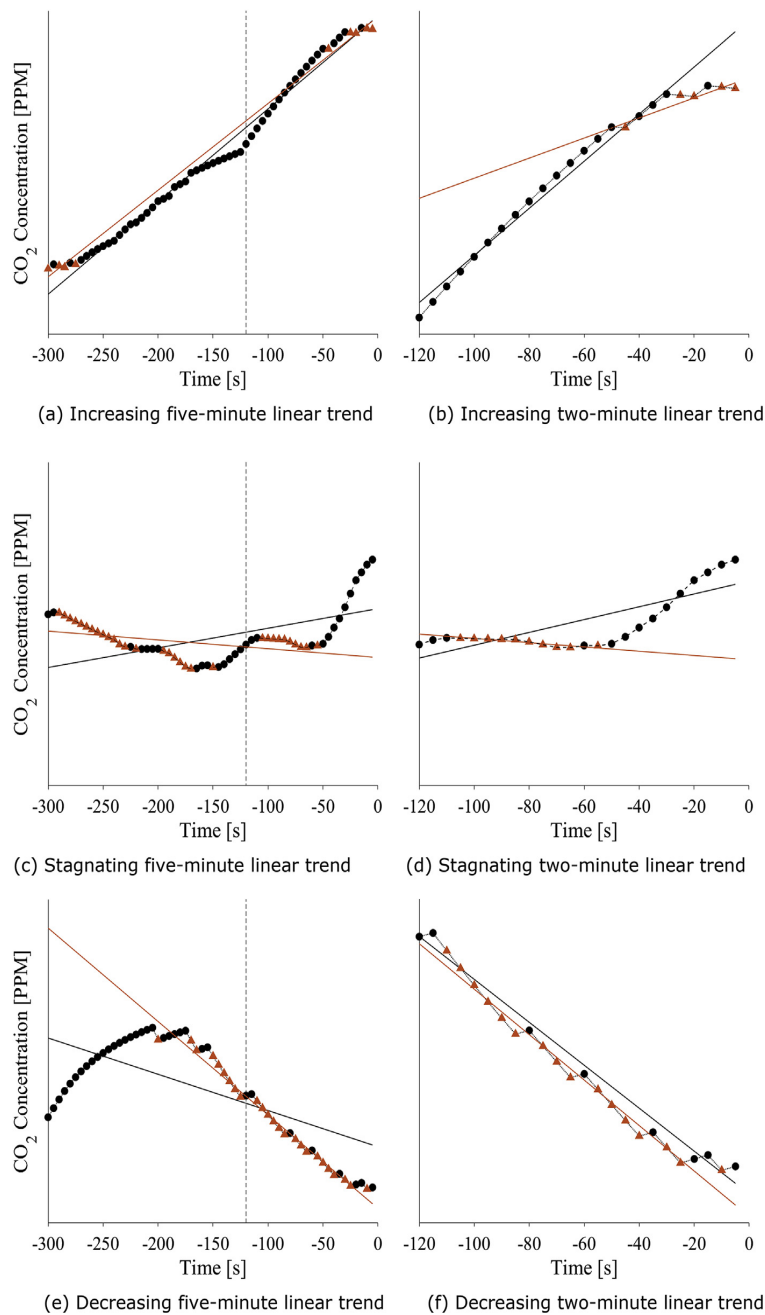
Fig. 3. The principle of occupancy detection based on the trajectory of sensor data.

trajectory.

Once the measured indoor climate data has been filtered, the following approach is applied to detect occupancy. In each time step the ZLEMA filtered data for a two and five-minute historic period is divided into two different groups of data depending on whether the data value in a certain time step is higher or lower than the data value in the previous time step. The two groups for two-minute historic periods are depicted in Fig. 3(b,d,f) and the five-minute historic periods in Fig. 3(a,c,e). A value marked with black indicates that the value is higher than the value in the previous time step, and a value marked with orange indicates that the value is lower than the value in the previous time step. Next, a linear regression of the black and orange data groups is determined (the black and orange lines in Fig. 3(a–e) for increasing and decaying instances, respectively) and the following set of rules is applied:

1. If both of the two-minute trends are positive (Fig. 3(b)) the probability of occupancy is set to $P = 1$, and consequently $C = 1$.
2. If one of the two-minute trends is positive and the other is negative (Fig. 3(d)), the probability of occupancy remains unchanged.
3. If the two-minute trends and the five-minute decaying trend are all negative (Fig. 3(e and f)), the probability of occupancy decays linearly. The rate at which the probability decays is determined each time rule 3 is first detected as $\Delta P = t/(S_0 - S_{ref})$, where S_0 is the sensor signal of the first two-minute data group value and t is the time at which the sensor reaches the reference level S_{ref} (pre-defined threshold, e.g. outdoor CO_2 concentration). The time t is determined by fitting an exponential regression. The reason for considering the five-minute decaying trend is to ensure that the decay is evolved before performing the exponential fit.

The probability is translated to a binary occupancy signal, where 'no occupancy' is determined with respect to a user-defined threshold (T_{decay}), i.e $C = 0$ when $P \leq T_{decay}$.

2.3. Data logger

The proposed occupancy detection method relies on indoor climate data, which may already be monitored by building management systems for other purposes than occupancy detection. However, to be independent of whether a case building has the required sensors installed or not, an inexpensive, mobile and non-intrusive online data logger for collection of sensor data was developed (Fig. 4). The data logger has sensors for measurement of air temperature, relative humidity, CO_2 concentration, total volatile organic compounds (VOC), noise and motion detection (PIR). Besides data from these six sensors, the absolute water content (AWT)

was calculated from the temperature and relative humidity measurements. The sensors were connected to an online Arduino Mega [49] which manages the sampling from the sensors and transmits sensor data to a MySQL database.

The temperature and humidity sensor was the AM2315 [50] which has a minimum sampling frequency of 0.5 Hz and a declared measurement error of ± 0.1 °C and $\pm 2\%$ RH. The CO_2 concentration sensor was the MG811 [51] which applies the solid electrolyte cell principle for CO_2 concentration measurements in the range of 350 to 10.000 ppm. Alcohol and solvent vapours (VOCs) are measured in the range of 50 to 5.000 ppm with the semiconductor gas sensor TGS 2620 [52]. The noise measurement was made using the omnidirectional microphone CMA-4544PF-W [53] with an integrated adjustable amplifier. Motion detection was detected using the prefabricated PIR motion sensor from Adafruit [54] with adjustable sensitivity.

The AM2315 sensor was pre-calibrated by the manufacturer but the remaining sensors required manual calibration. The accuracy of the remaining sensors therefore depends on how careful this calibration is performed. However, the absolute value of the measurement was not essential to the proposed method as the method simply tracks the trajectory of the measurements, but the sensors needed to provide a true image of the measurement process. Large measurement error could distort this progress but the magnitude of the measurement errors of the sensors used in this data logger was not observed to have any practical implication on the purpose of the proposed method.

2.4. Experimental setup

The proposed occupancy detection method was tested during two tests to verify its performance. The first test was conducted in a controlled test room in the Navitas building, Aarhus University, Denmark. Secondly, a comprehensive test was performed at a dormitory apartment. For each test case, ground truth data was collected using the camera technology described in Ref. [33]. Sensor data was collected in parallel to the ground truth using the data logger described in section 2.3. The detailed setups of the cases are described in the following sections.

2.4.1. Test room

The 1.8×2.8 m test room represented a single person office with a ceiling height of 3.0 m. No surfaces were exposed to the outdoor climate, and the room had only one entrance from a hallway (Fig. 5). The room had balanced mechanical ventilation with a constant air volume and a locally controllable radiator. The ground truth camera was installed outside the room above the entrance door and the online sensors were placed in the middle of the room at ceiling height. This was a simple test case where the
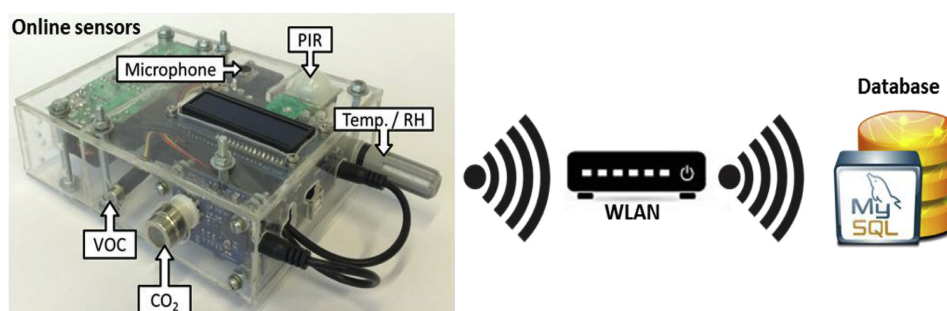
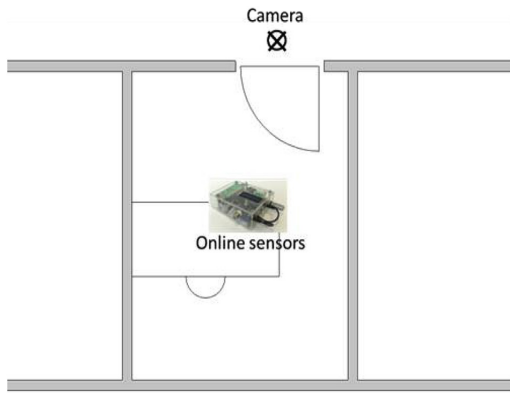

Fig. 4. Data logger setup.

Fig. 5. Setup of test room.

sensor data was only affected by the occupant of this specific room, i.e. no direct impact from weather conditions or open connections to adjacent occupied zones. Data was logged in a period from 26.11.2015 to 04.12.2015.

2.4.2. Dorm apartment

A three-room dorm apartment, shared by two persons, with one entrance from a hallway was selected as a second test case (Fig. 6). The two facades with windows were the only surfaces facing the outdoors. The apartment has mechanical ventilation with a constant air volume supplied in the two individual bed rooms and exhaust from the common bathroom, and a locally controllable radiator in each room. The ground truth camera was installed above the entrance door and the online sensors were placed in the living room at ceiling height. This was a more complex test case compared to the test room described in section 2.4.1 because 1) the sensor data can be affected directly by weather conditions, and 2) sensor data was only logged in the common room adjacent to the two individual bed rooms which might be the preferred staying zones. Consequently, it might be difficult to use sensor data for occupancy detection at apartment level. Data was logged in a period of 18 days from 7 to 25 January 2015.

3. Results and discussion

The following sections present the results of the proposed method from the two test cases. First, the mechanism is depicted
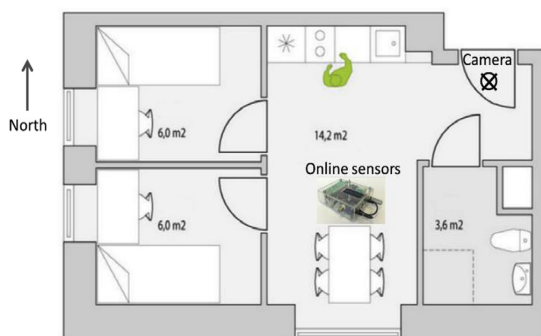

Fig. 6. Geometry and setup of the dorm apartment.

for one test day. Secondly, detections for a longer period are evaluated and lastly the mean absolute errors are determined for the entire test period. The threshold T_{decay}, used to convert occupancy probability into a binary occupancy value, has to be specified manually before operation. For the sensor data described in section 2.2, T_{decay} was set to 0.8 for the simple test room, while for the complex dorm apartment T_{decay} was set to 0.6, thus leading to more conservative binary occupancy state changes. For the PIR and noise sensor data, T_{decay} was set to 0 for both test cases, i.e. $i = 30$ min (see section 2.1).

3.1. Detection mechanism

Fig. 7 displays the mechanism of the proposed occupancy detection method during one day in the test room. Applying the method to the various sensor data provides fast detection when a person enters the room (i.e. state transition from 'unoccupied' to 'occupied'). At the specific day displayed in Fig. 7, the noise, RH and AWT led to occupancy detection before first arrival. At first arrival at 9, a limited time-delay is observed for occupancy detection based on sensor data from PIR (<1 min), noise (<1 min), CO_2 (5 min) and VOC (5 min), whereas temperature (17 min), RH (10 min) and AWT (11 min) reacted much slower. Sensor data from noise and CO_2 provided acceptable information on intermittent vacancy periods, whereas the other sensors only captured one shorter vacancy period. When the occupant left the room (i.e. state transition from 'occupied' to 'unoccupied'), the detection approach based on PIR and noise sensor data (described in section 2.1) was limited by the assumption of a 30 min hysteresis from last signal to state transition. The time-delay detection based on CO_2 (10 min), RH (12 min) and AWT (23 min) was limited, whereas VOC (39 min) and the room air temperature (63 min) reacted more slowly.

3.2. Occupancy detection

The binary occupancy schedules (i.e. C in Fig. 1) during a six-day period for the test room and dorm apartment are depicted in Fig. 8 and Fig. 9, respectively. The results from the test room suggest that under simple and controlled conditions, all indoor climate parameters are highly correlated with occupant presence. Thus using the trajectory of the sensor data enables convincing occupancy detection. However, detection based on relative humidity sensor signal and AWT led to false occupancy detections during the night between November 29 and 30. The results from the dorm apartment show a significant difference between the sensor-based detections. Furthermore, the results stress the challenge of measuring sensor data in the common room, while the occupants stayed in their individual bedrooms. This tendency is best observed by the detections based on the PIR sensor data which detected occupancy at the beginning and end of each stay when the occupants walked through the common room. Fig. 9 also shows that detections based on temperature sensor data in the dorm apartment primarily led to 'occupancy' state detections.

3.3. Mean absolute error

The percentage of false and true detections of the proposed method compared to the ground truth of the test room and the dorm apartment test case are listed in Table 1 and Table 2, respectively. Since the evaluated occupancy schedules are binary dichotomous sequences, each time step can be characterized as either:
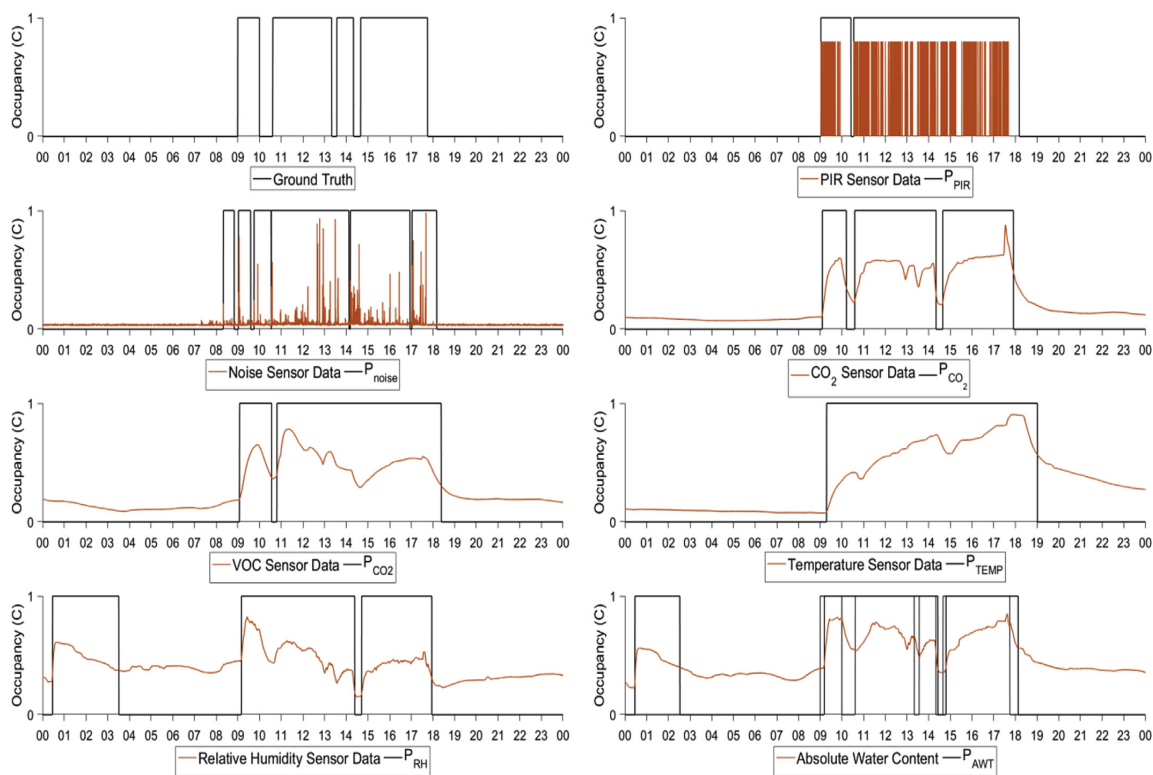
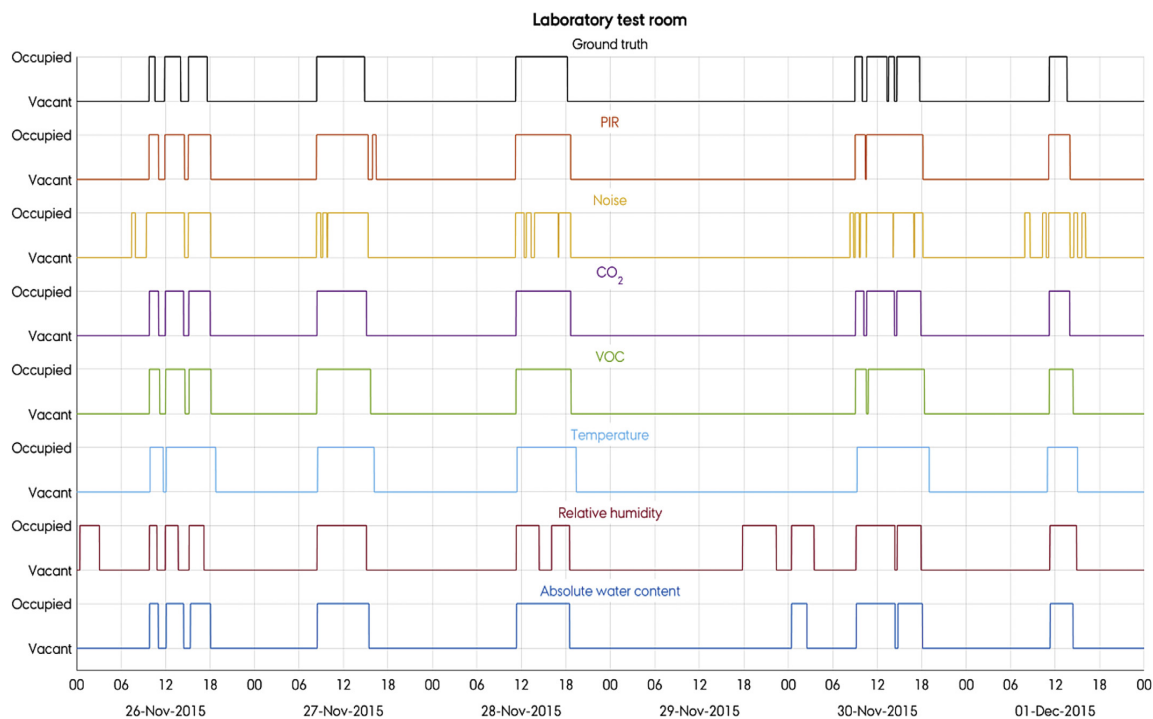**Fig. 7.** Detection mechanism illustrated for a period of 24 h.
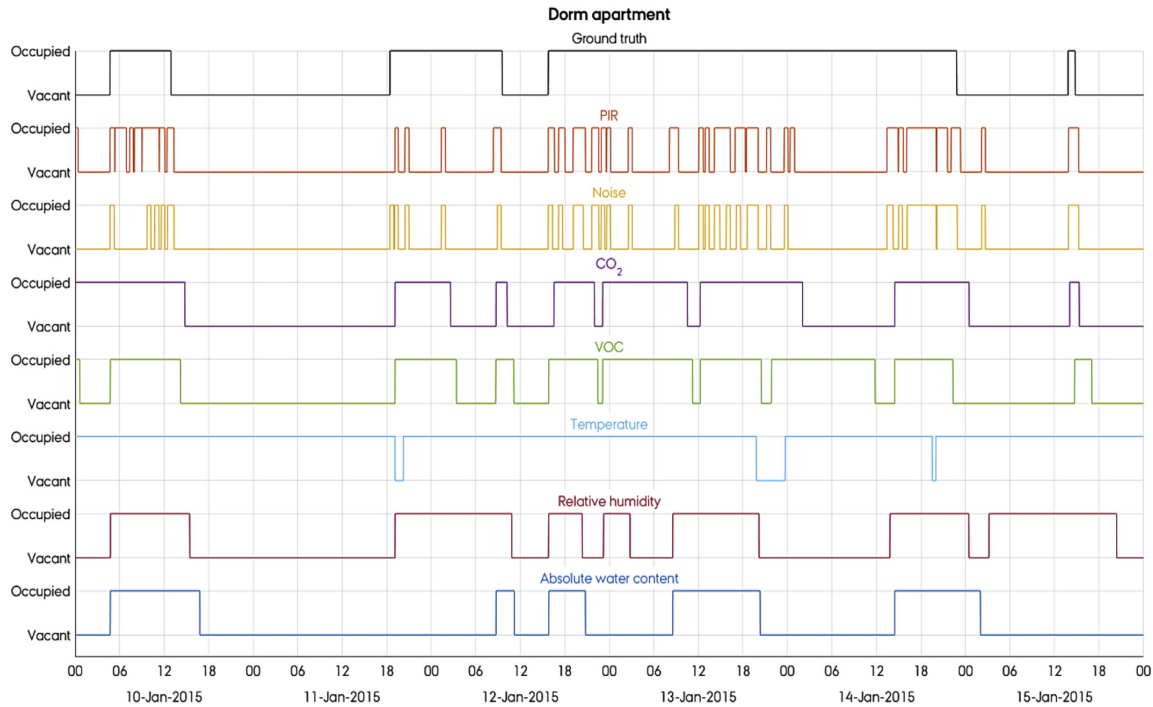

Fig. 8. Detection result from six days at the test room.

Fig. 9. Detection result from six days during the test at the dorm apartment.

Table 1
Results test room.

	False Negatives	False Positives	True Negatives	True Positives
PIR	0.0%	2.8%	78.9%	18.3%
Noise	1.3%	7.6%	74.1%	17.0%
CO_2	0.2%	1.7%	80.0%	18.1%
VOC	0.3%	4.0%	77.7%	18.0%
TEMP	0.5%	15.1%	66.6%	17.8%
RH	1.3%	19.7%	62.0%	17.0%
AWT	0.6%	11.5%	70.2%	17.7%
PIR&CO_2	0.0%	2.1%	79.6%	18.3%
PIR&VOC	0.1%	4.4%	77.3%	18.2%

Table 2
Results dorm apartment.

	False Negatives	False Positives	True Negatives	True Positives
PIR	43.5%	2.8%	21.0%	32.7%
Noise	52.5%	1.9%	21.9%	17.0%
CO_2	16.4%	11.0%	12.8%	59.8%
VOC	15.2%	10.1%	13.7%	61.0%
TEMP	5.4%	23.7%	0.1%	70.8%
RH	22.1%	13.9%	9.9%	54.1%
AWT	38.8%	8.4%	15.4%	37.4%
PIR&CO_2	14.6%	11.3%	12.5%	61.5%
PIR&VOC	14.0%	8.2%	15.6%	62.2%

a. False negative - ϵ_{neg} (i.e. ground truth state is 'occupancy' but method state is 'no occupancy', resulting in a reduction of HVAC systems which potentially leads to occupant discomfort)

b. False positive - ϵ_{pos} (i.e. method state is 'occupancy' but the ground truth state is 'no occupancy', potentially leading to unnecessary HVAC energy use to maintain the indoor climate)

c. True negative - τ_{neg} (i.e. method state is 'no occupancy' and the ground truth state is 'no occupancy')

d. True positive - τ_{pos} (i.e. method state is 'occupancy' and the ground truth state is 'occupancy').

Two controlled combinations of probability data were further investigated: PIR & CO_2 and PIR & VOC. The PIR sensor signal determined when the room transitioned from 'unoccupied' (C = 0) to 'occupied' (C = 1) while the change of state to 'unoccupied' (C = 1 to C = 0) was determined exclusively by the probability of occupancy calculated from the CO_2 or VOC sensor data, respectively.

The mean absolute error (ϵ) was calculated as the sum of ϵ_{neg} and ϵ_{pos}. Detections based solely on CO_2 sensor data had the lowest error ($\epsilon = 0.02$) for the test room (Table 1). However, applying the proposed method to PIR ($\epsilon = 0.03$), VOC ($\epsilon = 0.04$) and noise ($\epsilon = 0.09$), sensor data also yielded reliable occupancy detections, but the detections based on noise and VOC sensor data had a small fraction of false negative detections. The absolute water content of the indoor air ($\epsilon = 0.12$), derived from measurements of the temperature and relative humidity, was a better indicator of occupancy than temperature ($\epsilon = 0.16$) and relative humidity ($\epsilon = 0.21$) data, but the detection error was a factor 6 higher than detections based on CO_2 sensor data. The controlled combinations did not result in fewer errors than for CO_2 data alone. The true negatives show that the room was vacant for a large share of the time.

For the dorm apartment (Table 2), detections based solely on PIR ($\epsilon = 0.46$) and noise ($\epsilon = 0.54$) sensor data yielded high detection errors with a large fraction of false negative detections. This demonstrates the limitations of PIR sensors as the reason presumably is that occupants were in the apartment but outside the field-of-view of the PIR sensor and too far away from the noise sensor. Applying the proposed method to CO_2 ($\epsilon = 0.27$), VOC ($\epsilon = 0.25$), temperature ($\epsilon = 0.29$) and relative humidity ($\epsilon = 0.36$), sensor data

constituted a better indicator of occupancy. Detections based on temperature had the lowest fraction of false negative detections. As mentioned earlier, the reason was that the proposed method applied to the temperature data yielded very few periods of vacancy, also seen from the percentage of true negatives, because the correlation between the temperature measurements and occupancy is limited and also affected by disturbances like the ambient temperature and solar radiation (see Fig. 9). The occupants that lived in the dorm apartment often stayed for long periods; thus, the state of 'occupied' was often a good guess. However, the temperature data analysis did not capture the occupants' schedules and therefore provided very little occupancy information overall. The controlled combinations using PIR & VOC sensor data had the lowest detection error ($\varepsilon = 0.22$) and the controlled combinations using PIR & CO_2 slightly improved the detection based on CO_2 alone ($\varepsilon = 0.26$). This suggested that the PIR signal was the most appropriate probe for determining whether the state of the dorm apartment went from 'unoccupied' to 'occupied'. The VOC or CO_2 sensor data was used to determine when the room transitioned from 'occupied' to 'unoccupied' as this data was able to indicate when occupants stayed within the apartment but not necessarily in the room where the sensors were placed.

The results suggest that tracking the trajectory of the standalone CO_2, PIR or VOC sensor data is a good probe for determining occupancy in simple one-room zones, and applying the method on VOC or CO_2 concentration sensor data might be a good supplement to improve occupancy detection in building zones, where occupants may be in the zone but outside the field-of-view of the PIR sensor. It is also interesting that VOC sensor data seems to be an alternative to CO_2 sensor data as a probe for determining occupancy of building zones.

4. Conclusion

A novel plug-and-play method for occupancy detection based on sensor data, which often is available in most buildings for other reasons than occupancy detection, is proposed and evaluated. The proposed method is based on a set of rules applied to the trajectory of sensor data. Applying the proposed method using PIR, noise, CO_2 and VOC concentration, relative humidity and temperature sensor data obtained from a simple test room and a three-room dorm apartment resulted in a maximum accuracy of 98% and 78%, respectively. The reported accuracies are in the same range as existing physical and statistical data based methods (reported in section 1.1). However, contrary to existing methods, the proposed method is immediately operational (plug-and-play) as it does not require time-consuming gathering of detailed information about the physical conditions of the room or the need to wait for extensive training data prior to reliable operation.

Future work is needed to investigate how the method should deal with false negative and false positive detections in practice, and how to enable the method to detect the number of persons and any detailed occupant behavior such as window openings. Furthermore, exploring the sensitivity of different sensor combinations and locations to improve occupancy detection in various types of rooms constitutes future work.

Acknowledgement

References

[1] L. Pérez-Lombard, J. Ortiz, C. Pout, A review on buildings energy consumption information, Energy Build. 40 (2008) 394–398, http://dx.doi.org/10.1016/j.enbuild.2007.03.007.

[2] J. Yang, M. Santanouris, S.E. Lee, Review of occupancy sensing systems and occupancy modeling methodologies for the application in institutional buildings, Energy Build. 121 (2016) 344–349.

[3] C. Duarte, R. Budwig, K. Van den Wymelenberg, "Energy and demand implication of using recommended practice occupancy diversity factors compared to real occupancy data in whole building energy simulation, J. Build. Perform. Simul. 8 (6) (2014) 408–423.

[4] F. Tahmasebi, A. Mahdavi, The sensitivity of building performance simulation results to the choice of occupants' presence models: a case study, J. Build. Perform. Simul. (2015) 1–11, http://dx.doi.org/10.1080/19401493.2015.1117528.

[5] A. Mahdavi, F. Tahmasebi, The deployment-dependence of occupancy-related models in building performance simulation, Energy Build. 117 (2016) 313–320.

[6] Y. Agarwal, B. Balaji, S. Dutta, R.K. Gupta, T. Weng, Duty-cycling buildings aggresively: the next frontier in HVAC control, Chicago, Illinois, in: Information Processing in Sensor Network (ISPN), 2011.

[7] Y. Tachwali, H. Refai and J. E. Fagan, "Minimizing HVAC Energy Consumption Using a Wireless Sensor Network," in Annual Conference of the IEEE Industrial Electronics Society (IECON), Taipai, Taiwan, 2007.

[8] V. Dhummi, D. Demetriou, H.J. Palanthandalam-Madapusi, H.E. Khalifa, I. Isik, Robust occupancy-based distributed demand control ventilation, Int. J. Vent. 9 (4) (2011) 359–369.

[9] M.J. Brandemuehl, J.E. Braun, The Impact of Demand-controlled and Economizer Ventilation Strategies on Energy Use in Buildings, ASHRAE Transactions, Seattle, 1999.

[10] B. Dong, K.P. Lam, Building energy and comfort management through occupant behaviour pattern detection based on a large-scale environmental sensor network, J. Build. Perform. Simul. 4 (4) (2011) 359–369.

[11] J. Brooks, S. Kumar, S. Goyal, R. Subramany, P. Barooah, Energy-efficient control of under-actuated HVAC zones in commercial buildings, Energy Build. 93 (2015) 160–168.

[12] Z. Yang, B. Becerik-Gerber, How does building occupancy influence energy efficiency of HVAC systems? Energy Procedia 88 (2016) 775–780.

[13] Z. Yang, B. Bercerik-Gerber, Modeling personalized occupancy profiles for representing long term patterns by using ambient context, Build. Environ. 78 (2014) 23–35.

[14] S.S. Kwok, R.K. Yuen, E.W. Lee, An intelligent approach to assessing the effect of building occupancy on building cooling load prediction, Build. Environ. 46 (2011) 1681–1690.

[15] P. Correia da Silva, V. Leal, M. Andersen, Occupants interaction with electric lighting and shading systems in real single-occupied offices: results from a monitoring campaign, Build. Environ. 64 (2013) 152–168.

[16] T. Labeodan, C.D. Bakker, A. Rosemann, W. Zeiler, On the application of wireless sensors and actuators network in existing buildings for occupancy detection and occupancy-driven lighting control, Energy Build. 127 (2016) 75–83.

[17] A. Peruffo, A. Pandharipande, D. Caicedo, L. Schenato, Lighting control with distributed wireless sensing and actuation for daylight and occupancy adaption, Energy Build. 97 (2015) 13–20.

[18] C. Wang, D. Yan, H. Sun, Y. Jiang, A generalized probabilistic formula relating occupant behaviour to environmental conditions, Build. Environ. 95 (2016) 53–62.

[19] C.L. Erickson, M.Á. Carreira-Perpiñán, A.E. Cerpa, OBSERVE: occupancy-based system for efficient reduction of HVAC energy, Chicago, Illinois, in: Information Processing in Sensor Networks (IPSN), 2011.

[20] V.L. Erickson, M.Á. Carreira-Perpiñán, A.E. Cerpa, Occupancy modeling and prediction for building energy management, in: ACM Transactions of Sernsor Network, 2012.

[21] S. Goyal, H.A. Ingley, P. Barooah, Occupancy-based zone-climate control for energy-efficient buildings: complexity vs. performance, Appl. Energy 106 (2016) 209–221.

[22] S. Goyal, P. Barooah, T. Middelkoop, Experimental study of occupancy-based control of HVAC zones, Appl. Energy 140 (2015) 75–84.

[23] J. Page, D. Robinson, N. Morel, J.-L Scartezzini, A generalised stochastic model for the simulation of occupant presence, Energy Build. 40 (2008) 83–98.

[24] S. Lee, Y. Chon, Y. Kim, R. Ha, H. Cha, Occup. Predict. Algorithms Thermostat Control Syst. Using Mob. Devices 4 (3) (2013) 1332–1340.

[25] F. Oldewurtel, D. Sturznegger, M. Morari, Importance of occupancy information for building climate control, 101, Appl. Energy 101 (2013) 521–532.

[26] J.R. Dobbs, B.M. Hencey, Model Predictive HVAC control with online occupancy model, Energy Build. 82 (2014) 675–684.

[27] A. Mirakhorli, B. Dong, Occupancy behaviour based model predictive control for building indoor climate - a critical review, Energy Build. 129 (2016) 499–513.

[28] M. Gruber, A. Trüschel, J.-O. Dalenbäck, Co2 sensors for occupancy estimations: potential in building automation applications, Energy Build. 84 (2014) 548–556.

[29] T. H. Pedersen, M. D. Knudsen, R. E. Hadegaard and S. Petersen, "Handling

Stochastic Occupancy in an Economic Model Predictive Control Framework for Heatin system Operation in Dwellings," in CLIMA 2016-proceedings of the 12th REHVA World Congress: volume 10, Aalborg, Denmark, 2016.

[30] Y. Benezeth, H. Laurent, B. Emile, C. Rosenberger, Towards a sensor for detecting human presence and characterizing activity, Energy Build. 43 (2011) 305−314.

[31] H.-C. Shih, A robust occupancy detection and tracking algorithm for the automatic monitoring and commissioning of a building, Energy Build. 77 (2014) 270−280.

[32] X. Zhang, J. Yan, S. Feng, Z. Lei, D. Yi and S. Z. Li, "Water Filling: Unsupervised People Counting via Vertical Kinect Sensor," in IEEE Ninth International Conference on Advanced Video and Signal-Based Surveillance(AVSS '12), Washington, DC, USA, 2012.

[33] S. Petersen, T.H. Pedersen, K.U. Nielsen, M.D. Knudsen, Establishing an image-based ground truth for validation of sensor data-based room occupancy detection, Energy Build. 130 (2016) 787−793.

[34] Y. Zhao, W. Zeiler, G. Boxem, T. Labeodan, Virtual occupancy sensors for real-time occupancy information in buildings, Build. Environ. 93 (2015) 9−20.

[35] R.H. Dodier, G.P. Henze, D.K. Tiller, X. Guo, Building occupancy detection through sensor belief networks, Energy Build. 38 (2006) 1033−1043.

[36] C. Duarte, K. Van Den Wymelenberg, C. Rieger, Revealing occupancy patterns in an office building through the use of occupancy sensor data, Energy Build. 67 (2013) 587−595.

[37] B. Dong, B. Andrews, K.P. Lam, M. Höynck, R. Zhang, Y.-S. Chiou, D. Benitez, An information technology enabled sustainability test-bed (ITEST) for occupancy detection through an environmental sensing network, Energy Build. 42 (2010) 1038−1046.

[38] G. Ansanay-Alex, "Estimating Occupancy Using Indoor Carbon Dioxide Concentrations Only in an Office Building: a Method and Qualitative assessment," in 11th REHVA world congress Clima 2013, Praque, Czech Republic, 2013.

[39] C.C. Federspiel, Estimating the inputs of gas transport processes in buildings, IEEE Trans. Control Syst. Technol. 5 (5) (2002) 480−489.

[40] S. Wang, X. Jin, CO2-Based occupancy detection for on-line outdoor air flow control, Indoor Built Environ. 7 (1998) 165−181.

[41] S. Wang, J. Burnett, H. Chong, Experimental validation of CO2-based occupancy detection for demand-controlled ventilation, Indoor Built Environ. 8 (1998) 377−391.

[42] D. Calì, P. Matthes, K. Huchtemann, R. Streblow, D. Müller, CO2 based occupancy detection algorithm: experimental analysis and validation for office and residential buildings, Build. Environ. 86 (2015) 39−49.

[43] C. Jiang, M.K. Masood, Y.C. Soh, H. Li, Indoor occupancy estimation from carbon dioxide concentration, Energy Build. 131 (2016) 132−141.

[44] K. P. Lam, M. Höynck, R. Zhang, B. Andrews, Y.-S. Chiou, B. Dong and D. Benitez, "Information-Theoretic Environmental Features Selection for Occupancy Detection in open Offices," in Eleventh International IBPSA Conference, Glasgow, Scotland, 2009.

[45] L.M. Candanedo, V. Feldheim, Accurate occupancy detection of an office room from light, temperature, humidity and CO2 measurements using statistical learning models, Energy Build. 112 (2016) 28−39.

[46] S.H. Ryu, H.J. Moon, Development of an occupancy prediction model using indoor environmental data based on machine learning techniques, Build. Environ. 107 (2016) 1−9.

[47] X. Liang, T. Hong, G.Q. Shen, Occupancy data analytics and prediction: a case study, Build. Environ. 102 (2016) 179−192.

[48] J. Ehlers, R. Way, Zero Lag (Well, Almost), Technical Analysis of Stocks & Commodities, November 2010.

[49] Arduino [Online]. Available, www.arduino.cc, https://www.arduino.cc/en/Main/ArduinoBoardMega2560 [Accessed 21 October 2016].

[50] Adafruit [Online]. Available, www.adafruit.com, https://www.adafruit.com/products/1293 [Accessed 21 October 2016].

[51] Sandboxelectronics [Online]. Available, www.sandboxelectronics.com, http://sandboxelectronics.com/files/SEN-000007/MG811.pdf [Accessed 21 October 2016].

[52] Figarosensor [Online]. Available, www.figarosensor.com, http://www.figarosensor.com/products/2620pdf.pdf [Accessed 21 October 2016].

[53] C.U.I. Inc [Online]. Available, www.cui.com, http://www.cui.com/product/resource/cma-4544pf-w.pdf [Accessed 21 October 2016].

[54] Adafruit [Online]. Available, www.adafruit.com, https://learn.adafruit.com/pir-passive-infrared-proximity-motion-sensor/ [Accessed 21 October 2016].

48

P2 Space heating demand response potential of retrofitted residential apartment blocks
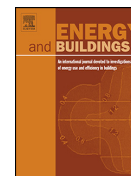
Contents lists available at ScienceDirect

Energy and Buildings

journal homepage: www.elsevier.com/locate/enbuild

Space heating demand response potential of retrofitted residential apartment blocks

Theis Heidmann Pedersen *, Rasmus Elbæk Hedegaard, Steffen Petersen

Department of Engineering, Inge Lehmanns Gade 10, Aarhus University, DK-8000 Aarhus C, Denmark

ARTICLE INFO

ABSTRACT

In future and smarter energy systems, time varying energy prices enable indirect demand response (DR) to assist the electricity supply system to meet demand. This simulation-based study investigates how economic model predictive control (E-MPC) schemes for space heating operation can utilize the thermal mass in an existing multi-story apartment block and eight retrofit scenarios to provide DR. The performance of the E-MPC scheme was evaluated in terms of its ability to enable end-user cost savings, reduce CO_2 emissions and to perform load shift of the heating demand compared to a conventional PI controller. Two E-MPC approaches were considered: centralized E-MPC where inter-zonal effects were considered and decentralized E-MPC that neglected heat transfer between adjacent apartments. The E-MPC schemes led to increasing cost savings (up to approx. 6%) and reduced CO_2 emissions (up to approx. 3%) as a function of increasing energy efficiency of the retrofit scenarios. The absolute amount of shifted power from peak load periods was rather consistent (approx. 2 kWh/m^2 heated net area) across all retrofit scenarios compared to the existing building. The centralized E-MPC scheme led to marginally better results than the decentralized E-MPC. The added complexity involved in establishing a centralized E-MPC compared to a decentralized E-MPC may therefore not be worth the effort.

© 2017 Elsevier B.V. All rights reserved.

1. Introduction

Instantaneous balance between supply and demand is a mandatory characteristic of the electricity supply system. Today, this balance is ensured almost exclusively by adjusting supply to meet demand. However, sheer supply-side management (SSM) is inefficient in systems with a high penetration of intermittent renewable energy sources (RES) such as wind turbines and photovoltaics [1]. Demand-side management (DSM) can to some extent assist supply-side management in such systems. There are different categories of DSM [2]. Traditionally, the most favored aspect of DSM has been energy efficiency [3,4] but recently several studies have explored the potential of demand response (DR), where consumers adjust their demand to meet supply [5–9]. It has mainly been applied by large scale industrial and commercial customers [10] but DR programs for space heating for residential customers could also be considered as they represents a large share of the total consumption: Private households accounted for approx. 25% of the total energy consumption in the European Union (EU) in 2011 [11] of

which approx. 67% was used for space heating in the Northern and Western regions of the EU [12].

Several studies have demonstrated DR potentials in residential space heating operation. A simulation-based study by Acvi et al. [13] obtained a 13% cost reduction and reduced the energy consumption in peak-hours by 23.6% compared to a baseline controller by applying real time prices (RTP) together with economic model predictive control (E-MPC) of an AC unit in a single residence. Halvgaard et al. [14] investigated the performance of a residential-scale heat pump operated by an E-MPC scheme using RTP. The control scheme achieved 25% cost savings using hard comfort constraints and 35% using softened constraints. Vrettos et al. [15] used day-ahead prices in an E-MPC scheme to investigate the DR potential of a residential building equipped with several installations for efficient DR (heat pump, slab cooling, electrical water heater, PV and battery) and achieved an energy consumption reduction of 20% and cost savings of 28% compared to a rule-based controller (RBC). Knudsen and Petersen [16] applied RTP and corresponding CO_2 intensity signals to an E-MPC scheme for space heating operation in a residential apartment and demonstrated a potential for cost savings together with CO_2 emission reductions as well as shifting consumption from periods of peak load to low load periods.

However, to the knowledge of the authors, there have been only a few studies on how the thermal characteristics of existing resi-

---

* Corresponding author.
E-mail address: thp@eng.au.dk (T.H. Pedersen).

Table 1
Construction characteristics of the existing building.

Construction type	Material	Thickness	Thermal Properties	
Interior Wall	Concrete	0.120 m	$\lambda = 1.10$ W/(m K)	$c = 920$ J/(kg K)
Floor/Ceiling	Wood	0.020 m	$\lambda = 0.15$ W/(m K)	$c = 1630$ J/(kg K)
	Insulation	0.050 m	$\lambda = 0.04$ W/(m K)	$c = 1210$ J/(kg K)
	Air space	0.050 m	$R = 0.18$ (m^2 K)/W	
	Hollow concrete slap	0.180 m	$\lambda = 1.29$ W/(m K)	$c = 270$ J/(kg K)
Exterior Wall – Facades	Concrete	0.070 m	$\lambda = 1.10$ W/(m K)	$c = 920$ J/(kg K)
	Insulation	0.060 m	$\lambda = 0.04$ W/(m K)	$c = 1210$ J/(kg K)
	Concrete	0.080 m	$\lambda = 1.10$ W/(m K)	$c = 920$ J/(kg K)
Exterior Wall – Gables	Concrete	0.095 m	$\lambda = 1.10$ W/(m K)	$c = 920$ J/(kg K)
	Insulation	0.060 m	$\lambda = 0.04$ W/(m K)	$c = 1210$ J/(kg K)
	Air space	0.015 m	$R = 0.15$ (m^2 K)/W	
	Concrete	0.150 m	$\lambda = 1.10$ W/(m K)	$c = 920$ J/(kg K)
	Air space	0.015 m	$R = 0.15$ (m^2 K)/W	
	Insulation	0.060 m	$\lambda = 0.04$ W/(m K)	$c = 1210$ J/(kg K)
	Concrete	0.090 m	$\lambda = 1.10$ W/(m K)	$c = 920$ J/(kg K)
Existing window	Double glazing (4-12Air-4)	0.020 m	$U_{glazing} = 2.84$ W/(m^2 K)	$g_{glazing} = 0.773$
	Wood frame		$U_{frame} = 1.700$ W/(m^2 K)	

Table 2
Facade retrofit measures.

Construction name	Material	Thickness	Thermal Properties	
Facade 1	External insulation	0.125 m	$\lambda = 0.036$ W/(m K)	$c = 920$ J/(kg K)
Facade 2	External insulation	0.205 m	$\lambda = 0.036$ W/(m K)	$c = 920$ J/(kg K)
2-layer window	Low-E glazing (4-14Ar-LowE4)	0.022 m	$U_{glazing} = 1.220$ W/(m^2 K)	$g_{glazing} = 0.671$
	Wood/Alu frame		$U_{frame} = 1.700$ W/(m^2 K)	
3-layer window	Low-E glazing (4LowE-14Ar-4-14Ar-LowE4)	0.040 m	$U_{glazing} = 0.688$ W/(m^2 K)	$g_{glazing} = 0.547$
	Wood/Alu frame		$U_{frame} = 1.700$ W/(m^2 K)	

dential buildings affect DR potentials of space heating operation. Reynders et al. [17] applied an RBC scheme to investigate the relation between energy efficiency of the building envelope and the potential for exploiting the structural thermal storage for DR in dwellings. Simulation results for six test cases showed that up to 40% of the stored energy was lost due to poor thermal characteristics. A subsequent parametric study of the building envelope thermal characteristics suggested that increased insulation level and air tightness were the two most important factors to increase the DR efficiency [18]. Upgrading the thermal performance of building envelopes of existing residential buildings in an energy system with a high penetration of renewable energy production therefore seems to be critical if space heating is to be used for DR.

The aim of the work reported in this paper is to contribute with further knowledge regarding the importance of the thermal characteristics of existing residential building envelopes on the latent DR potentials in residential space heating. The paper reports on a simulation-based study where centralized and decentralized E-MPC were used to operate the space heating in eight retrofit scenarios of an existing residential multi-story apartment block. The E-MPC scheme was evaluated in terms of its ability to reduce end-user cost, CO_2 emission and the resulting load shift of heating demand.

2. Method

A section of an existing apartment block was modelled in EnergyPlus (EP) [19] and represents as such an actual building to be controlled by E-MPC. The E-MPC scheme was implemented in MATLAB [20] and used to operate the space heating (electrical baseload) of the EP model through co-simulation using the Building Controls Virtual Test Bed (BCVTB) [21,22]. The following sections provide further information on the modelling of the test case in EP, the building model used in the E-MPC, the E-MPC scheme and the performance evaluation metrics used for performance evaluation of the E-MPC scheme.

2.1. EnergyPlus model

The third floor of an existing four-story apartment block was used as test case and thus modelled in EP. The EP files are provided in ref. [23]. The block was built in 1978 and has only undergone minor refurbishments since then. The geometry is depicted in Fig. 1 and consists of five stairwells (S) and ten apartments: one 1-room apartment (9), four 3-room apartments (1, 3, 5 and 7) and five 4-room apartments (2, 4, 6, 8 and 10) with east-west oriented facades where the west oriented facades have unheated balconies (blue boxes in Fig. 1). The stairwells and apartments were modelled as individual thermal zones with adiabatic horizontal surfaces (floor and roof). The stairwells were kept at a minimum temperature of 15 °C while the apartments had individual heating with different set points as explained in Section 2.4.

The thermal characteristics of the existing building envelope used in the EP model are specified in Table 1. The windows were modelled in WINDOW [24] and imported into the EP model. The infiltration air change rate was modelled as a constant rate of 0.5 h^{-1}. Internal loads from people and equipment were neglected to make the results easier to interpret. The Conduction Finite Difference algorithm in EP was used to calculate the construction heat balances with a 60 s time step. The standard EP weather data file for Copenhagen, Denmark was used in all simulations [25]. The simulation period was November 1, 2015 to February 28, 2016, which constitutes the coldest period of the heating season in Denmark.

To investigate the influence of the energy efficiency of the building envelope, a range of typically used retrofit solutions for existing Danish apartment blocks (Table 2) were combined into eight retrofit scenarios (Table 3) with gradually increasing energy efficiency. All scenarios were assumed to increase the air tightness due to the increased focus on the importance of building air tightness compared to when the existing building was constructed; hence, the infiltration rate was reduced to either 0.18 h^{-1} or 0.1 h^{-1} in an attempt to investigate the effect of different retrofit ambitions. Mechanical ventilation with heat recovery efficiency of 80% was assumed in all retrofit scenarios to ensure a constant air change of
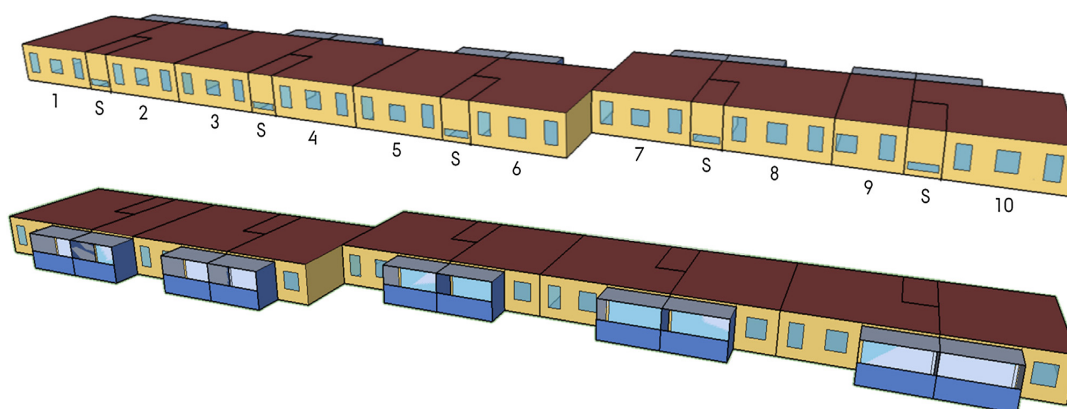
Fig. 1. Test case geometry as modelled in EnergyPlus with applied apartment numbering.

Table 3
Retrofit scenarios.

	External insulation	Window	Infiltration rate
Existing	–	existing	$0.50\,\mathrm{h^{-1}}$
Retrofit1	0.125 m	2-layer	$0.18\,\mathrm{h^{-1}}$
Retrofit2	0.125 m	2-layer	$0.10\,\mathrm{h^{-1}}$
Retrofit3	0.205 m	2-layer	$0.18\,\mathrm{h^{-1}}$
Retrofit4	0.205 m	2-layer	$0.10\,\mathrm{h^{-1}}$
Retrofit5	0.125 m	3-layer	$0.18\,\mathrm{h^{-1}}$
Retrofit6	0.125 m	3-layer	$0.10\,\mathrm{h^{-1}}$
Retrofit7	0.205 m	3-layer	$0.18\,\mathrm{h^{-1}}$
Retrofit8	0.205 m	3-layer	$0.10\,\mathrm{h^{-1}}$

Table 4
Average model fit-percentage compared to validation data.

	Multi-zone	Single-zone
Existing	84%	91%
Retrofit1	86%	88%
Retrofit2	84%	87%
Retrofit3	87%	88%
Retrofit4	85%	88%
Retrofit5	87%	85%
Retrofit6	86%	84%
Retrofit7	88%	86%
Retrofit8	87%	86%

$0.5\,\mathrm{h^{-1}}$ in all apartments. The retrofit measures facade 1 and facade 2 in Table 2 would, in practice, also consist of an external cladding and other materials but the thermal characteristics of these were neglected in the model.

2.2. Control model

A model describing the thermal dynamics of the building is required when applying MPC schemes. In this study, the model is defined as a discrete-time linear time-invariant system specified on state-space form (Eq. (1a)) with state matrix $\boldsymbol{A}$, system states x_k, input matrix $\boldsymbol{B}$, control inputs u_k, disturbance matrix $\boldsymbol{E}$, disturbances d_k and controlled system states y_k (Eq. (1b)) with output matrix $\boldsymbol{C}$.

$$x_{k+1} = \boldsymbol{A}x_k + \boldsymbol{B}u_k + \boldsymbol{E}d_k \tag{1a}$$

$$y_k = \boldsymbol{C}x_k \tag{1b}$$

There are several modelling techniques for representing the building dynamics [26] commonly categorized as white box (e.g. [19]), grey box (e.g. [27,28]) or black box model approaches (e.g. [29,30]). In this study, a grey box model approach was chosen as it provides the additional possibility of identifying the actual physical parameters of the building, e.g. the total heat loss coefficient, which could be beneficial to document the effects of retrofits in practice. Furthermore, grey box models are characterized by having relatively low requirements in terms of the amount of data needed to obtain them compared to the alternatives.

The model structure of the apartments was defined as a multi-zone model as illustrated in Fig. 2 for apartment j with adjacent apartments i, where T_{ext} is the external temperature [°C], Q_{sun} is the solar heat gains [W], Q_{heat} is the thermal energy from the space heating system [W], T is the temperature [°C], C is the thermal capacity [J/K], H is the heat transfer coefficients [W/K] and subscripts m, e and a represent the construction mass, ambient air and

room air, respectively. The multi-zone model can be reduced to a set of single-zone models by setting $H_{interaction} = 0$ throughout the model, i.e. neglecting the inter-zonal effects.

An inherent part of grey box modelling is to make data-based estimations of the parameters describing the thermal dynamic characteristics of the building (C and H in Fig. 2). The parameters were estimated for the multi-zone and the set of single-zone models, respectively, based on output data from a simulated experiment with a duration of 14 days (01.01.2016–14.01.2016). During the experiment the output of the heaters were controlled to follow a so-called Pseudo Random Binary Signals (PRBS) designed to excite systems with multiple time constants [31,32]. Ten different PRBS signals were used in the ten apartments. The output from the first seven days of data was used for parameter estimation using the MATLAB system identification toolbox [33,34] by minimizing the multiple-step ahead prediction error, while the output from the remaining seven days was used for model validation. The average model fits (NRMSE) [35] across all zones on the validation data for the multi-zone and single-zone model, respectively, are shown in Table 4. The fits of the multi-zone and single-zone model are within the same range. Differences in model fits are due to the different parameter estimations as shown in Fig. 3.

The estimated room air capacities for the two modelling approaches was similar, whereas the construction mass capacities differ slightly, presumably because the single-zone models lump the effects of inter-zonal heat exchange into other parameters. The complexity of one comprehensive multi-zone model also complicates the system identification, which is seen by the greater parameter estimation uncertainties.

When the multi-zone model is used in E-MPC as one comprehensive building model, the optimal control inputs for all apartments are calculated simultaneously for each discrete time step. This is called *centralized E-MPC* [36]. Using the set of single-zone models for E-MPC, i.e. each optimal control input is
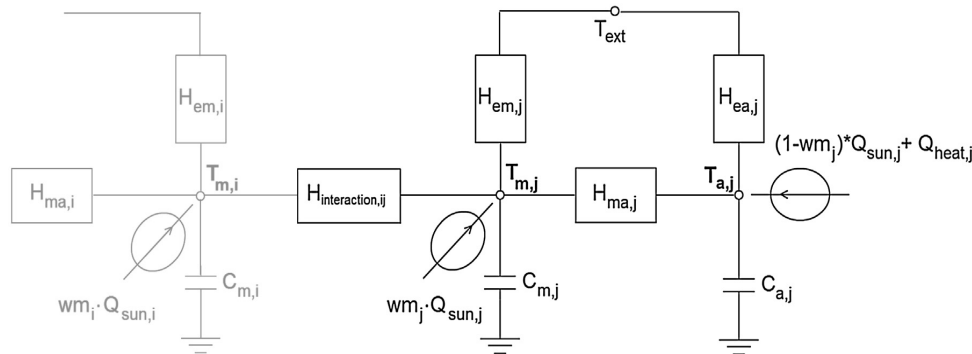
Fig. 2. Illustration of the model structure for apartment j and adjacent apartments i.
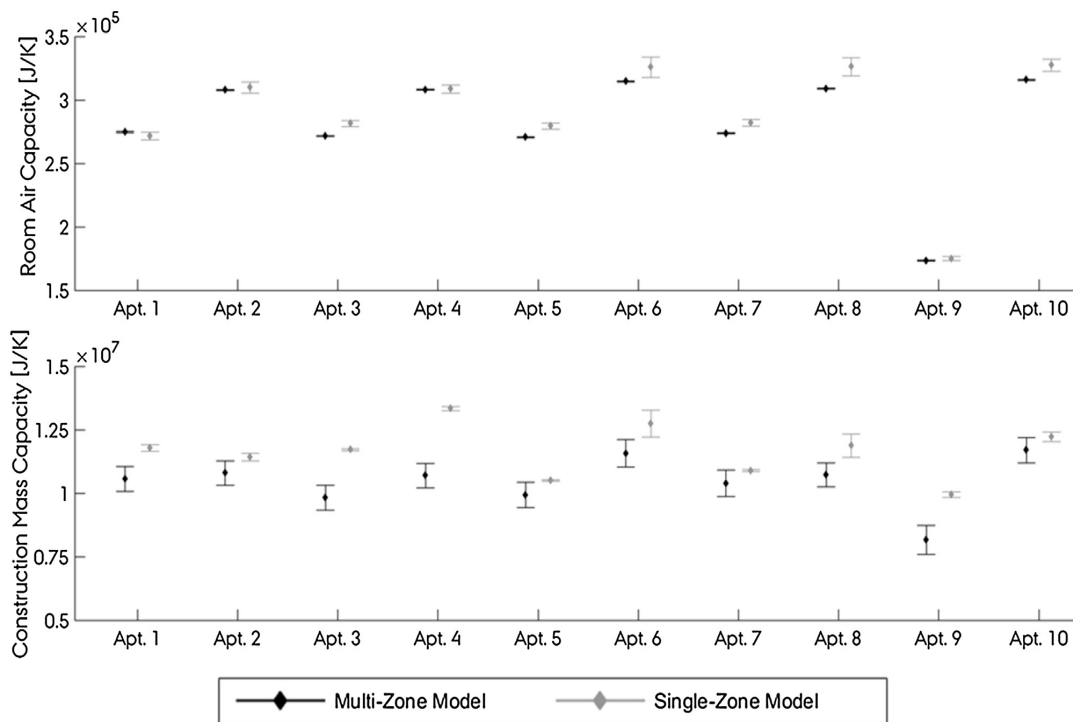

Fig. 3. Parameter estimations and standard deviation of the thermal capacity of the room air (top) and construction mass (bottom).

determined for each zone individually, is called *decentralized E-MPC* [36]. Thus, in theory, decentralized E-MPC will return a sub-optimal control strategy compared to the centralized E-MPC due to the neglect of inter-zonal effects. However, the decentralized control approach may be more practical since it does not require mapping of zone adjacency or exchange of information between controlled zones. This paper therefore investigates the performance differences between a decentralized and centralized control approach.

2.3. Economic model predictive control

The objective of the E-MPC scheme formulated in Eqs. (2a)–(2g) is to minimise the total operational cost for a finite prediction horizon N. At each discrete time step k, measurements of the room air temperatures are taken and the optimization problem is solved yielding a sequence of optimal space heating control input u^* [W]. The first element of u^* is then applied to the space heating system in the EP building model. At the next time-step $k+1$ the optimization problem is solved again with a prediction horizon shifted one time-step ahead in time and with updated room air temperature measurements. This receding horizon introduces feedback in the control scheme [37]. The optimal sequence of control inputs u^* is constrained by the maximum heating design power P_{max} (Eq. (2d)) and the value and rate of change of the room air temperatures y (Eqs. (2e) and (2f), respectively). All of the inequality constraints (Eqs. (2d)–(2f)) were enforced as equality constraints by introducing slack variables, which ensured that a feasible solution was always available. Furthermore, a low-level proportional controller is introduced in the EP model that ensures thermal comfort since model mismatch in the E-MPC scheme could lead to thermal comfort violations. The prediction horizon N and the discrete time step k were set to 3 days and 1 hour, respectively. To simplify the interpretation of the results, perfect predictions of the input weight c (Eq. (3)), in this case the electricity price and weather forecasts,
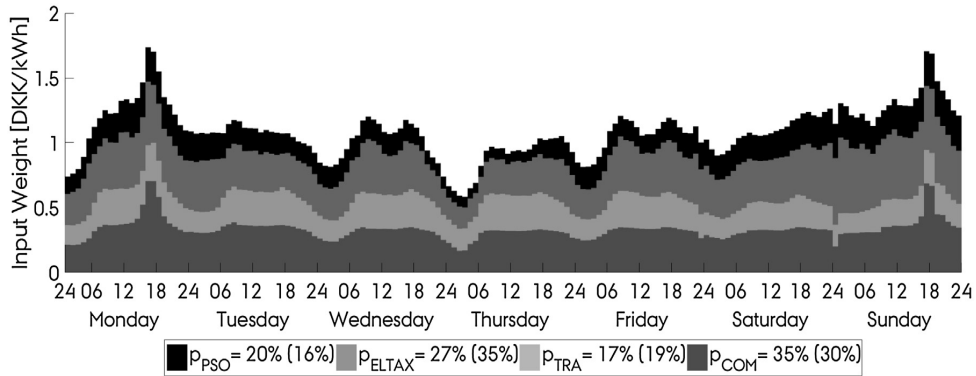
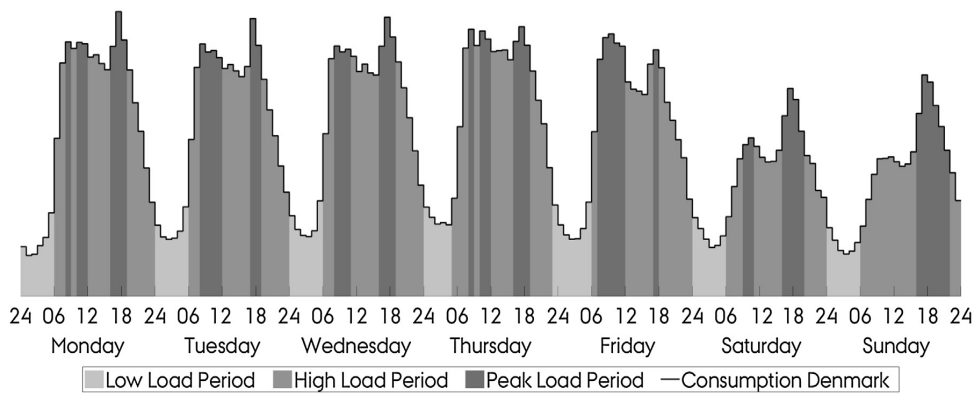**Fig. 4.** Input weight for the period of December 7–14, 2015.

Fig. 5. Partition of the daily consumption into periods of low, high and peak load for December 7–14 2015 [6](Nord Pool).

are assumed. Hence, the optimization problem forms a deterministic linear program (LP). The LP can be solved efficiently using the MOSEK solver [38].

$$\underset{u}{\text{minimize}} \sum_{k=1}^{N} c_k^T \cdot u_k \tag{2a}$$

$$\text{subject to } x_{k+1} = A x_k + B u_k + E d_k \tag{2b}$$

$$y_k = \boldsymbol{C} x_k \tag{2c}$$

$$0 \leq u_k \leq P_{max} \tag{2d}$$

$$T_{min,k} \leq y_k \leq T_{max,k} \tag{2e}$$

$$\Delta T_{min,k} \leq \frac{\Delta y_k}{\Delta t} \leq \Delta T_{max,k} \tag{2f}$$

$$x_0 = x(0) \tag{2g}$$

2.4. Constraints and input weight

In this study, the control input and state constraints (Eqs. (2d)–(2f)) are time-invariant but differ for each apartment as specified in Table 5.

The input weight vector c in Eq. (2a) is a signal designed to transform a multi-objective optimization problem into a single-

Table 5
Specification of input and state constraints.

Zone	P_{max}	T_{min}	T_{max}	ΔT_{min}	ΔT_{max}
Apartment 1	50 W/m²	20 °C	24 °C	−2.1 °C/h	2.1 °C/h
Apartment 2	50 W/m²	22 °C	26 °C	−2.1 °C/h	2.1 °C/h
Apartment 3	50 W/m²	20 °C	24 °C	−2.1 °C/h	2.1 °C/h
Apartment 4	50 W/m²	22 °C	26 °C	−2.1 °C/h	2.1 °C/h
Apartment 5	50 W/m²	20 °C	24 °C	−2.1 °C/h	2.1 °C/h
Apartment 6	50 W/m²	22 °C	26 °C	−2.1 °C/h	2.1 °C/h
Apartment 7	50 W/m²	20 °C	24 °C	−2.1 °C/h	2.1 °C/h
Apartment 8	50 W/m²	22 °C	26 °C	−2.1 °C/h	2.1 °C/h
Apartment 9	50 W/m²	20 °C	24 °C	−2.1 °C/h	2.1 °C/h
Apartment 10	50 W/m²	22 °C	26 °C	−2.1 °C/h	2.1 °C/h

objective optimization problem [16], which is summarised in Eq. (3).

$$c[k] = \underbrace{\frac{spot[k]}{\overline{spot}} \cdot c_{COM}}_{p_{COM}} + \underbrace{\frac{load[k]}{\overline{load}} \cdot c_{TRA}}_{p_{TRA}} + \underbrace{\frac{CO_2[k]}{\overline{CO_2}} \cdot c_{EL\_TAX}}_{p_{EL\_TAX}} + \underbrace{f_{PSO}[k] \cdot c_{PSO}}_{p_{PSO}} \tag{3}$$

where k is a discrete hourly time step, $spot$ is the hourly electricity spot price, $\overline{spot}$ is the mean electricity spot price, c_{COM} is the yearly average commercial tariff on electricity, $load$ is the hourly grid load, $\overline{load}$ is the mean grid load, c_{TRA} is the yearly average cost of electricity transportation through the transmission and distribution grid, CO_2 is the hourly CO_2 intensity associated with the electricity production, $\overline{CO_2}$ is the mean intensity and c_{EL_TAX} is the yearly average taxes and levies. c_{PSO} is the yearly average cost of a Danish public service obligation (PSO) levy put on electricity use
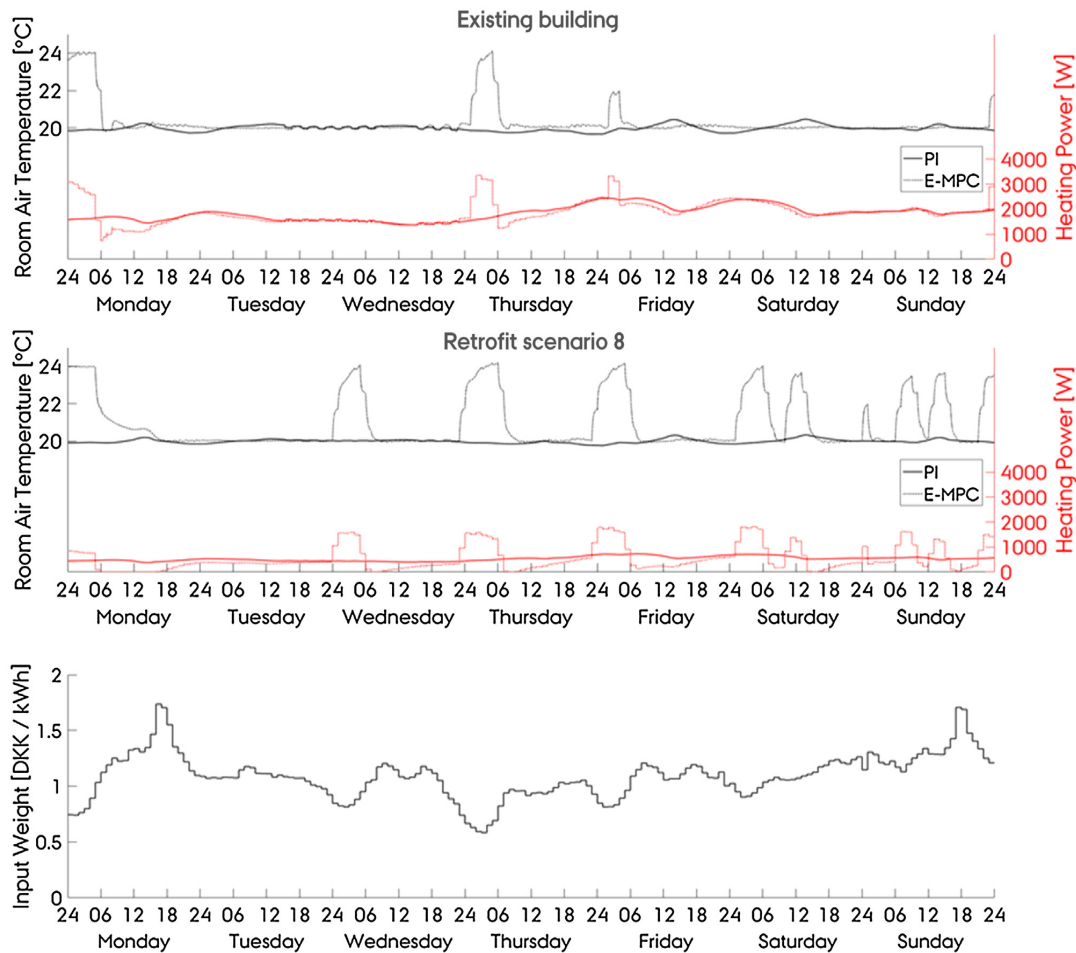
Fig. 6. Simulation results for apartment 7 for the existing building (top) and retrofit scenario 8 (middle) using a PI controller and E-MPC scheme, respectively, during the period December 7–14, 2015. The bottom chart shows the energy price (input weight c) during the same period.

where f_{PSO} is the PSO scaling factor. Approximately half of the PSO levy covers subsidies for wind turbines as supplement to the market price. The proposed f_{PSO} scaling factor is constructed in such a way that it is low in periods with low spot prices and high wind power production.

The data used in this study for Eq. (3) are electricity spot prices, grid load, CO_2 intensity signals and wind production from Nord Pool market data for Western Denmark during the simulation period [39] and Danish average component tariffs for 2015 [40]. Fig. 4 depicts an example of the input weight c as defined in Eq. (3) for the period December 7–14, 2015. The component share of the total tariff is specified in the legend where the percentage in brackets indicates the 2015 yearly shares.

2.5. E-MPC performance evaluation

Determining the true value of residential DR programs for the electricity supply system is a challenge of great concern [9]. The economic DR incentive may be limited on a household scale while significant on a societal level [6]. In this study, the performance of the E-MPC for residential space heating will be evaluated relative to a traditional PI controller in terms of achieved reductions of costs and CO_2 emissions as suggested by Knudsen and Petersen [16]. This form of evaluation will provide some insights into the

value of the proposed E-MPC, but it will not provide evaluation of other potential benefits such as the amount, time and duration of shifted energy which may affect production patterns and societal energy infrastructure investments. Several performance evaluation measures have been proposed to quantify the amount of shifted energy using active demand response [41,18]. However, quantifying the time to which the load is shifted is an equally relevant aspect of DR. A simple approach is to consider static periods of low, high and peak load; hence, evaluate the amount of energy shifted from peak periods to periods of low or high load [16]. In this study, the shifted energy of the E-MPC relative to the PI controller is evaluated with respect to a dynamic metric where each time step of the simulation period is categorized as either a period of low, high or peak load based on historical grid load data as illustrated in Fig. 5. For each day, the hours with grid load below the 25% quantile and above the 75% quantile were defined as low and peak load periods, respectively. The remaining hours were characterized as high load periods.

3. Results

To illustrate the mechanisms of the E-MPC scheme, Fig. 6 (top and middle) depicts the temperature conditions and heating consumption for apartment 7 in one week using the PI controller and

the centralized E-MPC, respectively. Fig. 6 (top) shows results from simulations of the existing building and Fig. 6 (middle) shows results from the most extensive energy retrofit scenario 8 (see Table 3 for details). In both cases, the PI controller maintained a room air temperature near the specified minimum comfort set point of 20 °C at all times, resulting in a smooth and fairly constant heating pattern. The E-MPC scheme, however, increased the room air temperature at times with low energy cost (Fig. 6 bottom) and thereby exploited the thermal mass of the constructions, which then reduced the need for space heating in the following periods characterized by higher energy cost.

Immediate comparison of the control actions in the two buildings indicates that improved energy efficiency of the building envelope increased the frequency at which load shifting was profitable.

3.1. Economic and environmental assessment

The cost and CO_2 emissions over the simulation period were accumulated for each combination of the nine buildings (the existing and the eight retrofit scenarios) and the three control schemes (PI, centralized E-MPC and decentralized E-MPC). Fig. 7 depicts the achieved cost and emission reductions for the centralized and decentralized E-MPC scenarios relative to the PI controller for all simulations. Both E-MPC schemes of the existing building led to minor cost savings while increasing CO_2 emissions slightly. In all retrofit scenarios both E-MPC schemes reduced the cost and CO_2 emissions compared to the PI controller. However, the centralized E-MPC had a marginally better performance than the decentralized E-MPC in all scenarios.

3.2. Load shifting potential

The absolute and relative ability of the E-MPC scheme to shift space heating consumption to low load periods as defined in Section 2.4 is exemplified by the performance of the centralized E-MPC in Fig. 8. Applying E-MPC on the existing building (R0) shifted
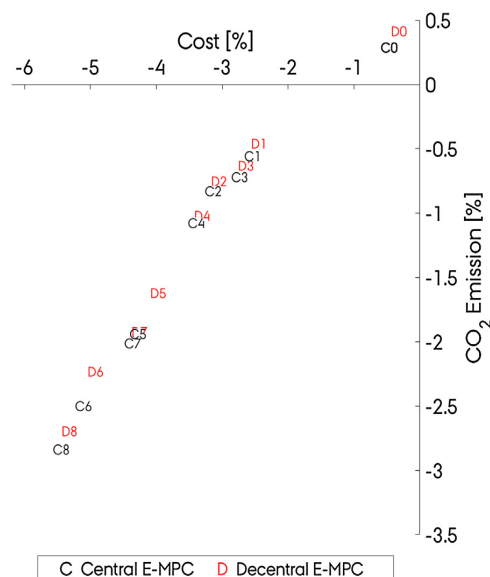

Fig. 7. Achieved cost and emission reductions for the centralized and decentralized E-MPC schemes relative to the PI controller for all simulations. The existing building is referred to with index 0 and the remaining numbers refer to the retrofit scenarios.

approx. 7% of the energy use away from peak load periods. For the retrofit scenarios, the shifted load was in the range of 30–47%.

4. Discussion

A tendency of decreasing cost and CO_2 emission as a function of the increasing energy efficiency can be observed in Fig. 7, which is a consequence of an increasing number of load shift events (as illustrated in Fig. 6). Fig. 7 suggests that reducing the infiltration
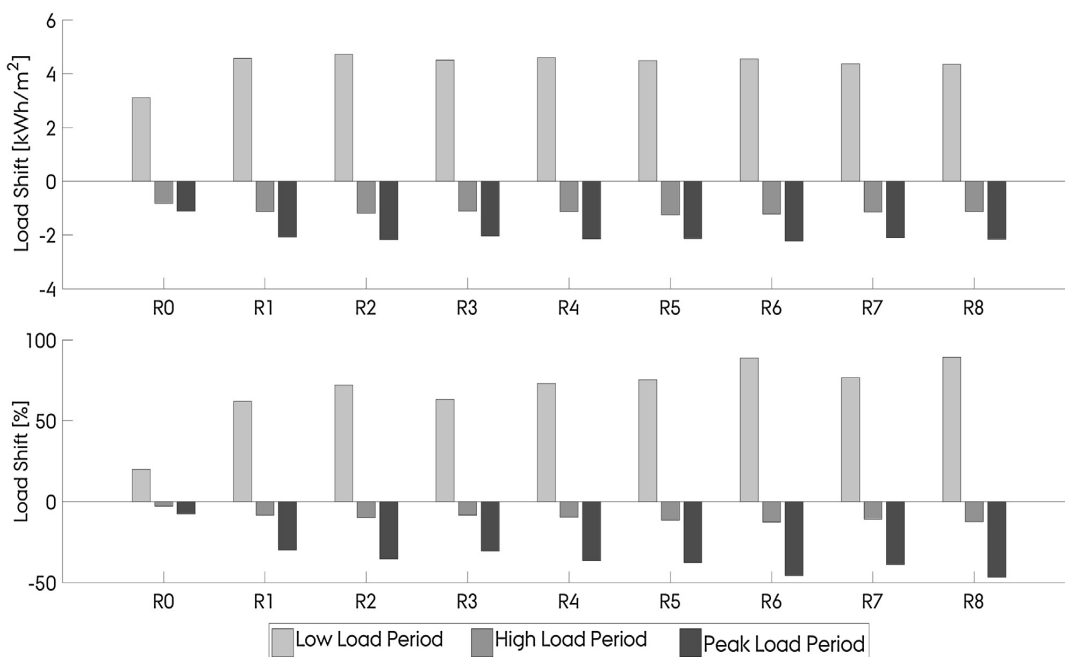

Fig. 8. Accumulated load shift of centralized E-MPC for all retrofit scenarios compared to the baseline PI control. Top: Absolute load shift. Bottom: Relative load shift.

air change rate was an important measure in terms of both cost and CO_2 emission reduction. The clustering of data with respect to the two types of window glazing indicates that reducing heat loss through windows influenced the potential. The added external insulation was most efficient in the buildings with 3-layer glazing since the heat loss through the envelope was a more dominating factor in these scenarios compared to the 2-layer glazing scenarios. While it is difficult to make a general valid ranking of the specific measures such as increasing the air tightness or lowering the transmission losses, the results show that reductions in the overall heat loss have a significant effect on cost savings, CO_2 emissions and load shifting in a building heated by a convective radiator system.

Fig. 8 shows that the relative load shift potential of the scenarios increased with increasing energy efficiency. This was primarily due to the corresponding reduction of the baseline space heating consumption: The absolute load shifting potential is seen to be rather constant across all retrofit scenarios.

The simulation results indicate that the centralized E-MPC scheme resulted in marginally better results than the decentralized E-MPC. Though not investigated, it is likely that inter-zonal effects would be less pronounced with insulated interior walls instead of the 0.12 m massive concrete walls used in this study. The difference in performance compared to the increased complexity of centralized E-MPC and the challenge of obtaining suitable multi-zone model suggests that decentralized E-MPC is sufficient for many practical applications.

5. Conclusion

This paper reports on a simulation-based study of the theoretical potential for utilizing the thermal mass in an existing and eight retrofit scenarios of a multi-story apartment block for demand response enabled by E-MPC of the space heating system. The control objective was to minimize the cost of space heating for the end-user, and performance was evaluated by comparison to a conventional controller. The E-MPC was also evaluated in terms of its ability to reduce CO_2 emissions and to perform load shift of the heating demand. Two E-MPC approaches were considered: centralized E-MPC where inter-zonal effects were considered and decentralized E-MPC that neglected heat transfer between adjacent apartments.

The E-MPC schemes yielded increased cost savings (up to approx. 6%) and reduced CO_2 emissions (up to approx. 3%) as a function of increasing energy efficiency of the retrofit scenarios. The centralized E-MPC only performed marginally better than the decentralized E-MPC, suggesting that using the more practical decentralized approach, which does not need configuration of zone adjacency or exchange of information between controlled zones, is sufficient in many situations.

The simulation results also suggest that the E-MPC schemes shifted consumption more frequently in the retrofit scenarios compared to the existing building. However, the absolute amount of shifted energy across the retrofit scenarios compared to the existing building was rather consistent. The relative amount of energy shifted from peak periods increased slightly with increasing energy efficiency due to the decreased baseline energy use in each retrofit scenario.

This study used perfect predictions of disturbances (weather and occupancy) to identify the theoretical potential of the E-MPC scheme. Future studies should include investigations on how this potential will be affected by uncertainties in weather forecasts and occupancy. Furthermore, experimental verification of the demonstrated potentials is recommended.

References

[1] M.H. Albadi, E.F. El-Saadany, A summeray of demand response in electricity markets, Electr. Power Syst. Res. 78 (2008) 1989–1996, http://dx.doi.org/10.1016/j.epsr.2008.04.002.

[2] North American Electric Reliability Corporation, Demand Response Availability Report, 2011 (03 2013. [Online]. Available: http://www.nerc.com/docs/pc/dadswg/2011%20DADS%20Report.pdf. [Senest hentet eller vist den 23 08 2016]).

[3] T. Ashrafian, A.Z. Yilmaz, S.P. Corgnati, N. Moazzen, Methodology to define cost-optimal level of architectural measures for enery efficient retrofits of existing detached residential buildings in Turkey, Energy Build. 120 (2016) 58–77, http://dx.doi.org/10.1016/j.enbuild.2016.03.074.

[4] D. Palensky, D. Dietrich, Demand side management: demand response, intelligent energy systems, and smart loads, IEEE Transactions on Industrial Informatics 7 (3) (2011), http://dx.doi.org/10.1109/tii.2011.2158841.

[5] R. D'Hulst, W. Labeeuw, B. Beusen, S. Claessens, G. Deconinck, K. Vanthournout, Demand response flexibility and flexibility potential of residential smart appliances: experiences from large pilot test in Belgium, Appl. Energ. 155 (2015) 79–90, http://dx.doi.org/10.1016/j.apenergy.2015.05.101.

[6] N. O'Connell, P. Pinson, H. Madsen, M. O'Malley, Benefits and challenges of electrical demand response: a critical review, Renew. Sustain. Energy Rev. 39 (2014) 686–699, http://dx.doi.org/10.1016/j.rser.2014.07.098.

[7] K.O. Aduda, T. Labeodan, W. Zeiler, G. Boxem, Y. Zhao, Demand side flexibility: potentials and building performace implications, Sustain. Cities Soc. 22 (2016) 146–163, http://dx.doi.org/10.1016/j.apenergy.2015.05.101.

[8] B.P. Esther, K.S. Kumar, A survey on residential Demand Side Management architecture, approaches, optimzation models and methods, Renew. Sustain. Energy Rev. 59 (2016) 342–351, http://dx.doi.org/10.1016/j.rser.2015.12.282.

[9] S. Nolan, M. O'Malley, Challenges and Barriers to demand response deployment and evaluation, Appl. Energ. 152 (2015) 1–10, http://dx.doi.org/10.1016/j.apenergy.2015.04.083.

[10] M. Gweder, D. Gyalistras, C. Sagerschnig, R.S. Smith, D. Sturznegger, FinalReport: Use of Weather And Occupancy Forecasts For Optimal BuildingClimate Control –Part II: Demonstration (OptiControl-II), 2013, Zürich, Switzerland.

[11] European Commission, Eurostat, 2017 (Online. Available: http://ec.europa.eu/eurostat. [Senest hentet eller vist den 30 03 2016]).

[12] Buildings Performace Institute Europe (BPIE), Europe's Buildings Under the Microscope ? A Country-by-country Review of the Energy Performance of Buildings, BPIE, 2011.

[13] M. Avci, M. Erkoc, A. Rahmani, S. Asfour, Model predictive HVAC load control in buildings using real-time electricity pricing, Energy Build. 60 (2013) 199–209, http://dx.doi.org/10.1016/j.enbuild.2013.01.008.

[14] R. Halvgaard, N.K. Poulsen, H. Madsen, J.B. Jørgensen, Economic Model predictive Control for Building Climate Control in a Smart Grid, in: IEEE PES Innovative Smart Grid Technologies (ISGT), Washington, D.C., United States, 2012, pp. 1–6, http://dx.doi.org/10.1109/ISGT.2012.6175631.

[15] E. Vrettos, K. Lai, F. Oldewurtel, G. Andersson, Predictive Control of Buildings for Demand Response with dynamic day-ahead and real-time prices, in: Control Conference (ECC), Zürich, 2013.

[16] M.D. Knudsen, S. Petersen, Demand response potential of model predictive control of space heating based on price and carbon dioxide intensity signals, Energy Build. 125 (2016) 196–204, http://dx.doi.org/10.1016/j.enbuild.2016.04.053.

[17] G. Reynders, T. Nuytten, D. Saelens, Potential of structural thermal mass for demand-side management in dwellings, Build. Environ. 64 (2013) 187–199, http://dx.doi.org/10.1016/j.buildenv.2013.03.010.

[18] G. Reynders, Quantifying the Impact of Building Design on the Potential of Structural Storage for Active Demand Response in Redisential Buildings, PhD Dissertation, 2015, KU Leuven.

[19] U.S. Department of Energy, EnergyPlus 8.1.0, [Online].

[20] The MathWorks, inc., MATLAB 2015 (8.6.0.267246), [Online].

[21] Lawrence Berkeley National Laboratory, Buildings Control Virtual Test Bed – BCVTB (1.4.0), [Online].

[22] M. Wetter, Co-simulation of building energy and control systems with the building controls virtual test bed, J. Build. Perform. Simul. 3 (4) (2010) 1–19, http://dx.doi.org/10.1080/19401493.2010.518631.

[23] Pedersen, Theis Heidmann, Hedegaard, Rasmus Elbæk, Petersen, Steffen (2017) "IDF EnergyPlus files of an existing Danish apartment block and eight

retrofit scenarios", Mendeley Data, v2 http://dx.doi.org/10.17632/6dhk66w5gj.2.

[24] Berkeley Lab WINDOW v7.4.8.0, (2016). [Online]. Available: https://windows.lbl.gov/software/window/7/index_7_4_8.html.

[25] U.S. Department of Energy, EnergyPlus Weather Data: Copenhagen 061800 (IWEC), [Online]. Available: https://energyplus.net/weather-region/europe_wmo_region_6/DNK%20%20. [Senest hentet eller vist den 06 04 2016].

[26] S. Prívara, J. Cigler, Z. Váňa, F. Oldewurtel, C. Sagerschnig, E. Žáčeková, Building modeling as a crucial part for building predictive control, Energy Build. 56 (2013) 8–22, http://dx.doi.org/10.1016/j.enbuild.2012.10.024.

[27] P. Bacher, H. Madsen, Identifying suitable models for the heat dynamics of buildings, Energy Build. 43 (2011) 1511–1522, http://dx.doi.org/10.1016/j.enbuild.2011.02.005.

[28] S. Goyal, C. Liao, P. Barooah, Identification of multi-zone building thermal interaction model from data, in: 50th IEEE Conference on Decision and Control, Orlando, FL, USA, 2011, http://dx.doi.org/10.1109/CDC.2011.6161387.

[29] S. Prívara, Z. Váňa, D. Gyalistras, J. Cigler, C. Sagerschnig, M. Morari, L. Ferkl, Modeling and identification of a large multi-zone office building, in: IEEE International Conference on Control Applications (CCA), Denver, CO, USA, 2011, http://dx.doi.org/10.1109/CCA.2011.6044402.

[30] J. Cigler, S. Prívara, Subspace idenfication and model predictive control for buildings, in: 1th International Conference Control, Automation, Robotics and Vision, Singapore, 2011, p. 1, http://dx.doi.org/10.1109/ICARCV.2010.5707821.

[31] S.V. Gaikwad, D.E. Rivera, Control-Relevant Input Signal Design for Multivariable System Identification: Application to High-Purity Distillation, 1996, San Francisco.

[32] R.E. Hedegaard, T.H. Pedersen, M.D.S. Knudsen Petersen, Identifying a comfortable excitation signal for generating building models for model predictive control: a simulation study, in: CLIMA 2016 ? Proceedings of the 12th REHVA World Congress: Volume 10, Aalborg, 2016.

[33] The MathWorks, inc., System Identification Toolbox 9.3, [Online].

[34] L. Ljung, System Identification. Theory for the User, Prentice Hall PTR, New Jersey, 1999.

[35] A.K. Tangirala, Principles of System Identification. Theory and Practice, CRC Press, Taylor & Francis Group, 2015.

[36] P.-D. Moroşan, R. Bourdais, D. Dumur, J. Buisson, Building temperature regulation using a distributed model predictive control, Energy Build. 42 (2010) 1445–1452, http://dx.doi.org/10.1016/j.enbuild.2010.03.014.

[37] F. Oldewurtel, A. Parisio, C.N. Jones, D. Gyalistras, M. Gweder, V. Stauch, B. Lehmann, M. Morari, Use of model predictive control and weather forecasts for energy efficient building climate control, energy and buildings, Energy Build. 45 (2012) 15–27.

[38] MOSEK ApS, The MOSEK optimization toolbox for MATLAB manual. Version 7.1 (Revision 49), (2015). [Online]. Available: http://docs.mosek.com/7.1/toolbox/index.html.

[39] Nord Pool, [Online]. Available: http://www.nordpoolspot.com/. [Senest hentet eller vist den 02 04 2016].

[40] Association of Danish Energy Companies, Elforsyningens tariffer & elpriser pr. 1. januar 2015, Dansk Energi, (2015).

[41] F. Oldewurtel, D. Sturznegger, G. Andersson, M. Morari, R.S. Smith, Towards a standardized building assessment for demand response, in: 52nd IEEE Conference on Decision and Control, Florence, Italy, 2013, http://dx.doi.org/10.1109/CDC.2013.6761012.
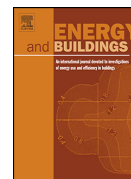
P3 Multi-market demand response using economic model predictive control of space heating in residential buildings

Contents lists available at ScienceDirect

Energy and Buildings

journal homepage: www.elsevier.com/locate/enbuild

Multi-market demand response using economic model predictive control of space heating in residential buildings

Rasmus Elbæk Hedegaard[*], Theis Heidmann Pedersen, Steffen Petersen

Department of Engineering, Inge Lehmanns Gade 10, Aarhus University, DK-8000 Aarhus C, Denmark

ARTICLE INFO

ABSTRACT

Several studies have evaluated the potential for residential buildings participating in demand response programs based on the day-ahead electricity market prices. However, little is known about the benefits of residential buildings providing demand response by engaging in trading on the intraday market. This paper presents a simulation-based study of the performance of an economic model predictive control scheme used to enable demand response through parallel utilization of day-ahead market prices and intraday market trading. The performance of the control scheme was evaluated by simulating ten apartments in a residential building located in Denmark through a heating season (four months) using historical market data. The results showed that the addition of intraday trading to the more conventional day-ahead market price-based control problem increased the total cost savings from 2.9% to 5.6% in the existing buildings, and 13%–19% in retrofitted buildings with higher energy-efficiency. In the existing building the proposed control scheme traded on average 12.7 kWh/m^2 on the intraday market throughout the simulation corresponding to 21% of the reference consumption. For a retrofitted building the traded volume was 9.6 kWh/m^2 which corresponds to 52% of the reference consumption. These results suggest that the benefits of considering intraday market trading as a demand response incentive mechanism apply to a wide range of buildings.

1. Introduction

As the penetration of intermittent renewable energy sources (RES) such as wind power increases, so will the uncertainty associated with electricity production prognoses because of the inherent uncertainties of weather forecasts. This uncertainty complicates the task of maintaining an instantaneous balance between electricity supply and demand [1,2]. A commonly suggested way of addressing the issue of grid balancing under more volatile electricity production is the implementation of smart grids [3–6]. A characteristic of smart grids is effective utilization of Demand Response (DR) programs, where consumers are encouraged to adjust their demand to meet supply and thereby increase the overall efficiency of the energy system. Energy use in residential buildings constitutes a significant potential for DR as it accounts for 25% of the total energy consumption in the EU of which 67% is used for space heating in the North and West regions of EU [7]. This flexible consumption can be activated through different types of DR programs.

1.1. Demand response programs

DR programs are often divided into *direct* and *indirect* control programs [4,8,9]. In direct control programs, the consumer entrusts the energy planners and operators (PO) with direct control of their electrical loads; the PO can change consumption pattern directly. In indirect control programs, the consumer has full control of the electrical loads and the PO can only provide incentives for consumers to change their consumption pattern. One incentive from PO to consumers is to provide time-varying energy prices, which motivates consumers to reduce consumption in high price periods, e.g. by shifting consumption to periods with lower prices. This approach is referred to as *indirect price-based* DR programs. Previous studies have demonstrated that residential building owners may benefit from this type of DR programs. Halvgaard et al. [10] operated a residential-scale heat pump using Economic Model Predictive Control (E-MPC) with day-ahead prices and achieved 25–35% cost savings compared to traditional set point control dependent on comfort constraints. Avci et al. [11] used E-MPC to achieve a 13% cost reduction compared to a two-position thermostatic control of a residential heat pump, and Oldewurtel et al. [12] used MPC with a multi-objective cost-function to reduce consumption peaks by up to 39% and costs by 31.2%. Knudsen and Petersen [13] demonstrated that using E-MPC for space heating can enable cost savings, CO_2

* Corresponding author.
   E-mail address: reh@eng.au.dk (R.E. Hedegaard).

Nomenclature

Abbreviations

DR	Demand response
E-MPC	Economic model predictive control
RES	Renewable energy sources
PO	(Energy) Planners and operators
SSM	Supply-side management
TSO	Transmission system operator
BRP	Balance responsible party
MILP	Mixed integer linear problem
ITH	Intraday trading horizon
ID	Intraday (market)
DA	Day-ahead (market)

Symbols

x	State vector of the resistance-capacitance building model
p_{da}	Vector containing forecasted day-ahead market prices
u_{da}^*	Optimal sequence of control actions with respect to day-ahead prices
p_{id}	Vector containing prices from intraday market trades
u_{id}^*	Optimal sequence of control actions after intraday optimization
J^*	Cost of implementing the entire optimal control strategy

---

emission reductions, and shift consumption from periods of peak load to low load periods. The large spread in savings found in the above-mentioned studies may be caused by several factors including the magnitude of price fluctuations, how the reference case is defined as well as the inclusion of taxes. For example, Knudsen et al. [14] demonstrated that the economic incentive of performing DR using E-MPC of residential space heating strongly depends on the taxation mechanism of energy: a case study led to end-user energy cost savings between 2% and 9% depending on the taxation. Furthermore, Pedersen et al. [15] demonstrated that the cost savings of indirect price-based DR programs using E-MPC depends on the energy-efficiency of the building envelope and consequently the storage efficiency, which relates the amount of energy lost during the storage process to the amount of energy actually stored.

All of the mentioned studies use forecasts of energy prices and weather with durations upwards of days to prepare the building for DR by utilizing the inherent thermal inertia of the building as an energy storage. However, previous studies have demonstrated that buildings can also help solve grid balancing issues that arise on a shorter time scale. Oldewurtel et al. [16] used MPC with critical peak pricing to quantify the flexible consumption immediately available in buildings that have not been prepared to deliver flexibility, by introducing two performance metrics: Power Shifting Potential and Power Shifting Efficiency. De Coninck et al. [17] used MPC to derive cost curves describing the costs associated with deviation from optimal control strategies to activate flexibility. Both studies conclude that the availability and associated cost of flexibility in building space heating depend on several dynamic factors such as the current thermal state of the building and weather conditions, but they do not attempt to investigate whether the cost of the flexibility is aligned and compatible with the current electricity markets or incentive mechanisms. The following section describes the structure of wholesale electricity markets and clarifies why these may be suitable for activating the DR potential in residential space heating.

1.2. Electricity markets as DR platforms

This study evaluates an indirect price-based DR program utilizing two European-based wholesale electricity markets: the day-ahead market Elspot and the intraday market Elbas. Both markets are a part of the cross-border electricity market Nord Pool. Each participating country is divided into individual bidding areas that reflect geographical and grid characteristics. For example, Denmark consists of two bidding areas of which the Western Denmark region (DK1) is characterized by a high penetration of wind power production [18]. In 2015 the accumulated annual wind power production constituted approximately 55% of the total annual consumption of the DK1 region [19].

In DK1, the majority of electricity is traded on the day-ahead market Elspot, where electricity trades confirmed upon market closure is to be delivered the following day. The market closes each day at 12:00 CET and shortly thereafter the hourly day-ahead prices (p_{da}) for the following day are available to the public. The hourly price is settled through the pay-as-clear principle in which, for each hour, the price that balances supply and demand applies to all electricity traded across different market regions. However, in periods where transmission lines between bidding areas are congested (bottlenecks), a market split occurs resulting in different prices on each side of the congestion. The physical limitations of transmission lines thus lead to increased price fluctuations in regions with high shares of intermittent RES such as DK1. Fig. 1 shows how high wind power production within the region has a tendency to reduce the DK1 day-ahead clearing prices in 2015. Furthermore, the production from wind exceeded the regional consumption in 1442 h while negative prices were observed in 65 h. It is these day-ahead prices that have served as the sole price signal in many E-MPC or rule-based studies on DR for space heating in buildings [10,12,13,20–23].

The significance of wind power production in the region for the day-ahead market principle means that the trades depend strongly on the accuracy of production (and consumption) prognoses. The market therefore needs a way of correcting the already traded quantities on the day-ahead market to be consistent with updated production prognoses. Such corrections can be made through trading on the intraday electricity market (Elbas) which remains open from the day-ahead market closure up until one hour before the electricity is to be delivered. Despite the fact that trades can be made up to 33 h before delivery, over 50% of all intraday trades are made within the last three hours before intraday market closure as the accuracy of prognoses increase [18]. The total volumes traded on the Elbas market are currently small, constituting only approximately 3% of the annually sold and bought electricity on Elspot in 2015 [19]. However, Scharff et al. [18] identified high shares of intermittent production from RES to be a contributing factor towards increased intraday trading.

In conventional power systems grid balancing is achieved through supply-side management (SSM) where the transmission system operator (TSO) hires power plants that are able to adjust their power output to address any imbalanced operation from market actors. In all trades on the day-ahead electricity market, one of the actors involved with the trade assumes the role of the Balance Responsible Party (BRP). The BRP is committed to cover any expenses of the TSO to counteract any imbalance associated with the trade. The balancing power price is thus directly linked to the expenses associated with balancing carried out by the TSO. As the share of fluctuating renewable production increases, the task of balancing the grid becomes increasingly complicated which, consequently, increases the expenses resulting from imbalanced operation. As the balancing expenses increase, BRPs are expected to be more involved in intraday trading to ensure a balanced operation.
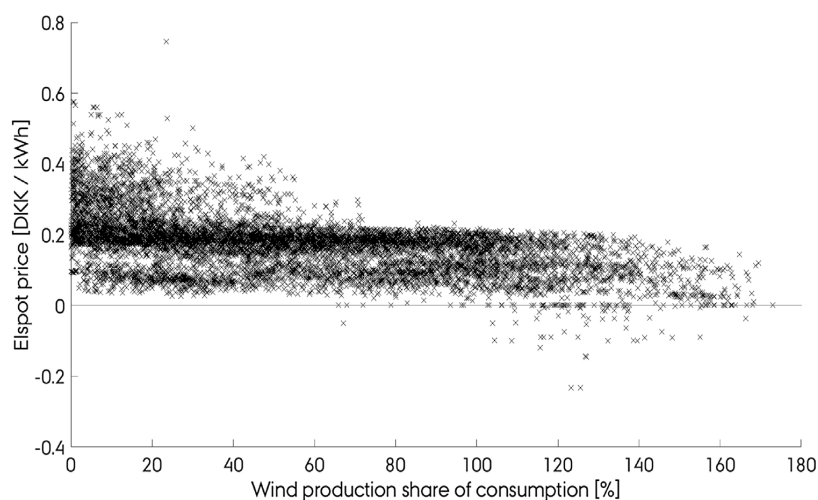
Fig. 1. The effect of wind power production on day-ahead electricity prices in the DK1 area. Source: Nord Pool, 2015 data.

The intraday electricity market prices (p_{id}) are settled according to the pay-as-bid principle, which means that individual trade prices are determined when market participants accept available offers. Therefore, prices may vary within any given hour [18]. Fig. 2 shows the marginal price of the day-ahead market and the interval for each hour in which trades settled on the intraday market over a three-day period in December 2015. The average intraday price and the day-ahead price are strongly correlated with a Pearson correlation factor of 0.91. However, as shown in Fig. 2, significant deviations between intraday and day-ahead prices occurred in several hours of the depicted period.

While the day-ahead price is a product of supply and demand, the intraday price is an indication of imbalances expected by the BRPs themselves. BRPs with flexible buildings in their own consumer portfolio may utilize this flexible demand to lower or avoid entirely the need for intraday trading. Similarly, other actors may use flexible consumption as a virtual power plant, offering energy on the intraday market.

1.3. Aim of this paper

Residential building owners or aggregators may increase their economic incentive to deliver DR to the electricity grid when mul-tiple electricity markets are considered. A study by Ali et al. [24] demonstrated that the charging pattern of domestic hot water tanks can be planned taking both day-ahead market prices and (artificial) instantaneous balancing events into consideration. It therefore seems reasonable to assume that space heating can be planned in a similar manner. However, to the knowledge of the authors, there have been no reported studies on whether space heating of residential buildings can participate in multiple DR programs using day-ahead and intraday prices simultaneously. This study therefore investigates whether space heating can be operated to respond to both day-ahead and intraday market-driven DR programs in parallel without compromising thermal comfort.

2. Method

The following sections introduce the proposed control scheme capable of utilizing market conditions on the day-ahead and intra-day market in parallel. First, Section 2.1 presents economic model predictive control in its more conventional configuration where only day-ahead prices are used to optimize operation of the building. Then, Section 2.2 expands upon the control scheme by introducing the expanded multi-market algorithm. Finally, Section
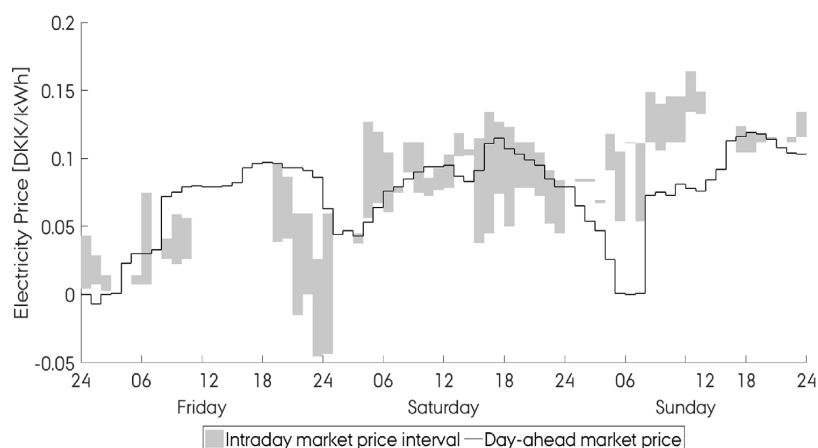

Fig. 2. Day-ahead clearing price and intraday market price-intervals (week 8, 2016).

2.3 presents the assumptions made for a case study used to illustrate the performance of the proposed control method.

2.1. Economic model predictive control

Economic model predictive control solves an optimization problem to determine the optimal sequence of control actions, u, for the space heating system by minimising the total operational cost for a finite prediction horizon N:

$$\underset{u}{\text{minimize}} \quad \sum_{k=1}^{N} C_k^T \cdot u_k \tag{2a}$$

$$\text{subject to } x_k = \boldsymbol{A}x_{k-1} + \boldsymbol{B}u_{k-1} + \boldsymbol{E}d_{k-1} \tag{2b}$$

$$y_k = \boldsymbol{C}x_k \tag{2c}$$

$$0 \le u_k \le P_{max} \tag{2d}$$

$$T_{min,k} \le y_k \le T_{max,k} \tag{2e}$$

$$\Delta T_{min,k} \le \frac{\Delta y_k}{\Delta t} \le \Delta T_{max,k} \tag{2f}$$

$$x_0 = x(0) \tag{2g}$$

where c_k is the time varying price associated with control action, u_k. The thermodynamics behaviour of the building to be controlled is described by Eqs. (2b) and (2c), and the control actions are constrained by the maximum design power of the space heating system by Eq. (2d). The controlled variable is the room air temperature, y_k, whose value and rate of change are constrained by Eqs. (2e) and (2f), respectively. Measurements are used to define the current state of the building in Eq. (2g), where the unobservable states are estimated using a Kalman Filter.

The model of the building thermodynamics used in this study was a grey-box model formulated in state space form. Grey-box models are categorised by having a predefined structure of physically meaningful parameters such as heat loss coefficients and thermal capacities. These parameters are estimated from measurement data through methods from the field of System Identification. The model used in this study is a simple two-state model, where the two states represent the lumped thermal capacity of the zone air and the construction components, respectively. Forecasts of ambient temperature, solar heat gains and space heating are treated as inputs from which the model produces a prediction of the zone air

temperature as output. A detailed description of the model structure used in this study is provided in Ref. [15].

At each discrete time step k, the states of the building model are updated and the optimization problem is solved using the MOSEK solver [25] resulting in a sequence of optimal space heating control inputs u^*. The output of the control scheme is thus the control strategy that, over a predefined prediction horizon N, satisfies the imposed constraints at the lowest operational cost. Only the first control action of each control sequence is implemented in the building after which a new sequence is computed at the start of the following time step – a control principle referred to as *receding horizon control* [26]. This approach allows for the control scheme to update weather and price forecasts continuously while enabling the use of building measurements to introduce feedback in the control loop.

2.2. Scenario-based optimization

The control scheme in Section 2.1 was expanded to enable the use of intraday price intervals in the optimization. A challenge in relation to this is to prevent the control scheme from purchasing and selling electricity within the same hour. One way of preventing such behaviour is to implement logic in the optimization problem that restricts the algorithm to be either in *selling-mode* or *buying-mode*. The resulting optimization problem would be a mixed integer linear problem (MILP) – an approach that was used in Bianchini et al. [27] to obtain on/off control of heaters. However, as the authors point out, MILPs are significantly more complex to solve than linear or quadratic programs, which limits the computationally tractable size of the problem. To avoid restricting the size of the optimization problem we chose a scenario-based approach instead, where optimization problems with different cost vectors corresponding to each relevant scenario were solved individually and then compared.

The decision making process including both the day-ahead and intraday market can be condensed to the principle described in Table 1. First, the optimal control strategy, u^*, is computed in each hour by solving the optimization problem defined in Eqs. (2a)–(2g) which only consider the day-ahead prices over a three day prediction horizon. While prices may not be available three days ahead, studies have shown E-MPC to be robust to simply repeating the price fluctuations from the first day [13]. This study assumes perfect price predictions for simplicity. Secondly, a shorter intraday trading horizon (ITH) is introduced – in this study ITHs of one and

Table 1
Breakdown of the new control algorithm.

| Control Algorithm |
|---|
| **for** *each timestep k = 1, 2, ...* **do** |
| **for** *each zone i = 1:10* **do** |
| measure zone states $\boldsymbol{x}_{0,i}$ |
| obtain weather and price forecasts |
| solve Eq. (2) using day-ahead prices, $\boldsymbol{p}_{da}$, to obtain control strategy $\boldsymbol{u}_{da}^*$ |
| **if** *intraday trading within ITH* **then** |
| **for** *scenario j = 1, 2, ...* **do** |
| solve Eq. (2) using intraday market prices, $\boldsymbol{p}_{id,j}$, within ITH to obtain control strategy, $\boldsymbol{u}_{id,j}^*$ |
| **end** |
| find minimal objective value J_j^* |
| implement first control action of $\boldsymbol{u}_{id,j}^*$ |
| **else** |
| implement first control action of $\boldsymbol{u}_{da}^*$ |
| **end** |
| **end** |
| **end** |
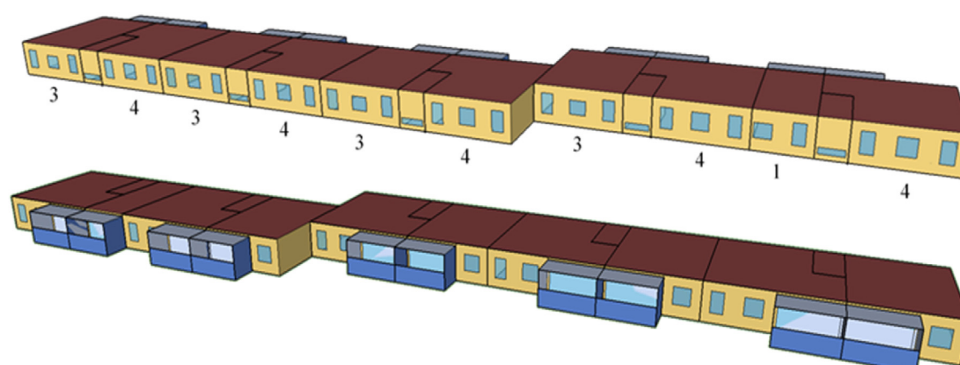
Fig. 3. Façades of case building with numbers indicating the apartments' number of rooms.

three hours were evaluated. Within the span of the ITH the algorithm evaluates currently available offers on the intraday market. If no offers are available, the intraday trading stage of the algorithm is not activated and the building is operated solely based on optimization using day-ahead prices. If trading offers are available inside the ITH, the algorithm treats the consumption procured on the day-ahead market as a trade commodity in the following intraday scenario optimization problems. These optimization problems evaluate all possible combinations of purchasing additional consumption or selling already procured consumption in each hour within the ITH. The controller then implements the intraday trading strategy that yields the highest profit, which may be to either store energy, sell part of the procured electricity back or stick to the original day-ahead optimized control sequence. In either case, the same comfort-related constraints used in the day-ahead optimization problem apply to all intraday scenarios, meaning that the algorithm will only sell energy in the extent that the thermal indoor climate remain within predefined comfort boundaries. To ensure compliance with the intraday market structure where the market closes one hour before delivery, each control strategy is computed one hour before implementation; hence, the strategy computed at time $t = 8:00$ is implemented in the building from $t = 9:00$ to 10:00.

An ITH of one hour results in three optimization problems to be solved: the initial *day-ahead problem*, a *sell-scenario* and a *buy-scenario*. Expanding the ITH by one hour introduces, in addition to the three previous scenarios, the two scenarios where electricity is bought in the first hour and sold in the second hour, and vice-versa. The number of scenarios and thereby optimization problems $n_{scenario} = 1 + 2^{ITH}$ to be solved in each time step increases exponentially with the ITH and is consequently

However, as mentioned in Section 1.2, approximately half of all trades are made within the last three hours before intraday market closure. Therefore, in order to limit the number of scenarios to evaluate, a maximum ITH of three hours was chosen in this study.

2.3. Case study

This section presents the simulation-based case study used for demonstrating the performance of the proposed control scheme. The building to be controlled is a four-story apartment block built in 1978 and located in Aarhus, Denmark. An EnergyPlus [28] model of the building serves as a representation of the actual building. The apartment block has east-west oriented window configurations and west-oriented open balconies, see Fig. 3. To simplify the modelling and simulation process, only the third floor was investigated which is comprised of ten differently sized apartments. All apartments were modelled as individual thermal zones with all

horizontal zone boundaries (ceiling, floor) assumed adiabatic. All thermal zones were modelled with electrical baseboard heating systems operated by the E-MPC control algorithm implemented in MATLAB [29]. The maximum allowed temperature increase of Eq. (2e) was chosen as four degrees above the set point in all apartments. Furthermore, the maximum rate of change in Eq. (2f) was specified as $2.1°$ per hour in accordance with ASHRAE's recommendations [30]. The link between MATLAB and EnergyPlus was facilitated with the Building Controls Virtual Test Bed (BCVTB) [31].

The simulation period was chosen as November 1 to February 28 corresponding to the main heating season in Denmark using the standard EnergyPlus weather data file of Copenhagen, Denmark [32]. Historical market data of electricity production, trading and prices (2015/16) from the day-ahead and intraday markets were used in the simulation as forecasts for operational planning of the building. The data was acquired through the Danish TSO, Energinet.dk [22] and Nord Pool [33,34]. Taxation of electricity was omitted in this study for the sake of simplicity in interpretation of results. Consequently, results presented in absolute values cannot be directly compared to the actual price paid by building owners. The case study does not investigate how weather and price forecast uncertainties affect the performance of the proposed control scheme.

Detailed information on the intraday trading was not available. The only data publicly available was the minimum, average and maximum prices of settled intraday trades for each hour. Because of this, optimal trading conditions were assumed, meaning that the algorithm achieves the lowest intraday price observed while energy is being purchased and highest when energy is sold back to the market. Another piece of information that was unavailable was the period during which a trade offer was available on the intraday market. Because of this, all trades settled during the ITH were assumed to be available at the beginning of the ITH. To reduce the significance of this assumption the ITH was limited to a maximum of three hours in this study. Finally, day-ahead prices were assumed outside the ITH interval.

Previous studies have indicated that the energy efficiency of the building envelope is an important factor in relation to DR quantity and duration [15,35]. The performance of the proposed control scheme was therefore also tested on two retrofitted versions of the existing building to investigate how increased energy-efficiency affected the potential for residential multi-market DR. Both retrofits involve more energy-efficient windows, additional external facade insulation, reduced infiltration rate, and a mechanical constant air volume ventilation rate of $0.5\,h^{-1}$ with 80% heat recovery efficiency as listed in Table 2. The table also lists the reference consumption for space heating over the four months sim-

Table 2
Specification of retrofit scenarios and reference consumption in the simulated period.

	Additional façade insulation	Infiltration rate	Window configuration	Reference consumption
Existing	–	0.50 [h^{-1}]	existing	59.9 kWh/m^2
Retrofit1	0.125 m	0.18 [h^{-1}]	2-layer glazing	28.1 kWh/m^2
Retrofit2	0.205 m	0.10 [h^{-1}]	3-layer glazing	18.6 kWh/m^2

ulated for each respective building controlled with a PI-controller with constant set point. A more detailed description of the building model and the retrofit scenarios can be found in ref. [15].

3. Results

The following sections present the results from the simulations of the case building. The mechanism of the proposed control scheme is illustrated and evaluated on its impact on energy consumption, overall cost savings, utilization of the intraday market, and the fraction of trades that contributed towards grid balance.

3.1. The mechanism

The air temperature and heating rate in a three-room apartment using a conventional PI-control scheme with a constant set point, E-MPC using only day-ahead prices, and the proposed multi-market control scheme are shown in Fig. 4 to illustrate the mechanism of the controller. The intraday action (Fig. 4 bottom) shows how the control scheme interacted with the intraday market in each time step. As a guide to the remaining figures of this article, it should be noted that any control scheme that involve intraday trading (marked ITH) also includes day-ahead trading.

It is not possible to compare results from the two E-MPC-based control schedules directly because they are outcomes of separate simulations where the state of the building may deviate significantly at any given time. However, on multiple occasions the effects of intraday trading are easily distinguishable. For example on Friday where the intraday trading resulted in additional temperature boosting before noon and again in the evening compared to the E-MPC based on only day-ahead prices. On Sunday the opposite happened, where extended periods of temperature boosting were cancelled since selling the procured energy was more profitable.

3.2. Energy consumption and cost savings

The extension of the E-MPC scheme to include intraday trading enables the building to participate in grid balancing while also increasing the potential for cost savings. Fig. 5 shows the performance of three E-MPC schemes when implemented in the case building and the two retrofit scenarios. For transparency, results are presented both in absolute and relative terms compared to a PI-controlled baseline of each building case (origo).

The results from the E-MPC based on day-ahead prices indicated that the retrofitted buildings (R1 and R2) only achieved moderately higher absolute cost savings compared to the existing building (R0). The reason is that, although the E-MPC scheme in the retrofitted buildings tended to load shift more often, the magnitude of load shifts in the existing building is larger due to the higher reference consumption, as also seen in [15]. The introduction of intraday trading reduces the difference in absolute cost savings achieved in the three buildings. This can be explained by relatively low fluctuations in the day-ahead prices that were only sufficient to make utilization of flexibility profitable in the retrofitted buildings, but not in the existing building where a higher loss is associated with the storage process. Since the prices on the two markets, as mentioned in Section 1.2, are strongly correlated, this often resulted in the energy-efficient buildings having already utilized all the available flexibility before trading on the intraday market, whereas this was not the case with the existing building. Ali et al. [24] addressed this issue by reserving part of the flexibility by using more restrictive comfort constraints in the initial day-ahead optimization than following intraday optimization problems. However, the authors argued that reserving flexibility may just as well influence the economic potential negatively as positively since the benefits and viability of reserving flexibility depend strongly on the frequency of DR-events, the size of the economic incentives offered, and the risk-willingness of the consumer.
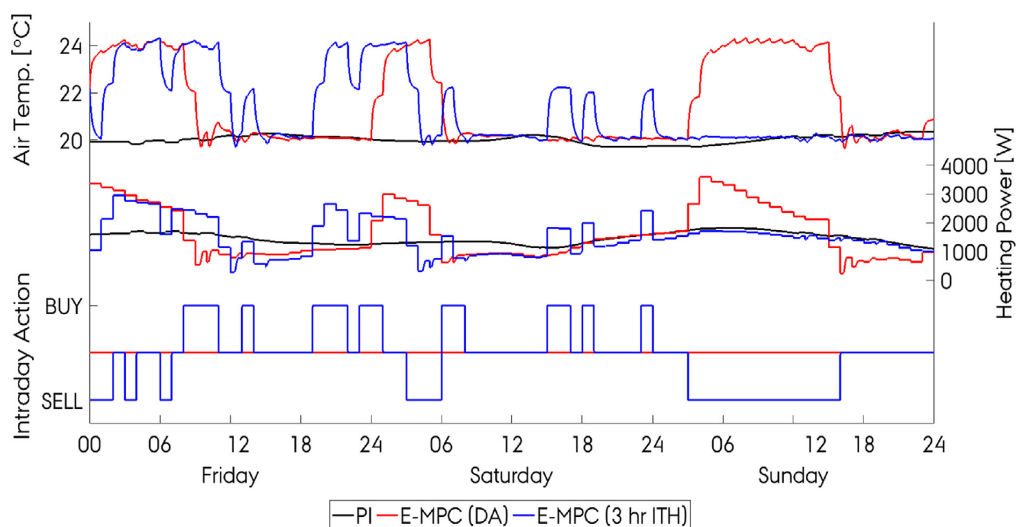

Fig. 4. Example period of both upward and downward regulation in the Retrofit2 building.
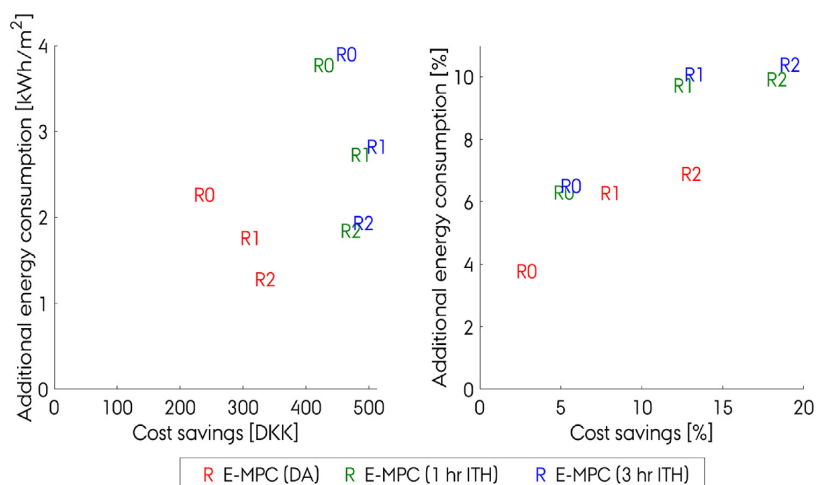
Fig. 5. Economic performance of the algorithm and effect on consumption aggregated for all apartments. Left (a) absolute differences from reference, right (b) relative to the reference.

Fig. 5b, which shows the cost savings in relative terms, indicates a significant difference in the achieved cost savings between the three buildings, suggesting that a higher fraction of the consumption can be made flexible in retrofitted buildings. Furthermore, the effect of enabling the control scheme to trade on the intraday market is seen to positively influence the potential in all cases significantly. The increase in consumed energy seen in Fig. 5 happens since heat is stored by increasing the air temperature. This increase in temperature naturally results in a higher heat loss to the surroundings, and thereby a higher overall consumption. The control algorithm determined when market conditions were sufficiently profitable to make up for the heat lost in the storage process. Finally, Fig. 5 suggest that the economic potential gained by increasing the ITH from one to three hours is marginal.

3.3. Interaction with the intraday market

This section presents how the proposed control scheme interacts with the two electricity markets. The electricity volumes traded by the E-MPC using day-ahead only and the proposed multimarket E-MPC are displayed in Fig. 6.

The results indicate that extending the ITH leads to a moderate increase in intraday trading activity. The reason is that this allows the control scheme to use more elaborate trading patterns including scenarios where electricity was bought in one hour in order to sell procured electricity in the next hour. Furthermore, the share of electricity procured through intraday trading increased for the retrofitted scenarios. This suggests that energy-efficient buildings, retrofitted or new, could on an aggregated level be considered assets in terms of short-notice residential DR.

As described in Section 1.2, BRPs with imbalanced operation are motivated to engage in intraday trading to avoid paying balancing prices. This suggests a certain correlation between the intraday trading and the expected grid balance. The philosophy behind the proposed control scheme is that, by contributing to the balance of individual market actors, the resulting DR will on average have contributed more to overall grid balance than imbalance. However, since balancing out a single BRP does not necessarily equate to increased grid balance, it is necessary to evaluate whether the performed DR actually contributed to balancing the grid.

This was done by labelling all intraday trades carried out by the control scheme based on whether it contributed to balancing
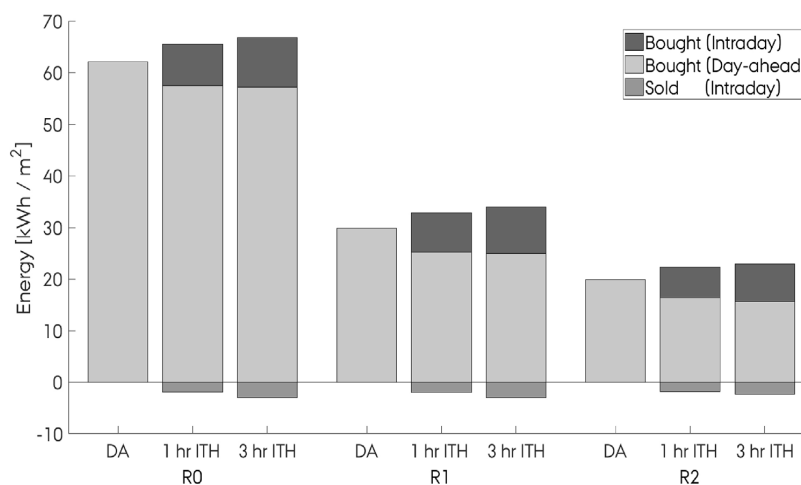

Fig. 6. Electricity traded on the day-ahead and intraday markets (mean of all zones).

Table 3
Percentage of time the DR contributed to balance and imbalance, respectively.

Grid state	Building	R0		R1		R2	
	Control action	1 h ITH	3 h ITH	1 h ITH	3 h ITH	1 h ITH	3 h ITH
Downregulation (48% of time)	Correct	33.1%	39.8%	36.9%	42.7%	35.0%	41.4%
	Incorrect	2.5%	8.1%	3.9%	8.8%	4.4%	7.7%
	No action	64.4%	52.1%	59.2%	48.5%	60.6%	50.9%
Upregulation (28% of time)	Correct	9.6%	17.8%	11.8%	18.6%	14.6%	17.4%
	Incorrect	17.4%	24.6%	17.4%	23.9%	15.6%	21.7%
	No action	72.9%	57.6%	70.9%	57.6%	69.8%	60.9%

the grid or introduced further imbalance. The terminology used in the following takes offset in the grid point of view. This means that buildings can provide *upward regulation* to the grid by lowering the consumption and, conversely, *downward regulation* by increasing consumption. According to Table 3, the grid was in need of downregulation 48% of the time and upregulation 28% of the time during the simulation period [19].

Furthermore, Table 3 indicates how the algorithm operated during these hours by dividing control actions into 'correct' ones that aided the grid and 'incorrect' ones that would have negatively impacted grid balance. As such, the following is an evaluation of both the proposed control scheme and the historical market conditions in relation to the needs of the electricity grid. Periods where the grid was not in need of balancing power was left out of this analysis.

It is seen that the control scheme, in a relatively large fraction of the time where the grid was in need of regulation, did not engage in intraday trading, but merely implemented the control action optimized with respect to day-ahead prices. Depending on the specific simulation, this tendency was observed between 48% and 73% of the time, which can be caused by e.g. poor price conditions or a lack of available flexibility.

The results in Table 3 also indicate that the algorithm performed well during times where the grid was in need of downregulation during which the actions carried out by the controller mostly favoured the grid. During these periods, the controller increased the consumption of the building to store energy between 33% and 43% of the time. On the other hand, it is seen that the control scheme was less efficient at providing services to a grid in need of upregulation. In these periods, more incorrect actions than correct were carried out. Inspecting the historical data revealed that the intraday prices often did not reflect the state of the grid correctly. When the grid needed downregulation, the prices indicated the opposite 22% of the time while in the upregulation scenario this was the case 47% of the time.

4. Discussion

The case results presented in Section 3.2 indicate that the majority of the economic benefits of including intraday trading can be achieved with a one-hour ITH, and thereby – compared to three-hour ITH – reduce the complexity of the planning phase. This implies that simple *one-way* trading patterns (i.e. buy-only or sell-only strategies) were sufficient. However, in real-world application, the ability to consider multiple offers at the same time may allow for easier integration with the market, where offers may be placed at any time throughout the trading window corresponding to the relevant hour. Longer trading horizons allowing utilization of offers entering the intraday market early may therefore be more practical, also bearing in mind that the computational time of the three-hour ITH control problem including both the day-ahead and all eight intraday scenarios for all ten zones was approximately 1.2 s. Rule-based logic could potentially speed this up further by ruling out

scenarios that are unlikely to produce optimal solutions based on price characteristics.

The economic optimization in the E-MPC control scheme will often result in the control scheme tracking the lower temperature set point to minimise the energy consumption – only raising the temperature when prices encourage it. During periods of set point tracking the building has, due to the zero-tolerance for comfort violations, no negative flexibility to offer to the intraday market. Consequently, the controller was only able to sell electricity when temperature boosting had occurred as a result of the day-ahead optimization. This relationship can be found in Fig. 4 where it is clear that electricity was only sold in periods where the day-ahead algorithm was performing temperature boosting. This limitation, in combination with misleading prices, is seen to impact the results of Section 3.3, where the control scheme is less efficient at reducing consumption (i.e. providing upward regulation) than increasing consumption (downward regulation). Enabling buildings to provide upward regulation could be done by allowing temperature violations based on either the profitability of prices or simply a certain fraction of time could to some extent address this limitation.

5. Conclusion

This simulation-based study indicates that consumers may increase their economic incentive to invest in economic predictive control of residential space heating by engaging in trades on the intraday electricity market in parallel with the day-ahead electricity market. Especially buildings that do not provide sufficient storage-efficiency to frequently exploit day-ahead price fluctuations through load shifting benefited from the multi-market approach; here, cost savings were approx. doubled compared to the single-market approach. The results also indicated that increasing the energy efficiency of the building, despite the reduction in overall consumption, only had a small negative impact on the quantities of energy traded on the intraday market. This suggests that also new or recently retrofitted buildings may benefit from participating in intraday market-driven demand response.

Finally, future work should investigate how an alternative formulation of comfort constraints that allows temporary set point violations increases the potential for buildings to provide services to electricity grids in need of upward regulation.

Acknowledgements

References

[1] C. Weber, Adequate intraday market design to enable the integration of wind energy into the European power systems, Energy Policy 38 (2010) 3155–3163, http://dx.doi.org/10.1016/j.enpol.2009.07.040.

[2] J. Kiviluoma, M. O'Malley, A. Tuohy, P. Meibom, M. Milligan, B. Lange, H. Holttinen, M. Gibescu, Impact of wind power on the unit commitment, operating reserves, and market design, in: IEEE Power and Energy Society General Meeting, San Diego, CA, 2011, http://dx.doi.org/10.1109/PES.2011.6039621.

[3] R. D'Hulst, W. Labeeuw, B. Beusen, S. Claessens, G. Deconinck, K. Vanthournout, Demand response flexibility and flexibility potential of residential smart appliances: experiences from large pilot test in Belgium, Appl. Energy 155 (2015) 79–90, http://dx.doi.org/10.1016/j.apenergy.2015.05.101.

[4] P. O'Connell, H. Madsen, M. O'Malley, Benefits and challenges of electrical demand response: a critical review, Renew. Sustain. Energy Rev. 39 (2014) 686–699, http://dx.doi.org/10.1016/j.rser.2014.07.098.

[5] S. Nolan, M. O'Malley, Challenges and Barriers to demand response deployment and evaluation, Appl. Energy 152 (2015), http://dx.doi.org/10.1016/j.apenergy.2015.04.083.

[6] B.P. Esther, K.S. Kumar, A survey on residential Demand Side Management architecture, approaches, Optimization models and methods, Renew. Sustain. Energy Rev. 59 (2016) 342–351, http://dx.doi.org/10.1016/j.rser.2015.12.282.

[7] Buildings Performace Institute Europe (BPIE), Europe's Buildings Under the Microscope – A Country-by-country Review of the Energy Performance of Buildings, BPIE, 2011.

[8] M.H. Albadi, E.F. El-Saadany, A summary of demand response in electricity markets, Electron. Power Syst. Res. 78 (11) (2008) 1989–1996, http://dx.doi.org/10.1016/j.epsr.2008.04.002.

[9] P. Siano, Demand response and smart grids – a survey, Renew. Sustain. Energy Rev. 30 (2014) 461–478, http://dx.doi.org/10.1016/j.rser.2013.10.022.

[10] R. Halvgaard, N.K. Poulsen, H. Madsen, J.B. Jørgensen, Economic Model Predictive Control for Building Climate Control in a Smart Grid, IEEE PES Innovative Smart Grid Technologies, Washington, DC, 2012, http://dx.doi.org/10.1109/ISGT.2012.6175631.

[11] M. Avci, M. Erkoca, A. Rahmanib, S. Asfoura, Model predictive HVAC load control in buildings using real-time electricity pricing, Energy Build. 60 (2013) 199–209, http://dx.doi.org/10.1016/j.enbuild.2013.01.008.

[12] F. Oldewurtel, A. Ulbig, A. Parisio, G. Anderson, M. Morari, Reducing peak electricity demand in building climate control using real-Time pricing and model predictive control, in: 49th IEEE Conference on Decision and Control 2010, Atlanta, GA, 2012, http://dx.doi.org/10.1109/CDC.2010.5717458.

[13] M.D. Knudsen, S. Petersen, Demand response potential of model predictive control of space heating based on price and carbon dioxide intensity signals, Energy Build. 125 (2016) 196–204, http://dx.doi.org/10.1016/j.enbuild.2016.04.053.

[14] M.D. Knudsen, S. Petersen, Demand response potential of model predictive control of space heating based on price and CO2 intensity signals, Energy Build. 125 (2016) 196–204 https://doi.org/10.1016/j.enbuild.2016.04.053.

[15] T.H. Pedersen, R.E. Hedegaard, S. Petersen, Space heating demand response potential of retrofitted residential apartment blocks, Energy Build. 141 (2017) 158–166 https://doi.org/10.1016/j.enbuild.2017.02.035.

[16] F. Oldewurtel, D. Sturznegger, G. Andersson, M. Morari, R.S. Smith, Towards a standardized building assessment for demand response, in: 52nd IEEE Conference on Decision and Control, Florence, Italy, 2013, http://dx.doi.org/10.1109/CDC.2013.6761012.

[17] R. De Coninck, L. Helsen, Quantification of flexibility in buildings by cost curves –methodology and application, Appl. Energy 162 (2016) 653–665, http://dx.doi.org/10.1016/j.apenergy.2015.10.114.

[18] R. Scharff, M. Amelin, Trading behaviour on the continuous intraday market ELBAS, Energy Policy 88 (2016) 544–557, http://dx.doi.org/10.1016/j.enpol.2015.10.045.

[19] Energinet.dk, The Wholesale Market: Download of Market Data (Accessed 23 04 2016) Available: http://www.energinet.dk/EN/El/Engrosmarked/Udtraek-af-markedsdata/Sider/default.aspx.

[20] D.I. Mendoza-Serrano, D.J. Chmielewski, Smart grid coordination in building HVAC systems: EMPC and the impact of forecasting, J. Process Control 24 (2014) 1301–1310 https://doi.org/10.1016/j.jprocont.2014.06.005.

[21] E. Vrettos, K. Lai, F. Oldewurtel, G. Andersson, Predictive Control of Buildings for Demand Response with Dynamic Day-ahead and Real-time Prices, in 2013, European Control Conference Zürich, 2013.

[22] L. Schibuola, M. Scarpa, C. Tambani, Demand response management by means of heat pumps controlled via real time pricing, Energy Build. 90 (2015) 15–28 https://doi.org/10.1016/j.enbuild.2014.12.047.

[23] A. Staino, H. Nagpal, B. Basu, Cooperative optimization of building energy systems in an economic model predictive control framework, Energy Build. 128 (2016) 713–722 https://doi.org/10.1016/j.enbuild.2016.07.009.

[24] M. Ali, A. Alahäivälä, F. Malik, M. Humayun, A. Safdarian, M. Lehtonen, A market-oriented hierarchical framework for residential demand response, Electr. Power Energy Syst. 69 (2015) 257–263, http://dx.doi.org/10.1016/j.ijepes.2015.01.020.

[25] MOSEK ApS, The MOSEK Optimization Toolbox for MATLAB Manual. Version 7.1 (Revision 49), 2015, Available: http://docs.mosek.com/7.1/toolbox/index.html.

[26] M. Gwerder, D. Gyalistras, C. Sagerschnig, R. Smith, D. Sturzenegger, Final Report: Use of Weather And Occupancy Forecasts For Optimal Building Climate Control – Part II: Demonstration (OptiControl-II), 2013.

[27] G. Bianchini, M. Casini, A. Vicino, D. Zarrilli, Demand-response in building heating systems: a model predictive control approach, Appl. Energy 168 (2016) 159–170, http://dx.doi.org/10.1016/j.apenergy.2016.01.088.

[28] U.S. Department of Energy, EnergyPlus 8.1.0, [Online].

[29] The MathWorks, inc., MATLAB 2015 (8.6.0.267246).

[30] ASHRAE, Standard 55-2010: Thermal Environmental Conditions for Human Occupancy, ASHRAE, Atlanta, 2010.

[31] M. Wetter, Co-simulation of building energy and control systems with the Building Controls Virtual Test Bed, J. Build. Perform. Simul. 3 (4) (2010) 1–19, http://dx.doi.org/10.1080/19401493.2010.518631.

[32] U.S. Department of Energy, EnergyPlus Weather Data: Copenhagen 061800 (IWEC) (Accessed 06 04 2016) Available: https://energyplus.net/weather-region/europe_wmo_region.6/DNK%20%20.

[33] Nord Pool, Elspot market data, [Online]. Available: http://www.nordpoolspot.com/Market-data1/Elspot/ (Accessed 29 04 2016).

[34] Nord Pool, Elbas market data, [Online]. Available: https://www.nordpoolspot.com/Market-data1/Elbas/ (Accessed 29 04 2016).

[35] G. Reynders, Quantifying the Impact of Building Design on the Potential of Structural Storage for Active Demand Response in Residential Buildings. PhD Dissertation, KU Leuven – Faculty of Engineering Science, 2015.

P4   Comparison of centralized and decentralized model predictive control in a building retrofit scenario

CISBAT 2017 International Conference – Future Buildings & Districts – Energy Efficiency from Nano to Urban Scale, CISBAT 2017 6-8 September 2017, Lausanne, Switzerland

Comparison of centralized and decentralized model predictive control in a building retrofit scenario

Theis Heidmann Pedersen[a],*, Rasmus Elbæk Hedegaard[a], Michael Dahl Knudsen[a], Steffen Petersen[a]

[a]Department of Engineering, Aarhus University, Inge Lehmanns Gade 10, 8000 Aarhus C, Denmark

Abstract

Heat transfer between apartments can challenge the positive effects of applying model predictive control (MPC) in multi-apartment buildings. This paper reports on an investigation of how the performance of two different MPC approaches – centralized and decentralized – may be affected by non-insulated and insulated partition walls between apartments. The results suggest that ignoring inter-zonal thermal effects using the less complicated decentralized approach leads to insignificant performance reductions compared to the more complicated centralized approach – especially if partition walls are insulated.

Keywords: Model predictive control; Building retrofit; Energy flexibility; Residential space heating; Demand response

1. Introduction

Current studies have demonstrated that model predictive control (MPC) of building systems may increase energy efficiency and ensure thermal comfort. MPC schemes rely on a model of the building dynamics, measurements of the state of the building and forecasts of disturbances (e.g. weather and occupancy) to determine a sequence of optimal

---

* Corresponding author.
E-mail address: thp@eng.au.dk

control actions [1-3]. Several studies have applied MPC to optimize the operation of heating, ventilation and air conditioning (HVAC) systems and have achieved significant energy savings. Sourbron et al. [2] applied MPC to operate a heat pump in an office building equipped with thermo active building systems, which reduced the electricity consumption by 15% while ensuring thermal comfort. Goyal et al. [3] used MPC to operate an air-handling unit and achieved energy savings of 55-60% compared to a dual-maximum baseline control. In a simulation study, Oldewurtel et al. [1] compared MPC to conventional rule-based control for various building typologies and locations, and found that MPC, in most cases, reduced energy consumption while improving thermal comfort.

Several studies have also considered time-varying energy prices together with MPC to minimize the operational cost, i.e. economic model predictive control (E-MPC), to provide flexibility to the energy grid through demand response [4-7]. A simulation study by Avci et al. [4] used real time prices together with an E-MPC scheme to operate an AC unit in a single residence and reduced the energy consumption in peak-hours by 23.6% and operational cost with 13% compared to a baseline controller. Pedersen et al. [5] used an E-MPC scheme and day-ahead power market prices to investigate the demand response potential in an existing residential multi-apartment building before and after retrofitting the building envelope. Compared to a baseline PI controller, the simulation results suggested that the E-MPC scheme reduced the energy consumption in peak-hours in the existing and retrofitted building by approx. 7% and up to 47%, respectively, while ensuring thermal comfort.

For multi-zone buildings, centralized and decentralized thermal control schemes exist [5, 8, 9]. Centralized MPC schemes require a detailed building model that accounts for heat transfer between adjacent zones to determine the operation in all zones simultaneously. Decentralized MPC relies on a set of single-zone models that neglect inter-zonal heat transfer, leading to multiple detached optimization problems. In theory, decentralized control schemes return a sub-optimal solution compared to centralized MPC. To show this, Moroşan et al. [8] compared a conventional baseline controller with a decentralized and centralized MPC scheme, which achieved energy savings of 5.5% and 13.4%, respectively. However, the authors noted that the performance difference depends on the coupling degree between zones. Pedersen et al. [5] likewise found a minor performance difference between centralized and decentralized control structures when applying E-MPC.

In existing apartment buildings, the interior partition walls often consist of heavy materials with high conductivity, such as concrete. However, in a retrofit situation, where the energy efficiency of the building is increased, insulation is often added to the partition walls to reduce inter-zonal noise. Consequently, the conductivity of the wall is reduced, which may diminish any advantage of including inter-zonal thermal effects. The decentralized control approach may therefore be more practical since it does not require mapping of zone-adjacency during model establishment or exchange information between controlled zones during operation. This paper therefore investigates the performance difference between centralized and decentralized MPC in an apartment building without and with insulated partition walls.

2. Method

The third floor of an existing residential building located in Aarhus, Denmark, consisting of ten apartments and five stairwells was modelled in EnergyPlus (EP) and used to represent the actual building to be controlled. In addition to the existing building, a case with a retrofitted building envelope was considered. Information on geometry and thermal characteristics of the existing and retrofitted buildings are provided in ref. [5] (the retrofitted building is denoted retrofit8 in the reference). The existing partition walls between apartments were assumed to consist of 120 mm concrete while additional 100mm mineral wool and 13mm gypsum was added when insulating the walls.

The MPC scheme was implemented in MATLAB and used to operate the space heating (electrical baseload) of the EP model through co-simulation facilitated by the Building Controls Virtual Test Bed (BCVTB) [10]. The simulations were carried out for the period December 1, 2016 to February 28, 2017, which constitutes the coldest period of the heating season in Denmark, using an EP weather data file based on on-site weather measurements. To ease the interpretation of the results, internal gains originating from occupants and equipment were omitted and perfect weather forecasts were assumed.

2.1. Centralized and decentralized model predictive control

MPC is an optimization-based control scheme, which at each time step determines a sequence of optimal space heating control actions by minimization of a cost function based on an input weight vector c associated with the control actions. The problem (eq. 1a-1g) is solved for a finite prediction horizon N which, in this study, was set to 72 hours. The control actions are restricted by the maximum design power P_{max} of the heating system (eq. 1d), and eq. 1e and eq. 1f constrain the apartment air temperatures and the temperature rate of change, respectively. Specifications for input and state constraints are listed in Table 1. The control actions are communicated to the space heating system in a receding horizon approach, i.e. only the first control action is implemented and the procedure is then repeated at the next time step based on recent apartment air temperature measurements and updated disturbance forecasts [1].

$$\underset{u_{0|t},\dots,u_{N|t}}{\text{minimize}} \quad J = \sum_{n=0}^{N-1} c_{n|t}^T \cdot u_{n|t} \tag{1a}$$

$$\text{subject to} \quad x_{n+1|t} = \mathbf{A}x_{n|t} + \mathbf{B}u_{n|t} + \mathbf{E}d_{n|t} \qquad \forall n = 0, \dots, N\text{-}1 \tag{1b}$$

$$y_{n+1|t} = \mathbf{C}x_{n+1|t} \qquad \forall n = 0, \dots, N\text{-}1 \tag{1c}$$

$$0 \leq u_{n|t} \leq P_{max} \qquad \forall n = 0, \dots, N\text{-}1 \tag{1d}$$

$$T_{min,n|t} \leq y_{n+1|t} \leq T_{max,n|t} \qquad \forall n = 0, \dots, N\text{-}1 \tag{1e}$$

$$\Delta T_{min,n|t} \leq \frac{y_{n+1|t}}{\Delta \tau} \leq \Delta T_{max,n|t} \qquad \forall n = 0, \dots, N\text{-}1 \tag{1f}$$

$$x_{0|t} = x_t \tag{1g}$$

The MPC scheme requires a reduced-order model that adequately describes the thermodynamics of the building, e.g. grey-box models. Grey-box models are characterized by having a pre-specified model structure consisting of physically meaningful parameters that are estimated from measurement data through methods from the field of system identification [11]. In a multi-apartment building, the model represents an interconnected system of subsystems (corresponding to apartments), where the interactions occur due to conduction between apartments [12]. Identifying suitable multi-zone models for centralized control schemes, thus considering the thermal interactions, can be difficult and requires time-consuming experiments, planning and modeling [12, 13]. Decentralized control schemes neglect the interactions and treat the thermal influences between subsystems as external unknown disturbances, thus adequate models are easier to identify. In this study, a two-state grey-box apartment model was used, where the two states represent the lumped thermal capacity of the zone air and the constructions. The applied state space representation is given in (1b-1c) with state matrix $\mathbf{A}$, system states x for time step $t+n$ forecasted at time t, input matrix $\mathbf{B}$, control actions u, disturbance matrix $\mathbf{E}$, disturbances d, output matrix $\mathbf{C}$ and output y (i.e. apartment air temperatures).

Table 1. Specification of input and state constraints

		Apt. 1	Apt. 2	Apt. 3	Apt. 4	Apt. 5	Apt. 6	Apt. 7	Apt. 8	Apt. 9	Apt. 10
Area	[m²]	81	94	81	94	81	94	81	94	50	94
P_{max}	[W/m²]	50	50	50	50	50	50	50	50	50	50
T_{min}	[°C]	20	22	20	22	20	22	20	22	20	22
T_{max}	[°C]	24	26	24	26	24	26	24	26	24	26
ΔT_{min}	[°C/h]	-2.1	-2.1	-2.1	-2.1	-2.1	-2.1	-2.1	-2.1	-2.1	-2.1
ΔT_{max}	[°C/h]	2.1	2.1	2.1	2.1	2.1	2.1	2.1	2.1	2.1	2.1

The centralized and decentralized MPC schemes were first evaluated in terms of their ability to track the lower comfort bounds, which constitutes the most energy efficient control approach. Secondly, the MPC schemes' ability to achieve end-user cost savings was assessed by considering time varying energy prices as input weights. Historical day-ahead power market prices for the simulation period were used, cleared for the bidding area western Denmark (DK1). For the sake of simplicity, taxation of electricity was omitted, thus results presented in absolute values are not directly comparable to actual costs paid by building owners.

3. Results and discussion

The ability of the centralized and decentralized MPC schemes to track the lower comfort bound for one week in apartment 9 in the retrofitted building, with and without insulated partition wall is displayed in Figure 1. For the building with existing partition walls, the centralized MPC scheme kept the air temperature close to the temperature set-point, whereas the decentralized MPC scheme overestimated the heating demand, leading to a positive temperature offset compared to the temperature set-point. The positive offset was caused by heat gains from adjacent apartments with higher temperature set-points (see Table 1). When insulating the partition walls, the heat exchange between adjacent apartments was reduced, resulting in a similar performance of the centralized and decentralized MPC schemes.
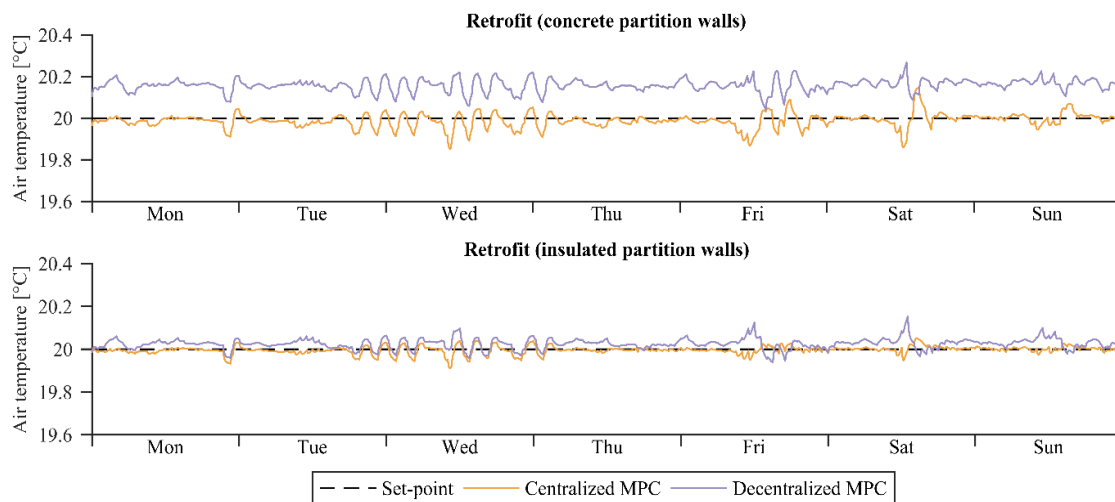

Figure 1. Simulation results of the room temperature in apt. 9 during one week.

The mean biased error (MBE) between the temperature set-points and the resulting air temperatures during the entire simulation period is specified in Table 2 (+ indicates insulated partition walls). The MBE supports the observations in Figure 1, where the decentralized MPC scheme in buildings with existing concrete partition walls led to positive and negative offsets for the apartments with a set-point of 20°C and 22°C, respectively. In the case with the insulated partition walls, the MBE for the two control schemes were very similar. In some apartments, the decentralized MPC scheme even achieved better results than centralized MPC, presumably because the required multi-apartment model was more difficult to identify than the single-apartment models, which led to a significant increase in the uncertainty of the parameter estimates [5].

Table 2. Mean biased error

Building	Control	Apt. 1	Apt. 2	Apt. 3	Apt. 4	Apt. 5	Apt. 6	Apt. 7	Apt. 8	Apt. 9	Apt. 10
Existing	Centralized	0.00	0.01	0.00	0.02	0.00	0.01	0.02	0.02	0.00	0.01
	Decentralized	0.06	-0.09	0.10	-0.07	0.12	-0.04	0.07	-0.07	0.12	-0.03
Existing+	Centralized	-0.01	0.03	-0.02	0.03	-0.01	0.01	-0.01	0.02	0.01	0.00
	Decentralized	0.01	-0.01	0.03	-0.01	0.03	-0.01	0.02	-0.01	0.03	0.00
Retrofit	Centralized	-0.01	0.03	-0.01	0.02	-0.02	0.02	-0.01	0.04	-0.02	0.00
	Decentralized	0.06	-0.09	0.10	-0.09	0.11	-0.05	0.06	-0.08	0.17	-0.05
Retrofit+	Centralized	-0.03	0.03	-0.02	0.02	-0.02	0.02	-0.04	0.03	0.00	-0.01
	Decentralized	0.00	-0.02	0.02	-0.02	0.02	-0.01	0.01	-0.02	0.03	-0.01

The mechanism of a conventional PI-controller and the E-MPC schemes using historical day-ahead prices during one week are displayed in Figure 2 for the retrofitted building with the existing partition walls and with insulated partition walls. In both cases, the conventional PI-controller maintained the air temperature close to the specified lower comfort set-point of 20°C at all times. The E-MPC schemes, however, exploited the structural thermal mass to reduce

the space heating consumption in high price periods by increasing the air temperature within the comfort bounds at times with low prices. Since the optimal control actions depend on the state of the building at any given time, direct comparison between the two control schemes at each time instance should be done carefully. However, in the case with the existing concrete partition walls, discrepancies between the two E-MPC schemes are clearly distinguishable on Thursday and Friday, where only the centralized E-MPC scheme increased the temperature. Furthermore, the temperature offset of the decentralized control scheme identified previously was also apparent in the case with the concrete partition walls. For the insulated partition walls, the control schemes led to almost identical operations.
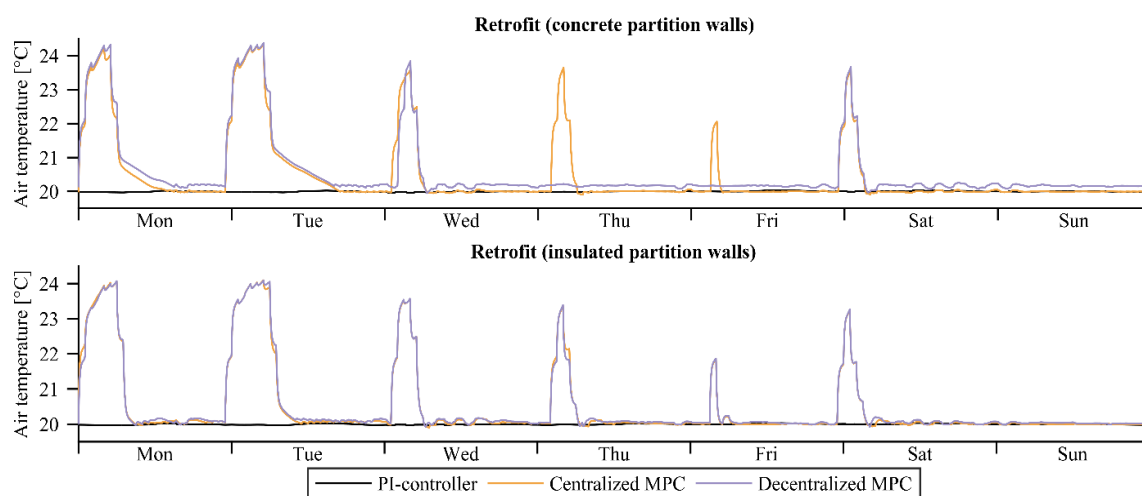

Figure 2. Simulation results of the room temperature in apt. 9 during one week using E-MPC.

Table 3 lists the total costs of each of the three control schemes (PI, centralized E-MPC and decentralized E-MPC) for the four building cases: before and after a general retrofit of the building envelope and with and without insulated partition walls. Furthermore, the total achieved cost savings and mean comfort violations compared to the PI-controller are specified. The standard deviations across the apartments are specified in the parentheses. The results suggest that centralized and decentralized E-MPC schemes achieved total cost savings similar to those of the PI controller. The decentralized control scheme, however, tended to distribute cost savings unevenly between the apartments in the scenarios without insulated partition walls. Further inspection of the simulation results indicated that this was due to lower achieved cost savings in the apartments with a lower comfort bound of 20°C; here, the E-MPC scheme planned the heating operation without considering the heat gains from adjacent apartments. This effect was significantly reduced in the scenarios with insulated partition walls. Furthermore, in the case with the insulated partition walls, the decentralized control scheme out-performed the centralized control scheme in terms of maintaining comfort, presumably because the multi-zone models are more challenging to identify.

Table 3. Summarized simulations results for all ten apartments

Building	Control	Total cost	Cost savings	Relative cost saving	Mean comfort violations
Existing	PI	€ 1040			89.7 (4.3) °Ch
	Centralized	€ 1010	€ 30 (0.66)	2.9%	18.1 (9.8) °Ch
	Decentralized	€ 1011	€ 29 (1.37)	2.8%	22.7 (9.4) °Ch
Existing+	PI	€ 1001			84.4 (2.9) °Ch
	Centralized	€ 977	€ 24 (0.42)	2.4%	15.9 (2.6) °Ch
	Decentralized	€ 979	€ 22 (0.50)	2.2%	11.2 (1.5) °Ch
Retrofit	PI	€ 327			43.9 (3.0) °Ch
	Centralized	€ 293	€ 34 (0.86)	10.4%	9.3 (8.7) °Ch
	Decentralized	€ 293	€ 34 (1.59)	10.4%	18.0 (8.7) °Ch
Retrofit+	PI	€ 323			38.5 (1.7) °Ch
	Centralized	€ 287	€ 36 (0.55)	11.1%	7.5 (3.0) °Ch
	Decentralized	€ 287	€ 36 (0.63)	11.1%	6.9 (2.2) °Ch

4. Conclusion

This paper reports on a simulation-based study of the performance differences between centralized and decentralized MPC schemes for optimal space heating operation in an existing and retrofitted multi-apartment building. The results of a 90-day simulation period showed that the decentralized MPC in buildings without insulated partition walls tended to result in a constant offset from the specified temperature set-point. Consequently, the achieved total cost savings for both schemes were found to be similar, but the decentralized control scheme failed to distribute the savings evenly across all apartments. Insulating the partition walls reduced the constant temperature offsets when applying the decentralized control scheme, which was reflected in the results. The decentralized control scheme was not only able to distribute cost savings evenly, but it also out-performed centralized control in terms of maintaining temperatures within the comfort bounds. This reversal in the optimal approach is likely caused by the fact that the advantages of centralized control diminish as insulation is added between zones, combined with the fact that the more complicated setup of the centralized control was more prone to uncertainty issues when identifying a building model for MPC.

Overall, the results suggest that decentralized control schemes can be applied in multi-apartment buildings, especially where partition walls are insulated for noise-reduction purposes. However, it is difficult to specify a general level of insulation, as the performance depends e.g. on the building, the modeling technique and the control purpose. Applying decentralized MPC also simplifies and reduces the time-consuming work involved when implementing MPC schemes. Furthermore, decentralized control schemes allow apartment owners to specify control objectives themselves, just as it allows for individual apartment owners to decide if and when to invest in advanced control.

Acknowledgements

References

[1] F. Oldewurtel, A. Parisio, C. N. Jones, D. Gyalistras, M. Gweder, V. Stauch, B. Lehmann and M. Morari. Use of Model Predictive Control and Weather Forecasts for Energy Efficient Building Climate Control. Energy Build. 45 (2012) 15-27.

[2] M. Sourbron, C. Verhelst and L. Helsen. Building models for model predictive control of office buildings with concrete core activation. J. Build. Perform. Simul. 6 (3) (2013) 175-198.

[3] S. Goyal, H. A. Ingley and P. Barooah. Occupancy-based zone-climate control for energy-efficient buildings: Complexity vs. performance. Appl. Energ. 106 (2016) 209-221.

[4] M. Avci, M. Erkoc, A. Rahmani and S. Asfour. Model predictive HVAC load control in buildings using real-time electricity pricing. Energy Build. 60 (2013) 199-209.

[5] T. H. Pedersen, R. E. Hedegaard and S. Petersen. Space heating demand response potential of retrofitted residential apartment blocks. Energy Build. 141 (2017) 158-166.

[6] M. D. Knudsen and S. Petersen. Demand response potential of model predictive control of Space heating based on price and carbon dioxide Intensity signals. Energy Build. 125 (2016) 196-204.

[7] R. Halvgaard, N. K. Poulsen, H. Madsen and J. B. Jørgensen. Economic Model predictive Control for Building Climate Control in a Smart Grid. in IEEE PES Innovative Smart Grid Technologies (ISGT) (2012) 1-6, Washington, D.C., United States.

[8] P.-D. Moroşan, R. Bourdais, D. Dumur and J. Buisson. Building temperature regulation using a distributed model predictive control. Energy Build. 42 (2010) 1445-1452.

[9] V. Chandan and A. G. Alleyne. Decentralized Architectures for Thermal Control of Buildings. in American Control Conference (2012), Montreal, Canada.

[10] M. Wetter. Co-simulation of building energy and control systems with the Building Controls Virtual Test Bed. J. Build. Perform. Simul. 3 (4) (2010) 1-19.

[11] R. E. Hedegaard and S. Petersen. Evaluation of Grey-Box Model Parameter Estimates Intended for Thermal Characterization of Buildings. in 11th Nordic Symposium on Building Physics (2017), Trondheim, Norway.

[12] S. Goyal, C. Liao and P. Barooah. Identification of multi-zone building thermal interaction model from data. in 50th IEEE Conference on Decision and Control (2011), Orlando, FL, USA.

[13] C. Agbi, Z. Song and B. Krogh. Parameter Identifiability for Multi-Zone Building Models. in 51st IEEE conference on Decision and Control (2012), Maui, Hawaii, USA.

P5 Handling thermal comfort in economic model predictive control schemes for demand response

CISBAT 2017 International Conference – Future Buildings & Districts – Energy Efficiency from Nano to Urban Scale, CISBAT 2017 6-8 September 2017, Lausanne, Switzerland

Handling thermal comfort in economic model predictive control schemes for demand response

Theis Heidmann Pedersen[a],*, Michael Dahl Knudsen[a],
Rasmus Elbæk Hedegaard[a], Steffen Petersen[a]

[a]Department of Engineering, Aarhus University, Inge Lehmanns Gade 10, 8000 Aarhus C, Denmark

Abstract

Addressing thermal comfort is an important aspect of applying economic model predictive control (E-MPC) schemes with the objective to perform demand response (DR), e.g. minimize operational cost. This paper compares the performance of four E-MPC schemes using both single-objective and multi-objective formulations to address thermal comfort. It is difficult to proclaim the superior formulation as the notion of thermal comfort is a subjective matter. However, the single-objective problem formulation proposed in this paper contains a parameter, ε_{max}, which describes the maximum acceptable deviations from the preferred indoor air temperature. This parameter can be regarded as a user-defined indicator of the acceptable deviations from the preferred temperature or, in other words, their 'DR willingness'.

───────

* Corresponding author.
E-mail address: thp@eng.au.dk

1. Introduction

Economic model predictive control (E-MPC) of building energy systems is an optimization based control scheme that uses a model of the building thermodynamics, forecasts of disturbances and measurements of the building state to determine a sequence of optimal control actions. Applying E-MPC together with time-varying energy prices to minimize the space heating operational cost and perform demand response (DR) have been investigated in several studies [1-4]. These E-MPC schemes achieve economic benefits by using the thermal capacity of the structural mass as storage by charging and discharging it with the room heating system in periods with low or high prices, respectively. The schemes therefore result in fluctuating indoor temperatures, and it is therefore necessary to ensure that economic benefits are not violating the thermal comfort of the occupants.

A simple E-MPC formulation in this regard is to assume that occupants are comfortable as long as temperatures are within a predefined comfort band, e.g. defined by a preferred temperature and an acceptable deviation from it. Using this comfort formulation, several studies have suggested significant cost savings and DR potentials. Halvgaard et al. [5] minimized the operational cost of a heat pump and achieved cost savings of 25% compared to traditional control. Pedersen et al. [4] optimized the space heating operation in a multi-apartment building which, compared to a conventional PI-controller, achieved cost savings of up to 6% and reduced energy consumption in peak-hours with up to 47%. Vrettos et al. [1] applied E-MPC for heat pump operation and achieved cost savings of 18.4% compared to a rule-based controller. However, an E-MPC scheme using this comfort formulation will often result in the controller tracking either the upper or the lower boundary of the comfort band [4]. This behavior means that the air temperature rarely is equal to the preferred temperature specified by the occupants. Another shortcoming of this formulation is that the building has no downward flexibility to offer in periods where the lower comfort bound is tracked, i.e. it is not possible to reduce the space heating demand if this service is requested by the supply side [6].

Another approach to ensure comfort is to formulate a multi-objective optimization (MOO) problem, i.e. simultaneously minimize operational costs and thermal comfort violations [2, 7-10]. Avci et al. [2] used an E-MPC scheme to minimize energy consumption and penalize temperature deviations from the preferred temperature, and introduced a discomfort tolerance index to weigh the objectives. Compared to a baseline controller, the E-MPC scheme reduced operational cost with 13% while increasing the mean temperature with 0.15°C. Morales-Valdés et al. [8] evaluated several MOO formulations and suggested to include Fanger's predicted mean vote (PMV) index or predicted percentage dissatisfied (PPD) index in the cost function which, however, led to a nonlinear optimization problem. Therefore, Cigler et al. [7] proposed a convex approximation of the PMV index in the cost function. However, including the PMV index in the cost function relies on assumptions regarding clothing level and metabolic rate, as well as measurement of air speed, relative humidity and the mean radiant temperature. Furthermore, the performance reported in the above-mentioned MOO studies depends on the selection of the assigned relative weights which essentially vary in time as they depend on the building conditions.

Current studies address thermal comfort in E-MPC formulations very differently, which may affect the reported DR potentials. This paper therefore reports on a simulation-based study, where the performance of an E-MPC scheme using both single-objective and multi-objective formulations to address thermal comfort violations is investigated. The aim is to provide a quantitative performance assessment of the different formulations in terms of comfort violations and operational cost, and to discuss their practical implications.

2. Method

A residential building consisting of ten apartments and five stairwells located in Aarhus, Denmark, was chosen as test case. A detailed EnergyPlus (EP) model was used to represent the building to be controlled; information on geometry and thermal characteristics of the building are provided in ref. [4] in which the building is denoted retrofit8. Furthermore, 100mm insulation was added to the partitioning walls to minimize the effect of inter-zonal heat exchange and thereby allow for a decentralized control principle [11]. The E-MPC scheme was implemented in MATLAB and used to operate the space heating of the EP model through co-simulation facilitated by the Building Controls Virtual Test Bed (BCVTB) [12]. The simulations were carried out for the period December 1, 2016 to February 28, 2017, which constitutes the coldest period of the heating season in Denmark, using an EP weather file based on on-site weather measurements. Historical day-ahead power market prices (cleared for Western Denmark, DK1 region) from the simulation period were used. To ease the interpretation of the results, internal gains originating from occupants and equipment were omitted, and perfect weather and price forecasts were assumed.

2.1. Economic model predictive control

At each time step the E-MPC scheme (eq. 1a-1g) determines a sequence of optimal space heating control actions which minimize temperature deviations from the preferred temperature (j_1) and the operational costs (j_2) for a finite prediction horizon N (set to 72 hours in this study).

$$\underset{\varepsilon,u}{\text{minimize}} \quad \underbrace{\epsilon^T \mathbf{Q}\, \epsilon}_{j_1} + \underbrace{c^T u}_{j_2} \tag{1a}$$

$$\text{subject to} \quad x_{n+1} = \mathbf{A}x_n + \mathbf{B}u_n + \mathbf{E}d_n \qquad \forall n = 0, \dots, N\text{-}1 \tag{1b}$$

$$y_{n+1} = \mathbf{C}x_{n+1} \qquad \forall n = 0, \dots, N\text{-}1 \tag{1c}$$

$$\epsilon_{n+1} = T_{\text{preferred}} - y_{n+1} \qquad \forall n = 0, \dots, N\text{-}1 \tag{1d}$$

$$0 \leq u_n \leq P_{\max} \qquad \forall n = 0, \dots, N\text{-}1 \tag{1e}$$

$$T_{\min} \leq y_{n+1} \leq T_{\max} \qquad \forall n = 0, \dots, N\text{-}1 \tag{1f}$$

$$x_0 = x(0) \tag{1g}$$

where $\mathbf{Q}$ is a time-invariant symmetric matrix with main diagonal elements and c is the time-varying day-ahead prices. A state space representation of the building's thermodynamics is specified in eq. 1b and eq. 1c. The control actions are restricted by the maximum power $P_{\max}$ of the heating system (eq. 1e), and the defined thermal comfort band (eq. 1f), which may vary between the apartments as listed in Table1. Recent measurements of the air temperature are used to update the current state of the building in eq. 1g with a Kalman Filter.

Table 1. Input and state constraints

	Apt. 1	Apt. 2	Apt. 3	Apt. 4	Apt. 5	Apt. 6	Apt. 7	Apt. 8	Apt. 9	Apt. 10
$P_{\max}$	50 W/m^2	50 W/m^2	50 W/m^2	50 W/m^2	50 W/m^2	50 W/m^2	50 W/m^2	50 W/m^2	50 W/m^2	50 W/m^2
$T_{\text{preferred}}$	20.5 °C	22.0 °C	21.5 °C	22.0 °C	20.5 °C	21.5 °C	21.0 °C	20.0 °C	22.0 °C	21.5 °C
$T_{\min}$	19.5 °C	20.5 °C	20.5 °C	20.0 °C	19.0 °C	19.5 °C	19.0 °C	19.0 °C	20.5 °C	19.5 °C
$T_{\max}$	21.5 °C	23.5 °C	22.5 °C	24.0 °C	22.0 °C	23.5 °C	23.0 °C	21.0 °C	23.5 °C	23.5 °C

Since the two objectives j_1 and j_2 are conflicting, there is generally no unique solution that optimizes both objectives simultaneously, which suggests that a useful approach to solving the MOO is that of Pareto optimality [13]. The set of Pareto optimal solutions, which from a mathematically point of view is equally acceptable, forms a Pareto front. The simplest method to obtain Pareto optimal solutions is convex combination of j_1 and j_2, e.g. the weighted sum approach (as used in ref. [2, 7, 8]): $J = \lambda \cdot j_1 + (1-\lambda) \cdot j_2$, where $\lambda \in [0,1]$. Note that if $\lambda=1$ the control scheme is a traditional reference tracking control problem, whereas if $\lambda=0$ the control scheme is similar to the ones used in ref. [1, 4, 5]. However, as mentioned in the introduction, the performance of this approach depends significantly on the assigned relative weights which are difficult to choose when the Pareto front is steep or if the objective functions have very different ranges [13, 14]. Furthermore, thermal discomfort can be difficult to quantify since thermal comfort has no direct economic translation. To overcome this, Das and Dennis [13] proposed a normal boundary intersection (NBI) method to approximate the Pareto front with evenly distributed discrete solutions that are independent of weights between objectives (see Figure 1).
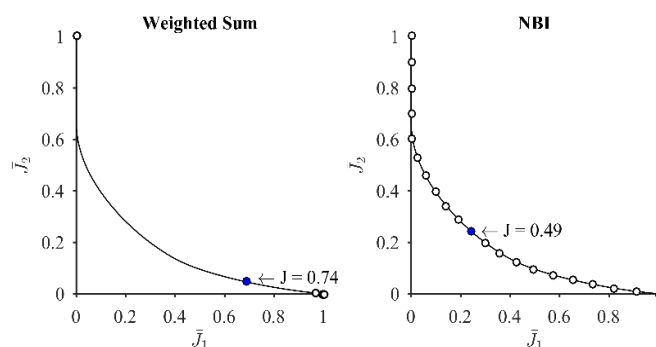

Figure 1. Normalized optimal Pareto solutions with λ increments of 0.05.

When the set of discrete Pareto solutions has been determined, several approaches exist to select and implement an agreeable trade-off between j_1 and j_2 [15]. In this study, the compromise solution is selected, which corresponds to the solution with the shortest Euclidean distance to the utopia point. The utopia point is, as the name suggests, an ideal solution when minimizing each objective independently. Figure 1 displays the results of the weighted sum and NBI methods for a scenario with two objectives with different ranges, and indicates that NBI is more resistant to ill-conditioned problems. The utopia point is origin, the solid line is the continuous Pareto front and the black and blue circles mark the obtained discrete Pareto solutions and the compromise solution, respectively.

Since an MOO problem is computationally demanding to solve compared to a single-objective optimization (SOO) problem, a SOO formulation is proposed which aims at imitating the behavior of MOO. The formulation builds on eq. 2a-2g. However, **Q** is an appropriate sized matrix of zeros (i.e. only objective j_2 is effective). Furthermore, additional state constraints are specified as illustrated in Figure 2, describing the maximum acceptable temperature deviations within the prediction horizon using the parameter ε_{max} [°Ch] which is then a tuning parameter to indicate preference between thermal discomfort and operational cost minimization.
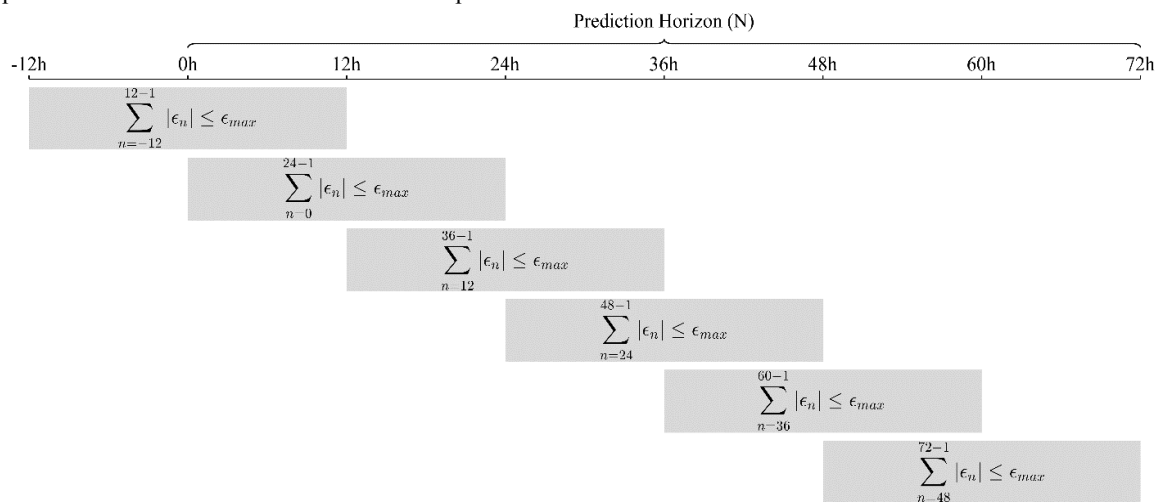

Figure 2. Principle of proposed additional six state constraints

3. Results and discussion

Simulation results obtained using the following four different E-MPC formulations have been evaluated with regard to their ability to reduce deviations from the preferred temperature (see Table 1) and to minimize operational costs:

a) Single objective: Minimize temperature deviations from the preferred temperature.
b) Single objective: Minimize operational costs.
c) Multi objective: Compromise solution (see Figure 1) between temperature deviations and cost.
d) Single objective: Minimize operational costs, but with additional state constraints (see Figure 2).

The objectives and constraints imposed in the four different control schemes vary as a result of the different formulations, thus rendering any direct comparison of results unfair from a mathematical point of view. The evaluation is therefore based on quantification of the four problem formulations on the achieved results. Figures 3a-d depict the indoor air temperature for a one week period in apartment 3 using the four E-MPC schemes with the time-varying energy prices *c* depicted at the bottom of Figure 3. Formulation a) ensured a temperature (solid line) close to the preferred temperature at all times, whereas the three other formulations utilized the thermal comfort band (dashed lines) to minimize operational cost. Formulation b) caused the E-MPC scheme to mainly track the lower and upper comfort bounds in order to exploit price fluctuations by charging and discharging the thermal capacity of the building. Formulation c) tracked the preferred temperature for the majority of the time, allowing deviations in temperature when prices encouraged it. The proposed formulation d) with $\varepsilon_{max} = 9\,°Ch$ exhibited similar behavior and DR-potential as c).
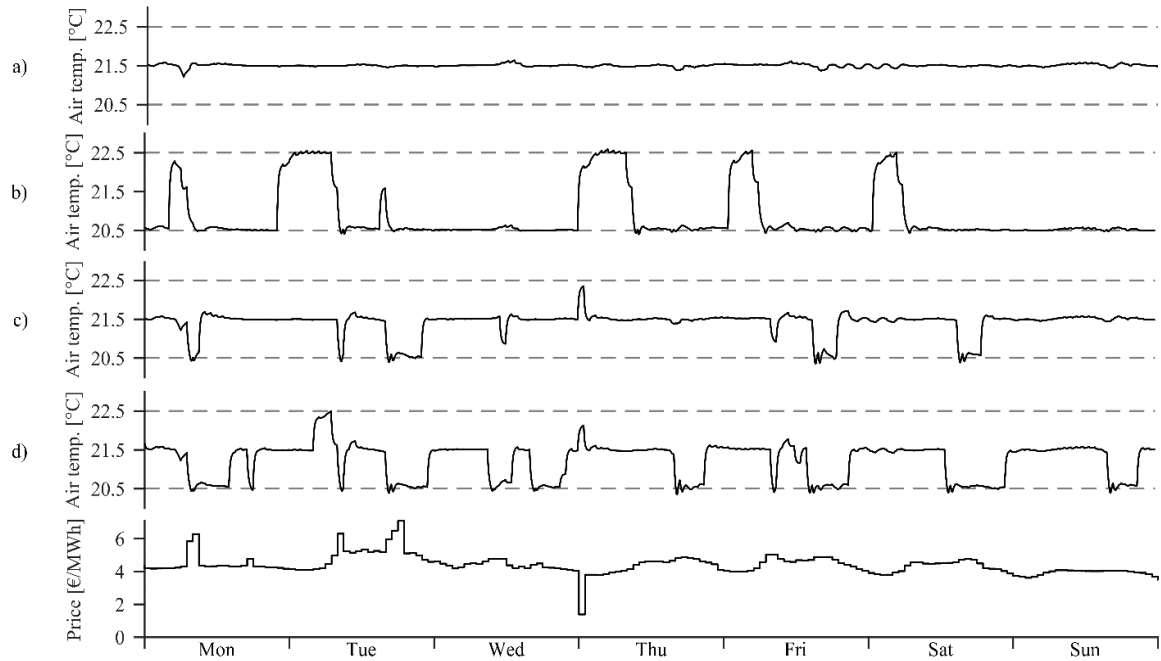
Figure 3. Mechanism of the four E-MPC schemes and the energy price during one week.

The normalized total operational cost during the entire 90-day simulation period as a function of the normalized average root-mean-square-error (RMSE) across the ten apartments is displayed in Figure 4 for the four formulations. The solutions obtained using problem formulations a), b) and c), respectively, are marked with "x" while solutions for formulation d) with different ε_{max} values are illustrated with "o" (displayed numbers are ε_{max}). Formulation a), which was a traditional set point tracking control problem, resulted in the lowest deviations from the preferred set point temperature but also the highest operational cost. Formulation b) achieved the lowest operational cost but also the highest RMSE. Formulation b) may therefore have overestimated the DR potential since occupants, in reality, may experience uncomfortable thermal conditions when tracking the lower comfort bound for long consecutive periods. Formulation c) demonstrated an acceptable compromise between the two objectives while formulation d) achieved similar performance as formulation c). Figure 4 indicates an almost convex combination of the two solutions a) and b) when choosing different values for ε_{max}, which could not be achieved by convex combination of the objectives (e.g. using the weighted sum approach) because of the different ranges of the objectives. Furthermore, formulation c) and d) enable downward flexibility, i.e. it is possible to reduce space heating if this service is sought by the grid.
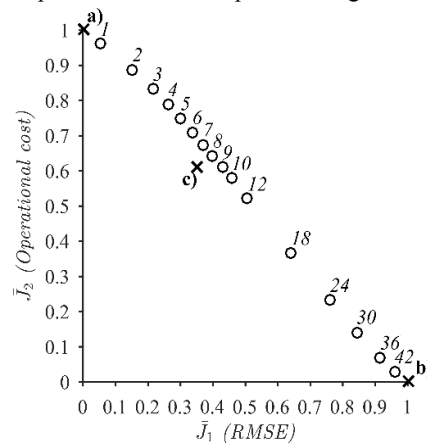

Figure 4. Normalized mean RMSE and total operational cost for all ten apartments.

79

4. Conclusion

This paper reports on a simulation-based study aimed at quantifying the performance of an E-MPC scheme using four different optimization problem formulations that handle thermal comfort in different ways. It is difficult to conclude which of the four formulations is preferable as it depends on whether – and how much – the occupants are willing to deviate from their preferred indoor air temperature to minimize operational cost through demand responses. However, the parameter ε_{max} in the proposed single-objective problem formulation – a parameter describing the maximum acceptable deviations from the preferred indoor air temperature – could be communicated to occupants as a personal indicator for the acceptable tradeoff between deviations from the preferred temperature and cost savings or, in other words, their 'DR willingness'.

Acknowledgements

References

[1] E. Vrettos, K. Lai, F. Oldewurtel and G. Andersson. Predictive Control of Buildings for Demand Response with dynamic day-ahead and real-time prices. in Control Conference (ECC) (2013), Zürich.

[2] M. Avci, M. Erkoc, A. Rahmani and S. Asfour. Model predictive HVAC load control in buildings using real-time electricity pricing. Energy Build. 60 (2013) 199-209.

[3] M. D. Knudsen and S. Petersen. Demand response potential of model predictive control of Space heating based on price and carbon dioxide Intensity signals. Energy Build. 125 (2016) 196-204.

[4] T. H. Pedersen, R. E. Hedegaard and S. Petersen. Space heating demand response potential of retrofitted residential apartment blocks. Energy Build. 141 (2017) 158-166.

[5] R. Halvgaard, N. K. Poulsen, H. Madsen and J. B. Jørgensen. Economic Model predictive Control for Building Climate Control in a Smart Grid. in IEEE PES Innovative Smart Grid Technologies (ISGT). (2012) 1-6, Washington, D.C., United States.

[6] R. E. Hedegaard, T. H. Pedersen and S. Petersen. Multi-market demand response using economic model predictive control of space heating in residential buildings. Energy Build.(2017), *in press*.

[7] J. Cigler, S. Prívara, Z. Váňa, E. Žáčeková and L. Ferkl. Optimization of Predicted Mean Vost index within Model Predictive Control framework: Computationally tractable solution. Energy Build. 52 (2012) 39-49.

[8] P. Moreles-Valdés, A. Flores-Tlacuahuac and V. M. Zavala. Analyzing the effects of comfort relaxation on energy demand flexibility of buildings: A multiobjective optimization approach. Energy Build. 85 (2014) 416-426.

[9] M. Castilla, J. Álvarez, M. Berenguel, F. Rodríguez, J. Guzmán and M. Pérez. A compariosn of thermal comfort predictive control strategies. Energy Build. 43 (2011) 2737-2746.

[10] F. Ascione, N. Bianco, C. De Stasio and G. M. Mauro. Simulation-based model predictive control by the multi-objective optimization of building energy performance and thermal comfort. Energy Build. 111 (2016) 131-144.

[11] T. H. Pedersen, R. E. Hedegaard, M. D. Knudsen and S. Petersen. Comparison of centralized and decentralized model predictive control in a building retrofit scenario. in CISBAT International Conference (2017), Lausanne, Switzerland, *submitted*.

[12] M. Wetter. Co-simulation of building energy and control systems with the Building Controls Virtual Test Bed. J. Build. Perform. Simul. 3 (4) (2010) 1-19.

[13] I. Das and J. E. Dennis. Normal-boundary intersection: A new method for generating the Pareto surface in nonlinear multicriteria optimization problems, SIAM J. Optim. 8 (3) (1998) 631-657.

[14] A. Gambier. MPC and PID Control Based on Multi-objective Optimization. in American Control Conference (2008), Washington, USA.

[15] V. M. Zavala. Real-Time Resolution of Conflicting Objectives in Building Energy Management: An Utopia-Tracking Approach. in Fiftth National Conference of IBPSA-USA (2012), Madison, Wisconsin.

P6   Investigating the performance of scenario-based model predictive control of space heating in residential buildings

Investigating the performance of scenario-based model predictive control of space heating in residential buildings

Theis Heidmann Pedersen & Steffen Petersen

Published online: 17 Nov 2017.

Submit your article to this journal

View related articles

View Crossmark data

Taylor & Francis
Taylor & Francis Group

Check for updates

Investigating the performance of scenario-based model predictive control of space heating in residential buildings

Theis Heidmann Pedersen ⓘ* and Steffen Petersen ⓘ

Department of Engineering, Aarhus University, Inge Lehmanns Gade 10, Aarhus C 8000, Denmark

This paper investigates the performance of scenario-based model predictive control (SB-MPC) for space heating operation to address the inherent uncertainty of weather forecasts and predictions of occupancy. In contrast to existing reported studies, this study relied on a sophisticated meteorological model and a higher order Markov chain occupancy model to generate stochastic disturbance scenarios. When applying the SB-MPC scheme for energy-efficient operation, simulation results suggested a slight increase in energy consumption (from approx. $27.7\,kWh/m^2$ to $28.0\,kWh/m^2$) when using one and 100 disturbance scenarios, respectively, while thermal comfort violations were reduced significantly (from 60°Ch to 10°Ch). Furthermore, the SB-MPC scheme was tailored to provide demand response and thereby achieved cost savings of 16.1% and 13.1% compared to conventional proportional-integral control when considering one and 100 disturbance scenarios, respectively. Choosing the appropriate number of disturbance scenarios thus relies on a consideration of the trade-off between the acceptable thermal comfort violations and energy-related benefits.

Keywords: energy-efficient control; demand response; weather ensembles; higher order Markov chain; stochastic occupancy model

1. Introduction

Demand-side management (DSM) can assist supply-side management in maintaining an instantaneous balance between supply and demand in energy systems with a high penetration of intermittent renewable energy sources (Wang, Xue, and Yan 2014). The two main components of DSM in relation to buildings are energy efficiency where the energy consumption is minimized, and adjustment of energy demand to meet supply through demand response (DR) programs. Several studies have demonstrated that buildings can meet both DSM objectives when applying model predictive control (MPC) for heating, ventilation and air conditioning (HVAC) systems operation (Oldewurtel et al. 2012; Corbin, Henze, and May-Ostendorp 2013; Henze 2013; Tanner and Henze 2014; Mirakhorli and Dong 2016; Salakij et al. 2016). MPC is an optimization-based control scheme, which requires a control-model of the building thermodynamics, measurements of current building state, forecasts of disturbances (e.g. weather and occupancy) and explicit constraints on input (e.g. heating power) and states (e.g. room air temperatures) to determine a sequence of control inputs.

The theoretical performance bound (PB), i.e. considering perfect disturbance predictions, of applying MPC schemes to minimize the energy consumption or to perform DR has been investigated in several simulation studies. Sourbron, Verhelst, and Helsen (2013) applied MPC for heat pump operation in an office building equipped with thermo-active building systems that, compared to a rule-based heating/cooling curve controller, reduced the electricity consumption by 15% while ensuring thermal comfort. Goyal, Ingley, and Barooah (2013) used MPC with perfect occupancy predictions to operate an air-handling unit and achieved energy savings of 55–60% compared to a dual-maximum baseline control. Oldewurtel, Sturzenegger, and Morari (2013) achieved energy savings of approx. 30% when considering perfect occupancy information in the associated MPC scheme compared to including static occupancy schedules. To investigate the DR potential of a residential air-conditioning unit, Avci et al. (2013) used an economic MPC (E-MPC) scheme together with real-time prices to minimize the operational cost, which reduced the energy cost with 13% and the energy consumption at peak-hours with 23.6%. Pedersen, Hedegaard, and Petersen (2017b) compared a conventional proportional-integral (PI) controller with an E-MPC scheme utilizing the day-ahead power market prices to investigate the DR potential in a residential apartment building prior to and after retrofitting the building envelope. The simulation results showed that the E-MPC scheme reduced the energy consumption in peak-hours in the existing and retrofitted building by approx. 7% and up to 47%, respectively, while ensuring thermal comfort.

The energy savings and DR potentials identified in the previously mentioned studies constitute a causal upper theoretical bound which, in practice, is unachievable since

---

*Corresponding author. Email: thp@eng.au.dk

the control scheme is affected by various structural uncertainties (i.e. building/control-model mismatch) and disturbance prediction uncertainties (i.e. weather forecasts and stochastic occupancy). The simplest approach to handle these uncertainties is to neglect their presence and assume that the control-model and disturbance predictions are equal to certain, often denoted deterministic MPC (DMPC) (Oldewurtel et al. 2012; Mayne 2014). Maasoumy et al. (2014) investigated how the performance of a DMPC scheme was affected by building/control-model mismatch and found that DMPC performed well when the mismatch was limited (presumably because of the feedback introduced by the receding horizon approach of MPC), but the theoretical energy saving potential of 37% diminished as the mismatch increased. Goyal, Ingley, and Barooah (2012b) likewise investigated the influence of building/control-model mismatch and found that the energy consumption increased with up to 35% due to different window and door resistances in the building and the control-model. They also found that occupancy uncertainties led to an increase in energy consumption of up to 25%. To further investigate the importance of reliable occupancy predictions, Dobbs and Hencey (2014) integrated an online inhomogeneous Markov chain occupancy model within a DMPC scheme, which reduced the space heating consumption by 19% compared to using pre-specified schedules. Pedersen et al. (2016) also integrated a stochastic occupancy model in a DMPC scheme with the objective of optimizing the space heating operation of four residential apartments, which reduced thermal comfort violations with up to 50% compared to utilizing static occupancy schedules.

Results from several of the studies mentioned above indicate that building/control-model mismatch and disturbance prediction uncertainties affect the potential for DMPC schemes significantly. Consequently, several approaches have been proposed to overcome the drawbacks of DMPC. One approach is to guarantee constraint satisfaction against all possible uncertainty outcomes, so-called robust MPC, where a min–max problem is solved, and the optimal control inputs are determined while enforcing constraints for all uncertainty realizations (Mayne 2014; Bayer et al. 2016; Mayne 2016). However, a robust MPC scheme may be too conservative and thus eliminate the benefits of applying MPC; especially if the set of possible uncertainty realizations is large since all realizations are treated as equally likely (Garatti and Campi 2013). Another less conservative approach is stochastic MPC (SMPC), which takes the stochastic properties of the uncertainties into consideration. Furthermore, SMPC enables probabilistic state constraints, thus allowing the constraints to be violated with a small probability (so-called chance constraints) (Farina, Giulioni, and Scattolini 2016). Oldewurtel et al. (2012) proposed an SMPC scheme where the control inputs were parameterized as affine functions of the yet unknown disturbances. Simulation

results of a building subject to uncertain weather forecasts suggested that SMPC was superior to DMPC in terms of both energy usage and thermal comfort violations. Ma and Borrelli (2012) applied SMPC to optimize the operation of an air-handling unit, and found that SMPC achieved energy savings of 30% compared to a baseline control. These studies demonstrate that SMPC schemes are superior to DMPC when the disturbance predictions are subject to uncertainty. However, the resulting stochastic optimization problem with probabilistic constraints is generally non-convex, except for a few specific cases (Calafiore and Campi 2006) and thus computationally intractable.

To obtain the advantages of SMPC while overcoming the computational drawbacks, recent research has focused on a tractable scenario-based approximation to SMPC. Scenario-based MPC (SB-MPC), sometimes also denoted randomized MPC, transforms the original stochastic optimization problem into a convex deterministic problem with a large number of constraints (Calafiore and Campi 2006; Calafiore 2009; Campi and Garatti 2011; Schildbach et al. 2014). The large number of deterministic constraints corresponds to the original constraints evaluated for multiple realizations of the disturbance outcomes according to their arbitrary probability density functions. Several studies have suggested that SB-MPC enables significant energy savings and thermal comfort improvements. Parisio et al. (2013, 2014) used SB-MPC to operate an HVAC system in a laboratory room, and found that SB-MPC led to fewer thermal comfort violations compared to a conventional PI controller. Zhang et al. (2013) applied SB-MPC in a building subject to weather and internal gains uncertainty. The simulation results suggested that DMPC and SMPC (as proposed by Oldewurtel et al. 2012) achieved similar results while both were outperformed by SB-MPC in terms of achieving energy savings and reducing thermal comfort violations.

1.1. *Aim of this paper*

The performance of SB-MPC inherently depends on the accuracy of the generated disturbance scenarios. Parisio et al. (2014) and Zhang et al. (2013) used statistical models to generate occupancy and weather forecast scenarios, but several studies using DMPC (Dobbs and Hencey 2014; Pedersen et al. 2016) have suggested to integrate a designated stochastic Markov chain occupancy model within the MPC scheme. To the best of the authors' knowledge, there have been no reported studies where such a designated occupancy model has been used to generate occupancy prediction scenarios within an SB-MPC scheme. This paper, therefore, reports on a simulation-based study that investigates the performance of an SB-MPC scheme using a higher order Markov chain occupancy model and a sophisticated meteorological model to generate disturbance scenarios.

Furthermore, MPC schemes have demonstrated significant potentials for achieving energy savings but, to the

knowledge of the authors, there have been no reported studies on how SB-MPC schemes affect the theoretically identified DR potentials when considering uncertain disturbance scenarios. The SB-MPC scheme was, therefore, also evaluated in terms of its ability to achieve end-user cost savings compared to a conventional PI controller.

2. Method

The performance of the SB-MPC scheme was investigated using co-simulation as illustrated in Figure 1. A residential building (see Section 2.3) located in Aarhus, Denmark, was modeled in EnergyPlus (EP) and represents the building to be controlled. The SB-MPC scheme was implemented in MATLAB and used to operate the space heating (electrical baseload) of the EP model through co-simulation facilitated by the Building Controls Virtual Test Bed (Wetter 2010). The EP model had a time step of 60 seconds, whereas the SB-MPC scheme had a time step of 60 minutes, i.e. a new space heating control input was exchanged hourly. Weather data provided by the Danish Meteorological Institute (2017) for a location in Aarhus ($56°10'22.56''$N, $10°8'2.20''$E) were used during the simulation period from 1 January 2016 to 28 February 2016, which is the coldest period of the heating season in Denmark. The following sections provide further information on the SB-MPC scheme, the disturbance scenarios and the building used as a test case.

2.1. Scenario-based model predictive control

In the proposed SB-MPC scheme, an optimization problem for a finite prediction horizon N is solved at each discrete time step t to determine a sequence of space heating control inputs $\boldsymbol{u}$. The control inputs are communicated to the EP representation in a receding horizon approach, thus only the first control input is implemented (Oldewurtel et al. 2012). At the next discrete time step, the optimization problem is solved again with a prediction horizon shifted one time step ahead in time, and with updated control-model states (see Equation (1)), weather forecast (see Section 2.2.1) and occupancy predictions (see Section 2.2.2). The different elements of the SB-MPC scheme are described in the following sections.
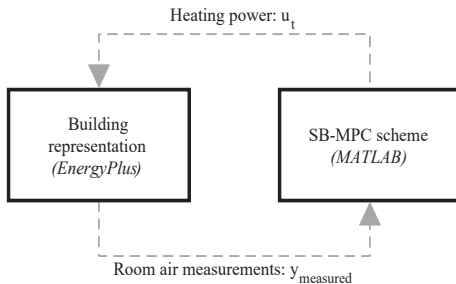

Figure 1. Illustration of the co-simulation process.

2.1.1. Control-model

The SB-MPC scheme relies on a simplified control-model of the building thermodynamics to optimize the control inputs. In this study, a grey-box modeling approach was chosen, which is characterized by having a pre-specified model structure consisting of physically interpretable parameters that are estimated from measurement data through methods from the field of system identification (Hedegaard and Petersen 2017). A two-state model representing the lumped thermal capacity of the zone air and the constructions was used (Pedersen, Hedegaard, and Petersen 2017b). The state space representation is given in Equation 1(a) and 1(b) with state matrix $\mathbf{A}$, system states $\boldsymbol{x}_t$ (i.e. room air and construction temperature), input matrix $\mathbf{B}$, control inputs u_t (i.e. space heating power), disturbance matrix $\mathbf{E}$, disturbances $\boldsymbol{d}_t$ (i.e. ambient temperature, direct and diffuse horizontal solar irradiance and occupancy), output matrix $\mathbf{C}$ and output y_t (i.e. room air temperature).

$$\boldsymbol{x}_{t+1} = \mathbf{A} \cdot \boldsymbol{x}_t + \mathbf{B} \cdot u_t + \mathbf{E} \cdot \boldsymbol{d}_t, \quad (1a)$$

$$y_t = \mathbf{C} \cdot \boldsymbol{x}_t. \quad (1b)$$

The control-model was estimated in continuous time and then discretized using the zero-order hold method with a time step of 60 minutes. At each time step, the room air temperature was measured (y_{measured}) and used to update the states of the control-model for time step t predicted at the last time step $t-1$. The states $\boldsymbol{x}_{t|t-1}$ was corrected using a Kalman filter to update the unobserved states according to Equation (2), where KG is the Kalman gain (Kalman 1960).

$$\boldsymbol{x}_{t|t} = \boldsymbol{x}_{t|t-1} + KG \cdot (y_{\text{measured}} - \mathbf{C} \cdot \boldsymbol{x}_{t|t-1}). \quad (2)$$

2.1.2. Control input and state constraints

The control input u_t was restricted by the maximum design heating power P_{max} of the space heating system by Equation (3).

$$0 \leq u_t \leq P_{\text{max}}. \quad (3)$$

Ensuring thermal comfort when applying MPC schemes can be handled in many ways (Pedersen et al. 2017). One approach is to formulate a multi-objective optimization problem, i.e. simultaneously minimize energy-related costs and thermal comfort violations (Avci et al. 2013; Dobbs and Hencey 2014). Another formulation is to assume that occupants are comfortable as long as the room air temperature is within a predefined comfort band defined by a preferred temperature and an acceptable deviation from this temperature (Pedersen, Hedegaard, and Petersen 2017b). In this study, the latter formulation was chosen, which led to a single objective problem formulation. The comfort band was defined according to Equation (4) by the

lower ($T_{\min}$) and upper ($T_{\max}$) comfort bounds.

$$T_{\min} \leq y_t \leq T_{\max}. \tag{4}$$

The comfort bounds were time invariant, thus not allowing for comfort bound setbacks if the room was predicted to be vacant. This was chosen to ease the interpretation of the results as the main aim of this study was to evaluate the SB-MPC scheme – not the occupancy prediction model.

2.1.3. Control scheme formulation

Scenario-based programs (SB-P) are a tractable approximation to a chance constrained optimization problem (CCP) that, with a high probability, computes a feasible solution to the original CCP. SB-P replaces the probabilistic state constraints with K deterministic constraints corresponding to $\boldsymbol{\delta}^{(1)}, \dots, \boldsymbol{\delta}^{(K)} \in \boldsymbol{\Delta}$ disturbance realizations (Calafoire and Campi 2006; Calafiore 2009; Campi and Garatti 2011; Zhang et al. 2013; Zhang et al. 2015). For convenience, the disturbance realizations are combined into full prediction horizon multi-samples in Equation (5), also called scenarios.

$$\boldsymbol{\omega}_t^{(k)} = \{\boldsymbol{\delta}_{1|t}^{(k)}, \dots, \boldsymbol{\delta}_{N|t}^{(k)}\}. \tag{5}$$

Each of the K number of disturbance scenarios will lead to K different state trajectories predicted by the control-model (Equation (1)) corresponding to each disturbance scenario $\boldsymbol{\omega}_t^{(k)}$. Consequently, the optimal control inputs are determined so all state trajectories satisfy the state constraints (Equation (4)). Using Equations (1)–(5), the resulting SB-MPC formulation at time step t for a prediction horizon N and using K number of disturbance scenarios is specified in Equation 6(a–f). The disturbance matrix $\mathbf{E}$ was discretized using a time step of 15 minutes, recognizing that occupancy can change significantly during the 60-minute time step of the SB-MPC scheme. The vector $\boldsymbol{c}$ is the cost signal containing the price, not necessarily money (see Sections 2.3.1 and 2.3.2), associated with the control input for time step $t + n$ forecasted at time step t.
SB-P[$\boldsymbol{\omega}$]:

$$\underset{u_{0|t}, \dots, u_{N|t}}{\text{minimize}} \quad J = \sum_{k=1}^{K} \sum_{n=0}^{N-1} c_{n|t} \cdot u_{n|t} \tag{6a}$$
$$\text{subject to} \quad \forall k = 1, \dots, K, \forall n = 0, \dots, N-1,$$

$$\boldsymbol{x}_{n+1|t}^{(k)} = \mathbf{A} \cdot \boldsymbol{x}_{n|t}^{(k)} + \mathbf{B} \cdot u_{n|t} + \mathbf{E} \cdot \boldsymbol{\omega}_{n|t}^{(k)}, \tag{6b}$$

$$y_{n|t}^{(k)} = \mathbf{C} \cdot \boldsymbol{x}_{n|t}^{(k)}, \tag{6c}$$

$$0 \leq u_{n|t} \leq P_{\max}, \tag{6d}$$

$$T_{\min} \leq y_{n|t}^{(k)} \leq T_{\max}, \tag{6e}$$

$$\boldsymbol{x}_{0|t}^{(k)} = \boldsymbol{x}_{0|t-1} + KG \cdot (y_{\text{measured}} - \mathbf{C} \cdot \boldsymbol{x}_{0|t-1}). \tag{6f}$$

2.1.4. Number of scenarios

Choosing the appropriate K number of scenarios to ensure that the solution to SB-P[$\boldsymbol{\omega}$] with high probability is a feasible solution to the original CCP is a topic of great research concern (Calafoire and Campi 2006; Calafiore 2009; Campi and Garatti 2011; Zhang et al. 2015). Introducing the confidence parameter $\beta \in [0,1]$ which bounds the risk of failure and the violation probability ϵ that represents a trade-off between cost function minimization and level of constraint satisfaction, Calafiore (2010) showed that if K satisfies Equation (7), the solution to SB-P[$\boldsymbol{\omega}$] is feasible to the original CPP(ϵ) with confidence at least $1 - \beta$.

$$K \geq \frac{2}{\varepsilon} \left(\ln \left(\frac{1}{\beta} \right) + \zeta - 1 \right), \tag{7}$$

where ζ is Helly's dimension of SB-P[$\boldsymbol{\omega}$] (Zhang et al. 2015). Computing ζ explicitly is, in general, very difficult; but ζ is upper bounded by the number of decision variables (Zhang et al. 2015). However, experiences from applying SB-MPC schemes for HVAC operation suggest that Equation (7) may be too pessimistic and that K could be chosen much smaller (Zhang et al. 2013), presumably because of the buildings' slow thermodynamics and the feedback introduced by the receding horizon approach.

2.2. Disturbance scenario

The disturbance scenarios consist of four disturbances: ambient temperature (T_{a}), direct horizontal solar irradiance (P_{dir}), diffuse horizontal solar irradiance (P_{dif}) and occupancy (P_{occ}). The predictions of occupancy were generated using a designated occupancy model (see Section 2.2.2), whereas the three weather forecasts were provided as weather ensembles (see Section 2.2.1). Since the weather ensembles and occupancy predictions originated from two distinct models, it was possible to differ the number of considered weather forecasts (K_{w}) and occupancy predictions (K_{occ}). The resulting number of disturbance scenarios therefore followed Equation (8).

$$K = K_{\text{w}} \cdot K_{\text{occ}}. \tag{8}$$

Forecasts for each of the four disturbances at time step t during the prediction horizon N were collected and constituted one of K scenarios, see Equation (9).

$$\boldsymbol{T_a}^{(k_{\text{w}})}[t] = \{T_{\text{a}}^{(k_{\text{w}})}[t + 1], T_{\text{a}}^{(k_{\text{w}})}[t + 2] \dots, T_{\text{a}}^{(k_{\text{w}})}[t + N]\}$$
$$\forall k_{\text{w}} = 1, \dots, K_{\text{w}}, \tag{9a}$$

$$\boldsymbol{P_{dir}}^{(k_{\text{w}})}[t] = \{P_{\text{dir}}^{(k_{\text{w}})}\}\{[t + 1], P_{\text{dir}}^{(k_{\text{w}})}[t + 2] \dots, P_{\text{dir}}^{(k_{\text{w}})}[t + N]\}, \tag{9b}$$

$$\boldsymbol{P}_{dif}^{(k_{\mathrm{w}})}[t] = \{P_{\mathrm{dif}}^{(k_{\mathrm{w}})}[t+1], P_{\mathrm{dif}}^{(k_{\mathrm{w}})}[t+2]\ldots, P_{\mathrm{dif}}^{(k_{\mathrm{w}})}[t+N]\}, \tag{9c}$$

$$\boldsymbol{P}_{occ}^{(k_{\mathrm{occ}})}[t] = \{P_{\mathrm{occ}}^{(k_{\mathrm{occ}})}[t+1], P_{\mathrm{occ}}^{(k_{\mathrm{occ}})}[t+2]\ldots, P_{\mathrm{occ}}^{(k_{\mathrm{occ}})}[t+N]\}$$
$$\forall k_{\mathrm{occ}} = 1, \ldots, K_{\mathrm{occ}}, \tag{9d}$$

$$\boldsymbol{\omega}^{(k)}[t] = \begin{bmatrix} \boldsymbol{T}_a^{(k_{\mathrm{w}})}[t] \\ \boldsymbol{P}_{dir}^{(k_{\mathrm{w}})}[t] \\ \boldsymbol{P}_{dif}^{(k_{\mathrm{w}})}[t] \\ \boldsymbol{P}_{occ}^{(k_{\mathrm{occ}})}[t] \end{bmatrix} \forall k_w = 1, \ldots, K_w, \forall k_{occ} = 1, \ldots, K_{\mathrm{occ}}. \tag{9e}$$

The following sections describe the weather ensembles and the higher order Markov chain occupancy model used to establish the *K* number of disturbance scenarios in the associated SB-MPC scheme.

2.2.1. *Weather ensembles*

A series of weather forecast ensembles, each consisting of 25 forecasts with hourly point values of ambient temperature [K], wind speed [m/s], global horizontal irradiance [W/m^2] and relative humidity [%], was provided by the Danish Meteorological Institute (2017). The 25 weather forecasts in an ensemble were generated with the HIRLAM numerical weather prediction model (Undén et al. 2002) by perturbing the initial conditions. Each forecast had a horizon of 54 hours, and a new ensemble was generated every sixth hour. Utilizing weather forecasts from the sophisticated HIRLAM weather model naturally captured cross-correlations between the weather variables. A randomly selected forecast was assumed to be the 'actual' weather,

thus the 24 remaining forecasts were used as weather forecast scenarios. An example of the 'actual' weather and 24 forecasts in one ensemble is displayed in Figure 2.

A boxplot of the differences between the forecast and the 'actual' weather is depicted in Figure 3 for 236 ensembles. The red line indicates the median, the box indicates the interquartile range (IQR) between the first and third quantile, the whiskers constitute 1.5 × IQR, and outliers are illustrated by points. It is noted that the hours where the solar irradiance equaled 0 W/m^2 (i.e. night-time) were omitted. Figure 3 shows that the IQR between the ambient temperature forecasts and the 'actual' weather was generally less than 1 K, and that the discrepancy is lower within the first six hours compared to the remaining forecast horizon. The highest discrepancies between the forecasted and 'actual' global irradiance are expected around noon where the highest absolute irradiance occurs. This is also the reason for the observed oscillating tendency. Since the forecasts were generated every sixth hour, i.e. at 06:00, 12:00, 18:00 and 24:00, the highest discrepancies will be located at multiples of six.

As specified in Equation (9), the disturbance scenarios consist of the ambient temperature and the direct and diffuse horizontal radiation. The global horizontal irradiance provided by the weather forecast service was therefore split into direct and diffuse horizontal irradiance using 'the clearness of sky' index (Reindl, Beckman, and Duffie 1990; Badescu 2008).

2.2.2. *Markov chain occupancy model*

Developing a reliable occupancy model is difficult because of the stochastic nature of humans. Many existing occupancy models for building simulation are based on the principles of the model proposed by Page et al. (2008) (referred to as Page-model) (e.g. Liao, Lin, and Barooah
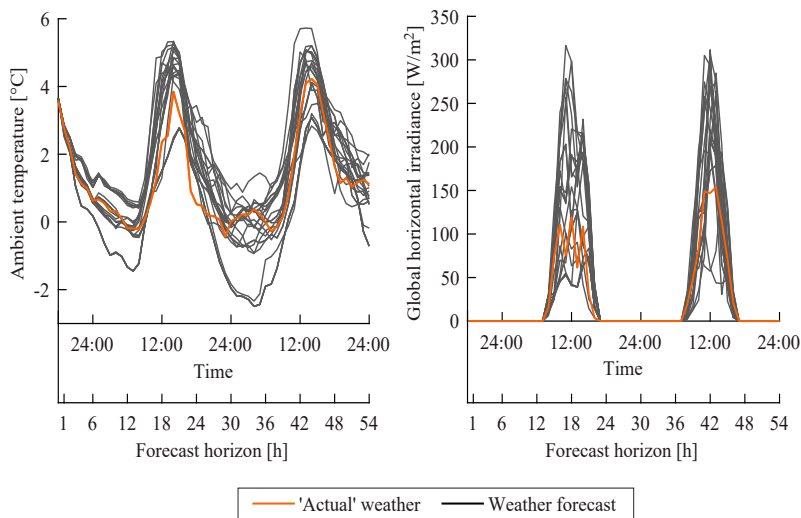

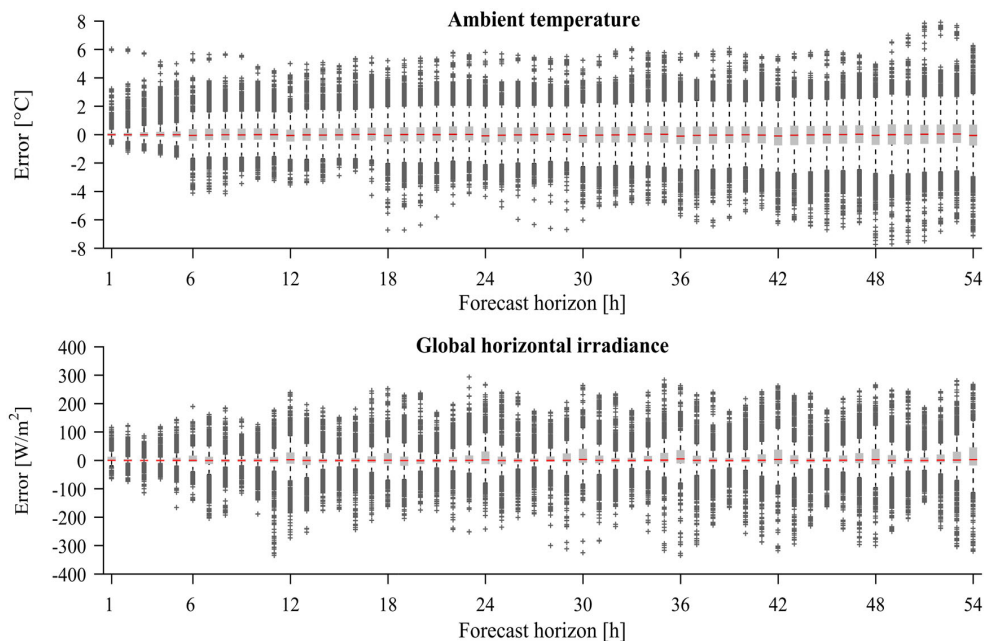Figure 2. Example of the 'actual' and forecasted weather in one ensemble.

Figure 3.   Weather forecast errors as a function of the forecast horizon.

2012; Chen, Xu, and Soh 2015; Feng, Yan, and Hong 2015; Mahdavi and Tahmasebi 2015; Tahmasebi and Mahdavi 2016). The Page-model relies on the assumption that occupancy in a time step only depends on the occupancy state at the preceding time step (first-order Markovian property), and was developed to evaluate building designs in terms of robustness towards stochastic user behaviour. Mahdavi and Tahmasebi (2015), however, investigated the use of the Page-model in building systems control compared to a non-probabilistic model, and found that the stochastic elements of the Page-model did not necessarily lead to a superior predictive performance, suggesting that the Page-model resulted in overly random occupancy predictions. Flett and Kelly (2016) proposed a higher order Markov chain model which also considered the duration of the occupancy state beyond the preceding time step. Using UK Time Use Survey data for 2500 persons, the authors found that the higher order Markov chain model performed moderately better than the first-order model. However, the aim of the model was not for control purposes.

In this study, a higher order inhomogeneous Markov chain model was used, which at each discrete time step yielded a binary occupancy state of either $\gamma_t = 0$ (absent) or $\gamma_t = 1$ (present). The probability of changing or continuing the occupancy state is described by transition probabilities p that depend on the current occupancy state, type of day, time of day and duration of the existing state. The principle of a higher order Markov chain is illustrated in Table 1 when the current state is present.

The transition probabilities were collected in a transition matrix **T** (Equation (10)). Table 1 illustrates the second

Table 1.   Principle of higher order Markov chain occupancy model.

Current state $\gamma_t = 1$ (present)	Duration (hours)	Future state	
		$\gamma_{t+1} = 0$ (absent)	$\gamma_{t+1} = 1$ (present)
	0–1	$p_{1\rightarrow 0}^{(1)}$	$p_{1\rightarrow 1}^{(1)}$
	1–2	$p_{1\rightarrow 0}^{(2)}$	$p_{1\rightarrow 1}^{(2)}$
	2–4	$p_{1\rightarrow 0}^{(4)}$	$p_{1\rightarrow 1}^{(4)}$
	4–6	$p_{1\rightarrow 0}^{(6)}$	$p_{1\rightarrow 1}^{(6)}$
	6+	$p_{1\rightarrow 0}^{(6+)}$	$p_{1\rightarrow 1}^{(6+)}$

row of **T**, but the same principle goes for the first row, i.e. when the current state is absent. The initial estimate of the transition matrix entries was the identity matrix, implying that the best guess of the future occupancy state is the current state, which has demonstrated satisfying results when used in an MPC scheme (Goyal, Ingley, and Barooah 2012a).

$$T = \begin{bmatrix} p_{0\rightarrow 0}(day, t, dur) & p_{0\rightarrow 1}(day, t, dur) \\ p_{1\rightarrow 0}(day, t, dur) & p_{1\rightarrow 1}(day, t, dur) \end{bmatrix}. \quad (10)$$

Since each row of **T** sums to one, only $p_{0\rightarrow 1}$ and $p_{1\rightarrow 0}$ need to be calculated. The value of $p_{0\rightarrow 1}$ was only updated if the state changed from absent, and $p_{1\rightarrow 0}$ only changed if the current state was present. The transition probabilities followed a binomial distribution with two outcomes: continuing or changing state. Thus, the maximum likelihood estimate of $p_{0\rightarrow 1}$ is simply the proportion of state transitions from vacant to present within a specific time
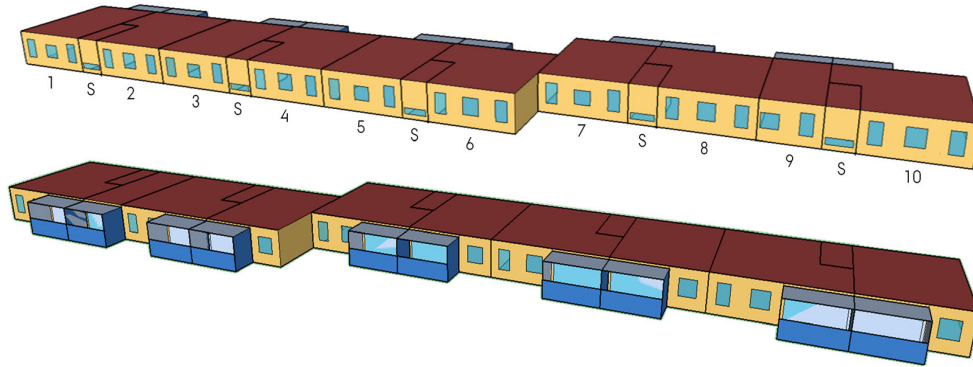
Figure 4. Test case geometry as modeled in EP with applied apartment numbering (Pedersen, Hedegaard, and Petersen 2017a, 2017b). Top: East facade. Bottom: West facade.

Table 2. Specification of input and state constraints.

Zone	Area (m²)	P_{max} (W)	T_{min} (°C)	T_{max} (°C)
Apartment 1	81	4050	20	24
Apartment 2	94	4700	22	26
Apartment 3	81	4050	20	24
Apartment 4	94	4700	22	26
Apartment 5	81	4050	20	24
Apartment 6	94	4700	22	26
Apartment 7	81	4050	20	24
Apartment 8	94	4700	22	26
Apartment 9	50	2500	20	24
Apartment 10	94	4700	22	26

Algorithm 1: Breakdown of occupancy model.

---

for each time step t = 1, 2, … **do**
  get current occupancy state γ_t
  if $\gamma_t \neq \gamma_{t-1}$ **then**
    | update transitions probabilities
  end
  for each scenario k = 1:K **do**
    if γ_t equals $\gamma_{t|t-1}^{(k)}$ **and** t > 1 **then**
      for prediction time step n = 0:N-2 **do**
        | $\gamma_{t+n|t}^{(k)} = \gamma_{t+n|t-1}^{(k)}$
      end
      deduce occupancy state $\gamma_{t+N-1|t}^{(k)}$
      using IFM
    else
      for prediction time step n = 0:N-1 **do**
        | deduce occupancy state $\gamma_{t+n|t}^{(k)}$
        | using IFM
      end
    end
  end
end

---

interval and conversely for $p_{1 \to 0}$. It was assumed that the transition probabilities were periodic with a period of 24 hours. However, a distinction between workdays and weekends was made. The occupancy state was established at each time step based on real-time CO_2 measurements using the detection method described by Pedersen, Nielsen, and Petersen (2017). Historical detections were used to train the transition probabilities prior to operation, while real-time CO_2 measurements were used to train the model continuously during operation, thus enabling the model to adapt to changes in room usage.

Updates of transition probabilities and predictions of occupancy were drawn according to Algorithm 1 for a prediction horizon N and K number of disturbance scenarios using the inverse function method (IFM) (Page et al. 2008).

2.3. Case study

A residential four-story apartment building constructed in 1978 located in Aarhus, Denmark, was used as a test case. The building has east–west-oriented window configurations and west-oriented open balconies, see Figure 4. To simplify the modeling and simulation, only the third floor was investigated, which consists of one 2-room apartment (9), four 3-room apartments (1, 3, 5 and 7), five 4-room apartments (2, 4, 6, 8 and 10) and five stairwells (S). The stairwells were kept at a minimum temperature of 15°C. The apartments were modeled as individual thermal zones, and all horizontal zone boundaries (i.e. ceiling and floor) were assumed adiabatic. Detailed descriptions of materials, constructions and systems are provided in Pedersen, Hedegaard, and Petersen (2017a, 2017b).

As described in Section 2.1.2, the space heating control inputs were restricted by the maximum heating power which differs for the apartments as specified in Table 2. Furthermore, the time invariant thermal comfort bounds are listed in Table 2, which also differ across the apartments.
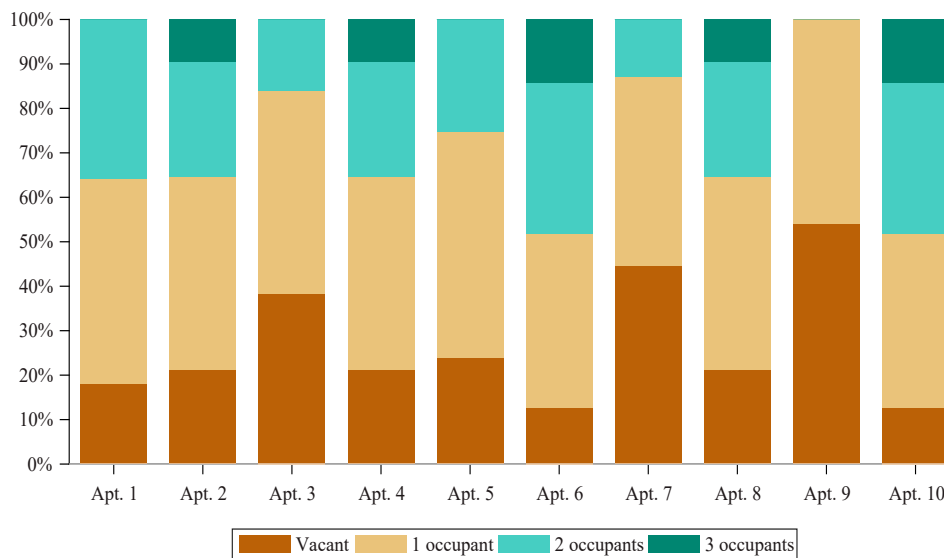
Figure 5.   Number of occupants during the simulation period.

2.3.1.   Occupancy schedules

As described earlier, occupancy detections were established based on CO2 measurements using the method described by Pedersen, Nielsen, and Petersen (2017) and assumed to be the ground truth. In this study, real CO_2 measurements from four single-person apartments were used as a basis for generating four ground truth occupancy schedules. These schedules were then combined randomly for each of the 10 apartments (where the maximum number of occupants was one, two and three for the 2-, 3- and 4-room apartments, respectively), assuming that the presence of individual occupants was independent. At each time step, the presence of occupants in the apartments was communicated to the EP representation where each occupant was assumed to generate 100 W. Figure 5 displays the percentage of time during which the apartments were vacant and occupied during the simulation period.

Since the presence of each occupant was assumed to be independent, it was straightforward to extend the occupancy model described in Section 2.2.2 to cope with multiple occupants. A transition matrix **T** was established for each occupant, and the resulting apartment state was determined by adding separate patterns for several occupants for each apartment.

2.3.2.   Energy efficiency potential

The SB-MPC scheme was first evaluated in terms of its ability to enable energy efficiency while restricting the room air temperature to be within the specified thermal comfort band according to Table 2. The most energy-efficient control approach is to track the lower thermal comfort bound, which was investigated by using a constant cost signal c (see Equation (6)). The prediction horizon N could be chosen small (chosen to be 24 hours) since the

objective of the SB-MPC scheme was to keep a constant temperature without any chance of temperature setback.

2.3.3.   DR potential

As described in the Introduction, the control scheme's ability to enable DR was also investigated. Evaluating the benefits of DR strongly depends on the chosen baseline. In Denmark, one of the most common space heating controls is conventional PI control which therefore was chosen to represent the baseline. Furthermore, many objectives can be considered when evaluating the potential for DR (Pedersen, Hedegaard, and Petersen 2017b). In this paper, the objective was to achieve end-user cost savings compared to the baseline PI controller. Historical day-ahead market prices acquired through the Danish TSO, Energinet.dk and Nord Pool spot for the bidding area DK1 were used as cost signal c (see Equation (6)). Since taxation is very country specific, taxation was omitted in this study to generalize the interpretation of the results; thus, results presented in absolute values cannot be directly compared to the actual price paid by building owners. Furthermore, perfect price predictions were assumed. To minimize the operational cost, the control scheme uses the thermal capacity of the structural mass as storage by charging and discharging it with the room heating system in periods with low or high prices, respectively. A prediction horizon N of 72 hours was, therefore, chosen to enable the control scheme to exploit the slow dynamics of the structures.

Furthermore, previous studies have suggested that the potential for DR (i.e. quantity and duration) is affected by the energy efficiency of the building envelope (Pedersen, Hedegaard, and Petersen 2017b). The performance of the proposed SB-MPC scheme was, therefore, evaluated based on simulations of the existing building and of a retrofitted
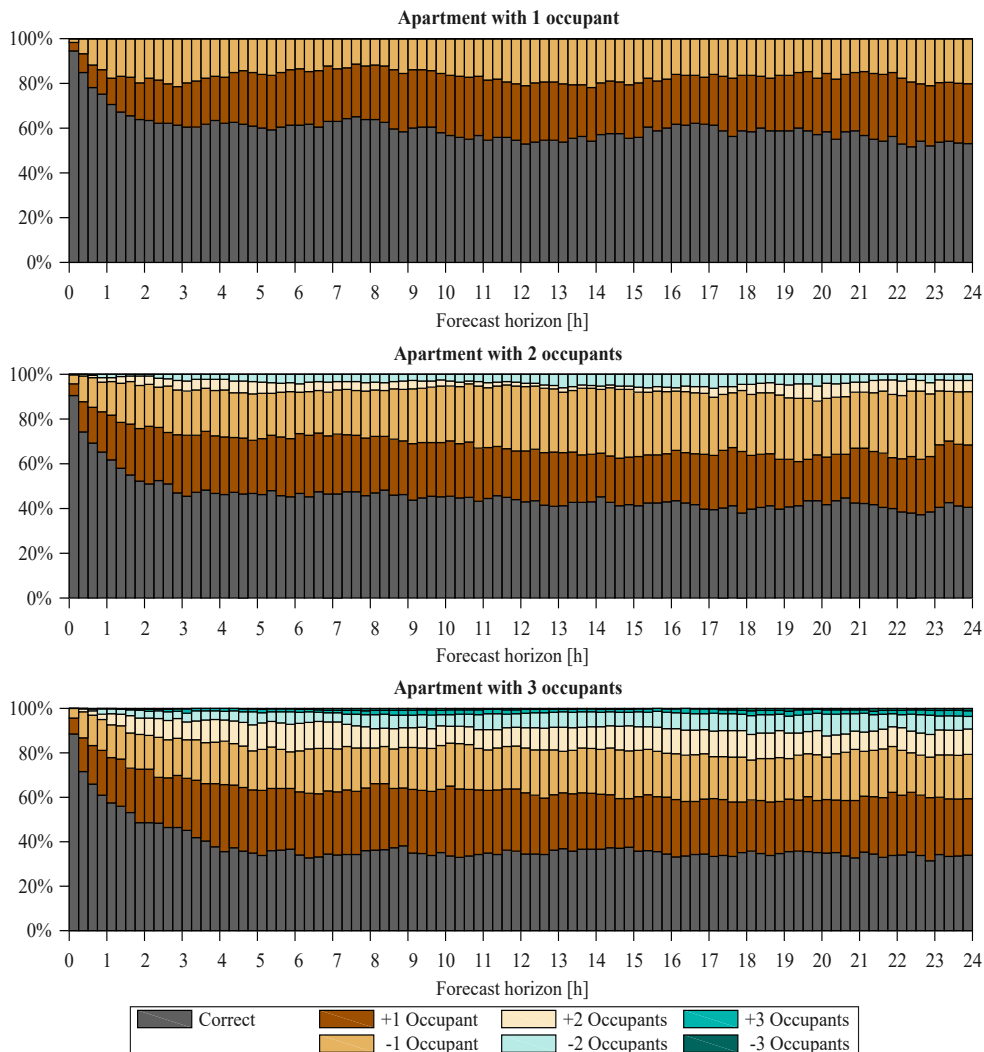
Figure 6.　Performance of the occupancy model.

building with energy-efficient windows, additional external facade insulation, a reduced infiltration rate, and a mechanical constant air volume ventilation rate of $0.5\,h^{-1}$ with 80% heat recovery efficiency (denoted retrofit 8 in Pedersen, Hedegaard, and Petersen 2017a, 2017b).

3.　Results

The following sections present the simulation results for the case building. First, the performance of the occupancy model was evaluated, and then the performance of the SB-MPC scheme was evaluated in terms of its ability to achieve energy and cost savings.

3.1.　Occupancy model

Figure 6 displays the percentage of time with correct and incorrect predictions as a function of the forecast horizon

for three apartments. Figure 6(a) shows that the occupancy model for a one-person apartment yielded the best predictions of occupancy a couple of hours ahead in time and then the accuracy dropped and stagnated at approx. 60%. The occupancy model predicted a fairly equal amount of false negatives and positives, thus the model was not biased towards a specific occupancy prediction error. The same tendency is observed in Figure 6(b) and 6(c) for apartments occupied by two and three persons, respectively. As the number of occupants increased, only a limited share of incorrect apartment state predictions (i.e. ±2 and ±3 occupants, respectively) was obtained.

3.2.　Energy efficiency

The mechanism of the SB-MPC scheme is displayed in Figure 7 for a 24-hour period with perfect occupancy predictions but uncertain weather forecasts. The top and
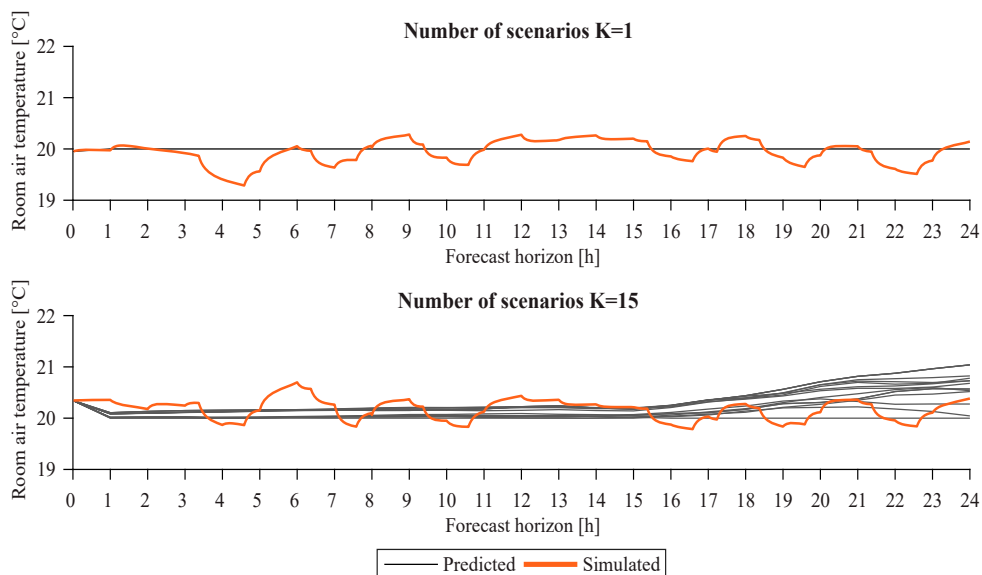
Figure 7.   Predicted and simulated air temperature for apartment 9 during a 24-hour period.

bottom charts show the predicted and the resulting EP simulated room air temperature when considering one weather forecast (i.e. $K = 1$, corresponding to DMPC) and 15 weather forecasts, respectively. Comparing the resulting room air temperatures shows that the SB-MPC scheme always planned the operation so the predicted state trajectories comply with the lower comfort bound. Nevertheless, the scenarios did not always capture the entire uncertainty spectrum (as would be the case for robust MPC) illustrated by the violations of the lower comfort band. However, increasing the number of disturbance scenarios led to fewer violations of the lower comfort bound.

The summarized thermal comfort violations and energy consumption for the existing building during the entire simulation period are displayed in Figure 8 as a function of the number of scenarios. Since the K number of disturbance scenarios was randomly selected, the resulting optimal solution is a random variable that depends on the disturbance scenario selection. Therefore, the results are shown for five simulations with the same configurations together with their mean. The dashed line indicates the theoretical PB, i.e. considering perfect disturbance predictions. Due to mismatch between the control-model and the EP representation, a certain amount of thermal comfort
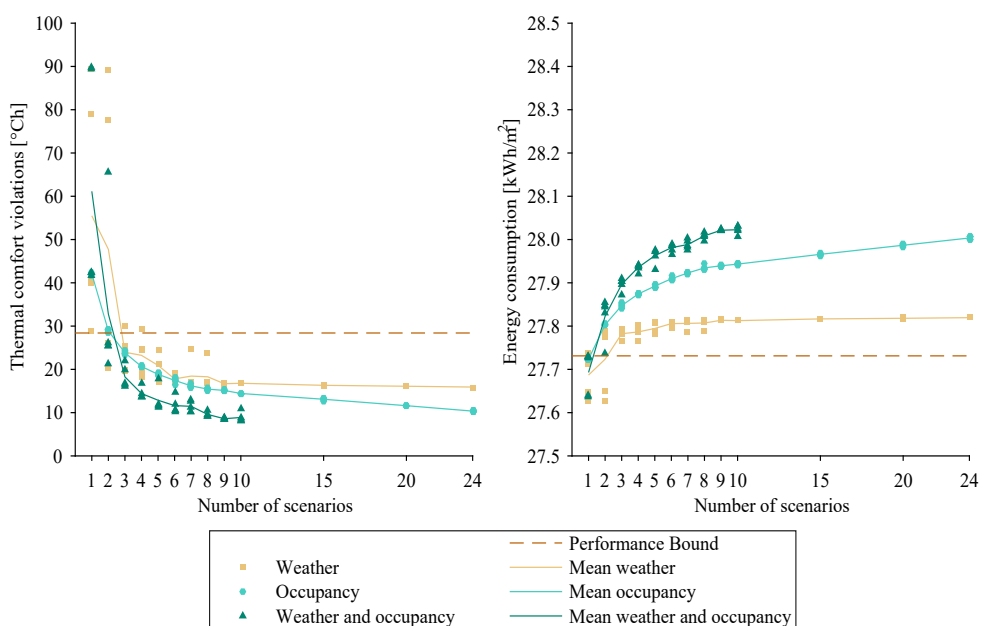

Figure 8.   Summarized thermal comfort violations and energy consumption for all 10 apartments as a function of the number of scenarios.
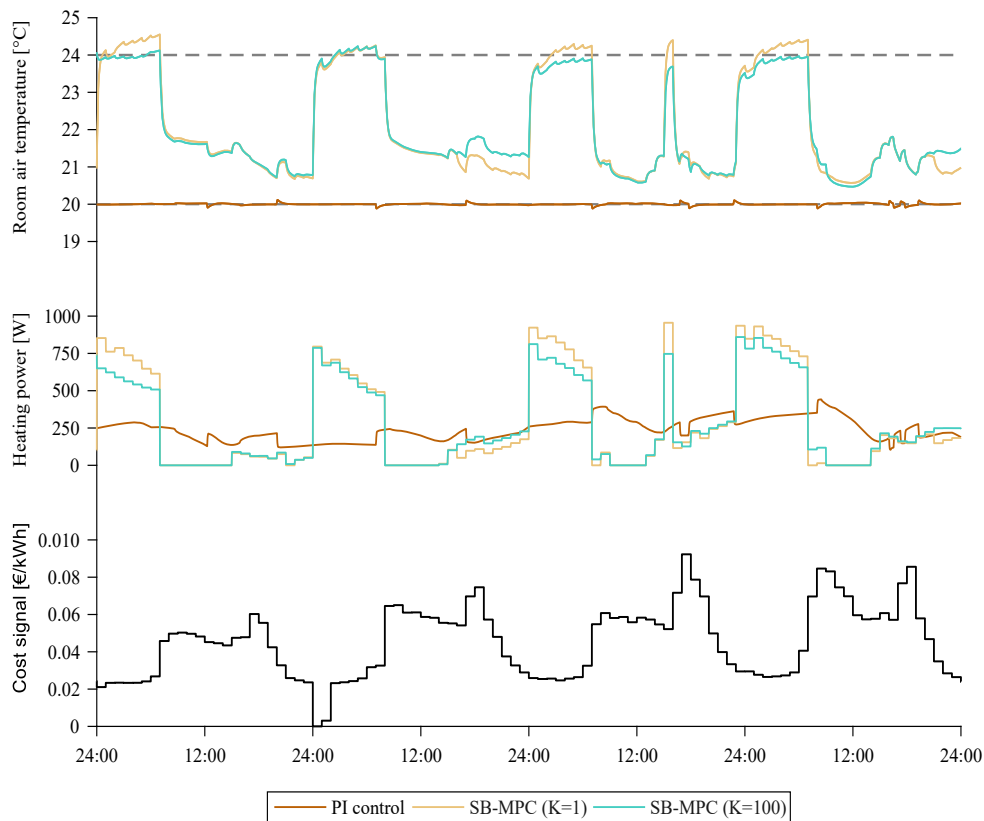
Figure 9. Simulation results from apartment 9 for the retrofitted building using a PI controller and the SB-MPC scheme with a different number of scenarios.

violations was obtained even for the PB. Figure 8 shows results for three cases:

(a) Uncertain weather forecasts with perfect occupancy predictions.
(b) Uncertain occupancy predictions with perfect weather forecasts.
(c) Uncertain weather forecasts and occupancy predictions.[1]

The results show that using only one disturbance scenario led to an increase in thermal comfort violations of up to a factor of three compared to the PB. As the number of scenarios increased, the thermal comfort violations decreased and became even lower than the PB. The reason was that the increased number of disturbance scenarios occasionally led to an overestimation of the space heating requirement which then compensated for the mismatch between the control-model and EP. Furthermore, the variation in the simulation results diminished as the number of scenarios increased. However, the introduced conservatism using an increased number of scenarios led to an increase in the overall energy use. This indicates a certain trade-off between the acceptable level of comfort violations and achieved energy savings.

3.3. DR potential

Figure 9 displays the mechanism of a conventional PI controller and the SB-MPC scheme for the retrofitted building subject to uncertain weather forecasts and occupancy predictions. The top chart shows the room air temperature, the middle chart shows the heating consumption and the bottom chart shows the time varying cost signal. The PI controller maintained a room air temperature near the specified lower comfort bound at all times (the small deviations were due to abrupt changes in occupancy), resulting in a fairly smooth heating pattern. The SB-MPC scheme, however, increased the room air temperature at times when prices were low and thereby exploited the structural thermal mass, which then reduced the need for space heating in the following high-price periods. Because of the high energy efficiency of the retrofitted building envelope, the heating consumption following a boosting period was often negligible.

On several occasions, multiple scenarios ($K = 100$) ensured compliance with the upper comfort constraint (dashed line in Figure 9), whereas the SB-MPC scheme using only one disturbance scenario ($K = 1$) violated the comfort constraint on multiple occasions.

The summarized operational costs and mean thermal comfort violations for all apartments during the simulation

Table 3. Summarized operational costs and mean thermal comfort violations for all 10 apartments.

	Operational cost	Cost savings	Comfort violations	Comfort difference
Existing building				
Baseline (PI)	€534		12.2°Ch	
SB-MPC ($K = 1$)	€519	€15 (2.8%)	27.1°Ch	14.9°Ch (122.1%)
SB-MPC ($K = 9$)	€523	€11 (2.1%)	15.1°Ch	2.9°Ch (23.8%)
SB-MPC ($K = 100$)	€527	€7 (1.3%)	8.6°Ch	− 3.6°Ch (− 29.5%)
PB	€520	€14 (2.6%)	14.0°Ch	1.8°Ch (14.8%)
Retrofitted building				
Baseline (PI)	€137		20.6°Ch	
SB-MPC ($K = 1$)	€115	€22 (16.1%)	28.4°Ch	7.8°Ch (37.9%)
SB-MPC ($K = 9$)	€118	€19 (13.9%)	20.7°Ch	0.1°Ch (0.5%)
SB-MPC ($K = 100$)	€119	€18 (13.1%)	15.6°Ch	− 5.0 °Ch (− 24.3%)
PB	€116	€21 (15.3%)	17.7°Ch	− 2.9°Ch (− 14.1%)

period for both the existing and retrofitted building are listed in Table 3. The presented results are the mean of five simulations with the same configurations. The cost savings and differences in thermal comfort violations compared to the conventional PI controller are also specified. The results show that using one scenario led to the highest cost savings and an increase in thermal comfort violations for both buildings. Using nine and 100 scenarios reduced the thermal comfort violations significantly while only reducing the cost savings moderately.

4. Discussion

The results indicated that the introduction of multiple disturbance scenarios reduced comfort violations significantly while only increasing energy consumption incrementally (see Figure 8). The reason for the sensitivity towards comfort violations is the structure of the SB-MPC scheme in which the space heating control input is a decision variable whereas thermal comfort is treated as a state constraint. The consequence of this structure is that deviations between predicted and actual disturbances can lead to a control input that is insufficient to fulfil the comfort constraints in the actual apartment. Given the 60-minute time step of the SB-MPC scheme, it takes one hour before the control scheme can correct the space heating control input, potentially resulting in comfort violations during the entire hour.

Figure 8 also indicated that the moderate increase in energy consumption using SB-MPC was most sensitive to uncertainties associated with occupancy predictions while the uncertainties associated with the weather forecasts caused most thermal comfort violations. The reason was that the SB-MPC scheme, at times with significant disturbance uncertainties, ensured compliance with the comfort bounds even for the least favourable considered disturbance scenario. Since the internal gain originating from the occupant metabolic rate covers a significant share of the total heating demand (100 W pr. occupant), this

would cause the SB-MPC to overestimate the space heating demand to ensure compliance with the lower comfort bound even for the fewest number of predicted occupants. However, the uncertainties associated with the weather forecast scenarios had a lesser absolute influence on the control inputs.

The results also indicated that SB-MPC displays similar space heating behaviour regardless of the number of scenarios used (see Figure 9). Using SB-MPC with multiple disturbance scenarios compared to DMPC ($K = 1$) did not affect the times at which boosting occurred but merely the amplitude of the control inputs, to ensure compliance with the thermal comfort bounds. A practical and computationally tractable alternative to SB-MPC could therefore be to implement DMPC together with a low-level PI controller, which could ensure a minimum of thermal comfort violations when the DMPC scheme underestimates/overestimates the disturbances.

5. Conclusion

This simulation-based study investigated the performance of an SB-MPC scheme using a sophisticated metrological model and a higher order Markov chain occupancy model to generate disturbance scenarios. The results suggest that choosing the appropriate number of disturbance scenarios relies on a consideration of the trade-off between the amount of acceptable thermal comfort violations and potential energy-related benefits. Furthermore, interpretation of the results indicates that future work should investigate whether SB-MPC could be substituted with the less computationally demanding DMPC in connection with a low-level PI controller.

Nomenclature

Abbreviations

DSM	demand-side management
DR	demand response
MPC	model predictive control
PB	performance bound
E-MPC	economic model predictive control
DMPC	deterministic model predictive control
SMPC	stochastic model predictive control
SB-MPC	scenario-based model predictive control
EP	EnergyPlus
CCP	chance constrained program
SB-P	scenario-based program
IQR	interquartile range
IFM	inverse function method
TSO	transmission system operator

Symbols

t	discrete time step SB-MPC scheme (60 min)
$\mathbf{A}$	state matrix
$\boldsymbol{x}_{t+n\|t}$	state vector predicted for time step $t + n$ at time step t
$\mathbf{B}$	input matrix
$\boldsymbol{u}$	control input vector
$\mathbf{E}$	disturbance matrix
$\boldsymbol{d}$	disturbance vector
KG	Kalman gain
K	number of disturbance scenarios
$\boldsymbol{\omega}^{(k)}$	k^{th} number of disturbance scenarios
N	prediction horizon
c	cost signal vector
γ	occupancy state
$\mathbf{T}$	transition matrix
$p_{z \to w}$	transition probability from occupancy state z to w

Note

1. The x-axis describes the number of disturbance scenarios for each uncertain disturbance according to Equation (8), thus K equals x^2 for case c).

ORCID

Theis Heidmann Pedersen http://orcid.org/0000-0002-0785-9294
Steffen Petersen http://orcid.org/0000-0002-7230-6207

References

Avci, Mesut, Murat Erkoc, Amir Rahmani, and Shihab Asfour. 2013. "Model Predictive HVAC Load Control in Buildings Using Real-Time Electricity Pricing." *Energy and Buildings* 60: 199–209. doi:10.1016/j.enbuild.2013.01.008.

Badescu, Viorel. 2008. *Modeling Solar Radiation at the Earth's Surface*. Berlin: Springer.

Bayer, Florian A., Matthias Lorenzen, Matthias A. Müller, and Frank Allgöwer. 2016. "Robust Economic Model Predictive Control Using Stochastic Information." *Automatica* 74: 151–161. doi:10.1016/j.automatica.2016.08.008.

Calafiore, Giuseppe C. 2009. "On the Expected Probability of Constraint Violation in Sampled Convex Programs." *Journal of Optimization Theory and Applications* 143 (2): 405–412. doi:10.1007/s10957-009-9579-3.

Calafiore, Giuseppe C. 2010. "Random Convex Programs." *SIAM Journal on Optimization* 20 (6): 3427–3464. doi:10.1137/090773490.

Calafoire, Giuseppe C., and Marco C. Campi. 2006. "The Scenario Approach to Robust Control Design." *IEEE Transactions on Automatic Control* 51 (5): 742–753. doi:10.1109/TAC.2006.875041.

Campi, Marco C., and Simone Garatti. 2011. "A Sampling-and-Discarding Approach to Chance-Constrained Optimization: Feasibility and Optimality." *Journal of Optimization Theory and Applications* 148 (2): 257–280. doi:10.1007/s10957-010-9754-6.

Chen, Zhenghua, Jinming Xu, and Yeng Chai Soh. 2015. "Modeling Regular Occupancy in Commercial Buildings Using Stochastic Models." *Energy and Buildings* 103: 216–223. doi:10.1016/j.enbuild.2015.06.009.

Corbin, Charles D., Gregor P. Henze, and Peter May-Ostendorp. 2013. "A Model Predictive Control Optimization Environment for Real-Time Commercial Building Application." *Journal of Building Performance Simulation* 6 (3): 159–174. doi:10.1080/19401493.2011.648343.

Danish Meteorological Institute. 2017. Accessed November 1 2017. http://www.dmi.dk/en/vejr.

Dobbs, Justin R., and Brandon M. Hencey. 2014. "Model Predictive HVAC Control with Online Occupancy Model." *Energy and Buildings* 82: 675–684. doi:10.1016/j.enbuild.2014.07.051.

Farina, Marcello, Luca Giulioni, and Riccardo Scattolini. 2016. "Stochastic Linear Model Predictive Control with Chance Constraint – A Review." *Journal of Process Control* 44: 53–67. doi:10.1016/j.jprocont.2016.03.005.

Feng, Xiaohang, Da Yan, and Tianzhen Hong. 2015. "Simulation of Occupancy in Buildings." *Energy and Buildings* 87: 348–359. doi:10.1016/j.enbuild.2014.11.067.

Flett, Graeme, and Nick Kelly. 2016. "An Occupant-Differentiated, Higher-Order Markov Chain Method for Prediction of Domestic Occupancy." *Energy and Buildings* 125: 219–230. doi:10.1016/j.enbuild.2016.05.015.

Garatti, Simone, and Marco C. Campi. 2013. "Modulating Robustness in Control Design. Principles and Algorithms." IEEE Control Systems Magazine, 36–51. doi:10.1109/MCS.2012.2234964.

Goyal, Siddharth, Herbert A. Ingley, and Prabir Barooah. 2012a. "Zone-Level Control Algorithms Based on Occupancy Information for Energy Efficient Buildings." American Control Conference (ACC), 3063–3068. doi:10.1109/ACC.2012.6315471.

Goyal, Siddharth, Herbert A. Ingley, and Prabir Barooah. 2012b. "Effect of Various Uncertainties on the Performance of Occupancy-Based Optimal Control of HVAC Zones." 51st IEEE Conference on Decision and Control, 7565–7570. doi:10.1109/CDC.2012.6426111.

Goyal, Siddharth, Herbert A. Ingley, and Prabir Barooah. 2013. "Occupancy-based Zone-Climate Control for Energy-Efficient Buildings: Complexity vs. Performance." *Applied Energy* 106: 209–221. doi:10.1016/j.apenergy.2013.01.039.

Hedegaard, Rasmus Elbæk, and Steffen Petersen. 2017. "Evaluation of Grey-Box Model Parameter Estimates Intended for Thermal Characterization of Buildings." 11th Nordic Symposium on Building Physics (NSB2017), Trondheim, Norway.

Henze, Gregor P. 2013. "Model Predictive Control for Buildings: A Quantum Leap?" *Journal of Building Performance Simulation* 6 (3): 157–158. doi:10.1080/19401493.2013.778519.

Kalman, R. E. 1960. "A New Approach to Linear Filtering and Prediction Problems." *Journal of Basic Engineering* 82 (1): 35–45. doi:10.115/1.3662552

Liao, Chenda, Yashen Lin, and Prabir Barooah. 2012. "Agent-based and Graphical Modelling of Building Occupancy." *Journal of Building Performance Simulation* 5 (1): 5–25. doi:10.1080/19401493.2010.531143.

Ma, Yodong, and Francesco Borrelli. 2012. "Fast Stochastic Predictive Control for Building Temperature Regulation." American Control Conference (ACC), 3075–3080. doi:10.1109/ACC.2012.6315347

Maasoumy, M., M. Razmara, M. Shahbakhti, and A. Sangiovanni Vincentelli. 2014. "Handling Model Uncertainty in Model Predictive Control for Energy Efficient Buildings." *Energy and Buildings* 77: 377–392. doi:10.1016/j.enbuild.2014.03.057.

Mahdavi, Ardeshir, and Farhang Tahmasebi. 2015. "Predicting People's Presence in Buildings: An Empirically Based Model Performance Analysis." *Energy and Buildings* 86: 349–355. doi:10.1016/j.enbuild.2014.10.027.

Mayne, David Q. 2014. "Model Predictive Control: Recent Developments and Future Promise." *Automatica* 50: 2967–2986. doi:10.1016/j.automatica.2014.128.

Mayne, David Q. 2016. "Robust and Stochastic Model Predictive Control: Are We Going in the Right Direction?" *Annual Reviews in Control* 41: 184–192. doi:10.1016/j.arcontrol.2016.04.006.

Mirakhorli, Amin, and Bing Dong. 2016. "Occupancy Behavior Based Model Predictive Control for Building Indoor Climate – A Critical Review." *Energy and Buildings* 129: 499–513. doi:10.1016/j.enbuild.2016.07.036.

Oldewurtel, Frauke, Allessandra Parisio, Colin N. Jones, Dimitrios Gyalistras, Markus Gwerder, Vanessa Stauch, Beat Lehmann, and Manfred Morari. 2012. "Use of Model Predictive Control and Weather Forecasts for Energy Efficient Building Climate Control." *Energy and Buildings* 45: 15–27. doi:10.1016/j.enbuild.2011.09.022.

Oldewurtel, Frauke, David Sturznegger, and Manfred Morari. 2013. "Importance of Occupancy Information for Building Climate Control." *Applied Energy* 101: 521–532. doi:10.1016/j.apenergy.2012.06.014.

Page, J., D. Robinson, N. Morel, and J.-L. Scartezzini. 2008. "A Generalised Stochastic Model for the Simulation of Occupant Presence." *Energy and Buildings* 40: 83–98. doi:10.1016/j.enbuild.2007.01.018.

Parisio, Alessandr, Damiano Varagnolo, Marco Molinari, Giorgio Pattarello,Luca Fabietti, and Karl H. Johansson. 2014. "Implementation of a Scenario-based MPC for HVAC Systems: an Experimental Case Study." 19th IFAC World Congress, 599–605. doi:10.3182/20140824-6-ZA-1003.02629.

Parisio, Alessandra, Damiano Varagnolo, Daniel Risberg, Giorgio Pattarello, Marco Molinari, and Karl H. Johansson. 2013. "Randomized Model Predictive Control for HVAC Systems." 5th ACM Workshop on Embedded Systems For Energy-Efficient Buildings (BuildSys'13). doi:10.1145/2528282.2528299.

Pedersen, Theis Heidmann, Rasmus Elbæk Hedegaard, and Steffen Petersen. 2017a. "IDF EnergyPlus Files of an Existing Danish Apartment Block and Eight Retrofit Scenarios." Mendeley Data doi:10.17632/6dhk66w5gj.1.

Pedersen, Theis Heidmann, Rasmus Elbæk Hedegaard, and Steffen Petersen. 2017b. "Space Heating Demand Response Potential of Retrofitted Residential Apartment Blocks." *Energy and Buildings* 141: 158–166. doi:10.1016/j.enbuild.2017.02.035.

Pedersen, Theis Heidmann, Michael Dahl Knudsen, Rasmus Elbæk Hedegaard, and Steffen Petersen. 2016. "Handling Stochastic Occupancy in an Economic Model Predictive Control Framework for Heating System Operation in Dwellings." CLIMA2016 – 12th REHVA World Congress (10), Aalborg, Denmark.

Pedersen, Theis Heidmann, Michael Dahl Knudsen, Rasmus Elbæk Hedegaard, and Steffen Petersen. 2017. "Handling Thermal Comfort in Economic Model Predictive Control Schemes for Demand Response." *Energy Procedia* 122: 985–990. doi:10.1016/j.egypro.2017.07.458.

Pedersen, Theis Heidmann, Kasper Ubbe Nielsen, and Steffen Petersen. 2017. "Method for Room Occupancy Detection Based on Trajectory of Indoor Climate Sensor Data." *Building and Environment* 115: 147–156. doi:10.1016/j.buildenv.2017.01.023.

Reindl, D. T., W. A. Beckman, and J. A. Duffie. 1990. "Diffuse Fraction Correlations." *Solar Energy* 45 (1): 1–7. doi:10.1016/0038-092X(90)90060-P.

Salakij, Saran, Na Yu, Samuel Paolucci, and Panos Antsaklis. 2016. "Model-Based Predictive Control for Building Energy Management. I: Energy Modeling and Optimal Control." *Energy and Buildings* 133: 345–358. doi:10.1016/j.enbuild.2016.09.044.

Schildbach, George, Lorenzo Fagiano, Christoph Frei, and Manfred Morari. 2014. "The Scenario Approach for Stochastic Model Predictive Control with Bounds on Closed-Loop Constraint Violations." *Automatica* 50: 3009–3018. doi:10.1016/j.automatica.2014.10.035.

Sourbron, Maarten, Clara Verhelst, and Lieve Helsen. 2013. "Building Models for Model Predictive Control of Office Buildings with Concrete Core Activation." *Journal of Building Performance Simulation* 6 (3): 175–198. doi:10.1080/19401493.2012.680497.

Tahmasebi, Farhang, and Ardeshir Mahdavi. 2016. "Stochastic Models of Occupants' Presence in the Context Building Systems Control." *Advances in Building Energy Research* 10 (1): 1–9. doi:10.1080/17512549.2015.1050693.

Tanner, Ryan A., and Gregor P. Henze. 2014. "Stochastic Control Optimization for a Mixed Mode Building Considering Occupant Window Opening Behaviour." *Journal of Building Performance Simulation* 7 (6): 427–444. doi:10.1080/19401493.2013.863384.

Undén, Per, Laura Rontu, Heikki Järvinen, Peter Lynch, Javier Calvo, Gerard Cats, Joan Cuxart, et al. 2002. "Hirlam-5 scientific documentation." Technical Report, Swedish Meteorological and Hydrological Institute.

Wang, Shengwei, Xue Xue, and Chengchu Yan. 2014. "Building Power Demand Response Methods Toward Smart Grid." *HVAC&R Research* 20 (6): 665–687. doi:10.1080/10789669.2014.929887.

Wetter, Michael. 2010. "Co-simulation of Building Energy and Control Systems with the Building Controls Virtual Test Bed." *Journal of Building Performance Simulation* 3 (4): 1–19. doi:10.1080/19401493.2010.518631.

Zhang, Xiaojing, Sergio Grammatico, Georg Schildbach, Paul Goulart, and John Lygeros. 2015. "On the Sample Size of Random Convex Programs with Structured Dependence on the Uncertainty." *Automatica* 60: 182–188. doi:10.1016/j.automatica.2015.07.013.

Zhang, Xiaojing, Georg Schildbach, David Sturznegger, and Manfred Morari. 2013. "Scenario-Based MPC for Energy-Efficient Building Climate Control under Weather and Occupancy Uncertainty." European Control Conference (ECC), Zürich, Switzerland, 1029–1034.

P7 The effect of including hydronic radiator dynamics in model predictive control of space heating

The effect of including hydronic radiator dynamics in model predictive control of space heating

Theis Heidmann Pedersen [1], Rasmus Elbæk Hedegaard, Kristian Fogh Kristensen, Benjamin Gadgaard, Steffen Petersen

Department of Engineering, Aarhus University, Inge Lehmanns Gade 10, 8000 Aarhus C, Denmark

_____

Abstract

Existing simulation-based studies on applying model predictive control (MPC) schemes for space heating operation to enable demand response (DR) make use of linear models for the heating system, usually by assuming convective electrical baseboard heaters. However, buildings connected to district heating networks are typically equipped with hydronic heat emitters, such as radiators, that are nonlinear in their behavior. This paper therefore investigates the effect of including the nonlinear dynamics of a hydronic heat emitter on the DR potential of MPC for space heating. Furthermore, the performance of a practical two-level control approach suitable for real application, in which a heating setpoint was determined by a linear MPC and communicated to a conventional proportional integral controller, was investigated. The simulation framework for the investigation was based on the application of an experimentally obtained hydronic radiator model applied in different co-simulation setups, featuring a model of a poorly and a highly insulated apartment, respectively. The results indicated that inclusion of the nonlinear thermal effects of hydronic radiators did not significantly affect the DR performance when compared to the results of an MPC scheme controlling convective electrical baseboard heaters. In general, both setup achieved operational cost savings of approx. 5% and 18% in an existing and retrofitted building, respectively, while restricting the amount of thermal comfort violations to a limited extent. This suggests that results obtained in previous studies featuring electrical baseboard heaters also apply to buildings equipped with hydronic heating systems, and that future simulation-based studies and practical implementation of MPC for space heating can continue to rely on the use of far less computationally demanding linear control-models. Furthermore, the results suggest that the two-level control scheme seems like an appropriate control setup suitable for real applications.

Keywords: model predictive control; demand response; dynamic radiator model; space heating; hydronic heating;

_____

[1] Corresponding author. Tel: +45 20822070
E-mail address: thp@eng.au.dk

Nomenclature

Abbreviations

DR	Demand response
MPC	Model predictive control
E-MPC	Economic model predictive control
DH	District heating
N-MPC	Nonlinear model predictive control
PRBS	Pseudo-random binary signal
PRMS	Pseudo-random multi-level signal

Symbols

τ	Time step	[seconds]
t	Temperature	[°C]
T	Temperature	[K]
N_s	Number of sections	[-]
C	Heat capacity	[J/K]
c_p	Specific heat capacity	[J/(kg·K)]
ρ	Density	[kg/m^3]
q	Flow rate	[m^3/s]
Q	Energy	[J]
ϕ	Heat power	[W]
n	Radiator exponent	[-]
Δt_{ar}	Arithmetic temperature difference	[°C]
Δt_{lg}	Logarithmic temperature difference	[°C]
β_C	Fraction of convective heat emission	[-]
β_R	Fraction of radiative heat emission	[-]
A	State matrix	
$\boldsymbol{x}_{\tau+n\|\tau}$	State vector predicted for time step $\tau+n$ at time step τ	
B	Input matrix	
$\boldsymbol{u}$	Control actions vector	
E	Disturbance matrix	
$\boldsymbol{d}$	Disturbance vector	
KG	Kalman gain	

Subscripts

j	Section number
inlet	Inlet water temperature
outlet	Outlet water temperature
w	Water
N	Nominal (standard conditions)

1   Introduction

Demand response (DR) programs where building owners adjust their consumption in response to an external request have been proposed in several studies to overcome challenges related to power imbalances and peak load issues in the electricity grid, e.g. [1, 2] to mention a few. However, district heating (DH) networks may also benefit from building owners participating in DR programs as DH networks, in the near future, will be strongly coupled with the electricity grid to increase integration of renewable energy sources [3, 4]. Several studies have thus investigated the ability of buildings to provide DR using thermal energy storages, including both active storage (e.g. domestic hot water tanks) [5, 6] and passive storage obtained by exploiting their thermal mass [7-13].

Several control approaches can be used to enable DR of which especially the concept of model predictive control (MPC) has received significant research attention lately [7, 8, 11, 12]. MPC is an optimization-based control scheme that relies on a simplified control-model of the building thermodynamics to determine an optimal control strategy. Knudsen and Petersen [5] applied an economic MPC (E-MPC) scheme with the objective of minimizing operational costs of domestic hot water preparation in an ultra-low temperature DH system. Considering time varying electricity and district heating prices, the proposed E-MPC scheme simultaneously enabled load-shift from peak periods and operational cost savings of approx. 5%. Avci et al. [11] applied E-MPC together with day-ahead electricity prices to minimize the weighted sum of the operational cost and the temperature deviations from a preferred room air setpoint. Applying the proposed E-MPC scheme to operate an AC unit reduced the energy consumption in peak-hours by 23.6% compared to a conventional two-position control approach. Pedersen, Hedegaard and Petersen [7] applied E-MPC and day-ahead wholesale electricity prices for optimal operation of convective electrical space heaters in ten apartments. Compared to a conventional constant setpoint tracking proportional-integral (PI) controller, the E-MPC scheme achieved load reductions of up to 47% in peak load periods, depending on the energy efficiency and, accordingly, the storage efficiency of the building envelope. However, as suggested by Le Dréau and Heiselberg [9], the type of heat emitter significantly affects the magnitude and duration of DR events. They applied rule-based control to increase and decrease the temperature setpoint for varying durations using two types of heat emitters (i.e. radiators and underfloor heating), and found that the modulation potential differed significantly for the two considered heat emitters.

Existing simulation studies on applying E-MPC schemes to operate the space heating system to enable DR make use of convective electrical baseboard heaters that behave linearly. However, typical heating systems in buildings connected to DH networks consists of hydronic heat emitters, such as radiators, that are characterized by nonlinearities in their heat output, driven by the temperature difference between the radiator and room. Using E-MPC for real applications to operate hydronic heat emitters therefore introduces nonlinearities that, consequently, lead to a less practical and computationally demanding nonlinear MPC (N-MPC) scheme.

To the best of the authors' knowledge, there are no reported studies on whether the nonlinear dynamics of a hydronic heat emitter affect the potential of DR when exploiting the structural thermal mass to shift energy consumption in buildings. This paper therefore reports on a simulation-based study, applying an N-MPC scheme with the objective of minimizing operational cost to investigate the effect of the DR potential. Furthermore, the performance of a two-level MPC scheme suitable for real applications, which allow for a practical coupling between the MPC scheme and existing setpoint-tracking controllers was evaluated.

2   Method

A dynamic radiator model was needed to accurately evaluate the impact of hydronic heating systems; therefore this paper first presents a nonlinear radiator model that adequately represents the thermodynamics of a hydronic radiator (section 2.1). Subsequently, three MPC scheme setups were formulated: a linear MPC scheme, a two-level MPC scheme, and an N-MPC scheme (section 2.2). The performance of the three setups was investigated through co-simulations facilitated by the Building Controls Virtual Test Bed [15] of an apartment located in Aarhus, Denmark (see section 2.3). The apartment was represented by an EnergyPlus (EP) model while the dynamic radiator model and the MPC schemes were implemented in MATLAB.

2.1   Dynamic radiator model

A nonlinear grey-box model of a particular hydronic panel radiator (DeLonghi Radel type 22 [16]) was established. The thermal behavior of the radiator was modeled as a system of nonlinear ordinary differential equations based on the laws of thermodynamics [17], thus the radiator was lumped into N_S equally sized homogeneous horizontal sections in serial connection. The particular radiator dimensions and inlet/outlet locations are illustrated in Fig. 1. Preliminary thermographic investigations confirmed that the assumption about approximately homogeneous horizontal sections of this specific radiator was acceptable (see Fig. 2).
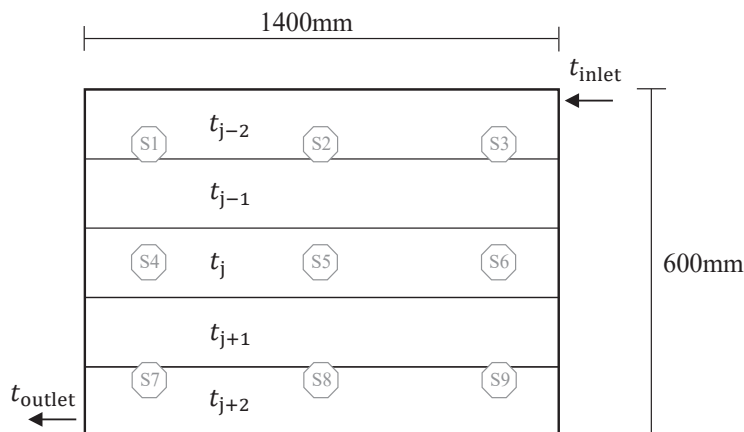

Fig. 1. Principle of the dynamic radiator model exemplified with N_S = 5 horizontal sections with different temperatures t. The octagons mark the position of nine thermocouples (type K) used to measure the surface temperature.

However, it is noted that the modeling was specific to this particular radiator since model parameters, such as heat capacity and nominal power, vary with the size of the radiator while position of the inlet and outlet affects the charging pattern, i.e. the stratification in the radiator.
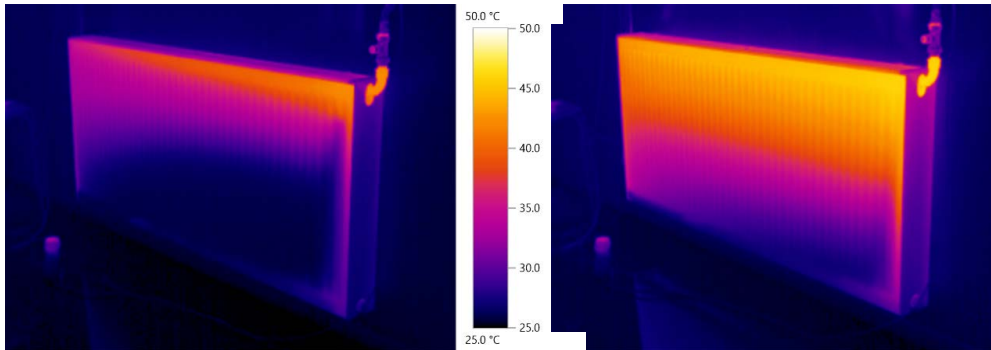

Fig. 2. Thermographic images during heat-up. Left) after 5 minutes. Right) after 8 minutes.

The energy balance of each section was expressed as an ordinary differential equation (see Eq. (1)), where Q_{stored} denotes the stored heat, and ϕ_{in} and ϕ_{out} denote the power flowing in and out of the radiator, respectively. The ordinary differential equation is specified in detail for the j'th section of the radiator in Eq. (2) (see Appendix A for the full set of radiator model equations). C_{Rad} is the combined heat capacity of the water and radiator material, q is the flow rate, while $c_{p,w}$ and ρ_w are the specific heat capacity and density of the water, respectively. The nominal power of the radiator determined at standard conditions is denoted ϕ_N, while $\Delta t_{ar,N}$ and n are the arithmetic temperature difference at standard conditions and the radiator exponent, respectively. The water in each radiator sub-section was assumed incompressible and fully mixed, thus the entire water-volume in each section j has temperature t_j (see Fig. 1).

$$\frac{dQ_{stored}}{d\tau} = \sum \phi_{in} - \sum \phi_{out} \tag{1}$$

$$\frac{C_{Rad}}{N_S} \cdot \frac{dt_j}{d\tau} = c_{p,w} \cdot \rho_w \cdot q \cdot (t_{j-1} - t_j) - \frac{\phi_N}{N_S} \cdot \left(\frac{t_j - t_{room}}{\Delta t_{ar,N}} \right)^n \tag{2}$$

The model requires the inlet temperature (t_{j-1} for the first section, see Appendix A), the room temperature and the flow rate as inputs. The output of the model is the temperature of the water in the last section, which is assumed to be equal to the outlet water temperature. Modeling the outlet water temperature enables a simple calculation of the heating power to the room, which equals the change in energy of the water (see Eq. (3)).

$$\phi_{Rad} = c_{p,w} \cdot \rho_w \cdot q \cdot (t_{inlet} - t_{outlet}) \tag{3}$$

The heating power is delivered to the room by convective and radiative heat transfer. The fraction of convection and radiation denoted β_C and β_R, respectively, depend on the radiator and room temperature conditions. Knowing $\beta_{R,N}$, i.e. the radiative fraction at standard conditions, enables the calculation of β_R according to Eq. (4) [18]. In this study, $\beta_{R,N}$ was assumed to be 0.3 which is in accordance with other studies [19, 20] for a double panel radiator.

$$\beta_{\text{R}} = \beta_{\text{R,N}} \cdot \frac{\frac{\left(T_{\text{room}} + \Delta t_{lg}\right)^4 - T_{\text{room}}^{\,4}}{\left(T_{\text{room}} + \Delta t_{lg,\text{N}}\right)^4 - T_{\text{room}}^{\,4}}}{\left(\frac{\Delta t_{lg}}{\Delta t_{lg,\text{N}}}\right)^n} \tag{4}$$

2.1.1   Calibration of radiator model parameters

The model parameters were calibrated based on measurement data from experiments where the radiator was excited by controlling the flow rate according to four experiments as specified in Table 1. The temperatures of inlet, outlet and room air were, in all experiments, measured at a sampling rate of 15 seconds along with nine surface temperatures (see Fig. 1). Three experiments were conducted using pseudo-random multi-level signals (PRMS) generated by the software Galois [21], and one experiment was conducted using a pseudo-random binary signal (PRBS) generated using the MATLAB function *idinput*. The use of both PRBS and PRMS signals was to test the prevailing notion in literature that a PRBS signal may not provide sufficient perturbation to identify nonlinear models [22]. The duration of the experiments is denoted *P,* and the number of levels was the number of different flowrates, ranging from a fully closed to a fully open valve position. The switching time, i.e. the shortest amount of time between changing flowrates, was set to 300 seconds for all four experiments.

Table 1. Parameters defining the four experiments

	Experiment 1 *Training data*	**Experiment 2** *Training data*	**Experiment 3** *Training data*	**Experiment 4** *Validation data*
Excitation signal	PRMS	PRMS	PRBS	PRMS
Number of levels	5	13	2	5
Duration (*P*)	14 hours	14 hours	14 hours	50 hours

The radiator model in Eq. (2) contains five unknown parameters. However, the model structure only allows for calibration of two parameters due to issues regarding structural identifiability [17]. To reduce the number of unknown parameters, the parameters describing the properties of water, $c_{p,\text{w}}$ and ρ_{w}, were assumed to be temperature invariant. This assumption seems reasonable as the temperature fluctuations between 30°C-60°C, only leads to approximately 0.2% and 1.5% variation of $c_{p,\text{w}}$ and ρ_{w}, respectively. For convenience, the material property H_{w} is introduced according to Eq. (5).

$$H_{\text{w}} = c_{p,\text{w}} \cdot \rho_{\text{w}} \tag{5}$$

Fixing the material properties of the hydronic fluid leaves three unknown parameters: the nominal power at standard conditions, the thermal capacity of the radiator and the radiator exponent. The radiator exponent *n* was estimated using the standard static least-squares calibration method [23] based on measurements of the nominal power at three standard temperature conditions as stated in Table 2 [16]. The two remaining parameters, i.e. the nominal power and the thermal capacity, were calibrated with the objective to minimize

the outlet temperature residuals using the time-series measurements obtained during the experiments. Furthermore, the radiator models were calibrated for $\{N_s \in \mathbb{Z} \mid 2 \leq N_s \leq 100\}$ to identify the optimal N_s.

Table 2. Specifications from data sheet

t_{inlet}	t_{outlet}	t_{room}	ϕ_{N}	$\Delta t_{ar,\text{N}}$
75 °C	65 °C	20 °C	2479 W	50.0 °C
70 °C	55 °C	20 °C	2001 W	42.5 °C
55 °C	45 °C	20 °C	1264 W	30.0 °C

The first three experiments were used as separate training data sets for calibrating three versions of the radiator model, and data from the fourth experiment was used to validate the calibrated models. Measurements from experiment 4, i.e. the validation data, are depicted in Fig. 3. It is seen that the room air temperature had an increasing trend during the experiment by a couple of degrees because of the high amount of heat injected into the room. The calibrated models were evaluated in terms of the two standard metrics root mean square error (RMSE) and normalized root mean square error (NRMSE) as defined in Eq. (6) and (7), respectively. *P* is the duration of the experiment where the index $\tau s = \{1, 2,..., P\}$ denotes the time in 15 seconds increments, *z* and $\hat{z}$ are timeseries of the measured data and the output of the model, respectively, and $\|\cdot\|$ denotes the Euclidean norm. Considering both metrics in the evaluation ensures reliable evaluation when using three distinct experiments with varying variability to calibrate the models.

$$RMSE \;\;= \sqrt{\frac{\sum_{\tau s=1}^{P}(z_{\tau s} - \hat{z}_{\tau s})^2}{P}} \tag{6}$$

$$NRMSE = \left(1 - \frac{\|z - \hat{z}\|}{\|z - \text{mean}(z)\|}\right) \cdot 100 \tag{7}$$
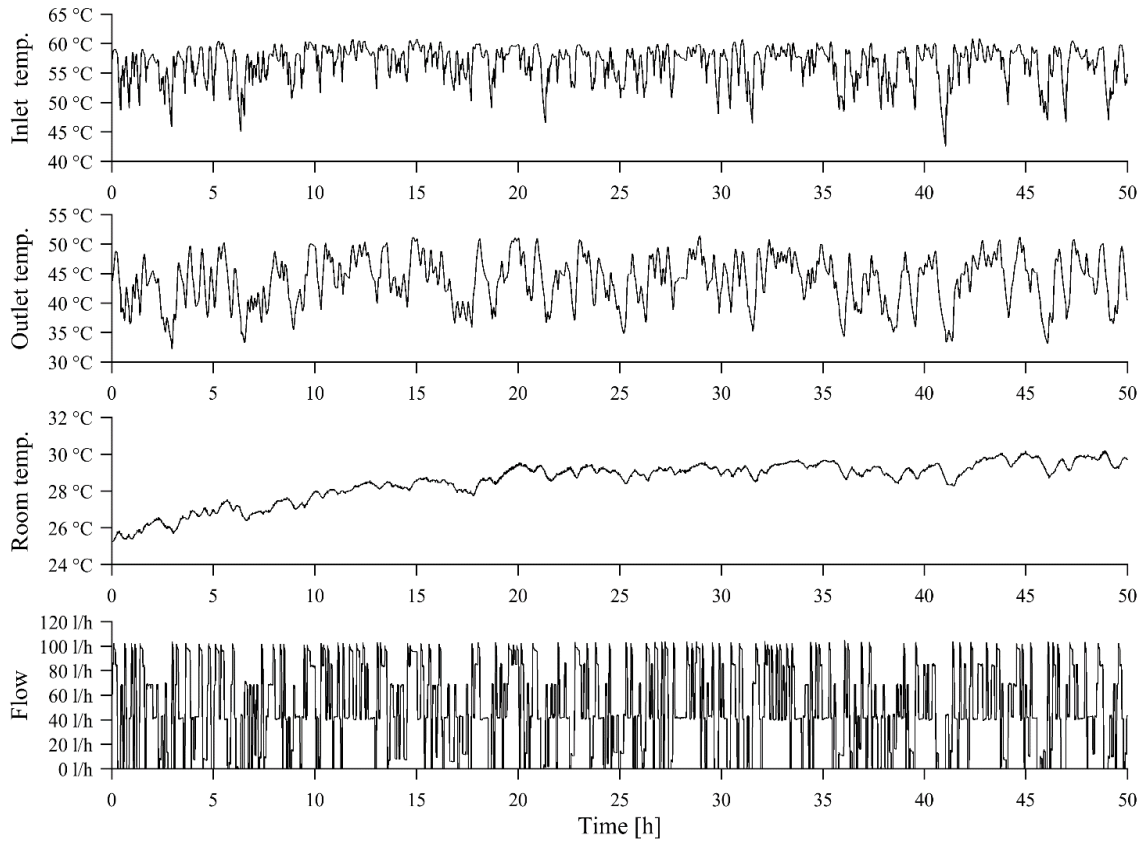
Fig. 3. Data from experiment 4 used for model validation

2.2 Model predictive control

MPC is an optimization based control scheme that, in each discrete time step τ_{MPC}, determines an optimal control sequence for a finite prediction horizon N. The controllable decision variables $\boldsymbol{u}$, i.e. space heating control actions, are communicated to the EP representation of the building in a receding horizon approach, where only the first action of the optimal sequence is actually implemented [24]. At the next discrete time step, the optimization problem is solved again with a prediction horizon shifted one time step ahead in time. In this study, a linear objective function was considered for the MPC scheme using a time varying cost signal $\boldsymbol{f}$, as specified in Eq. (8).

$$\underset{\boldsymbol{u}}{\text{minimize}} \; J = \sum_{\tau=0}^{N-1} f_\tau \cdot u_\tau \tag{8}$$

The MPC scheme is subject to multiple constraints (Eq. (9) – (12)). Firstly, the scheme is constrained by a control-model which describes the thermodynamics of the system to be controlled. The dynamics are specified in Eq. (9), and are a function of the system states $\boldsymbol{x}_\tau$, control action u_τ and disturbances $\boldsymbol{d}_\tau$ (i.e. ambient temperature and transmitted solar irradiance).

$$\boldsymbol{x}_{\tau+1} = g(\boldsymbol{x}_\tau, u_\tau, \boldsymbol{d}_\tau) \tag{9}$$

At each time step τ_{MPC}, the room air temperature was measured from the EP representation (y^{measured}) and used to correct the states of the control-model using a Kalman filter that updates the observed and unobserved states according to Eq. (10), where KG is the Kalman gain [25].

$$\boldsymbol{x}_{\tau|\tau} = \boldsymbol{x}_{\tau|\tau-1} + KG \cdot \left(y_\tau^{\text{measured}} - \boldsymbol{C} \cdot \boldsymbol{x}_{\tau|\tau-1}\right) \tag{10}$$

Addressing thermal comfort when applying MPC schemes can be handled in various ways [26]. One approach is to formulate a multi-objective optimization problem, which simultaneously minimizes operational costs and thermal comfort deviations [11, 27]. Another approach is to assume that occupants are comfortable as long as the room air temperature is within a predefined comfort band [7, 8]. In this study, the latter approach was chosen, which led to a single objective formulation. The comfort band was defined by the time invariant lower ($t_{\min}$) and upper ($t_{\max}$) comfort bounds, see Eq. (11).

$$t_{min} \le y_\tau \le t_{max} \tag{11}$$

Furthermore, the space heating control action u_τ was restricted by the maximum design heating power according to Eq. (12).

$$0 \le u_\tau \le u_{max} \tag{12}$$

2.2.1 Investigated MPC setups

In theory, the control-model of the room and heating system dynamics specified in Eq. (9) is a nonlinear function. However, many studies approximate the room thermodynamics as a linear function by neglecting the nonlinear dynamics of hydraulic systems, and assume electrical baseboard heaters in the simulations, thus resulting in a convex linear program, see e.g. [7, 8]. To investigate how this approximation affects the control performance, simulations of three MPC setups were carried out:

a) Linear MPC controlling an electrical baseboard heater[2].

b) Two-level control where a linear MPC determined the optimal heating setpoint to be maintained by a conventional PI-controller[3] adjusting the water flow to the hydronic radiator model.

c) N-MPC scheme, i.e. including the hydronic radiator in the control-model.

The three setups led to distinct co-simulation setups as illustrated in Fig. 4, facilitated by the Building Controls Virtual Test Bed [15].

---

[2] A constant radiative fraction β_R of 0.3 was assumed.
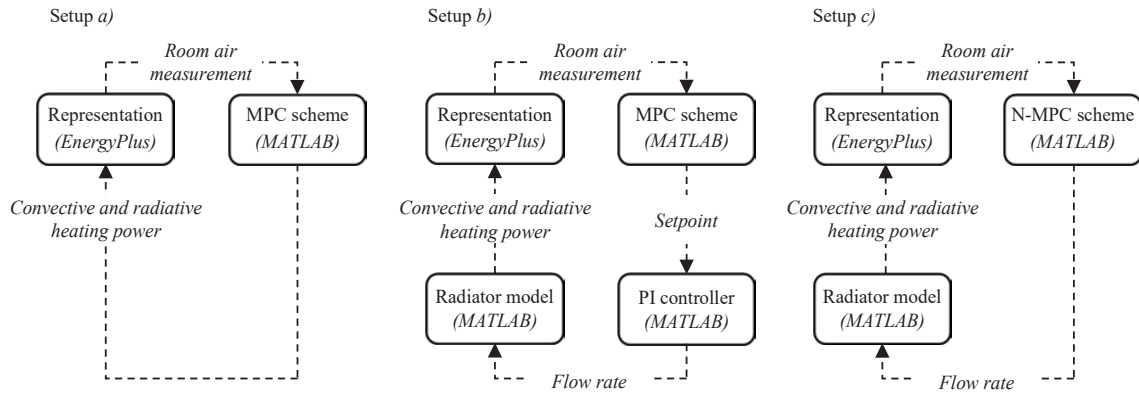[3] The PI controller was tuned using the MATLAB function *pidtune*.

Fig. 4. Co-simulation setups for the three investigated MPC setups.

Setups *a)* and *b)* relied on a linear two-state grey-box control-model representing the lumped thermal capacity of the zone air and the construction elements. The state space representation of the model is given in Eq. (13) and (14) with state matrix $\mathbf{A}$, input matrix $\mathbf{B}$, disturbance matrix $\mathbf{E}$ and output matrix $\mathbf{C}$. The control-model was estimated in continuous time and then discretized using the zero-order hold method with a time step of 60 seconds.

$$x_{\tau+1} = \mathbf{A} \cdot x_\tau + \mathbf{B} \cdot u_\tau + \mathbf{E} \cdot d_\tau \qquad (13)$$

$$y_\tau \quad = \mathbf{C} \cdot x_\tau \qquad (14)$$

The commercial solver *CPLEX* was used to solve the convex linear program and returned the optimal sequence of control actions u [W], constrained by the maximum installed heating power, i.e. $u_{max} = \phi_{max}$ (Eq. (12)). In setup *b)* the predicted temperatures, resulting from applying the optimal sequence u, were communicated as a setpoint to the low-level PI-controller which then adjusted the flow rate of the hydronic radiator accordingly (hence the name *two-level control*).

For setup *c)* the control-model combined the linear room model (Eq. (13) and (14)) with the model of the hydronic radiators (Eq. (2) and Appendix A) leading to a nonlinear control-model and a nonconvex optimization formulation. Instead of linearizing and discretizing the control-model, the MATLAB functions *ode45* and *fmincon* were used to simulate and optimize the model, respectively. The controllable decision variable was the sequence of flow rates q which was constrained by the maximum flow rate, i.e. $u_{max} = q_{max}$ (Eq. (12)). The *ode45* function simulated the system of ordinary differential equations using the fourth and fifth order Runge Kutta to determine an adequate time step size, thus ensuring a reliable simulation. The function *fmincon* contains several optimization algorithms of which the *active set* algorithm was used for the purposes of this study since it has been demonstrated to be able to achieve adequate results in a timely manner [14]. However, we found that the solver algorithm was sensitive towards the initial sequence of control actions. Especially in cases where the initial sequence of flowrates would lead to comfort violations, the algorithm tended to arrive at locally optimal solutions. The optimization problem in this study was therefore solved using

two initial guesses, and the resulting solution with the lowest objective value was implemented. The first initial guess was determined by taking the solution obtained when neglecting the hydronic system and translating it into flowrates using Eq. (3). The second initial guess vector was a constant flow rate which was determined so the room air temperature was within the comfort bounds during the entire prediction horizon. After determining the optimal flow rates q, the resulting radiant and convective emitted heating power were calculated using Eq. (3) and (4).

2.3   Test case

The three MPC setups were tested on an EP model representing an apartment located in Aarhus, Denmark. The apartment has east-west oriented windows and a west-oriented open balcony illustrated with yellow in Fig. 5. The horizontal zone boundaries (i.e. ceiling and floor) were assumed adiabatic. Insulation was added to the partitioning wall to make it reasonable to neglect heat transfer to the adjacent apartment as suggested in [28], and the temperature in the adjacent apartment was kept constant at 20°C. Previous studies have suggested that the DR potential depends on the energy efficiency of the building envelope [7]. Therefore, the simulations were performed for the existing building and a building with an improved energy efficiency. Further specifications of materials and constructions are provided in ref. [7] where the building configurations used in this study are denoted *Retrofit0* and *Retrofit8*.
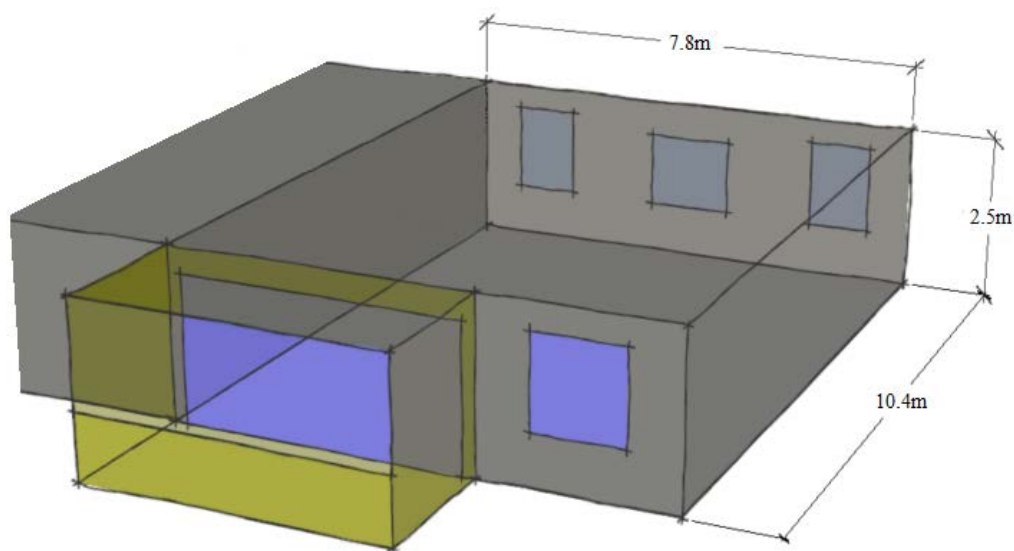

Fig. 5. Test case geometry as modeled in EP.

The EP model had a time step of 60 seconds, whereas the MPC scheme determined new control actions every 15 minutes (τ_{MPC} of 900 seconds). On-site weather measurements (see Fig. 6) were used during the one week simulation period from December 12, 2016, to December 18, 2016.
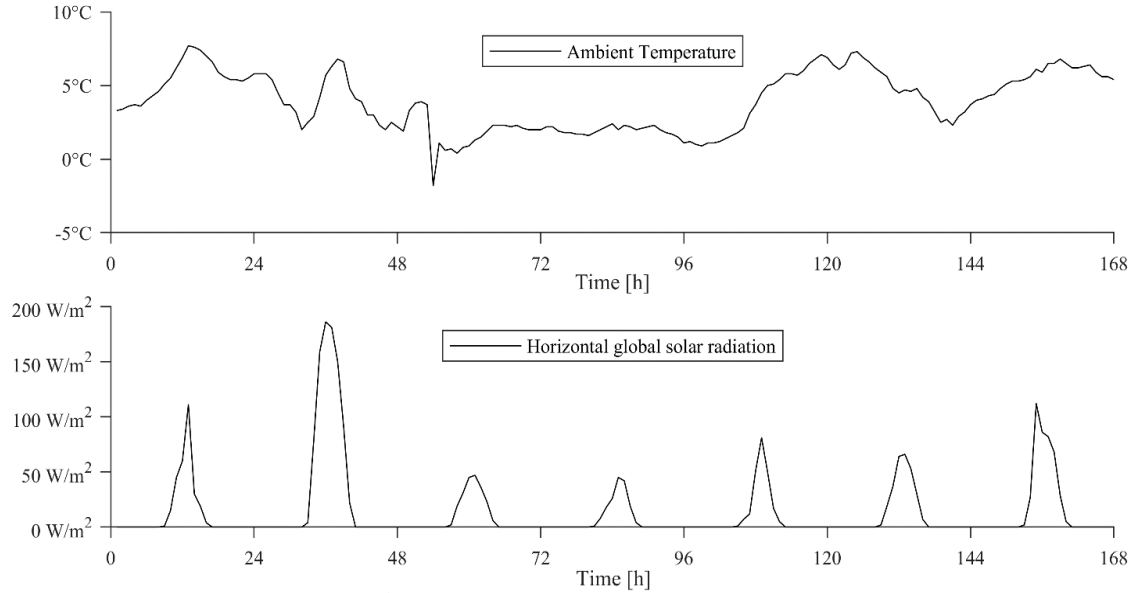
Fig. 6. Weather conditions during the simulation period

As stated in Eq. (11), the MPC scheme was constrained to maintain a room air temperature within certain comfort bounds. The potential of exploiting the thermal mass as a sensible heat storage depends on the comfort interval, i.e. how large temperature fluctuations occupants will allow. In this study, a rather restrictive comfort interval was chosen with comfort bounds t_{min} and t_{max} set to 20°C and 23°C, respectively. The apartment was assumed to be equipped with two radiators which, as described in section 2.2.1, constrained the linear MPC and N-MPC scheme by the radiator characteristics of $\phi_{max} = 2025W$ and $q_{max} = 110$ l/h, respectively.

The potential of DR can be evaluated with respect to various objectives [5, 7, 8]. This study considers price-based demand response, where the objective was to achieve operational cost savings compared to a reference scenario with a control scheme tracking a constant setpoint t_{min}. Historical day-ahead wholesale electricity prices for the bidding area DK1 were used as cost signal f (see Eq. (8)) in all control setups. The efficiency factor in the conversion of electricity to thermal energy in setups that include a hydronic heating system, i.e. setups *b)* and *c)*, was assumed to be equal to one. This allowed for a direct performance comparison of the three MPC setups, as well as comparisons with results obtained in previous studies. In practice, however, a heat pump would significantly improve the economic performance of setups *b)* and *c)*. Taxation tariffs are very country specific and were therefore neglected to generalize the interpretation of the results. Consequently, the resulting operational costs cannot be expected to match the actual operational costs paid by consumers. Furthermore, perfect predictions of *f* were assumed. A prediction horizon *N*=48 hours was chosen to ensure that the control scheme utilized the full storage capacity of the thermal mass.

Three key performance indicators were used to evaluate the DR potential. One indicator was the ability of the MPC schemes to achieve operational cost savings relative to a reference controller according to Eq. (15), where c_τ denotes the operational cost for time step τ.

$$\overline{\Delta c} = \sum_{\tau=1}^{P} \frac{c_\tau^{MPC} - c_\tau^{ref}}{c_\tau^{MPC}} \tag{15}$$

The other indicator was the absolute and relative ability of the MPC schemes to shift space heating consumption in each time step compared to a reference controller according to Eq. (16) and (17), respectively.

$$\Delta\phi_\tau = \phi_\tau - \phi_\tau^{ref} \qquad \forall \tau = 1, \dots, P \tag{16}$$

$$\overline{\Delta\phi_\tau} = \frac{\phi_\tau - \phi_\tau^{ref}}{\phi_\tau^{ref}} \qquad \forall \tau = 1, \dots, P \tag{17}$$

Furthermore, the shifting efficiency, which is the ratio between decreased and increased heating consumption during charging and discharging periods, was evaluated according to Eq. (18) [9]. The durations of charging and discharging periods is denoted τ^{charge} and $\tau^{discharge}$ and is determined at each load shift event (see Fig. 12).

$$\eta_{shifting} = \frac{-\int_0^{\tau^{discharge}} \Delta\phi_\tau (\Delta\phi_{\tau s} < 0) d\tau}{\int_0^{\tau^{charge}} \Delta\phi_\tau (\Delta\phi_\tau > 0) d\tau} \tag{18}$$

3   Results

3.1   Dynamic radiator model

Three dynamic radiator models were calibrated based on the three separate training datasets (see Table 1) and with an increasing number of horizontal sections. Fig. 7 displays the performance indicators RMSE and NRMSE for the identified models evaluated on the validation data. The results suggest that the models derived using data generated from PRBS excitation signals (experiment 3) were less capable of accurately predicting the outlet temperature of the radiator compared to models derived using data generated from PRMS excitation signals (experiment 1 and 2). This is in agreement with the prevailing notion in literature that PRBS signals are suitable for linear systems, whereas calibration of nonlinear systems benefits from the use of PRMS excitation signals, as they are better at revealing the behavior of dynamic systems [22]. The models calibrated using Experiment 1 and 2 data achieved similar performance. Generally, the performance increases as the number of sections approaches six; hereafter the performance stagnates.
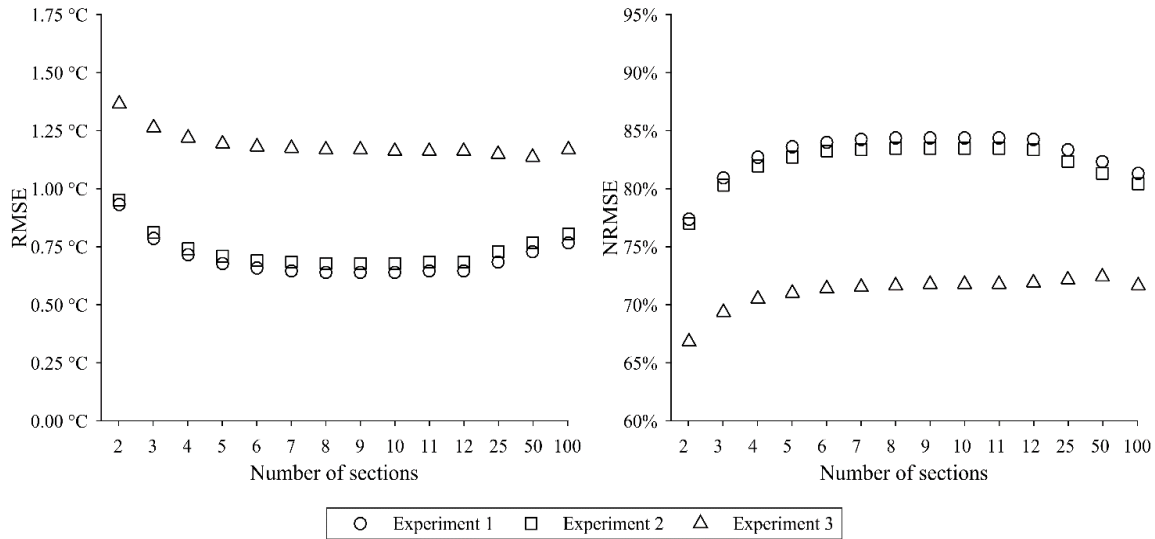
Fig. 7. RMSE and NRMSE values on validation data for radiator models calibrated based on the three distinct experiments with varying number of sections N_S.

The best performing radiator model was achieved using Experiment 1 as training data and with nine horizontal sections (RMSE = 0.64°C and NRMSE = 84% on the validation data). This model was therefore chosen for the following investigations of the MPC schemes. The model parameters are stated in Table 3. It can be seen that the calibrated nominal power ϕ_N of 1874 W (using $\Delta t_{ar,N}$ = 42.5 °C) is consistent with the declared ϕ_N of 2001W from the manufacturer (second row of Table 2) with a deviation of approx. 6%.

Table 3. Calibrated and calculated model parameters of the proposed dynamic radiator model.

N_s	C_{Rad} [J/K]	H_w [kJ/(m³·K)]	ϕ_N [W]	$\Delta t_{ar,N}$ [°C]	n
9	43254.3	4113.7	1873.7	42.5	1.32

Fig. 8 shows a comparison of the measured surface temperatures during the experiment used for model validation (Experiment 4) and the simulated states of the horizontal sections in the model using the parameters in Table 3. The measured surface temperatures (see Fig. 1 for their placements) were averaged horizontally and compared with the simulated temperatures of sections two, five and eight. Fig. 8 left column shows the temperature during 12 hours of the experiment, and Fig. 8 right column shows the histogram of residuals during the entire experiment (50 hours). The temperature deviations increased slightly from the bottom section towards the top section, where the RMSE for the four sections was 3.55°C, 1.77°C, 0.95°C and 0.64°C, respectively. As expected, the residuals of the outlet temperature were the lowest since the model was calibrated with the objective of minimizing the outlet residuals. Another reason for this vertical increment is the model structure, where the heat loss for each horizontal section is a function of the room air temperature.

However, the temperature of the ambient air surrounding the radiator increases vertically, thus the model structure overestimates the heat loss especially in the top sections.
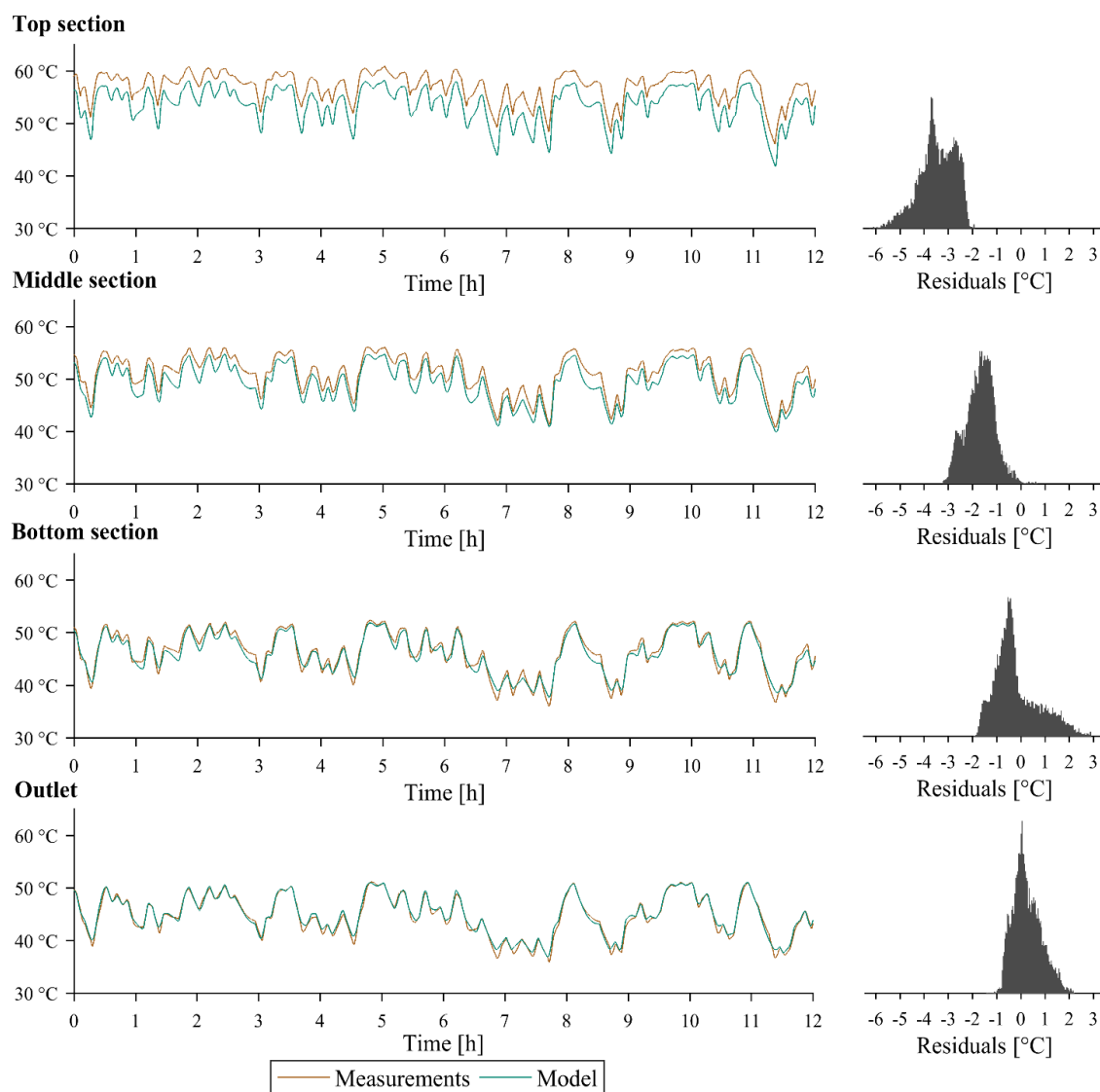
Top section

Middle section

Bottom section

Outlet

Fig. 8. Simulated system states compared to surface temperature measurements.

3.2   Performance of MPC schemes

The indoor air temperatures for the existing building in the simulated one-week period, using the constant setpoint tracking controller (reference) and the three MPC setups, respectively, are depicted in Fig. 9. The grey dashed lines indicate the thermal comfort bounds, and the bottom chart displays the historical time varying wholesale electricity prices. Compared to the reference controller, all the E-MPC schemes increased the space heating consumption and, consequently, increased the air temperatures in low price periods. Consequently, the

thermal mass of the building constructions was charged and the heating consumption in the following high price periods was reduced. Overall, the trajectories depicted in Fig. 9 suggest that the three MPC setups resulted in similar space heating strategies.
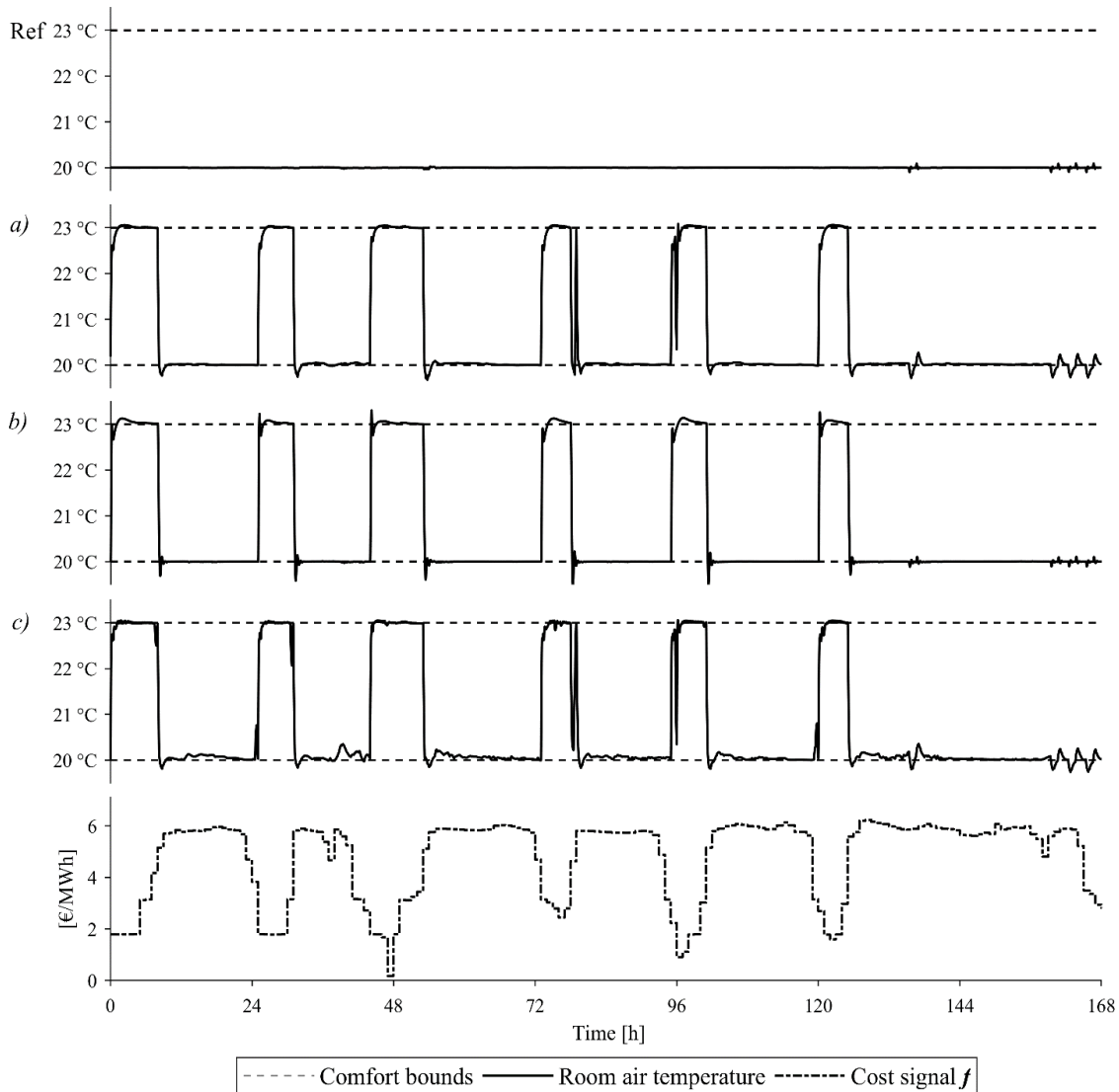
Fig. 9. One-week simulation results and associated cost signal.

It is noted that the simulations were only performed for a period of one week and for one specific apartment, which is why the specific absolute results cannot be used for generalizations on the effect of the MPC schemes. However, the observed tendencies are considered generalizable as they are consistent with previously obtained results investigating the performance of E-MPC [7, 8, 11].

The summarized results for the simulation week is presented in Table 4 and confirm that the three MPC setups achieved similar performance. Evaluation of the ability to achieve operational cost savings (Eq. (15)) showed

that the three MPC setups achieved operational cost savings of approx. 5% and 18% for the existing and retrofitted building, respectively. Furthermore, the ability to maintain an air temperature within the comfort bounds was evaluated as the number of degree hours where the air temperature violated the lower and upper temperature bounds. The performance was similar for all MPC setups, and the level of comfort violations was generally limited – a fact also indicated by Fig. 9. The reason for the minor comfort violations in setups *a)* and *c)*, which solely relied on the control-model to predict the required space heating consumption, was the practically unavoidable building/control-model mismatch. In setup *b)*, which relied on a low-level PI controller to track the setpoints specified by the MPC scheme, minor temperature over- and undershoots were observed when the low-level PI controller was switching between the upper and lower comfort bounds as setpoints.

Table 4. Summarized simulation results.

		Energy	**Operational cost**	**Cost savings**	**Comfort violations**
Existing building	Reference	4.1 kWh/m²	€ 12.0		0.4 °Ch
	Scenario *a)*	4.3 kWh/m²	€ 11.3	€ 0.7 (5.8%)	3.2 °Ch
	Scenario *b)*	4.3 kWh/m²	€ 11.3	€ 0.7 (5.8%)	3.7 °Ch
	Scenario *c)*	4.4 kWh/m²	€ 11.4	€ 0.6 (5.0%)	2.1 °Ch
Retrofitted building	Reference	1.4 kWh/m²	€ 3.9		0.1 °Ch
	Scenario *a)*	1.5 kWh/m²	€ 3.2	€ 0.7 (18.0%)	2.3 °Ch
	Scenario *b)*	1.5 kWh/m²	€ 3.2	€ 0.7 (18.0%)	2.6 °Ch
	Scenario *c)*	1.5 kWh/m²	€ 3.2	€ 0.7 (18.0%)	1.6 °Ch

The relative ability of the MPC setups to shift space heating consumption by exploiting the thermal mass as heat storage (Eq. (17)) is depicted in Fig. 10 and Fig. 11 for the existing and retrofitted building, respectively. A positive difference indicates a boosting period, where the room air temperature was increased to store heat, whereas a negative difference occurs at high price periods, where the heat storage was discharged. A negative difference of -100% indicates a period where the space heating was completely shut off. In general, the three MPC setups led to similar charging and discharging patterns.
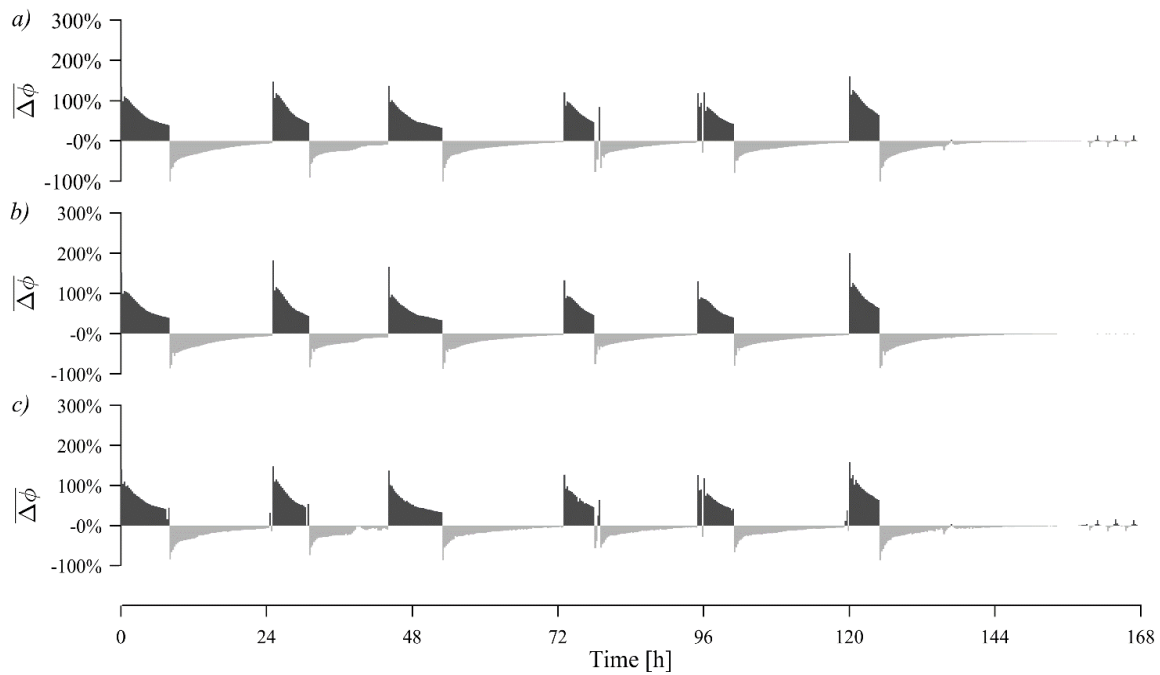
Fig. 10. Potential for exploiting the thermal mass as heat storage for the existing building.

The relative shifting potential was highest in the retrofitted building because of the lower reference heating consumption. The periods of complete heating shut-off were very limited in the existing building, whereas a total shut-off was possible for extended periods in the retrofitted building. Furthermore, Fig. 10 and Fig. 11 show that the temperature boosts resulted in space heating increases of up to approx. 100% and 300% compared to the reference controller for the existing and retrofitted building, respectively. For this to be possible, radiators have to be over-dimensioned when installed, which is typically the case in many existing Danish residential buildings in order to ensure fast response times and sufficient heating power given the worst-case weather conditions [29].
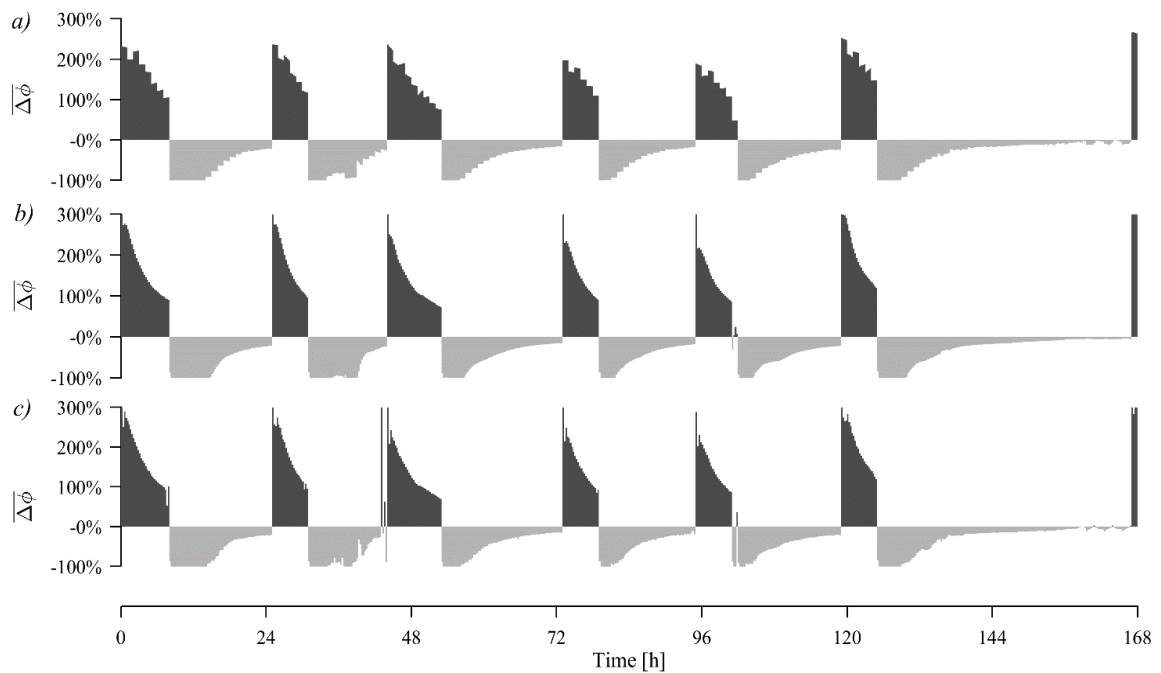
Fig. 11. Potential for exploiting the thermal mass as heat storage for the retrofitted building.

Fig. 12 displays the absolute shifting potential according to Eq. (16) for the existing and retrofitted building, respectively, using MPC setup *b)*. The simulation period was divided into six load shift events consisting of a charging and discharging period (see Eq. (18)). Overall, the existing building enabled the highest shifted consumption due to the generally higher reference consumption, whereas the retrofitted building enabled shifts over longer periods because of the increased storage efficiency. Information on the absolute charge and discharged heat in individual events is specified in Table 5 together with the shifting efficiency. In contrast to previous studies that used rule-based control to investigate the heat storage efficiency of thermal mass [9, 30], the charging and discharging periods in this study varied in duration since the control was optimized based on the cost signal *f*.

Table 5. Specification of load shifting events.

		Charging	**Discharging**	η_{shifting}
Existing building	Event 1	108.1 Wh/m^2	-65.4 Wh/m^2	60.6%
	Event 2	86.8 Wh/m^2	-52.9 Wh/m^2	61.0%
	Event 3	102.8 Wh/m^2	-74.3 Wh/m^2	72.4%
	Event 4	79.7 Wh/m^2	-57.6 Wh/m^2	72.3%
	Event 5	88.5 Wh/m^2	-62.5 Wh/m^2	70.6%
	Event 6	79.4 Wh/m^2	-60.0 Wh/m^2	75.5%
Retrofitted building	Event 1	89.0 Wh/m^2	-57.9 Wh/m^2	65.1%
	Event 2	68.5 Wh/m^2	-53.3 Wh/m^2	77.9%
	Event 3	81.4 Wh/m^2	-69.3 Wh/m^2	85.1%
	Event 4	70.1 Wh/m^2	-56.6 Wh/m^2	80.7%
	Event 5	71.7 Wh/m^2	-57.7 Wh/m^2	80.5%
	Event 6	69.3 Wh/m^2	-70.4 Wh/m^2	101.5%

As expected, the quantity of shifted consumption was slightly higher for the existing building; however, the shifting efficiency was significantly higher for the retrofitted building. The efficiency of Event 6 was even above 100% since heat stored at previous events was not yet fully discharged coming into the event. This mechanism can also be observed in Fig. 11 where the relative consumption at the end of the fifth discharging period was still below zero before charging period six was initiated. The observed shifted quantities and efficiencies are consistent with the results in [9].

Fig. 12. Absolute shifting potential for the existing and retrofitted building using MPC setup b).

4   Discussion

The results of this study showed very limited differences in performance between setups *a)* and *b)*. This suggests that findings from previous studies using electrical baseboard heaters as in setup *a)*, e.g. [7, 8], also apply to buildings equipped with hydronic heating systems. Besides enabling a more broad generalization of previous research results, this equivalency also has a practical advantage. The simulation time for setup *c)* significantly increased compared to setups *a)* and *b)* with a factor of up to 50. Based on the findings of this study, it therefore seems practically reasonable that future simulation-based studies as well as real application of E-MPC for single-zone residential space heating rely on setup *b)*. However, it may be necessary to include the dynamics of the radiator when operating multi-zone hydronic space heating systems or to investigate the dynamic response of the heating system.

Furthermore, in agreement with previous studies [7, 8, 9], the results suggest that the potential for shifting space heating consumption depends on the energy efficiency of the building envelope. The absolute potential for shifting energy on the short term was greater in the existing building because of the higher reference consumption, whereas the higher storage efficiency of the retrofitted building made it more suited for shifting loads over longer periods. Similarly, the retrofitted building allowed space heating to be completely shut off for multiple consecutive hours, while the existing building was incapable of sustaining comfortable temperatures without space heating. Despite these differences, the absolute loads shifted during the load shifting events were similar.

5   Conclusion

This paper reported on the development of a reliable dynamic hydronic radiator model and an investigation of the effect of including the radiator dynamics in an associated MPC scheme for residential space heating with the objective to perform price-based demand response. Three MPC setups were defined: *a)* a linear MPC controlling an electrical baseboard heater, *b)* a two-level controller where a linear MPC calculated the heating setpoint for conventional PI-control of the hydronic radiator model, and *c)* an N-MPC scheme that included the hydronic radiator in the control-model. The three MPC setups obtained similar simulation results, i.e. operational cost savings of approx. 5% and 18% in an existing and retrofitted building, respectively, while restricting the amount of thermal comfort violations to a limited extent. This suggest that the more practical two-level MPC implementation is preferable for real applications compared to the significantly more computational demanding N-MPC scheme for real applications.

The calibrated dynamic radiator model developed for this study was able to adequately simulate the behavior of the actual radiator when comparing measured experiment data with the states of the proposed dynamic model. As such, this paper also provides a reliable radiator model suitable for any simulation-based research study in which accurate representation of the dynamic behavior of hydronic radiators is desirable.

6   Acknowledgement

Appendix A

The complete system of non-linear ordinary differential equations of the hydronic radiator model.

$$C_{\text{Rad}} \cdot \frac{dt_1}{d\tau} = H_{\text{w}} \cdot q \cdot (t_{\text{inlet}} - t_1) \cdot N_{\text{S}} - \phi_{\text{N}} \cdot \left(\frac{t_1 - t_{\text{room}}}{\Delta t_{ar,\text{N}}} \right)^n \qquad (A.1)$$

$$C_{\text{Rad}} \cdot \frac{dt_2}{d\tau} = H_{\text{w}} \cdot q \cdot (t_1 - t_2) \cdot N_{\text{S}} - \phi_{\text{N}} \cdot \left(\frac{t_2 - t_{\text{room}}}{\Delta t_{ar,\text{N}}} \right)^n \qquad (A.2)$$

$$C_{\text{Rad}} \cdot \frac{dt_3}{d\tau} = H_{\text{w}} \cdot q \cdot (t_2 - t_3) \cdot N_{\text{S}} - \phi_{\text{N}} \cdot \left(\frac{t_3 - t_{\text{room}}}{\Delta t_{ar,\text{N}}} \right)^n \qquad (A.3)$$

$$C_{\text{Rad}} \cdot \frac{dt_4}{d\tau} = H_{\text{w}} \cdot q \cdot (t_3 - t_4) \cdot N_{\text{S}} - \phi_{\text{N}} \cdot \left(\frac{t_4 - t_{\text{room}}}{\Delta t_{ar,\text{N}}} \right)^n \qquad (A.4)$$

$$C_{\text{Rad}} \cdot \frac{dt_5}{d\tau} = H_{\text{w}} \cdot q \cdot (t_4 - t_5) \cdot N_{\text{S}} - \phi_{\text{N}} \cdot \left(\frac{t_5 - t_{\text{room}}}{\Delta t_{ar,\text{N}}} \right)^n \qquad (A.5)$$

$$C_{\text{Rad}} \cdot \frac{dt_6}{d\tau} = H_{\text{w}} \cdot q \cdot (t_5 - t_6) \cdot N_{\text{S}} - \phi_{\text{N}} \cdot \left(\frac{t_6 - t_{\text{room}}}{\Delta t_{ar,\text{N}}} \right)^n \qquad (A.6)$$

$$C_{\text{Rad}} \cdot \frac{dt_7}{d\tau} = H_{\text{w}} \cdot q \cdot (t_6 - t_7) \cdot N_{\text{S}} - \phi_{\text{N}} \cdot \left(\frac{t_7 - t_{\text{room}}}{\Delta t_{ar,\text{N}}} \right)^n \qquad (A.7)$$

$$C_{\text{Rad}} \cdot \frac{dt_8}{d\tau} = H_{\text{w}} \cdot q \cdot (t_7 - t_8) \cdot N_{\text{S}} - \phi_{\text{N}} \cdot \left(\frac{t_8 - t_{\text{room}}}{\Delta t_{ar,\text{N}}} \right)^n \qquad (A.8)$$

$$C_{\text{Rad}} \cdot \frac{dt_9}{d\tau} = H_{\text{w}} \cdot q \cdot (t_8 - t_9) \cdot N_{\text{S}} - \phi_{\text{N}} \cdot \left(\frac{t_9 - t_{\text{room}}}{\Delta t_{ar,\text{N}}} \right)^n \qquad (A.9)$$

$$t_{\text{outlet}} = t_9 \qquad (A.10)$$

References

[1] S. Wang, X. Xue and C. Yan, "Building power demand response methods toward smart grid," HVAC&R Research 20:6, pp. 665-687, 2014.

[2] E. Nyholm, S. Puranik, É. Mata, M. Odenberger and F. Johnsson, "Demand response potential of electrical space heating in Swedish single-family dwellings," Building and Environment 96, pp. 270-282, 2016.

[3] H. Lund, A. N. Andersen, P. A. Østergaard, B. V. Mathiesen and D. Connolly, "From electricity smart grids to smart energy systems - A market operation based approach and understanding," Energy 42, pp. 96-102, 2012.

[4] J. Wang, H. Zhong, Z. Ma, Q. Xia and C. Kang, "Review and prospect of integrated demand response in multi-energy system," Applied Energy 202, pp. 772-782, 2017.

[5] M. D. Knudsen and S. Petersen, "Model predictive control for demand repsonse of domestic hot water preparation in ultra-low temperature district heating systemsq," Energy and Buildings 146, pp. 55-64, 2017.

[6] S. Stinner, K. Huchtemann and D. Müller, "Quantifying the operational flexibility of building energy systems with thermal energy storgaes," Applied Energy 181, pp. 140-154, 2016.

[7] T. H. Pedersen, R. E. Hedegaard and S. Petersen, "Space heating demand response potential of retrofitted residential apartment blocks," Energy and Buildings 141, pp. 158-166, 2017.

[8] R. E. Hedegaard, T. H. Pedersen and S. Petersen, "Multi-market demand response using economic model predictive control of space heating in residential buildings," Energy and Buildings 150, pp. 253-261, 2017.

[9] J. Le Dréau and P. Heiselberg, "Energy flexibility of residential buildings using short term heat storage in the thermal mass," Energy 111, pp. 991-1002, 2016.

[10] J. Široký, F. Oldewurtel, J. Cigler and S. Prívara, "Experimental analysis of model predictive control for an energy efficient building heating system," Applied Energy 88, pp. 3079-3087, 2011.

[11] M. Avci, M. Erkoc, A. Rahmani and S. Asfour, "Model predictive HVAC load control in buildings using real-time electricity pricing," Energy and Buildings 60, pp. 199-209, 2013.

[12] G. Bianchini, M. Casini, A. Vicino and D. Zarrilli, "Demand-response in building heating systems: A Model Predictive Control Approach," Applied Energy 168 , pp. 159-170, 2016.

[13] J. Kensby, A. Trüschel and J.-O. Dalenbäck, "Potential of residential buildings as thermal energy storage in district heating systems - Results from a pilot test," Applied Energy 137, pp. 773-781, 2015.

[14] A. Acosta, A. I. González, J. M. Zamarreño and V. Álvarez, "Energy savings and guaranteed thermal comfort in hotel rooms through nonlinear model predictive controllers," Energy and Buildings 129, pp. 59-68, 2016.

[15] M. Wetter, "Co-simulation of building energy and control systems with the Building Controls Virtual Test Bed," *Journal of Building Performance Simulation (2010),* vol. 3, no. 4, pp. 1-19.

[16] DL Radiators, "Radiatorji Radel in Delonghi 2013".

[17] L. H. Hansen, Stochastic modelling of central heating systems, Lyngby: IMM - DTU, 1997.

[18] S. Holst, "TRNSYS-Models for Radiator Heating Systems," München, 1996.

[19] D. Risberg, M. Risberg and L. Westerlund, "CFD modelling of radiators in buildings with user-defined wall functions," Applied Thermal Engineering 94, pp. 266-273, 2016.

[20] Danfoss Heating Solutions, "Introduction to Hydronic Floor Heating," 2010.

[21] H. A. Barker, "GALOIS - A Program for Generating Pseudo-Random Pertubation Signals," in 12th IFAC Symposium on System Identification (SYSID 2000), Santa Barbara, 2000.

[22] M. W. Braun, D. E. Rivera, A. Stenman, W. Foslien and C. Hrenya, "Multi-level pseudo-random signal design and "model-on-demand" estimation applied to nonlinear identification of a RTP wafer reactor," in *American Control Conference*, San Diego, California, 1999.

[23] EN 442-2:2014, Radiators and convectors - Part 2: Test methods and rating, Brussels: CEN - European committee for standardization, 2014.

[24] F. Oldewurtel, A. Parisio, C. N. Jones, D. Gyalistras, M. Gweder, V. Stauch, B. Lehmann and M. Morari, "Use of Model Predictive Control and Weather Forecasts for Energy Efficient Building Climate Control," Energy and Buildings 45, pp. 15-27, 2012.

[25] R. E. Kalman, "A New Approach to Linear Filtering and Prediction Problems," Journal of basic engineering 82(1), pp. 35-45, 1960.

[26] T. H. Pedersen, M. D. Knudsen, R. E. Hedegaard and S. Petersen, "Handling thermal comfort in economic model predictive control schemes for demand response," Energy Procedia (122), pp. 985-990, 2017.

[27] J. R. Dobbs and B. M. Hencey, "Model Predictive HVAC control with online occupancy model," Energy and Buildings 82, pp. 675-684, 2014.

[28] T. H. Pederesen, R. E. Hedegaard, M. D. Knudsen and S. Petersen, "Comparison of centralized and decentralized model predictive control in a building retrofit scenario," Energy Procedia 122, pp. 979-984, 2017.

[29] D. S. Østergaard and S. Svendsen, "Theoretical overview of heating power and necessary heating supply temperatures in typical Danish single-family houses from the 1900s," Energy and Buildings 126, pp. 375-383, 2016.

[30] G. Reynders, J. Diriken and D. Saelens, "Quantification Method For The Active Demand Response Potential By Structural Storage In Buildings," in 14th International Conference of the International Building Performance Simulation Association, Hyderabad, India, 2015.

Project application to ForskEL (in Danish)

Projektbeskrivelse

ForskEL- og ForskVE-udbud 2015

Program der ansøges *(angiv ForskEL eller ForskVE):*	ForskEL
Ansøgning nr.:	12305
Projekttitel:	**READY.DK**
Ansøger:	Aarhus Universitet
Dato:	26.08.2014.

Indholdsfortegnelse

1. Generel beskrivelse af teknologien

I projektet READY.DK udvikles der en metodik der detaljeret kan kortlægge smart grid potentialet for den enkelte bygning i forbindelse med en energirenovering. Metodikken faciliteres af et EDB-program. Dette program vil indgå i et større kompleks af programmer, der udvikles i forbindelse med det internationale EU-FP7 projekt "READY", der arbejder med energirenoveringspotentialer på bydelsniveau. READY.DK vil dermed bidrage med et vigtigt input til en platform der skal balancere det privat-, og socio-økonomiske trade-off mellem investeringer i energibesparelse, investeringer i teknologi der kan høste "Smart Grid Potentiale", og energiproduktion.

2. Projektbeskrivelse

a.   Projektets formål

Indeværende projekt "READY.DK" er et "ad-on" projekt til det 33,5 mio. € store internationale EU-FP7 projekt "READY". Original FP 7 ansøgning vedlagt, og både indhold og økonomi er godkendt af EU. READY forventes at starte ultimo 2014.

READY er primært et demonstrationsprojekt, men Aarhus Universitet (AU) har ansvar for nogle få forskningsaktiviteter indarbejdet i projektet. Et af områderne er arbejdspakke *3.5.1: Opimization of building retrofit*, og her ønsker vi med denne ansøgning at udvide omfanget af forskningsområdet, resultaterne og formidlingen af smart grid-integrerede løsninger i forbindelse med bygningsrenovering. Omfangsmæssigt ønsker vi at udbygge forskningsområdet med tre årsværk svarende til en fuldtids Ph.d. studerende på Aarhus Universitet, Institut for Ingeniørvidenskab.

Vedlagt forefindes et "2 siders" dansk resume af FP 7 READY-projektet samt original og godkendt FP 7 ansøgning.

I resten af denne ansøgning vil vi koncentrere os om at forklare den ønskede udbygning af arbejdspakken 3.5.1 i EU FP 7 READY projektet. Overordnet set ønsker vi at skærpe smart grid elementet i FP7 ansøgningen, som primært er et energirenoverings-demonstrationsprojekt for boligbyggeri med fokus på energibesparelser. I FP7 projektet behandles smart grid potentialet af eksisterende byggeri på "makroskala". I READY.DK vil vi bevæge os ned på "mikroskala" og skærpe fokus på hvorledes man kan integrere konkrete løsninger, der fremmer eksisterende bygningers "Smart Grid Potentiale" i forbindelse med en energirenovering. Dermed får vi mere viden om hvor det privat-, og socio-økonomiske trade-off mellem investeringer i energibesparelser og investeringer i teknologi der kan høste "Smart Grid Potentiale" ligger. Målet er at bidrage med forskningsbaseret viden til at skabe en metodik der med udgangspunkt i det enkelte byggeris potentiale for energibesparelser og smart grid fleksibilitet kan bruges til projektering af en totalløsning i forbindelse med renovering af boliger.

b.   Beskrivelse af projektets indhold

Der gives i det efterfølgende en kort opsummering af delopgaven 5.3.1 i READY der omhandler optimering af energirenoveringer: *Investeringer i energirenovering af boliger nedbringer energiefterspørgslen gennem et reduceret forbrug. Bygningers masse, lokal lagring og intelligente apparater kan øge forbrugernes fleksibilitet og lette integrationen af vedvarende energi til opvarmning og elforsyning. Med udgangspunkt i energirenoveringsdelen i demonstrationsprojektet*

READY samt resultaterne af underopgave 2.1, (selve energirenoveringen) har denne delopgave til formål at etablere en generel platform for i grove tal at kvantificere de operationelle krav til energipriser og "demand-side" fleksibilitet af typiske bygninger i et større område. Der er fokus på koste optimale løsninger, der minimerer levetids energiforbruget (dvs. omfatter indeholdt energi fra produktion m.v.), og sikre størst mulig demand-side fleksibilitet og garanterer en høj kvalitet af indendørs klima og miljø forhold til slutbrugeren.

Indholdet af projektet READY.DK vil være at generere viden og data om konkrete smart grid løsninger der kan indarbejdes i danske energirenoveringer. Dermed vil man flytte sig fra de "grove" betragtninger af potentialer i READY (byniveau) til mere konkret/lokale vurderinger af potentialer (bygningsniveau). Det er vigtigt for den enkelte bygningsejer samt energisystemet at kunne kvantificere smart grid potentialet i den konkrete bygning rimeligt præcist for at kunne foretage rentable investeringer og opstille de rette betingelser i forbindelse med en demand respose handel.

READY.DK vil gennemføre analyser og eksperimenter der kortlægger smart grid potentialet for en række af de enkelte bygninger der indgår i energirenoveringsprojektet FP7 *før* energirenove-ringerne. Dernæst foretages analytiske beregninger af løsninger der teoretisk set maksimerer bygningernes smart grid potentiale i forbindelse med en energirenovering. Disse løsninger ind-arbejdes i energirenoveringsprojekterne, og disse testes eksperimentelt i perioden *efter* energi-renoveringen. Erfaringerne fra projektet vil blive brugt til at opstille en metodik der kan bruges til at identificere og kvantificere effekten af fleksibilitetsteknologier i forbindelse med energire-novering.

c. Beskrivelse af arbejdspakker

Arbejdspakke og -nummer	AP1 – Projektledelse
Resourcer	Tidsforbrug: 500 timer

Formål
Denne AP har til formål at sikre en effektiv forvaltning af aktiviteterne i projektet, herunder især koordinering med aktiviteterne i READY projektet. Projektledelsen skal også sikre en høj kvalitet af forskningsarbejdet og de rapporter og publikationer der produceres. Arbejdspak-ken tager sig af den administrative og finansielle forvaltning af projektet, herunder overvåg-ning og rapportering af status til Energinet.dk; risikostyring; tilrettelæggelse af projektmø-der; og kvalitetssikring.

Arbejdspakke og -nummer	AP2 – Smart grid potentiale i energirenoveringer
Resourcer	Tidsforbrug: 5771 timer

Formål
Denne AP genererer viden og data om konkrete smart grid løsninger der kan indarbejdes i danske energirenoveringer gennem demonstrationsprojektet EU-FP7 READY. Arbejdspakken beskæftiger sig dermed med konkrete bygninger og deres ejere – både analytisk og ekspe-rimentelt. Formålet er at skabe en valideret metodik der kan benyttes til at kortlægge smart grid potentialet for den enkelte bygning og deres ejer(e) i forbindelse med en energirenove-

ring.
Opgavebeskrivelse Opgave 2.1: Smart grid potentiale i eksisterende byggeri Der udvælges en række bygninger som er repræsentativ for de bygninger der indgår i ener-girenoveringerne i READY (en-familiehuse og etageboligbyggeri). Disse bygninger analyseres teoretisk for deres smart grid potentiale *før* de renoveres, og der udføres eksperimenter med bygningerne for at undersøge om de teoretiske potentialer kan indfries. *Milepæl: Smart grid potentiale for bygningerne identificeret (før energirenovering) – 0.-6. måned* Opgave 2.2: Identifikation og test af løsninger der øger bygningernes smart grid potentiale. Viden om de eksisterende bygnings fra arbejdspakke 2.1 benyttes til at identificere løsnin-ger der potentielt kan øge bygningernes fleksibilitet i forhold til et smart grid. Løsningerne indarbejdes i energirenoveringsprojekterne, og disse testes eksperimentelt i perioden *efter* energirenoveringen. *Milepæl: Løsninger der øger smart grid potentialet i forbindelse med en renovering identifice-ret (før energirenovering) – 6.-12. måned* *Milepæl: Eksperimentel test af smart grid løsninger i renoveringsprojekterne gennemført – 12.-24. måned* Opgave 2.3: Metodik På baggrund med erfaringerne i opgave 2.1 og 2.2 opstilles en metodik der kan bruges til at identificere og kvantificere effekten af fleksibilitetsteknologier i forbindelse med energireno-vering. Metodikken er operationaliseret i et EDB-program, der faciliterer opgaven. Program-met giver et værdifuldt input til den overordnede renoveringsmodel i EU-FP7, der skal balan-cere det privat-, og socio-økonomiske trade-off mellem investeringer i energibesparelse, investeringer i teknologi der kan høste "Smart Grid Potentiale", og energiproduktion. *Milepæl: Metodik færdig – 0.-36. måned*

d.   Risikovurdering

Der vurder ikke at være de store risici forbundet med projekt, da dette "Ad On" projekt er en udbygning af et allerede godkendt EU FP 7 projekt.

e.   Miljøpåvirkninger

e.1 Miljøkonsekvenser og milepæle for miljøforbedringer

		Karakter af miljøpåvirkning			Handling i projektet	
	(Slet ikke dette skema og uddyb efterføl-gende)	Ikke relevant	En mindre (X) eller væsent-lig (XX) på-virkning	Positiv (+) eller negativ (-) påvirk-ning	Håndteres i projektet	En milepæl i projektet
	Eksempel på indtastning		XX	-	X	
Påvirkninger fra valg af materialer	Brug af sjældne metaller og grundstoffer (f.eks. i magneter, katalysatorer, solceller)	x				
	Brug af byggematerialer (f.eks. stål, ce-ment)		XX	-	X	
	Brug af miljøskadelige stoffer (f.eks. for-maldehyd, PCB) samt andre forbrugsstoffer	X				
	Mulighed for at genbruge eller genvinde emner	X				
Påvirkninger fra processer	Energiforbrug og udledning til luften (fra rejser og fra produktion, transport og drift af udstyr)		x	+	X	
	Særlige arbejdsmiljøforhold ved produktion og drift, herunder håndtering af kemikalier og risiko for ulykker	x				
	Lokalitetsspecifikke konsekvenser, herunder ulempe for folk i omegnen og påvirkning af natur (f.eks. støj, lugt, udledninger)	x				
	Produktion af restprodukter og affald, her-under spildevand, samt behov for specialbe-handling af affald	x				
Påvirkninger i forhold til energisystemet	Ændring i virkningsgrad/effektivitet (både teknologi og system)		x	+		
	Påvirkning af eksisterende infrastruktur (behov for ny/forstærkning eller redukti-on/undgå)	x				
	Miljøkonsekvens af ændret fleksibilitet i forhold til brændselstyper	X				
	Miljøkonsekvens af ændring i fleksibilitet i forhold til produkt (fx el/varme)		XX	+	X	

Bygninger med øget fleksibilitet i forhold til et smart grid kan kræve investeringer i ekstra byg-gematerialer, men ikke nødvendigvis. Fleksibiliteten kan udnyttes til at minimere energiforbrug og udledning til luften hvis man ønsker dette som objektfunktion i styringen af systemet. Fleksi-bilitet vil øge effektiviteten af energiforsyningen.

e.2 Bidrag til politiske mål for et mere miljøvenligt energisystem

(slet ikke denne tabel)	Ikke relevant	Mindre bidrag	Væsentligt bidrag
Hele energiforsyningen dækkes af vedvarende energi i 2050.			x
Elektricitet og varme dækkes af vedvarende energi i 2035.			x
Udfasning af kul på kraftværker og udfasning af oliefyrede kedler i 2035.			x
Integration af 50 pct. vindkraft i 2020.			x
20 pct. reducering af CO_2 udledning i 2020.			x
20 pct. energivirkningsgrad i 2020.			x

3. Projektets relevans

Fremtidens elektriske system vil være væsentligt forskellig fra det elektriske systemet vi kender i dag. Store og markante ændringer er nødvendige, hvis den meget store mængde vedvarende energi, fra primært vindmøller og solceller, skal blive integreret og udnyttet optimalt. Der skal udvikles tekniske og økonomiske løsninger, der sikre en balance mellem produktion og forbrug mellem de mange forskellige energiforbrugende enheder og operatører i det samlede energisystem.

I fremtidens elsystem, "Smart Grid", vil der være behov for en væsentligt større fleksibilitet hos elkunderne, og det betyder at samspillet mellem de forskellige energisystemer skal udnyttes i langt større grad end det gøres i dag samt at kunderne skal inddrages på en sådan måde, at de bliver et vigtigt og nyttigt "aktiv" i balanceringen af el-systemet og effektiv udnyttelse af den fluktuerende el-produktion fra sol og vind.

Med dette "Ad on" projekt vil vi sikre at overordnet energirenovering ikke modarbejder men bidrager positivt til et fleksibelt energisystem ved at indarbejde Smart Grid løsninger i arbejdet med energirenoveringer.

Generelt vil vi med dette projekt bidrager væsentligt til at nå Danmark's og EU's mål for nedbringelse af CO_2 udledningen, udbygningen og implementeringen af vedvarende energi og ikke mindst understøtter strategierne inden for smart grid og smart energy.

4. Formidlingsplan og forankring

Resultaterne fra projektet vil have en betydelig indflydelse på den nuværende state-of-the-art ud fra både videnskabelige og teknologiske synspunkter.

Aarhus Universitet planlægger at formidle resultaterne af projektet gennem præsentationer i internationale videnskabelige konferencer og workshops, samt gennem videnskabelige publikationer i dedikerede, internationale forskningstidsskrifter. Derudover udføres der minimum tre populærartikler i danske tidsskrifter, og projektets tema og resultater vil indgå i projektlederens blog.

READY.DK vil også udnytte den unikke mulighed for formidling og forankring af viden som projektet opnår gennem det integrerede samarbejde med EU-FP7 projektet READY.

5. Organisering og kompetencer for aktører

Projektet er organiseret som et ph.d. projekt ved Aarhus Universitet. Projektet forankres i forskergruppen Indeklima og Energi, som bl.a. beskæftiger sig med bygningers rolle i fremtidens smart grid (http://eng.au.dk/forskning/forskningsomraader/byggeri-og-bygningsdesign/indeklima-energi/)

Forskergruppen udfører forskningen i samarbejde med nationale og internationale samarbejdspartnere. Forskergruppen er også ansvarlig for den forskningsbaserede undervisning i civilingeniøruddannelsen i Integrated Energy Design.

6. Finansiering og generelle kommentarer til budget

Der søges midler til en Ph.d. studerende under gældende regler for Ph.d. ansættelse, lønninger m.v.

7. Tilskyndelsesvirkning

Indeværende projekt READY.DK, et ad-on projekt til EU projektet READY, vil ikke bliver ført ud i livet, medmindre at der opnås støtte og dermed finansiering fra ForskEL af en hel ph.d. studerende. Der er ikke muligt at allokere og flytte midler fra i READY projektet til en detaljeret, forskningsbaseret udvikling af integrerede løsninger, der fremmer eksisterende bygningers "Smart Grid Potentiale" i forbindelse med en energirenovering, da READY primært er et demonstrationsprojekt. Vi mener at området er af meget stor betydning for udviklingen af fremtids energisystemer og søger derfor ForskEL om finansiering af projektet READY.DK.

8. Markedet

a.   Målgruppe og merværdi for forbrugere

Boligforeninger, virksomheder og private boliger mf. der står foran en energirenovering. Vi skal sikre der bliver Smart Grid renoveret og ikke kun energirenoveret.

Aggregatorer (balance kraft m.v.) og el-handlere kan udvikle nye forretningskoncepter og forretningsmuligheder i krydsfeltet mellem regulerede aktiviteter og udvikling af det frie marked, når de får adgang til "Smart Grid" potentialet i den store bygningsmasse.

Alle fremtidige el-kunder, der har et "ikke ubetydelig" elforbrug og ikke mindst et elforbrug, der kan reguleres ved prissignaler mv.

Fremtidige el-forbrugere og bygninger vil have optimale betingelser for at sikre den bedste "driftsøkonomi" af det samlede energiforbrug, da de er sikret billigere og renere elektricitet gennem deres omdannelse til at være "Smart Grid Ready", gennem deres Smart Grid renovering.

Levandører af Smart Grid komponeter, systemer og serviceses m.v.

b.   Konkurrenceanalyse

Ikke relevant for nuværende.

c.   Markedspotentiale af "Smart Grid Ready"

Antallet af bygninger i Danmark der bør/skal energi/smart-grid renoveres fremover er meget stort. Der er tale om mere end 90.000 etageboliger og mere end 72.000 kontor-og erhvervsbyggeri. Mange af disse bygninger er nødt til at gå igennem en "Smart Grid Ready" renovering og en energioptimerings renovering i løbet af de næste 10 til 20 år. Antages det, at kun 33 % af disse bygninger bliver "Smart Grid Ready" over en periode på 15 år, vil det give den potentielle af over 3.100 bygninger pr. år, og det er kun i Danmark.

Derudover vil der være mere end 1 mio. enfamiliehuse, der skal/bør energirenoveres og få varmepumper installeret i de næste mange år. I 2030 forventes det, at omkring 300.000 individuelle varmepumper vil blive installeret i enfamilieshuse, og det alene i Danmark! Derfor er det vigtigt med en metodik til smart grid renovering.

d.   Markedsføringsplan

Se under "Formidlingsplan og forankring".

9. Forskning

a.   Forskningsindhold

Når vi har omstillet vores energiproduktion til vedvarende energi, er det ikke nødvendigvis økonomisk rentabelt at energirenovere i det omfang man hidtil har set i forskningsbaserede demonstrationsbyggerier (renovering). Der er en tendens til at energirenovere til "0-energi" niveau, endda "aktiv-energi" niveau (enheder der over et år producerer mere energi end de bruger). Det er langt fra sikkert om dette er fornuftigt i alle renoveringsprojekter – på kort eller længere sigt.

Det forskningsmæssige indhold af dette projekt er at bidrage til en mere nuanceret tilgang til energirenovering, der bør inkludere balancen mellem investeringer i energibesparelser, energiforsyning og teknologier til smart grid fleksibilitet.

b.   Forskningsbaseret bemanding

Sektion for Byggeri og Bygningsdesign

Sektion for Byggeri og Bygningsdesign under Institut for Ingeniørvidenskab på AU vil bidrage med viden og ekspertise i bygningsfysik og -installationer. Hovedinteressen i dette projekt er modellering af energiforholdene i bygninger, herunder verifikation på grundlag af empiriske data indsamlet i projektet med henblik på at gøre simulation-baserede forudsigelser om smart grid potentialer mere pålidelige.

Kontaktinformation på nøgleperson
Steffen Petersen, Ph.D
Adjunkt, Ph.D.
Leder af Indeklima og Energi

Aarhus University Department of Engineering, Aarhus University
Inge Lehmanns Gade 10, 8000 Aarhus C, Danmark
Email: stp@eng.au.dk
Phone: +45 4189 3347

Steffen Petersen er projektleder for READY.DK.

En egnet kandidat til Ph.d. studiet i READY.DK arbejdspakke 2 vil blive optaget på Graduate School at Science and Technology (Aarhus Universitet).

Institut for Ingeniørvidenskab, Smart Grid program

Smart Grid programmet på Institut for Ingeniørvidenskab vil støtte projektet i dag-til-dag ledelse, kommunikation, gennemførelse af aktiviteter og udvikling af initiativer og nye projekter.

Kontaktinformation på nøgleperson
Peter Harling Lykke

Aarhus University Department of Engineering, Aarhus University
Finlandsgade 22, 8200 Aarhus N, Danmark
Email: ply@eng.au.dk
Phone: +45 4189 3325
Autoriseret underskriver

Thomas Skjødeberg Toftegaard, Institutleder

Kontaktinformation
Thomas Skjødebjerg Toftegaard, institutleder

Department of Engineering, Aarhus University
Finlandsgade 22, 8200, Aarhus N, Danmark
Email: tst@cs.au.dk
Phone (direct): +45 8715 6168
Phone (mobile): +45 2137 9470

c.   Forskningsplan
Se beskrivelse af arbejdspakke 2 i afsnit 2c af denne ansøgning.

10. CV'er Nøglepersoner

Curriculum Vitae – Steffen Petersen (AU-ENG)

Born 3 April 1979, Danish.

Education:
2011	Ph.D., Department of Civil Engineering, Technical University of Denmark. Title: Simulation-based support for design of new low-energy office buildings.
2005	M.Sc. in engineering, Department of Civil Engineering, Technical University of Denmark.

Employment:
2013-present	Assistant professor, Aarhus University Department of Engineering
2005-present	Consultant engineer, ALECTIA A/S
2006-2011	PhD Student, Dept. Civil Engineering, Technical University of Denmark
2008 (March-August)	Guest researcher at Lawrence Berkeley National Laboratory – Building Technology
2005-2006	Research assistant at Section of Building Physics and Services, Dept. Civil Engineering, Technical University of Denmark

Research areas:
Method and tools for simulation-based design support; predictive control of building systems operation; calculated vs. measured performance; smart grid potentials in building operation.

Keywords: Energy and buildings, Building physics, Indoor climate (thermal, air quality, daylight), Building simulation, Integrated energy design (process).

Relevant publications:
Petersen S. and Bundgaard BW. The effect of weather forecast uncertainty on a predictive control concept for building systems operation. *Applied Energy* 116 (2014) 311–321

Petersen S. and Svendsen S. Method for component-based economical optimisation for use in design of new low-energy buildings. *Renewable Energy* 38 (1) (2012) 173-180

Petersen S. and Svendsen S. Method for simulating predictive control of building systems operation in the early stages of building design. *Applied Energy* 88 (2011) 4597–4606

Curriculum Vitae – Peter Harling Lykke (AU-ENG)

Born 17 June 1965, Danish.

Education and academic degrees
Project Manager, 2010
Euro Consultant. On year course in Aarhus. November 92 - August 93.
Introduction to the use of "European system", Including funds, subsidies, grants etc., supple-
mented with accounts and contacts and network development.

Bachelor of Engineering, Odense (completed in Copenhagen), August 87 - February 92.
Specializing in Energy and Environment. My thesis was in "Future energy supply". Solar thermal
power plant based on SOFC - fuel cells.

Current and recent positions held:
2012 -   Smart Grid Programme Manager Aarhus University School of Engineering, Aahus
University, Denmark

2012 – 2010 Innovation Manager NRGi Net A/S
2010 – 2004 Head of research and development NRGi Amba
2004 – 2004 Head of department (Development) NRGi Construction A/S
2004 – 1997 Head of department (Sale) NRGi Construction A/S
1997 – 1995 Energy- and development ingineer NRGi Construction A/S (ARKE)

Management experience:
More than 20 years of R&D management experience from the energy sector including manage-
ment of project management office. I have managed innovation and product development
teams in national environment. The last five years with focus on rollout of smart meters and
preparation for Smart Grids.

Board of Directors:
2004 – 2012 Member of Board of Directors for Varmepumpefabrikantforeningen
2004 – 2008 Member of Board of Directors for Electronic Housekeeper
2008 – 2012 Member of Board of Directors for Samsø Energiakademi

Expert records:
Member of the Council of Regions Midtjyllands "mega" investment in renewable energy by 2007
Member of the Danish Energy's F & I Committee from 2007-2012
Member of Danish Electric Vehicle Alliance from 2010-2012
Member of DI Energy industry R & I Committee from 2008-2012